Comparative Analysis and Characterization of Ubiquilin Proteins in Ubiquitin Signaling and Neurodegenerative Disease

By

Bennett William Fox

A dissertation submitted in partial fulfillment of

the requirements for the degree of

Doctor of Philosophy

(Chemistry)

at the

University of Wisconsin – Madison

2016

Date of final oral examination: 8/2/2016

This dissertation is approved by the following members of the Final Oral Committee:

Randal S. Tibbetts, Professor, Department of Human Oncology
Laura L. Kiessling, Professor, Departments of Chemistry and Biochemistry
Shigeki Miyamoto, Professor, Department of Oncology
Elizabeth A. Craig, Professor, Department of Biochemistry
David A. Wassarman, Professor, Department of Cell and Regenerative Biology

Dedication

This work is dedicated in loving memory of my mom, Andrea Fox.

Acknowledgements

There are so many people that I'd like to thank that I'm going to work through chronologically, starting with people in science and then people in my personal life.

I am deeply indebted to Frank Schroeder, my research mentor during my time as an undergraduate at Cornell University. Frank is unrivaled in his intelligence and curiosity. He pushed me to my limit – to the point of tears – and he never treated me like I was just a kid, even though I was. Frank is full of bizarre ideas that are insightful and occasionally of an otherworldly quality. Frank is a model scientist and a great human being, I feel so lucky that we met when we did… otherwise I might have gone to law school!

When I arrived at Madison, I hit it off with Eric Strieter, a new professor who was starting his lab doing something that I didn't know very much about, which was this small protein called ubiquitin. Eric is awesome – he is a bit bonkers – and he is also fearless with big ideas and contagious enthusiasm. I learned molecular biology, data organization, and protein purification from Eric. I also consumed scientific literature while in his lab, mostly in an effort to keep up with him. Eric's interests in building ubiquitin chains informed my interest in how those different ubiquitin chains would be decoded in the cell, leading the lab down a new avenue.

I am grateful to Rachel Sheridan, of Laura Kiessling's lab, and to Dave Taggart, of Paul Friesen's lab, who taught me cell culture and insect cell culture techniques that I brought back to Eric's lab. I think all of my original cohort in Eric's lab – Vivian, Ellen, Steven, Robert, and HP – deserve my thanks, and also probably an apology, as I was a bit of an ego back at the beginning of grad school (I'd like to think that I'm reformed now). At some point, my relationship with Eric began to deteriorate and I left his lab in a blaze; happily, I have since rebuilt my bridge with him. I thank Laura Kiessling and Matt Sanders for support during this time – Laura allowed me to stay on CBI funding and encouraged me to find a new mentor during a difficult transition. I was considering a semester leave to collect my head, but Frank flew into town to spend a couple days convincing me that it's easier to "go back to school if I never leave." Thanks again to Frank for believing in me, for making the trip out and helping me retrieve my head from somewhere south of its normal place.

In March of 2011, I joined the Tibbetts lab and I hit the ground running. Randy and I got along well; he had high expectations for me and pushed me to take over a nascent project in the lab about ubiquitin-binding proteins called ubiquilins (the subject of my dissertation). Randy is a laissez faire advisor, allowing me to explore many ideas, working on related, tangential, and occasionally unrelated ideas. He's a sharp scientist – he designs experiments that are clean and insightful – he's taught me that the best experiments are informative regardless of the outcome. My understanding and appreciation for controls in cell biology comes from his scrutiny of my work, and also from our discussions of published literature, which we both enjoy dissecting.

I owe many thanks to the people in Randy's lab over the years, for the camaraderie, friendship, scientific discussions, and all of that. To Keith, my original mentor, thanks for taking me under your wing; to Tony, thanks for making yourself available and being such a softie, I enjoyed our talks; to JJ, my main man, for all the laughs, the shared love of music, and for our enduring friendship; to Sang Hwa, for sharing home-brewed Kombucha and keeping the lab running, thanks for tolerating me, good luck with the ubiquilin project; to Lihong, a careful and meticulous scientist with a level head and a gift for making chicken wings; to Weiyan, who always cracks me up, keep up the good work in the lab and with your English – what's up brother. And of course, Adam Mastrocola, Dr. Cola, Dr. Coco Beans, one of the most talented, generous, and thoughtful scientists/humans I've ever known. Lots of love to Dr. Cola, who taught me so much about experimental design and the power of designing both positive and negative controls. To the army of undergrads who have come and gone – we couldn't have done it without you. Special thanks to Logan, aka Dr. Juice, and Krystal (KO), my mentees, who did their best as I learned how difficult it is to mentor others. And double special thanks to Chi Chi, my fly collaborator. Chi Chi, you're the boss. I hope grad school is a great time for you.

I would like to thank my committee members and collaborators for their intellectual input and contributions. To Betty, thanks for your suggestions on writing and organizing work – I hope that the quality of my work will be proof that I took those suggestions seriously. To David, who carefully looks at my data and asks tough questions, thank you for your interest and time. You were right about the PRR insertion, by the way – more on that in chapter 4! To Shigeki – where would I be without you? You were instrumental in helping us appreciate the difference between Ub binding and Ub modification of ubiquilins. Quite literally, I could not have done it without you. And via Shigeki, thanks also to Chris Hooper, whose *in vitro* expertise helped us put the nails in the coffin of a hypothesis that was dismantled – thanks again, Hoop. To Mark Scalf, my MS collaborator – thanks for providing us with a solid foundation. I learned so much about setting up a successful collaboration from working with you – mainly that I need to have my plan together before the collaboration starts! Also thanks to Darryl Wesener, from the Kiessling lab, who taught me about Gibson cloning and helped me to design the $UQ1^{+PRR}$ insertion constructs.

To Laura – I think I've had roughly one class per semester with you, and I was your next-door lab neighbor for a couple years, so you've been a staple of my graduate school experience. It's been really cool being a part of CBI and I thank you for your leadership in that realm, especially the career conference that you organized. Thanks also for hosting a seminar class that I thoroughly enjoyed – I think every grad student should participate in a seminar like that. And I am deeply grateful for your emotional support during trying times, back when I switched out of Eric's lab and also during my mom's illness. Thanks also for your big picture suggestions on my project – your ideas were always a few steps ahead of the work while I sweated the details.

Then there are the people in my life who tolerated me during graduate school – my family: my dad, Thadlaw aka Puff Thaddy aka P. Thiddy; my brother, Eli, my sister, Emily and my other brother from another mother, Michael, my darling niece, Lainie. To my Aunt Moe and my "frousins," and specifically to all of my Madison friends who made life here great: Ethan and Laura, Tom and Laura, Kevin, J McD, Luke and Kelsey, Julia K-D, Purba "Pamela Turbo," Luke Boralsky, Dave Mortenson. Thanks for all the laughs and the fun. Thanks for canoeing on the frozen lake and disc golf on the weekends and late night skate sessions and the piano bar. Thanks for bike rides and croquet on the lawn or just sitting on the Square having a cup of coffee. Most of all, thanks to Steph – I couldn't have done it without you, I love you and I'm excited for what's next.

Randy – It's been a wild, mostly good, sometimes rocky time. I had no idea what I was getting into when I joined your lab, and I think you could say the same thing. I know the ubiquilin project will wander and sample the noise, but I'm pretty sure we're onto something. Thanks for your patience, your guidance, and your support. I'm excited to leave and I'm sad to go, getting teary-eyed writing this. Looking forward to publishing some sick papes with you in the very near future, fingers crossed on the climbing assay

Abstract

This thesis encompasses the analysis of two highly related ubiquitin (Ub)-binding proteins, ubiquilin 1 (UQ1) and ubiquilin 2 (UQ2). Ubiquilins participate in proteasome-mediated protein degradation and are broadly implicated in the adaptive stress response and neurodegenerative diseases. UQ1 and UQ2 contain the same type, number, and arrangement of modular domains, with the exception of a proline-rich-repeat (PRR) domain that is only present in UQ2. Notably, mutations clustered in the PRR of UQ2 cause X-linked amyotrophic lateral sclerosis (ALS) and/or frontotemporal lobar degeneration; however, neither the normal functions of the PRR nor impacts of ALS-associated mutations in UQ2 are well understood. This body of work is guided by two major objectives: to understand the normal function of the PRR in the context of UQ2, and to investigate ALS-causing mutations in the protein. Through a variety of biochemical, cytological, and cellular assays, we characterized the protein-protein interactions and post-translational modifications of ubiquilins, as well as their roles in cellular degradation pathways. Our principal findings indicate that the PRR domain contributes to ubiquitylation of UQ2, which is ablated by disruption of the Ub-binding domain. Surprisingly, removal or replacement of the first 30aa of UQ2 also strongly reduces its ubiquitylation, indicating that the PRR and the amino-terminus cooperate to direct ubiquitylation. Investigation of $UQ2^{ALS}$ mutants revealed increased ubiquitylation and reduced solubility of a single mutant, $UQ2^{P497H}$, whereas other ALS mutants were similar to wild type UQ2 in these assays. Characterization of cellular degradation pathways suggest that ubiquilins stabilize cytosolic substrates through both Ub-dependent and –independent mechanisms, depending on the substrate and technique. Collectively,

these data contribute to the characterization of ubiquilin proteins and provide a simple experimental framework to investigate the relationship between Ub-binding, Ub modification, and alterations to protein solubility, which comprise hallmark pathologic features of neurodegenerative disease

Table of Contents

Chapter 1) Introduction

1.1 ALS

Amyotrophic lateral sclerosis (ALS) is a fatal neurodegenerative disease that specifically targets motor neurons. People with ALS experience progressive paralysis and typically die from respiratory failure within 2-3 years of symptom onset. There are no effective treatments for the disease, which is most often diagnosed in middle-aged people during otherwise healthy and productive years. The single FDA-approved drug to ameliorate ALS, riluzole (brand name: Rilutek), is of limited efficacy[1]. Riluzole treatment extends lifespan by 3 months on average through a poorly defined mechanism[2]. There is clearly much to be desired and much work to do in the way of therapeutic intervention for ALS, which has entered the media limelight during my graduate school tenure with a social media movement known as the "ALS Ice Bucket Challenge." It would be wonderful if public awareness of the disease increases interest (and funding), helping to propel scientists, clinicians, and people affected by ALS to overcome this devastating degenerative condition.

1.2 Genetics of ALS

The etiology of ALS is similar to other neurodegenerative diseases: roughly 10% of ALS is classified as familial, in that there is a specific genetic mutation that causes disease, while the other 90% of cases are "sporadic," meaning that there are no known genetic mutations. During my time in graduate school, there has been tremendous progress in understanding ALS genetics and its surprisingly close relationship with a clinically distinct neurodegenerative condition, frontotemporal lobar degeneration with ubiquitin inclusions (FTLD-U)[3]. To date, mutations in more than 20 different genes have

been found to cause ALS. With few exceptions, these genes encode proteins that function in two major cellular facets: RNA-binding and protein trafficking[4]. There are many excellent reviews on RNA-binding proteins and the complex genetics of ALS, including a review written by a former graduate student in the lab[5]. The most recent, major discovery in ALS and FTLD-U genetics has been the identification of a hexanucleotide repeat expansion (HRE) in the intron of a poorly characterized gene, *c9ORF72*[6,7]. The *c9ORF72* HRE is the most common cause of both familial and sporadic ALS and FTLD-U[8], generating tremendous interest in characterizing the clinical, behavioral, and pathological features of the c9ORF72 HRE in neurodegeneration[9].

1.3 Hallmarks of ALS pathology

The presence of intracellular aggregates containing misfolded and Ub-modified proteins is a common hallmark of ALS and of many other neurodegenerative diseases, e.g., Alzheimer's Disease (AD), Parkinson's Disease, and Huntington's Disease. These heterogeneous conditions are collectively referred to as proteinopathies, in which pathology is characterized by toxic aggregates of disease-specific proteins in particular regions of the central nervous system. To date, many proteins have been conclusively linked to proteinopathies—including several distinct genetic forms of ALS (for review, see [10])—in which mutations disrupt normal protein folding and promote the formation of intracellular aggregates. Among the most prominent pathological features of ALS is the 43kDa TAR DNA-binding protein (TDP-43). Mutations in TDP-43 were shown to cause dominantly inherited ALS, but even in cases of sporadic ALS that lack TDP-43 mutations, cytosolic accumulations of ubiquitylated TDP-43 are a near universal occurrence[11]. Additional proteins that are frequently observed in ALS pathology include

p62/SQSTM1 and ubiquilins, Ub-binding proteins with the capacity to form oligomers and inclusion bodies[12,13]. Notably, mutations in either UQ2 or p62/SQSTM1 can also cause familial ALS, lending support to the idea that proteins enriched in pathological inclusions are of general relevance to disease progression and etiology[14,15]. In cases of the *c9ORF72* HRE, an unusual form of repeat-associated non-ATG (RAN) translation occurs, producing a variety of toxic dipeptides that are prominently featured in pathological aggregates[16-18].

1.4 The ubiquitin-proteasome system

Different neurodegenerative diseases are characterized by inclusions of disease-specific proteins – even distinct genetic forms of ALS are classified by distinct populations of proteins in inclusions[19]. Despite this heterogeneity, the accumulation of insoluble Ub is a common pathological feature that unites a variety of clinically distinct neurodegenerative conditions, including sporadic and familial forms of ALS. Ub is a small, highly conserved protein that is covalently appended to other proteins in an ATP-dependent process requiring at least three classes of enzymes[20]. There are several coding genes for Ub, many of which produce Ub as a fusion to another protein, typically a ribosomal protein[21,22]. Upon translation, the Ub-ribosomal protein fusion is recognized by Ub-specific proteases (USP) that recognize the C-terminus of Ub and cleave after the di-glycine motif, revealing free Ub and a free ribosomal protein. Additionally, there are stress-induced genes that encode polyUb as a multimeric series of head-to-tail units, which, when translated, are cleaved by USPs to reveal monomers, allowing for increased Ub synthesis during periods of stress[23].

The most well studied function of Ub is in protein degradation, in which covalent modification of a substrate by a polyUb chain signals for degradation by a large, cylindrical assembly of multiple gated proteases, known as the proteasome[24]. Ubiquitin is covalently appended to substrate proteins through nucleophilic attack of an amine on thioesterified Ub, resulting in an isopeptide bond between the substrate lysine (or free amine group of the N-terminus) and C-terminal glycine of Ub. At this point the Ub, bearing seven lysine amino acids and an N-terminal amine, can serve as the subsequent point of Ub conjugation, resulting in the construction of polyUb chains. A minimum of four Ub monomers is required for efficient proteasome targeting, and the range of polyUb chain length is estimated to vary widely from one to dozens of Ub moieties [25,26].

Due to the large number of lysine amino acids in Ub and the stochastic nature of Ub modification, a massive diversity of polyUb chains can be built, consisting of homotypic chains, in which all of the Ub monomers in a chain are linked through the same lysine; heterotypic chains, in which different lysine amino acids are used for conjugation of Ub monomers; and "forked" chains, which occurs when two lysine amino acids within the same Ub serve as conjugation points[27]. Additional layers of complexity, e.g., phosphorylation and acetylation of Ub, affect its recognition and the kinetics of chain formation[28,29]. For more information, I recommend the following excellent reviews on ubiquitylation and Ub signaling[30-32].

As it stands, ubiquitylation can result in a huge array of structurally and functionally distinct modifications, as homotypic polyUb chains linked through K48 are typically thought to target proteins for degradation, whereas K63-linked polyUb chains

are best studied in DNA damage signaling. The characterization of specificity in this system – from the E2/E3 enzymes that build Ub chains to the deubiquitylases (DUBs) that destroy chains – have revealed incredible, dynamic signaling events[33,34]. Recognition of different polyUb chains is mediated by Ub-binding domains, many of which show specificity for chain linkage and for specific subunits within a chain[35,36]. There is, therefore, tremendous complexity in the construction of polyUb chains, the "ubiquitin code," resulting in interaction with Ub-binding proteins that act to decode and transduce the signal[30].

1.5 Structure and function of ubiquilin proteins

Ubiquilin proteins comprise a family of related proteins that function in Ub-mediated proteolysis. At the N-terminus, ubiquilins contain a Ub-like (UBL) domain that is highly similar to the three-dimensional fold of Ub. The UBL domain contains abundant lysine amino acids and can serve as an Ub acceptor, resulting in monoUb-modified ubiquilins. In this work, I characterized Ub modification of ubiquilins by mass spectrometry (Chapter 3) and assessed the impacts of monoUb modification on Ub binding and solubility of ubiquilin proteins (Chapter 4). At the C-terminus, ubiquilins contain a Ub-associated (UBA) domain that binds with roughly equal affinity to homotypic polyUb chains of any linkage, and also displays modest affinity for monoUb[37,38]. Owing to its nonspecific interactions with Ub chains, synthetic constructs of ubiquilin UBA repeats have been coupled to agarose beads for protection and enrichment of polyUb from complex mixtures, known as tandem Ub-binding entities (TUBEs)[39]. The UBA domains of ubiquilins are unique because of their nonspecific, high affinity interactions, suggesting that ubiquilins can interact with a wide variety of Ub-

modified clients. This is reflected by observations that overexpression of ubiquilins stabilizes many different substrates, discussed at length in Chapter 4, section 4.4, and explored experimentally in chapter 5.

The central region of ubiquilins is Met-rich and contains four STI1 motifs of unknown significance, but there are reports suggesting that this central region is involved in homo- and hetero-dimerization and the recruitment of other cellular chaperones, including HSP70 family members and PDI[40-42]. Additional patterns of interest include a dozen tetrapeptide motifs of the sequence N-P-X-Ψ (in which X is any amino acid and Ψ is an aliphatic amino acid) of unknown function. Even less is known about the extreme N-terminus of ubiquilins, ~30aa of predicted unstructured sequence which is absent from UQ4. In chapter 4, I explore the function of the N-terminal 30aa of UQ2 in directing ubiquitylation of the UBL domain (section 4.3.4). Notably, in UQ2 this N-term extension preceding the UBL contains two PXXP motifs flanked by basic amino acids, which comprises a minimal SH3-binding motif that is absent from UQ1.

1.6 Mutations in UQ2 cause ALS

It was discovered in 2011 that missense mutations in *UBQLN2* cause dominantly inherited ALS and ALS with dementia[14]. Disease-causing mutations in UQ2 are clustered in a proline-rich-repeat (PRR) domain not present in UQ1. In fact, UQ1 and UQ2 share 95% similarity and otherwise harbor the same type, number, and arrangement of modular domains. Regardless of *UBQLN2* mutations (rare: less than 1% of disease population), UQ2 protein is frequently observed in insoluble, Ub-rich inclusions by post-mortem immunohistochemistry of neurons of affected individuals, one of the pathological hallmarks of ALS[13,43]. Additionally, ubiquilins are observed in Ub-positive pathology of

Parkinson's, Huntington's, and Alzheimer's diseases, suggesting that these proteins are important regulators of Ub-mediated aggregation[44,45].

1.7 Foreword

I performed my thesis research to investigate how mutations in the PRR of UQ2 may instigate neurodegenerative disease. Because the function of the PRR domain is unknown, I compared UQ2 with UQ1 as a reference point, given the high degree of similarity and the conservation of domains between the two proteins. Therefore my thesis work can be summarized as two major questions: 1) How does the PRR impact the function of UQ2 as compared to UQ1? 2) What are the effects of mutations in the PRR domain? As it turns out, neither question is straightforward to address.

My approach entailed systematic cytological and biochemical characterizations of ubiquilins, including point mutants and chimeras, in immortal cell lines and with recombinant proteins. Due to the prevalence of Ub-positive inclusions in post-mortem pathology, much of my work focused on the intertwined properties of Ub-binding, Ub-modification, and protein solubility. In chapter 2, I cover the first project I had in the lab, including its mistakes, and what I learned from them. In chapter 3, my hypothesis that the PRR might serve as a protein-protein interaction domain led me to characterize the ubiquilin interactome through co-immunoprecipitation (IP) / mass spectrometry (MS) experiments. During the course of MS characterization, I found that ubiquilin proteins are Ub-modified, and I explored the sequence determinants and consequences of this modification in chapter 4. I simultaneously attempted to ascertain a functional role for ubiquilins in protein degradation, which is the subject of chapter 5. My outlook on the

project, future directions for the work, and a discussion of literature on ubiquilins, protein solubility, disease models, and what it all might mean comprise chapter 6.

1.8 A note to new students

At the beginning of graduate school, I eagerly read papers in journals like Molecular Cell and Nature Cell Biology, fascinated and excited by panels of western blotting data. Inexperienced in the techniques, I typically accepted western blotting and IP data at face value, meaning I believed what was published. Although I have had my fair share of issues with reproducing published work, I don't mean to imply that there's foul play (although in my experience sometimes there is). In complex experiments, it is easy to make assumptions that preclude an accurate assessment of a given system. When I started grad school, I was satisfied to use the lysis buffer historically relevant to my lab, not considering the profound impact that buffer can have on the experimental outcome. As I write my thesis and come to the close of my time in graduate school, I have gained much experience. I have spent years learning "simple" techniques – because the choice of buffer (which can encompass ionic strength, detergent, counter ions, glycerol, and concentration of interacting proteins) makes all the difference, both in the outcome of the experiment and its interpretation. I have spent considerable effort developing a cursory understanding of different biological detergents, and in so doing have made some interesting discoveries about the biochemistry and regulation of ubiquilin proteins. The choice of detergent still cannot account for some of the greatest variability in antibody-based experiments, which is derived from the use of antibodies themselves. That said I have made my best effort to use the same epitope and antibody throughout my graduate

career, so that my results can be compared not only within an experiment, but also between experiments and across the years.

1.9 References

1. McGoldrick, P., Joyce, P. I., Fisher, E. M. C. & Greensmith, L. Biochimica et Biophysica Acta. *BBA - Molecular Basis of Disease* **1832,** 1421–1436 (2013).
2. Vucic, S. *et al.* Riluzole exerts central and peripheral modulating effects in amyotrophic lateral sclerosis. *Brain* **136,** 1361–1370 (2013).
3. Lattante, S., Ciura, S., Rouleau, G. A. & Kabashi, E. Defining the genetic connection linking amyotrophic lateral sclerosis (ALS) with frontotemporal dementia (FTD). *Trends Genet.* **31,** 263–273 (2015).
4. Renton, A. E., Chiò, A. & Traynor, B. J. State of play in amyotrophic lateral sclerosis genetics. *Nature neuroscience* **17,** 17–23 (2013).
5. Hanson, K. A., Kim, S. H. & Tibbetts, R. S. RNA-binding proteins in neurodegenerative disease: TDP-43 and beyond. *WIREs RNA* n/a–n/a (2011). doi:10.1002/wrna.111
6. DeJesus-Hernandez, M. *et al.* Expanded GGGGCC Hexanucleotide Repeat in Noncoding Region of C9ORF72 Causes Chromosome 9p-Linked FTD and ALS. *Neuron* 1–12 (2011). doi:10.1016/j.neuron.2011.09.011
7. Renton, A. E. *et al.* A Hexanucleotide Repeat Expansion in C9ORF72 Is the Cause of Chromosome 9p21-Linked ALS-FTD. *Neuron* 1–12 (2011). doi:10.1016/j.neuron.2011.09.010
8. van Rheenen, W. *et al.* Hexanucleotide repeat expansions in C9ORF72 in the spectrum of motor neuron diseases. *Neurology* (2012). doi:10.1212/WNL.0b013e3182661d14
9. Gitler, A. D. & Tsuiji, H. Brain Research. *Brain Res* 1–11 (2016). doi:10.1016/j.brainres.2016.04.004
10. Andersen, P. M. & Al-Chalabi, A. Clinical genetics of amyotrophic lateral sclerosis: what do we really know? *Nat Rev Neurol* **7,** 603–615 (2011).
11. Neumann, M. *et al.* Ubiquitinated TDP-43 in frontotemporal lobar degeneration and amyotrophic lateral sclerosis. *Science* **314,** 130–133 (2006).
12. King, A., Maekawa, S., Bodi, I., Troakes, C. & Al-Sarraj, S. Ubiquitinated, p62 immunopositive cerebellar cortical neuronal inclusions are evident across the spectrum of TDP-43 proteinopathies but are only rarely additionally immunopositive for phosphorylation-dependent TDP-43. *Neuropathology* **31,** 239–249 (2011).
13. Brettschneider, J. *et al.* Pattern of ubiquilin pathology in ALS and FTLD indicates presence of C9ORF72 hexanucleotide expansion. *Acta Neuropathol* (2012). doi:10.1007/s00401-012-0970-z
14. Deng, H.-X. *et al.* Mutations in UBQLN2 cause dominant X-linked juvenile and adult-onset ALS and ALS/dementia. *Nature* 1–7 (2011). doi:10.1038/nature10353
15. Fecto, F. *et al.* SQSTM1 Mutations in Familial and Sporadic Amyotrophic Lateral Sclerosis. *Arch Neurol* **68,** 1440–1446 (2011).
16. Zu, T. *et al.* Non-ATG-initiated translation directed by microsatellite expansions.

Proceedings of the National Academy of Sciences **108,** 260–265 (2011).
17. Mizielinska, S. *et al.* C9orf72 repeat expansions cause neurodegeneration in Drosophila through arginine-rich proteins. *Science* **345,** 1192–1194 (2014).
18. Chew, J. *et al.* Neurodegeneration. C9ORF72 repeat expansions in mice cause TDP-43 pathology, neuronal loss, and behavioral deficits. *Science* **348,** 1151–1154 (2015).
19. Mackenzie, I. R. A. *et al.* Pathological TDP-43 distinguishes sporadic amyotrophic lateral sclerosis from amyotrophic lateral sclerosis with SOD1 mutations. *Ann Neurol* **61,** 427–434 (2007).
20. Pickart, C. M ECHANISMS U NDERLYING U BIQUITINATION. *Annu Rev Biochem* (2001).
21. Ozkaynak, E., Finley, D., Solomon, M. J. & Varshavsky, A. The yeast ubiquitin genes: a family of natural gene fusions. *EMBO J* **6,** 1429–1439 (1987).
22. Redman, K. L. & Rechsteiner, M. Identification of the long ubiquitin extension as ribosomal protein S27a. *Nature* **338,** 438–440 (1989).
23. Finley, D., Ozkaynak, E. & Varshavsky, A. The yeast polyubiquitin gene is essential for resistance to high temperatures, starvation, and other stresses. *Cell* **48,** 1035–1046 (1987).
24. Pickart, C. & Cohen, R. Proteasomes and their kin: proteases in the machine age. *Nat Rev Mol Cell Biol* **5,** 177–187 (2004).
25. Thrower, J. S., Hoffman, L., Rechsteiner, M. & Pickart, C. M. Recognition of the polyubiquitin proteolytic signal. *EMBO J* **19,** 94–102 (2000).
26. Hochstrasser, M. Lingering Mysteries of Ubiquitin-Chain Assembly. *Cell* **124,** 27–34 (2006).
27. Kim, H. T. *et al.* Certain pairs of ubiquitin-conjugating enzymes (E2s) and ubiquitin-protein ligases (E3s) synthesize nondegradable forked ubiquitin chains containing all possible isopeptide linkages. *J Biol Chem* **282,** 17375–17386 (2007).
28. Wauer, T. *et al.* Ubiquitin Ser65 phosphorylation affects ubiquitin structure, chain assembly and hydrolysis. *EMBO J* **34,** 307–325 (2015).
29. Ohtake, F. *et al.* Ubiquitin acetylation inhibits polyubiquitin chain elongation. *EMBO Rep* **16,** 192–201 (2015).
30. Komander, D. & Rape, M. The Ubiquitin Code. *Annu Rev Biochem* (2012). doi:10.1146/annurev-biochem-060310-170328
31. Deshaies, R. J. & Joazeiro, C. A. P. RING domain E3 ubiquitin ligases. *Annu Rev Biochem* **78,** 399–434 (2009).
32. Pickart, C. M. & Fushman, D. Polyubiquitin chains: polymeric protein signals. *Curr Opin Chem Biol* **8,** 610–616 (2004).
33. Mevissen, T. E. T. *et al.* OTU deubiquitinases reveal mechanisms of linkage specificity and enable ubiquitin chain restriction analysis. *Cell* **154,** 169–184 (2013).
34. Strieter, E. & Korasick, D. Unraveling the Complexity of Ubiquitin Signaling. *ACS Chem Biol* (2011). doi:10.1021/cb2004059
35. Kristariyanto, Y. A. *et al.* K29-Selective Ubiquitin Binding Domain Reveals Structural Basis of Specificity and Heterotypic Nature of K29 Polyubiquitin. *Molecular cell* **58,** 83–94 (2015).
36. Walters, K. J. & Chen, X. Measuring ubiquitin chain linkage: Rap80 uses a

molecular ruler mechanism for ubiquitin linkage specificity. *EMBO J* **28,** 2307–2308 (2009).

37. Raasi, S., Ranjani Varadan, Fushman, D. & Pickart, C. M. Diverse polyubiquitin interaction properties of ubiquitin-associated domains. *Nat Struct Mol Biol* **12,** 708–714 (2005).
38. Zhang, D., Raasi, S. & Fushman, D. Affinity makes the difference: nonselective interaction of the UBA domain of Ubiquilin-1 with monomeric ubiquitin and polyubiquitin chains. *J Mol Biol* **377,** 162–180 (2008).
39. Hjerpe, R. *et al.* scientific report. *EMBO Rep* **10,** 1250–1258 (2009).
40. Kaye, F. J. *et al.* A family of ubiquitin-like proteins binds the ATPase domain of Hsp70-like Stch. *FEBS Lett* **467,** 348–355 (2000).
41. Ford, D. L. & Monteiro, M. J. Dimerization of ubiquilin is dependent upon the central region of the protein: evidence that the monomer, but not the dimer, is involved in binding presenilins. *Biochem J* **399,** 397–404 (2006).
42. Itakura, E. *et al.* Ubiquilins Chaperone and Triage Mitochondrial Membrane Proteins for Degradation. *Molecular cell* **63,** 21–33 (2016).
43. Williams, K. L. *et al.* UBQLN2/ubiquilin 2 mutation and pathology in familial amyotrophic lateral sclerosis. *Neurobiol Aging* (2012). doi:10.1016/j.neurobiolaging.2012.05.008
44. Mah, A. L., Perry, G., Smith, M. A. & Monteiro, M. J. Identification of ubiquilin, a novel presenilin interactor that increases presenilin protein accumulation. *J Cell Biol* **151,** 847–862 (2000).
45. Rutherford, N. J. *et al.* Unbiased screen reveals ubiquilin-1 and -2 highly associated with huntingtin inclusions. *Brain Res* 1–12 (2013). doi:10.1016/j.brainres.2013.06.006

Chapter 2) The UQ1^{8i} Story

Overview

This is a story that I worked on for my first ~ 2 years in the Tibbetts lab, here in its uncorrected form. I began this project under the guidance of a former graduate student, Dr. Keith Hanson. Keith was studying a splice variant of UQ1, termed UQ1^{8i} (also known as UQ1 isoform 2), which is purportedly associated with late-onset Alzheimer's disease[1], although there are reports in roughly equal number suggesting that this association is weak or non-existent[2-4].

It is important to say up front that I discovered a point mutation in UQ1^{8i} in the UBL domain (I65T) that is responsible for the majority of its interesting phenotype (unfortunately I figured this out after working through the revision process at JBC). This mutation results in a protein that binds to Ub with higher affinity, as assessed by co-IP and Ub-binding assays. The I65T mutation also disrupts the localization of UQ1^{8i}, preventing association with autophagosomes as assessed by localization with the autophagosome protein, LC3, as well as with the autophagosome / inclusion body protein, p62. In this chapter, I'll present the data and our interpretation of the data as it was collected. I'll follow this with a revised analysis of UQ1^{8i}, and finish with some suggestions for a follow-up project.

2.1 Abstract

Members of the ubiquilin (UBQLN) family of molecular chaperones play key roles in proteasome- and autophagosome-mediated protein degradation, and are increasingly implicated in neurodegenerative disease. A splicing mutation of *UBQLN1* that leads to skipping of exon 8 (UBQLN1^{8i}) is associated with late-onset Alzheimer's disease, whereas point mutations in the closely related *UBQLN2* gene cause X-linked

amyotrophic lateral sclerosis (ALS) and ALS/dementia. In this study, we sought to characterize the properties of disease-relevant ubiquilin mutants. We found that UBQLN1^{8i} displays intracellular targeting deficiencies and dominantly interferes with the targeting of wild-type UBQLN1 and UBQLN2 proteins to autophagosomes. UBQLN1^{8i} exhibited an intrinsic increase in its ubiquitin (Ub)-binding affinity, consistent with deregulation of its C-terminal Ub-associated (UBA) domain. ALS-associated mutations in UBQLN2, although impacting a domain that is not shared with UBQLN1, also increased Ub-binding affinity. We propose that altered intramolecular regulation is coupled to Ub-binding and constitutes a common biochemical theme linking distinct neurodegeneration-associated ubiquilin mutants.

2.2 Introduction

The presence of intracellular aggregates containing misfolded and Ub-modified proteins is a common hallmark of many neurodegenerative diseases, including Alzheimer's Disease (AD), Parkinson's Disease, Huntington's Disease, and amyotrophic lateral sclerosis (ALS) [5,6]. These heterogeneous conditions are collectively referred to as proteinopathies, in which pathology is characterized by toxic aggregates of disease-specific proteins in particular regions of the central nervous system[7]. To date, many proteins have been conclusively linked to proteinopathies—including several distinct genetic forms of ALS (for review, see[8])—in which mutations disrupt normal protein folding and promote the formation of intracellular aggregates. Dominant mutations in the 43 kDa TAR DNA-binding protein (TDP-43) were shown to cause dominantly inherited ALS[9-14]. Of note, even in cases of sporadic ALS that lack TDP-43 mutations, cytosolic accumulations of ubiquitylated TDP-43 are a near universal occurrence[15], implying that

aberrant protein aggregation might also reflect a decline in cellular proteostasis associated with aging. If so, one connection between protein aggregation and neurodegeneration could include dominant mutations in proteins that regulate cellular proteostasis[16,17].

In support of this idea, several proteins implicated in neurodegeneration are participants in the two major protein degradation pathways of eukaryotic cells: the Ub-proteasome pathway (UPP) and macroautophagy (hereafter referred to as autophagy). For instance, mutations in the multifaceted AAA^+ ATPase, valosin-containing protein (VCP), cause inclusion body myopathy with Paget's disease of bone and are responsible for 1-2% of inherited ALS cases[18,19]. Additionally, Sequestosome-1/p62 was also identified as a genetic component of ALS, and is prevalent in insoluble inclusions across a wide spectrum of disease[20-22]. Very recently, Siddique and colleagues demonstrated that dominant mutations in *UBQLN2* cause X-linked forms of ALS and ALS/dementia[23]. This was especially interesting to our lab in light of recent findings that UBQLN1 binds to TDP-43 [24], and ectopic expression of UBQLN1 exacerbates an ALS-phenotype in a *Drosophila* model of TDP-43-driven neurodegeneration[25].

UBQLN1 and UBQLN2 belong to a broader family of evolutionarily conserved ubiquilins; there are four distinct ubiquilin proteins, and each contains a modular architecture in which N-terminal Ub-like domains (UBL) and C-terminal Ub-associated domains (UBA) are separated by a structurally divergent central region bearing two to four stress-inducible protein (STI1) repeats (Fig. 2.1). Ubiquilins are believed to function as UPP shuttling factors by delivering Ub-modified proteins for degradation—the UBA domain binds ubiquitylated target proteins and the UBL domain engages components of

the proteasome[26,27]. The STI1 motifs found in the central region of ubiquilins are important for regulation of dimerization and interaction with additional cellular chaperones, including protein-disulfide isomerase (PDI) and the HSP70-family member STCH, implicating ubiquilin proteins in diverse proteostatic networks[28-30]. Additionally, UBQLN1 localizes to autophagosomes and is reported to be required for proper maturation of vesicles destined for degradation, although its exact role in this process is unknown[31].

Bertram et al. reported that a genetic variant of *UBQLN1*, in which a mutation promotes the skipping of an alternative exon 8 (UBQLN1^{8i}), is associated with late-onset AD, although this linkage was not observed in all studies[1-3,32,33]. The UBQLN1^{8i} mutation disrupts the fourth STI1 repeat (Fig. 2.1) and in *Drosophila*, UBQLN1^{8i} expression enhances neurodegeneration as compared to expression of the wild-type protein[34]. Wild-type UBQLN1 expression has been reported to confer protective effects in cell culture and *C. elegans* models of HD[35,36], and in *Drosophila* models of AD[35].

Interestingly, although UBQLN1 and UBQLN2 are closely related proteins (74% amino acid identity), five ALS-associated mutations identified in UBQLN2 occur at proline residues within a proline-rich repeat (PRR) that is not conserved in UBQLN1 or any other non-mammalian ubiquilin ortholog[23]. Following this discovery, exome screening identified an additional missense mutation in *UBQLN2* implicated in familial ALS, immediately upstream of the PRR (Fig. 2.1)[37]. Deng et al. demonstrated that UBQLN2 ALS mutants exhibited reduced activity toward a proteasome-dependent test substrate as assessed by overexpression assays[23]; however, as is the case for the

UBQLN1^{8i} mutation, the biochemical impacts of ALS-associated PRR mutations in UBQLN2 are largely uncharacterized.

We sought to characterize the properties of disease-relevant UBQLN1 and UBQLN2 proteins in cells, with the hope of identifying distinctions among the different disease alleles. We found that the AD-associated UBQLN1^{8i} mutant is deficient in targeting to autophagosomes and *trans*-dominantly inhibits the localization of wild type UBQLN1 and UBQLN2. Moreover, we observed a dramatic increase in Ub-binding affinity of UBQLN1^{8i} relative to UBQLN1^{WT}, and observed a similar trend for ALS-associated mutants relative to UBQLN2^{WT}. Surprisingly, we also observed increased Ub-binding affinity of UBQLN2 relative to UBQLN1 in a PRR-dependent manner, suggesting that the presence of the PRR contributes to a unique aspect of UBQLN2 function and may underlie the differential disease relevance of agnate chaperones.

2.3 Results

2.3.1 UBQLN1^{8i} binds to but does not colocalize with TDP-43

We set out to characterize the intracellular targeting and biochemical properties of the UBQLN1^{8i} variant, which lacks 28 amino acids encoded by exon 8, encompassing the fourth STI1 repeat (Fig. 2.1). In earlier studies, we found that UBQLN1^{WT} binds to TDP-43 *in vitro* and promotes the localization of both overexpressed and endogenous TDP-43 to cytoplasmic structures that stain positive for autophagosome markers[24]. These data suggested that UBQLN1^{WT} might be involved in targeting TDP-43 to the autophagosome for degradation. We therefore tested whether UBQLN1^{8i} could also recruit TDP-43 to similar cytoplasmic structures. When expressed in HeLa cells, TDP-43 localizes to the nucleus (Fig. 2.2A, top); when coexpressed with UBQLN1^{WT}, both proteins colocalize in

cytoplasmic punctate structures (Fig. 2.2A, middle). However, when coexpressed with UBQLN1^{8i}, TDP-43 remains confined to the nucleus (Fig. 2.2A, bottom). Despite a lack of colocalization with TDP-43, UBQLN1^{8i} nevertheless forms cytoplasmic structures that appear similar to those observed with UBQLN1^{WT}. These data suggest that UBQLN1^{8i} does not recruit TDP-43 to the autophagosome and provided the first clue that UBQLN1^{8i} may harbor an intrinsic cellular targeting defect.

One explanation for the lack of colocalization between UBQLN1^{8i} and TDP-43 is that, unlike the wild-type protein, UBQLN1^{8i} does not bind to TDP-43. Detection of UBQLN1^{WT} and TDP-43 binding is complicated by the observation that co-expression of both UBQLN1^{WT} and TDP-43 in cells promotes dramatic insolubility of both proteins. In fact, when expressed at similar levels in cells, UBQLN1^{8i} was consistently more insoluble than UBQLN1^{WT}, and exhibited higher molecular weight species consistent with Ub modifications (Fig. 2.2B). In order to avoid this solubility problem, we immunoprecipitated either UBQLN1^{WT} or UBQLN1^{8i} from cells and then applied lysate containing HA-tagged TDP-43 to the immunoprecipitate. Surprisingly, we found that TDP-43 bound equally well to both UBQLN1^{WT} and UBQLN1^{8i} (Fig. 2.2C). Therefore, it seemed unlikely that decreased binding affinity contributes to lack of colocalization between UBQLN1^{8i} and TDP-43.

2.3.2 UBQLN1^{8i} does not target to autophagosomes

Previously, we found that UBQLN1^{WT} and TDP-43 colocalizes with the autophagosome marker, microtubule-associated protein light chain 3 (LC3)[24]. We sought to extend this observation and determine if UBQLN1^{8i} puncta also stain positive for LC3. Unlike wild-type protein, UBQLN1^{8i} did not colocalize with GFP-LC3 when coexpressed

in HeLa cells (Fig. 2.2D), suggesting that the mutant protein is not a component of the autophagosome. To account for GFP-LC3 overexpression artifacts and to further confirm that UBQLN1^{8i} puncta are not autophagosomes, we stained HeLa cells expressing either UBQLN1^{WT} or UBQLN1^{8i} for endogenous LC3 (Fig. 2.2E). UBQLN1^{WT}, but not UBQLN1^{8i} colocalized with endogenous LC3, confirming that the mutant protein is defective in autophagosome targeting.

We further profiled autophagosome targeting with the endogenous autophagy adaptor, p62, an Ub-binding protein critical to the regulated formation of cellular inclusions and also implicated in familial ALS[20,38,39]. We found that overexpressed UBQLN1^{WT} targeted to p62-containing foci in HeLa cells under basal conditions (Fig. 2.3A, top), following brief amino acid starvation (Fig. 2.3A, second row), following proteasome inhibition by treatment with MG132 (Fig. 2.3A, third row), or following autophagy inhibition with bafilomycin A1 (Fig. 2.3A, bottom). However, the vast majority of UBQLN1^{8i} structures did not colocalize with p62 under any of the conditions tested (Fig. 2.3A, right panel). Interestingly, in cells with lower UBQLN1^{8i} expression, we observed colocalization with p62 after proteasome inhibition; however, these structures appeared abnormal with respect to structures formed by wild-type UBQLN1 (Fig. 2.3B). These findings suggest that UBQLN1^{8i} structures are not degradation-competent or perhaps detrimental to cellular degradation, as p62 contributes to both proteasome- and autophagy-mediated protein degradation[40,41].

The observation that UBQLN1^{8i} often formed elongated perinuclear inclusions suggested that it targeted to different subcellular compartments than its wild-type counterpart (Fig. 2.3B, arrows). In order to determine the identity of puncta formed by

UBQLN1^{WT} and UBQLN1^{8i}, we used a panel of antibodies for markers of different subcellular compartments and vesicles. UBQLN1^{WT} and UBQLN1^{8i} both colocalized with EEA1, a marker of the early endosome, and with Hrs, a component of the ESCRT-0 complex found in both early and intermediate endosomes that is involved in recognition and internalization of ubiquitylated substrates (Fig. 2.4A) [42,43]. Both proteins also colocalized with EPS15, a protein involved in recognition and sorting of ubiquitylated membrane receptors (Fig. 2.4A) [43,44]. Neither UBQLN1^{WT} nor UBQLN1^{8i} consistently localized with the lysosomal marker LAMP1 (Fig. 2.4A) and neither protein exhibited complete colocalization with any of the above markers, suggesting that these compartments are dynamic and non-overlapping. We also employed the markers p58 and golgin, and found that neither UBQLN1^{WT} nor UBQLN1^{8i} were trafficked through the Golgi apparatus (Fig. 2.4B). Thus, the only striking difference between wild-type and mutant protein localization is the lack of targeting of UBQLN1^{8i} to the autophagosome.

2.3.3 UBQLN1^{8i} inhibits autophagosome targeting of wild-type UBQLN1 and UBQLN2

Because of this difference in cellular compartment occupancy, we next asked whether UBQLN1^{WT} and UBQLN1^{8i} would localize to the same or to distinct compartments when coexpressed in cells. In order to address this question, we cotransfected DsRed-tagged UBQLN1^{WT} with either myc-UBQLN1^{WT} or myc-UBQLN1^{8i} and examined the cells by immunofluorescence (IF) microscopy. As expected, DsRed-UBQLN1^{WT} and myc-UBQLN1^{WT} colocalized in cytoplasmic puncta (Fig. 2.5A, top). Interestingly, in every cell examined, DsRed-UBQLN1^{WT} colocalized with myc-UBQLN1^{8i} (Fig. 2.5A, bottom). Furthermore, the structures containing both DsRed-UBQLN1^{WT} and UBQLN1^{8i} appeared similar to the tubular, perinuclear

UBQLN1^{8i} puncta previously observed (Fig. 2.5A, arrow), suggesting that UBQLN1^{8i} recruited UBQLN1^{WT} to these aberrant compartments.

We hypothesized that UBQLN1^{8i} may sequester UBQLN1^{WT} and prevent its localization to the autophagosome. To test this hypothesis, we co-transfected DsRed-UBQLN1^{WT} and GFP-LC3, along with either myc-UBQLN1^{WT} or myc-UBQLN1^{8i}, and then assayed for colocalization of the DsRed and GFP signals. As expected, DsRed-UBQLN1^{WT} colocalized with GFP-LC3 in the presence of myc-UBQLN1^{WT}. However, when myc-UBQLN1^{8i} was expressed, DsRed-UBQLN1^{WT} failed to localize with GFP-LC3 (Fig. 2.5B). This experiment was also performed with endogenous LC3 and produced the same results (Fig. 2.5C). As a further control, expression of myc-UBQLN1^{8i} did not affect the localization of DsRed-UBQLN1^{WT} with Hrs in early endosomes (Fig. 2.5D), confirming that this disrupted localization is specific to autophagosomes. Similarly, we found that expression of myc-UBQLN1^{WT} did not alter localization of DsRed-UBQLN1^{WT} with p62 (Fig. 2.5E), whereas expression of myc-UBQLN1^{8i} sequestered DsRed-UBQLN1^{WT} into tubular, p62-negative structures (Fig. 2.5E, arrows). We conclude that UBQLN1^{8i} has the capacity to titrate UBQLN1^{WT} protein away from LC3- and p62-positive structures.

We also tested if UBQLN1^{8i} could disrupt targeting of UBQLN2^{WT}. We coexpressed HA-UBQLN2^{WT} with either myc-UBQLN1^{WT} or myc-UBQLN1^{8i} in HeLa cells and observed strong colocalization between myc-UBQLN1^{WT} and HA-UBQLN2^{WT}, as well as between myc-UBQLN1^{8i} and HA-UBQLN2^{WT}, as analyzed by IF microscopy (Fig. 2.5F). UBQLN2^{WT} puncta assumed the characteristic fused appearance of UBQLN1^{8i} puncta, suggesting that UBQLN^{8i} also dominantly inhibits UBQLN2^{WT} (Fig.

2.5F, arrows). Consistent with this, UBQLN1^{8i} disrupted the colocalization of UBQLN2^{WT} with p62 (Fig. 2.5G), in some cases promoting colocalization of HA-UBQLN2^{WT} and endogenous p62 in tubular structures and in other cells preventing it altogether (Fig. 2.6A). As expected, UBQLN1^{WT} did not disrupt localization of UBQLN2^{WT} (Fig. 2.6B). In sum, these data suggest that expression of UBQLN1^{8i} disrupts recruitment of both UBQLN1 and UBQLN2 to degradation-competent vesicles.

2.3.4 UBQLN1^{8i} exhibits enhanced dimerization and Ub-binding

Ubiquilins are known to dimerize in a manner dependent on the central region of the protein, independent of the UBL and UBA domains, suggesting a function of the STI1 motifs with respect to self-recognition[28]. Thus, the sequestration of UBQLN1^{WT} by UBQLN1^{8i} into perinuclear puncta could reflect an intrinsic increase in UBQLN1^{8i} dimerization potential. To test this hypothesis, we conducted co-IP experiments using DsRed-UBQLN1^{WT} and either myc-UBQLN1^{WT} or myc-UBQLN1^{8i}. Interestingly, myc-UBQLN1^{8i} consistently bound more DsRed-UBQLN1^{WT} as compared to myc-UBQLN1^{WT} (Fig. 2.5H), and this interaction was independent of a functional UBA domain (Fig. 2.7), suggesting that the interaction between UBQLN1^{WT} and UBQLN1^{8i} may be more stable relative to wild-type homodimers. The increased dimerization affinity of UBQLN1^{8i} is plausibly linked to the *trans*-dominant sequestration of wild-type UBQLN in intact cells.

We further hypothesized that enhanced dimerization of ubiquilins could lead to local enrichment of UBA domains, thereby altering Ub-binding properties of the mutant protein. Consistent with this possibility, UBQLN1^{8i} bound more strongly to monoUb-conjugated agarose beads *in vitro* as compared to UBQLN1^{WT} (Fig. 2.8A). To further

compare the Ub-binding properties of UBQLN1^{WT} and UBQLN1^{8i}, we treated cells with the proteasome inhibitor, MG132, to induce accumulation of endogenous polyUb chains tethered to substrates. We subsequently performed IP of the myc-tagged ubiquilins and measured the amount of ubiquitylated substrate that retained association with either the wild-type or mutant proteins. The intensity of the Ub laddering was clearly stronger in the UBQLN1^{8i} samples versus UBQLN1^{WT} samples, supporting the conclusion that UBQLN1^{8i} binds more avidly to Ub-substrates than UBQLN1^{WT} (Fig. 2.8B). We also performed these experiments with ubiquilin proteins bearing point mutations in the UBA domains. Previous studies of the *S. cerevisiae* UBQLN1 ortholog, Dsk2, revealed that mutation of a Phe residue in the highly conserved Met-Gly-Phe motif of the UBA domain greatly diminished the interaction with mono- and polyUb[45,46]. As expected, the analogous mutation (F559A) abolished binding of UBQLN1^{WT} to monoUb and polyUb (Fig. 2.8A, 2.8B). The equivalent F531A mutation in UBQLN1^{8i} (UBQLN1^{8i} is 28 amino acids shorter due to deletion of exon 8) dramatically attenuated mono- and polyUb-binding, but did not abolish it altogether (Fig. 2.8A, 2.8B). Residual Ub-binding activity of UBQLN1$^{8i/F531A}$ is likely mediated through dimerization with wild-type endogenous UBQLN1. Finally, the UBA domain point mutations abolished colocalization of both myc-UBQLN1^{WT} and myc-UBQLN1^{8i} with HA-Ub in intact cells (Fig. 2.8C), which is similar to results obtained upon truncation of the UBA domain[24]. These findings indicate that the 8i mutation increased the UBA domain-dependent binding of UBQLN1 to both monoUb and polyUb substrates.

Given the dramatic difference in Ub-binding between UBQLN1^{WT} and UBQLN1^{8i}, we hypothesized that loss of the fourth STI1 repeat might alter

intramolecular folding of UBQLN1^{8i}, such that its UBA domain is more accessible for binding Ub-substrates. Structurally similar chaperones bearing modular UBL-UBA and UBL-UIM domains have been shown to undergo intramolecular interactions between the complementary Ub-like and Ub-binding domains[47,48]. It has been previously demonstrated that a construct of UBQLN1 in which the UBL domain is truncated (UBQLN1Δ^{UBL}) serves as a dominant-negative inhibitor of cellular transport[49]. Heir et al. concluded that defective targeting of UBQLN1Δ^{UBL} was due to lack of UBL interactions with other proteins bearing Ub-binding modules. We reasoned that disruption of the UBL domain would also influence Ub binding by rendering the UBQLN1 UBA domain hyper-accessible for substrate binding. We therefore introduced two simultaneous point mutations in the UBL domain predicted to disrupt its interaction with Ub-binding domains: Thr-43→Ala and Ile-79→Thr (herein referred to as UBQLN1^{UBLpm}), and measured the impact on Ub binding[47].

UBQLN1^{UBLpm} exhibited disrupted intracellular targeting (Fig. 2.8D), consistent with published findings regarding UBQLN1Δ^{UBL}, and confirming that these point mutations functioned as expected. Co-IP studies revealed that the UBQLN1^{UBLpm} displayed a level of polyUb binding that exceeded that observed for UBQLN1^{8i} (Fig. 2.8E). Interestingly, UBQLN1^{UBLpm} did not possess enhanced dimerization potential, as assessed by co-IP of co-expressed DsRed-UBQLN1^{WT} (Fig. 2.8F), demonstrating that dimerization and Ub-binding activities of UBQLN1^{8i} are biochemically separable.

2.3.5 The PRR regulates UBQLN2 Ub-binding affinity

Mutations in the unique PRR domain of UBQLN2 cause ALS and ALS/dementia, but the biochemical impacts of these mutations are unknown. IF studies revealed that

UBQLN2^{WT}, ALS-associated mutants of UBQLN2 (UBQLN2^{P497H}, UBQLN2^{P525S}), and a construct of UBQLN2 lacking the PRR (UBQLN2Δ^{PRR}) targeted equivalently to p62-positive structures, suggesting that mutations in the PRR domain do not grossly disrupt cellular targeting, and that the PRR is dispensable for localization (Fig. 2.9). We explored the binding affinities of UBQLN2^{WT}, UBQLN2Δ^{PRR}, and all five UBQLN2^{ALS} Pro mutants for polyUb in co-IP experiments. We found that polyUb ladders were clearly increased for the UBQLN2^{ALS} mutants relative to UBQLN2^{WT} in cells treated with MG132 (Fig. 2.10A). UBQLN2^{ALS} mutants also bound more strongly to polyUb chains than UBQLN2^{WT} in the absence of MG132, indicating that the observed phenotype is not an artifact of proteasome inhibition (Fig. 2.10B). As expected, an inactivating point mutation in the UBA domain (UBQLN2^{F594A}) largely abolished polyUb binding of UBQLN2 (Fig. 2.12). Finally, we consistently observed a decrease in polyUb binding of UBQLN2Δ^{PRR} relative to UBQLN2^{WT}, which implies a role for the PRR domain in regulating UBQLN2-substrate interactions (Fig. 2.10C, Fig. 2.12).

The observation that UBQLN2^{WT} possesses intrinsically elevated Ub-binding activity relative to UBQLN2Δ^{PRR} suggested that there might be differences between the Ub-binding activities of UBQLN1^{WT} and UBQLN2^{WT}. This was experimentally observed in side-by-side co-IP experiments in the presence or absence of MG132 pretreatment (Fig. 2.12C). That the residual Ub-binding potential of UBQLN2Δ^{PRR} was still elevated relative to UBQLN1^{WT} suggests that minor differences outside the PRR might also contribute to differential Ub-binding (Fig. 2.12C). Although these results must be interpreted cautiously, they suggest that UBQLN2^{WT} has a higher affinity for

endogenous polyUb than UBQLN1^{WT}, and this intrinsic difference is augmented by ALS-associated mutations in the UBQLN2 PRR.

2.4 Discussion

In this study, we investigated the intracellular targeting and biochemical properties of disease-relevant mutations in UBQLN1 and UBQLN2. We found that the AD-associated variant of UBQLN1, UBQLN1^{8i}, exhibits intracellular targeting defects that are coupled to increased dimerization capacity and dramatically elevated Ub-binding potential. These findings, combined with the observation that UBQLN1^{8i} *trans*-dominantly disrupted autophagosome targeting of UBQLN1 and UBQLN2, provide a possible explanation for the proposed contribution of UBQLN1^{8i} to late-onset AD[1]. Although the targeting of UBQLN2 was largely unaffected by ALS-associated mutations, these mutations also caused a strong increase in Ub-binding activity. These changes in Ub-binding appear to occur independently of obvious changes in localization or dimerization, which provides functional distinction of UBQLN2^{ALS} mutants from the UBQLN1^{8i} mutation.

It is important to note that our lab and others have observed endogenous ubiquilin proteins by IF and found they are typically cytoplasmic and occasionally appear as speckles, but do not tend to form large puncta under basal conditions. Under conditions of stress, such as treatment with proteasome inhibitor or oxidative insult, ubiquilins do form punctate structures that colocalize with autophagosome markers and ubiquitin[24,29,50,51]. It is plausible that the level of expression in our studies leads to the formation of inclusion bodies in response to stress induced by ectopic expression of ubiquilin. It seems reasonable that expression of these proteins would cause a stress

response, as overexpression of the *S. cerevesiae* ortholog of UBQLN1, Dsk2, is toxic to yeast[52]. With this in mind, we find noteworthy the clear differences between UBQLN1^{WT} and UBQLN1^{8i} targeting to the autophagosome.

The mechanisms by which ubiquilins target to the autophagosome are not known; both early endosomes and multivesicular bodies can fuse with autophagosomes, and the finding that UBQLN1^{WT} colocalizes with EEA1 and Hrs suggests that one possible route for UBQLN1^{WT} delivery to autophagosomes is through the endosomal pathway. That UBQLN1^{8i} colocalizes with the same endosomal markers as UBQLN1^{WT} could mean that this mutant does not successfully enter the autophagosome pathway and is instead retained in endosomal compartments. One intriguing possibility is that the enhanced Ub-binding of UBQLN1^{8i} is responsible for its retention in the endosome, suggested by the fact that UBQLN1 interacts with Hrs and EPS15[43], which are known to be mono-ubiquitylated[44,53]. However, we would expect that UBQLN2 ALS mutants should exhibit a similar defect if enhanced Ub-binding were responsible for disrupted autophagosome targeting. Because we observed no such defect with the ALS mutants, it is possible that the STI1 motif is in some way required for proper cellular localization, or that UBQLN1 and UBQLN2 utilize distinct pathways to target to the autophagosome.

A remarkable feature of UBQLN1^{8i} is its dramatically increased dimerization potential, which may be linked to both the increased Ub-binding capacity and altered targeting of the mutant protein. Ford and Monteiro demonstrated that monomeric ubiquilin proteins interacted with Ub-substrates, and proposed that dimerization toggled ubiquilins to an inactive state. They also found that the central region of UBQLN1, spanning the four STI1 repeats, mediates dimerization[28]. Our findings indicate that

deletion of the fourth STI1 motif leads to increased dimerization. Based on this idea, it is conceivable that enhanced dimerization of UBQLN1^{8i} contributes to enhanced Ub binding through local enrichment of UBA domains. However, it seems unlikely that altered dimerization can fully account for the massive increase in polyUb-binding of the UBQLN1^{8i} mutant that was observed in co-IP assays.

We propose that deletion of the STI1 motif disrupts intramolecular folding, such that the UBQLN1 UBA domain becomes hyper-accessible for substrate/Ub interactions (Fig. 2.13). In this simplified model, UBQLN1 is in a conformational equilibrium between closed and open states. In the closed state, the UBL and UBA domains interact, preventing association with Ub-modified substrates. Mutations that directly (UBL domain mutations) or indirectly (the 8i mutation) diminish the UBL-UBA interaction extend the half-life of the open state, resulting in greater Ub-binding. This model can reconcile the seemingly contradictory role of ubiquilins in cellular protein degradation. Studies employing overexpression of wild-type ubiquilin proteins have found that they stabilize model substrates, whereas experiments exploring knockdown of ubiquilins produced similar results[54-56]. Overexpression is expected to increase both the open and closed states of ubiquilins. It is possible that a minor increase in the open form of ubiquilin leads to premature Ub-substrate interactions that disrupt rather than facilitate proteolysis. Structural studies will be required to define the impact of STI1 repeats and the 8i mutation on the accessibility and function of the UBQLN1 UBA domain.

UBQLN2 is virtually identical to UBQLN1 with the exception of its conspicuous PRR. Neither the function of this unusual domain nor the consequences of ALS-linked mutations within it are defined; however, our studies reveal that enhanced polyUb-

binding activity is one biochemical phenotype shared across all the mutants tested. Proline-rich motifs are enriched in proteins that localize to membranes or participate in vesicle trafficking, and often mediate protein-protein interactions[57,58]. Thus, the enhanced polyUb-binding of UBQLN2^{ALS} mutants could arise from altered protein interaction profiles.

Alternatively, the PRR may fulfill a unique structural function that enhances the availability of the UBA domain for substrate interactions. This hypothesis is consistent with the finding that UBQLN2 bound more polyUb than either UBQLN1 or UBQLN2Δ^{PRR}. Similar to the model described for UBQLN1^{8i}, we speculate that ALS-associated mutations in the PRR disrupt the structure of the motif, leading to aberrant Ub-binding by disrupting the equilibrium between closed and open states of UBQLN2. Over time, the altered Ub-binding profile of UBQLN2^{ALS} mutants may compromise proteostasis, leading to protein aggregation and cellular injury. Future studies addressing functional impacts of the PRR domain and ALS-associated mutations will undoubtedly illuminate such possibilities.

2.5 Materials and Methods

DNA Construction

The open reading frames of human UBQLN1 and TDP-43 were PCR amplified and subcloned into the pCMV-myc or pCMV-HA vectors for expression in mammalian cells, as described previously[24] (Clontech). UBQLN1^{8i} was generated by the splice overlap extension method, which introduced a BglII restriction site in place of exon 8. The open reading frame of human UBQLN2 was PCR amplified and subcloned into pCMV-myc and pCMV-HA vectors using restriction enzymes EcoRI and XhoI (New

England Biolabs). UBQLN2Δ^{PRR} was generated by splice overlap extension and the incorporation of a KpnI restriction site in place of the PRR. A 48 amino-acid stretch was excised: The core twelve P-X-X repeats and six amino acids on either side of the tripeptide repeat sequence, resulting in a final construct that is 578 amino acids. Point mutations were introduced by site-directed mutagenesis using *Pfu* Turbo DNA polymerase (Stratagene); primers and PCR conditions are available upon request. Sequencing was performed at the UW-Madison Biotechnology Center DNA sequence facility using ABI 3730xl DNA analyzers.

Cell Culture and Transfections

HeLa cells and HEK 293T cells were maintained in Dulbecco's modified Eagle's medium (DMEM) containing 10% fetal bovine serum and 100U/ml of penicillin and streptomycin in a 5% CO_2 atmosphere (Cellgro). HeLa cells were transfected with Lipofectamine 2000 (Invitrogen) according to the manufacturer's instructions. Prior to transfection, cells were washed and incubated in antibiotic-free DMEM containing 2% fetal bovine serum. HEK 293T cells were transfected with the calcium phosphate method with varying amounts of plasmid DNA depending on the experiment (between 2-6 μg), routinely in 60mm or 100mm plates at 40-60% confluency.

Antibodies

Antibody suppliers included: Santa Cruz Biotechnology Inc. (α-myc 9e10, α-myc A-14, α-HA F-7, α-HA Y-11, α-Ubiquitin P4D1, α-HDAC6 H-300, α-EPS15 C-20, α-VCP H-120), Abcam (α-p62 ab56416, α-S5a ab20239), and Invitrogen (α-UBQLN 37-7700). Antibodies against golgin, p58, CD63, EEA1, LAMP1, and Hrs were kind gifts from Professor Richard Anderson, University of Wisconsin-Madison. The secondary

antibody suppliers included: Jackson (horseradish peroxidase-conjugated goat α-rabbit IgG), GE Healthcare (horseradish peroxidase-conjugated sheep α-mouse IgG), and Invitrogen (Alexa Fluor 594 goat α-rabbit IgG, Alexa Fluor 488 goat α-rabbit IgG, Alexa Fluor 594 goat α-mouse IgG, Alexa Fluor 488 goat α-mouse IgG).

Immunoprecipitation

HEK 293T cells were transfected with varying amounts of plasmid DNA and incubated for 18-24 h. In certain experiments, four h prior to lysis, cells were treated with MG132 or DMSO to achieve a final concentration of 4μM (or the equivalent volume of DMSO vehicle). Cells were washed 2x in PBS, harvested by centrifugation, and resuspended in ice-cold buffer (20 mM HEPES pH 7.4, 150 mM NaCl, .2% NP-40, 1.5 mM $MgCl_2$, 1 mM EDTA) containing a protease/phosphatase inhibitor mixture (50 mM β-glycerophosphate, 10 mM sodium fluoride, 20 nM microcystin, 10 μg/ml leupeptin, 5 μg/ml aprotinin, 5 μg/ml pepstatin A, 0.2 mM PMSF, 1mM DTT). For experiments denoted as "high salt," cells were harvested in the same manner and resuspended in ice-cold buffer (20 mM HEPES pH 7.4, 300 mM NaCl, .5% Triton-X-100, 1.5 mM $MgCl_2$, 1 mM EDTA with identical protease/phosphatase inhibitor mixture) and treated identically to cells lysed in IP buffer, as follows: Cells were subjected to 10-second vortex pulses and incubated on ice for 10-15 min. Cell extracts were clarified by centrifugation at 20,000g for 10 min. The soluble fraction was transferred to a new tube and protein concentration was determined by Bradford assay. An insoluble fraction was prepared by washing the pellet twice in lysis buffer followed by boiling in 1x SDS-PAGE sample buffer. For IP, lysate was transferred to a new tube, and ice-cold lysis buffer was added proportionately to adjust the concentration of the lysate such that IP was typically

performed between 1-1.5 mg/ml total lysate. Lysate was incubated with 1 μg antibody/500 μg total lysate and mixed with gentle inversion at 4°C for four h, after which either Protein-A or Protein-G sepharose was added (roughly 15 μl slurry per IP). After incubation with gentle inversion mixing for sixteen h at 4°C, the beads were collected and washed four times with lysis buffer. Bound proteins were analyzed by SDS-PAGE and immunoblotting using the indicated antibodies.

Ub-agarose Binding

HEK 293T cells were transfected and lysed in the same manner as described for IP experiments. Following lysis, a soluble fraction was transferred to a new tube containing 25μl Ub-agarose slurry (Boston Biochem), equilibrated in lysis buffer. Beads were rotated with gentle inversion at 4°C for sixteen h, collected and washed four times with lysis buffer. Bound proteins were analyzed by SDS-PAGE and immunoblotting using the indicated antibodies.

Immunofluorescence

HeLa cells were grown on glass coverslips and a total of 0.8 μg of plasmid DNA was introduced into each well of a 12-well plate, or 2 μg of plasmid DNA was transfected in 60mm plates that had been fitted with six coverslips, using Lipofectamine 2000 (Invitrogen) according to manufacturer's instructions. Cells were washed with PBS and fixed with 4% paraformaldehyde in PBS either twenty or forty-eight h after transfection, as indicated in the experiment. Fixed cells were permeabilized with 0.2% Triton-X100 (in PBS) for 15 minutes at room temperature, followed by three washes with PBS. Cells were blocked in sterile-filtered 3% bovine serum albumin in PBS (w/v) for thirty minutes at room temperature, followed by a one-hour incubation at room temperature with

primary antibody at a final concentration of 0.1-0.5 μg/ml in 3% BSA, depending on the antibody. Cells were washed five times in ice-cold tris-buffered saline containing Tween-20 (TBST). Following wash, cells were incubated with appropriate Alexa-Fluor secondary antibody, varying between experimental conditions, at a final concentration of 1:1000. Cells were washed five times with TBST and then incubated for fifteen minutes at room temperature with DAPI diluted in PBS at a final concentration of 0.15μg/ml. Cells were washed again with TBST and then mounted on glass coverslips using Vectashield mounting medium (Vector Labs, Inc. H-1000). Once dried, coverslips were sealed using clear nail polish and stored at -20^{0}C. Photographs were taken on a Nikon Eclipse Ti-U Epifluorescence microscope with Plan Fluor objectives (20x/0.5, 40x/0.75, 60x/0.5-1.25 Oil Iris with Zeiss Immersol 518N). Images were acquired using NIS Elements D3.10 software and the microscope was outfitted with the following filter cubes: DAPI (Excitation 340-380nM, Dichromatic Mirror (DM) at 400nM with medium bandpass, Emission 435-485nM), FITC (Excitation 465-495nM, DM at 505nM with medium bandpass, Emission 515-555nM), TRITC (Excitation 528-553nM, DM at 565nM with narrow bandpass filter combination, Emission 590-650nM). Images were further imported into ImageJ 1.45q for processing and arrangement into figures.

2.6 Revised Analysis

As I indicated in the overview, there was a missense mutation in the UBL domain of UQ1^{8i}, resulting in the replacement of a highly conserved isoleucine with a smaller, polar threonine (I65T) (Fig. 2.14A). I discovered this mutation while cloning the ubiquilins into new vectors for the next phase of the project. Unfortunately, as I sequenced other UQ1^{8i} vectors, I discovered that the mutation was present in all of them,

and then learned that the plasmid had not been sequenced outside of the deletion region. $UQ1^{8i}$ was originally constructed by splice overlap extension with a low fidelity polymerase, and the mutation occurred completely by chance. I also discovered two additional point mutations present in both $UQ1^{WT}$ and $UQ1^{8i}$ that were in the original cDNA purchased by the lab. The two SNPs in UQ1 are A25T (predicted neutral) and P202H (predicted disruptive). The P202H mutation sits in an NPXΨ tetrapeptide that is highly conserved (Fig. 2.14B).

Reversion of the mutation in the UBL domain of $UQ1^{8i}$ reverts the localization phenotype and reduces the amount of precipitated Ub to levels similar to $UQ1^{WT}$ (Fig. 2.15). Unfortunately, I threw out the film for the IP – I think I was both disgusted and disappointed – but I don't have a record of this data. In some ways, this was a blessing and a curse because our original analysis was deeply flawed. The following paragraph was cut from the manuscript during the revision process: "Surprisingly, the enhanced affinity of $UBQLN2^{WT}$ for polyUb did not translate to an equivalent increase in monoUb-binding affinity relative to $UBQLN1^{WT}$. The reason for this discrepancy is presently unclear; it is possible that $UBQLN2^{WT}$ may bind polyUb-conjugated substrates through a bipartite mechanism in which it engages both the substrate and the polyUb chain. Alternatively, it is conceivable that $UBQLN2^{WT}$ is fully charged with endogenous polyUb-conjugated substrates from cell extracts, which competitively inhibits binding to monoUb-agarose beads *in vitro*."

As it turns out, UQ1 and UQ2 have similar affinity for Ub, as do the ALS mutants of $UQ2^{WT}$, despite our claim that the ALS mutations uniformly increased Ub-binding. We had assumed that the Ub being precipitated in IPs was non-covalently associated

through the UBA domain. This is not a very careful assumption, and Shigeki was a non-believer. I remember meeting with him and he said something along the lines of, "how can UQ1 bind monoUb equally well to UQ2, but not polyUb? They should have the same affinity if they bind the monomer the same." He was correct – the differential IP of polyUb by ubiquilins reflects a detergent-sensitive mixture of covalent Ub modification and non-covalent Ub bound via the UBA domain (spoiler alert, this is essentially the nutshell version of Chapter 4).

So what of the UQ2 ALS mutants binding more polyUb? It's a little embarrassing, but I chalk it up to wishful thinking, biased interpretation, and a strong sense of pressure to produce interesting data. This was my first project in the Tibbetts lab, I felt I had a lot to prove, and I had inexperienced hands and an incomplete understanding of the techniques – it was a good story, not broken, so I didn't fix it. I feel fortunate that we did not publish this story. Although it was harrowing at the time, looking back it was a great lesson in experimental design and analysis.

2.7 Future Directions (UQ1^{8i} Specific)

Not sure if there's a lot of interest in UQ1^{8i} in terms of its relationship with Alzheimer's Disease, but because it is a naturally occurring splice variant, I think it would be interesting to study UQ1 lacking its fourth STI1 motif, especially in light of a recent report that the more highly structured STI1 motif of UQ4 engenders a novel function in the capture of mislocalized proteins harboring a transmembrane domain[59].

A few ideas and observations to follow up: 1) The UQ1^{8i} mutant exhibits increased dimerization, which is not observed for UQ1^{UBL*}. I think this is interesting, as it could be one of the only meaningful biochemical findings of this work. The enhanced

dimerization is also observed for the $UQ1^{8i/UBA*}$ mutant, so it's not simply a manner of enriching Ub-binding proteins. The splicing of $UQ1^{WT}$ to form $UQ1^{8i}$ may result in enhanced dimerization or oligomerization of ubiquilin proteins, which is an interesting idea in light of a recent paper proposing that ubiquilins exist as inactive dimers that are released into the active, monomeric form during certain stressors[60]. It might be interesting to assess if $UQ1^{8i}$ expression is inducible, and if so, under what conditions. 2) Another clear conclusion is that the UBL domain of ubiquilins is required for their targeting to autophagosomes, but not for targeting to endosomes. Ubiquilin proteins therefore enter the endosome pathway independently of the UBL domain, but the UBL is required to exit this pathway. Ubiquilin constructs lacking the UBL are thought to dominantly disrupt vesicle trafficking, and this was perhaps reflected in the accumulation of strangely shaped $UQ1^{8i}$ structures[49]. 3) Finally, in recent work, I found that the SNPs present in UQ1 (A25T and P202H) result in reduced solubility of the protein as assessed by extraction in common detergents. I therefore corrected both the A25T and P202H mutations, and in subsequent work presented in this thesis, employed the NCBI reference form of the protein. It might be interesting to functionally characterize UQ1 SNPs and analyze the prevalence of these mutations in the general and disease populations through resources like the 1000 genomes project.

2.8 Figures

Figure 2.1

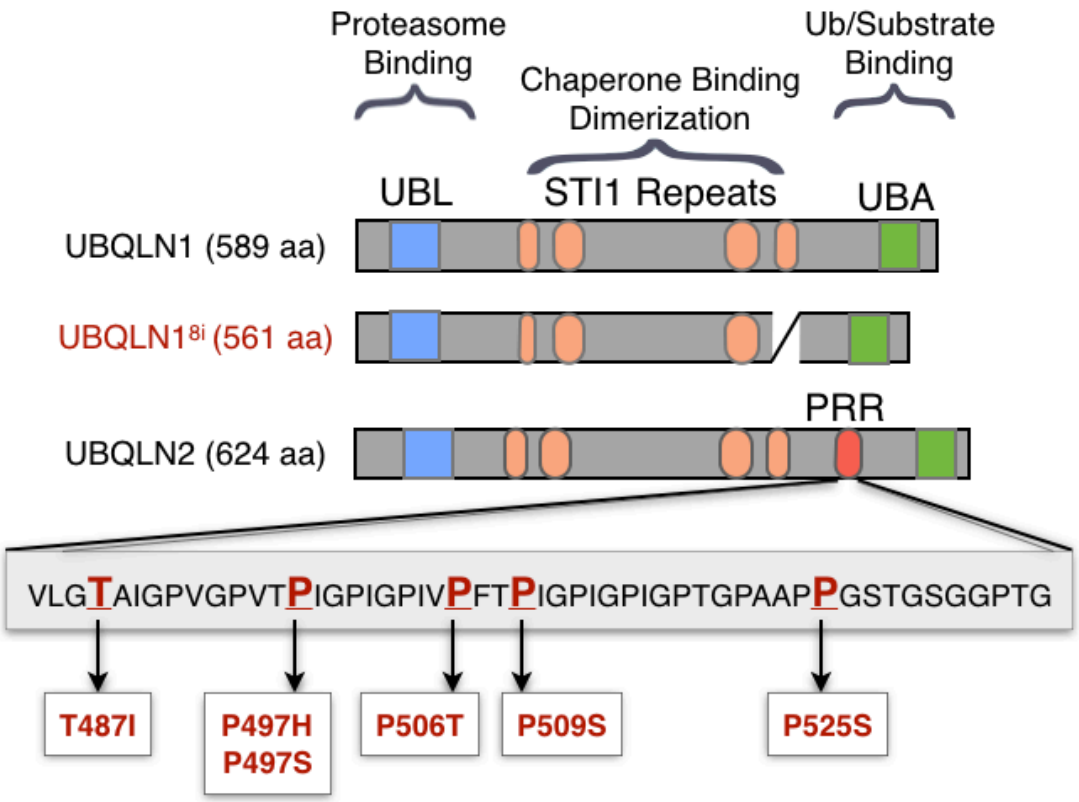

Schematic representations of UBQLN1^{WT}, UBQLN1^{8i}, and UBQLN2^{WT}. The UBQLN1^{8i} mutation promotes aberrant splicing of the *UBQLN1* transcript, resulting in the exclusion of exon 8. As a result, UBQLN1^{8i} is missing the fourth STI1 repeat in the central region, but is otherwise identical to UBQLN1^{WT}. UBQLN1^{WT} and UBQLN2^{WT} share 74% amino acid identity. The fundamental difference is a unique proline-rich-repeat located upstream of the UBA domain in UBQLN2^{WT}. Enlarged, red amino acids represent missense mutations in this domain, and arrows denote the resulting mutations.

Figure 2.2

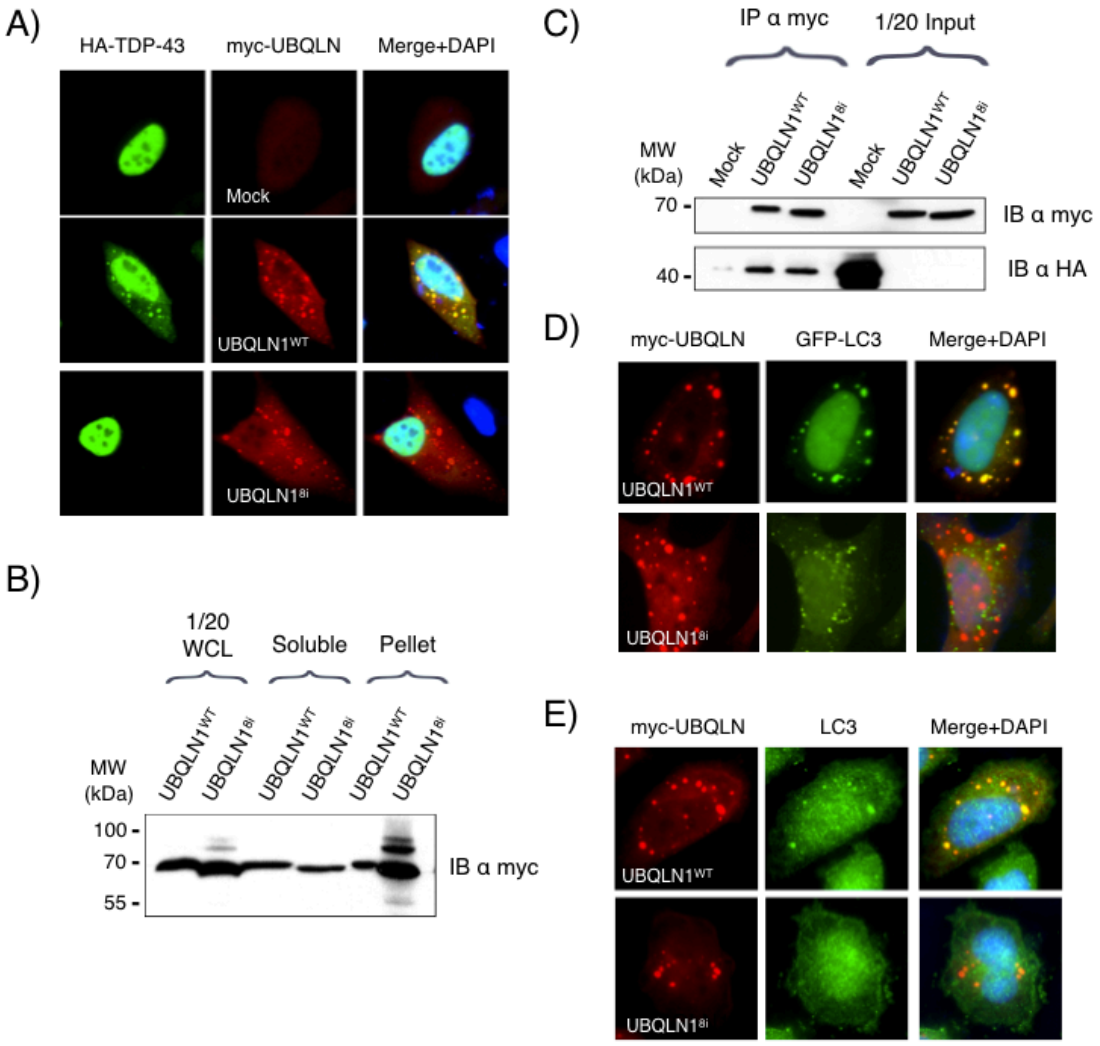

Different localization patterns of UBQLN1^{WT} and UBQLN1^{8i} with TDP-43 and LC3 **A)** TDP-43 colocalizes with UBQLN1^{WT} but not UBQLN1^{8i}. HeLa cells were transfected with HA-TDP-43, either alone or in combination with myc-UBQLN1^{WT} (middle) or myc-UBQLN1^{8i} (bottom). Cells were stained 48 h later using α-HA (green) and α-myc (red) antibodies. **B)** HEK 293T cells expressing either myc-UBQLN1^{WT} or myc-UBQLN1^{8i} were fractioned, followed by SDS-PAGE and blotting with α-myc antibody. **C)** HEK 293T cells were transfected separately with HA-TDP-43, myc-UBQLN1^{WT}, or myc-UBQLN1^{8i} plasmids. Ubiquilin proteins were IP with a-myc and incubated with cell extract containing HA-TDP-43. Bound proteins analyzed by blotting with α-HA and α-myc antibodies. **D)** HeLa cells were transfected with myc-UBQLN1^{WT} or myc-UBQLN1^{8i} and GFP-LC3 plasmids, and 48 h later stained with α-myc (red) antibody. **E)** HeLa cells were transfected with myc-UBQLN1^{WT} or myc-UBQLN1^{8i}, and 48 hrs later stained with α-myc (red) and α-LC3 (green) antibody.

Figure 2.3

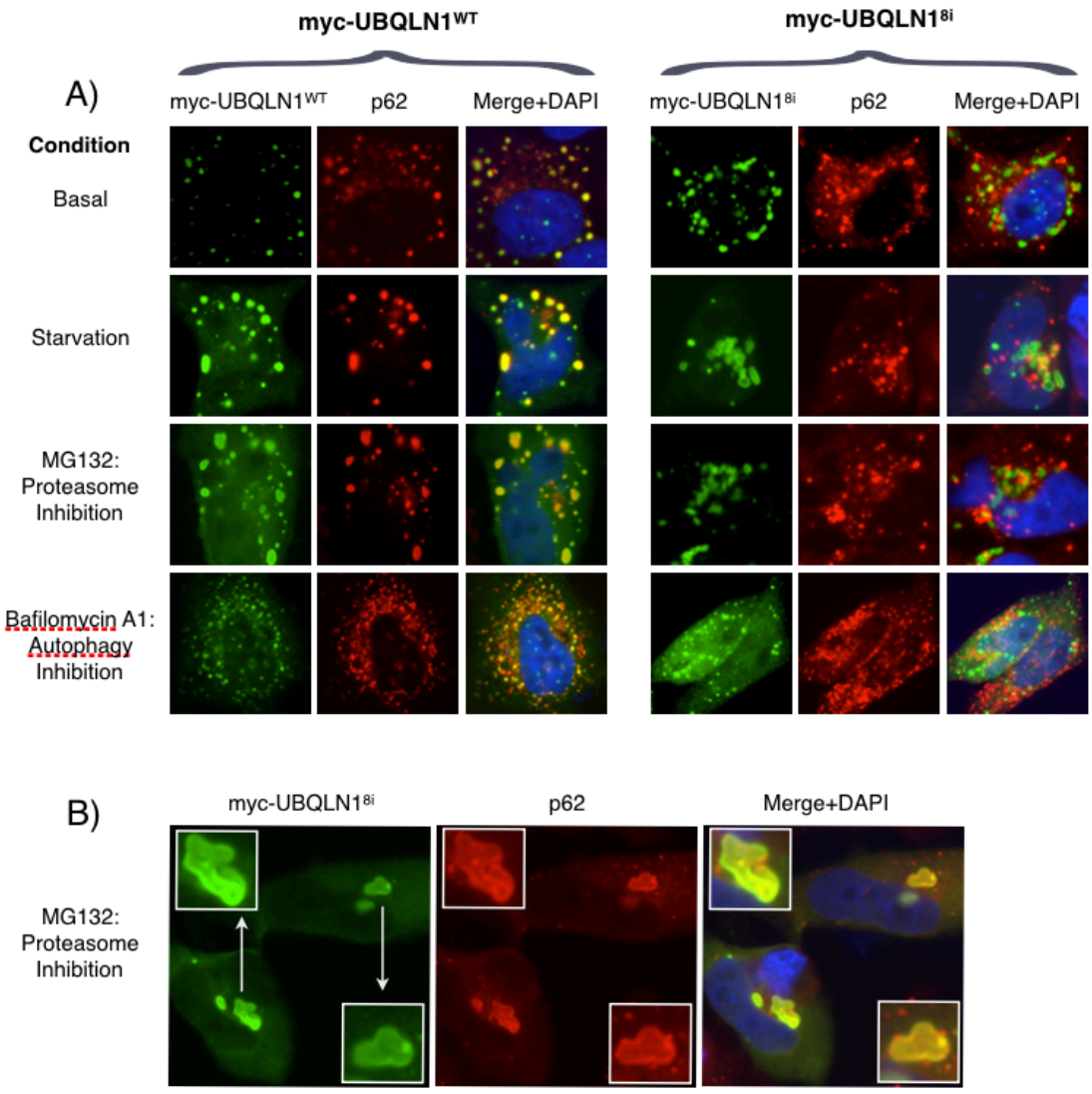

Differential localization of UBQLN1^{WT} and UBQLN^{8i} with p62. HeLa cells were transfected with either myc-UBQLN1^{WT} or myc-UBQLN1^{8i}, fixed, and stained 20 h later using α-myc (green) and α-p62 (red) antibodies. **A)** UBQLN1^{WT} localizes with endogenous p62 under basal conditions, following amino acid starvation (30m), following treatment with MG132 (4μM 2h), and following treatment with Baf A1 (100nM 4h). Right side: UBQLN1^{8i} does not localize with p62 under the conditions described **B)** Following MG132 treatment, UBQLN1^{8} displays two localization modes with endogenous p62: multiple p62-negative UBQLN1^{8i} structures as in (A), and tightly packed, perinuclear UBQLN1^{8i} punctate structures that stain positive for p62. Arrows denote unique vesicular structures formed by UBQLN1^{8i}, appearing as fused or elongated in many cells at varying expression levels.

Figure 2.4

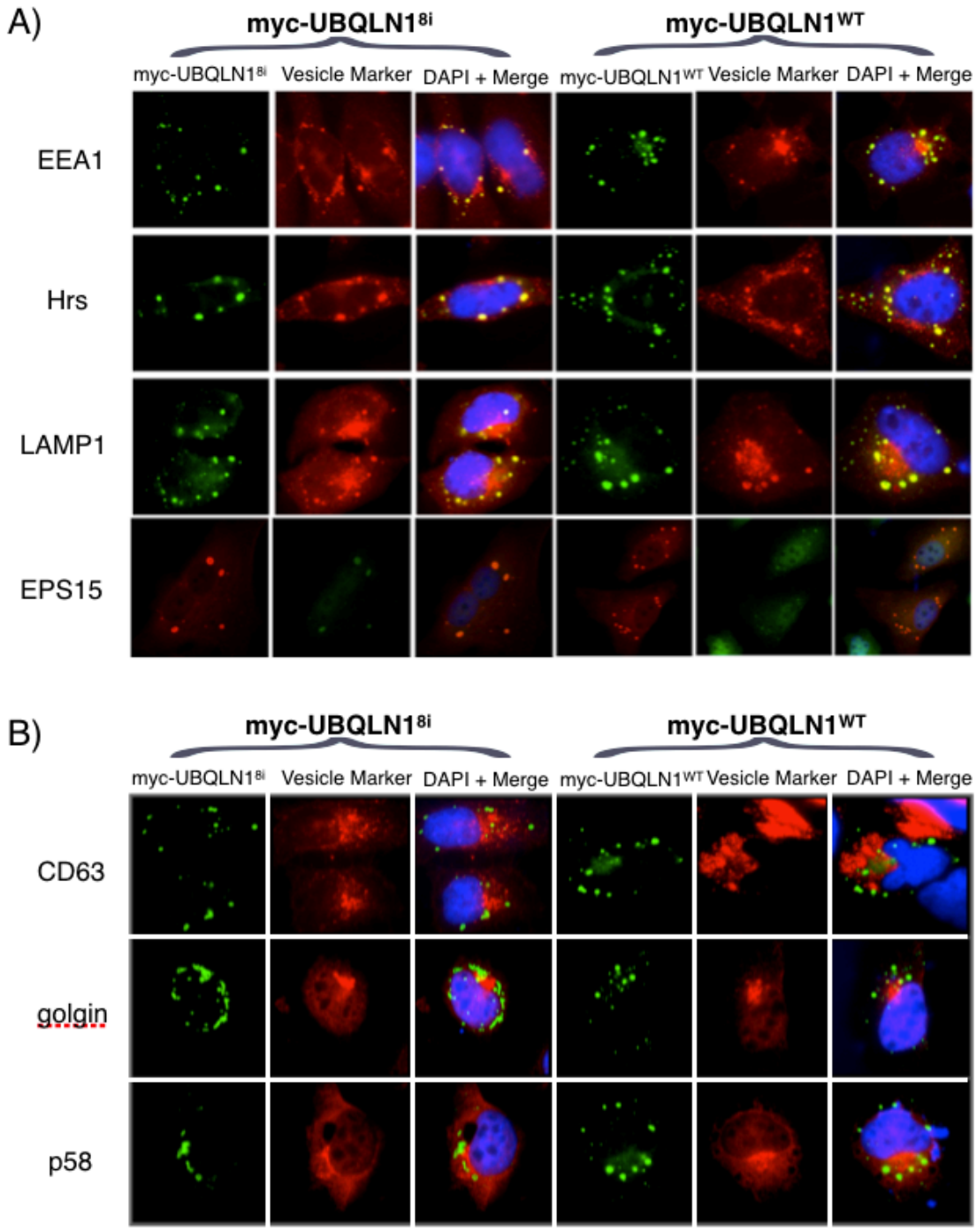

UQ1^{WT} and UQ1^{8i} localize with endocytic and lysosomal proteins. **A)** Localization of UQ1^{WT} and UQ1^{8i} is shared with endosomal proteins (EEA1, Hrs, and EPS15) and lysosomal proteins (LAMP1). **B)** UQ1^{WT} and UQ1^{8i} do not localize with markers of the multivesicular body (CD63) or the golgi apparatus (golgin, p58).

Figure 2.5

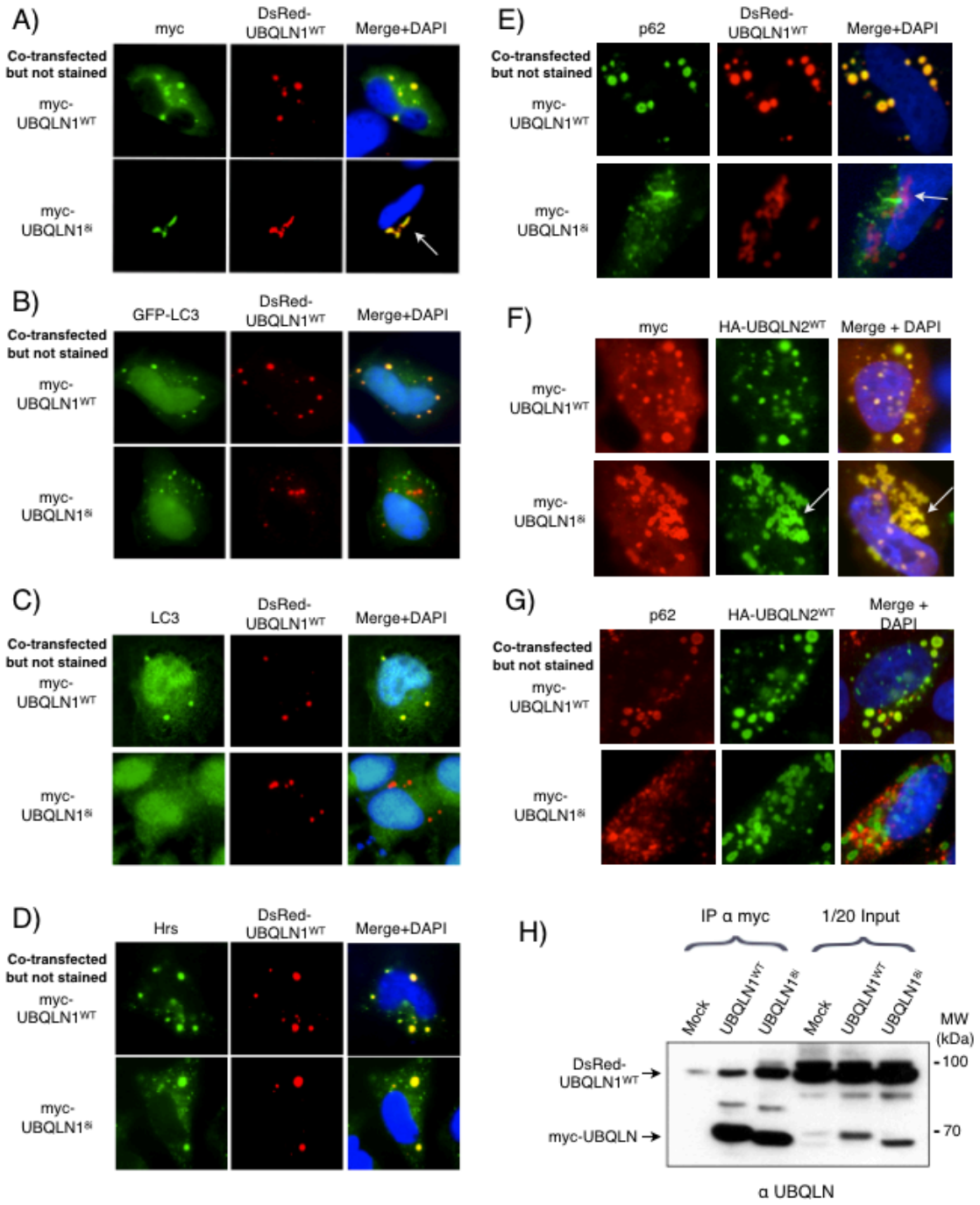

Disruptive interactions between UBQLN^{8i} and UQ1^{WT} and between UBQLN1^{8i} and UQ2^{WT}. **A)** HeLa cells were transfected with DsRed-UBQLN1^{WT} and either myc-UBQLN1^{WT} (top) or myc-UBQLN1^{8i} (bottom). Cells were stained 48 h later with α-myc antibody (green). Arrow highlights the incorporation of DsRed-UBQLN1^{WT} into an aberrant punctate structure by association with UBQLN1^{8i}. **B)** UQ1^{8i} disrupts the localization of DsRed-UBQLN1^{WT} with GFP-LC3. **C)** UQ1^{8i} disrupts the localization of DsRed-UBQLN1^{WT} with endogenous LC3. **D)** UQ1^{8i} does not disrupt localization with

endocytic protein, Hrs. **E)** $UQ1^{8i}$ disrupts the localization of DsRed-$UBQLN1^{WT}$ with p62. **F)** $UQ1^{8i}$ can sequester $UQ2^{WT}$ into aberrant structures, indicated by arrow. **G)** $UQ1^{8i}$ disrupts the localization of $UQ2^{WT}$ with p62. **H)** HEK 293T cells were transfected with DsRed-$UBQLN1^{WT}$ alone or in combination with myc-$UBQLN1^{WT}$ or myc-$UBQLN1^{8i}$ and 24 h later, cell extracts were IP with α-myc. Bound proteins were analyzed by SDS-PAGE and immunoblotting with α-UBQLN antibody, which reacts with both myc- and DsRed-tagged UBQLN proteins, as indicated by arrows.

Figure 2.6

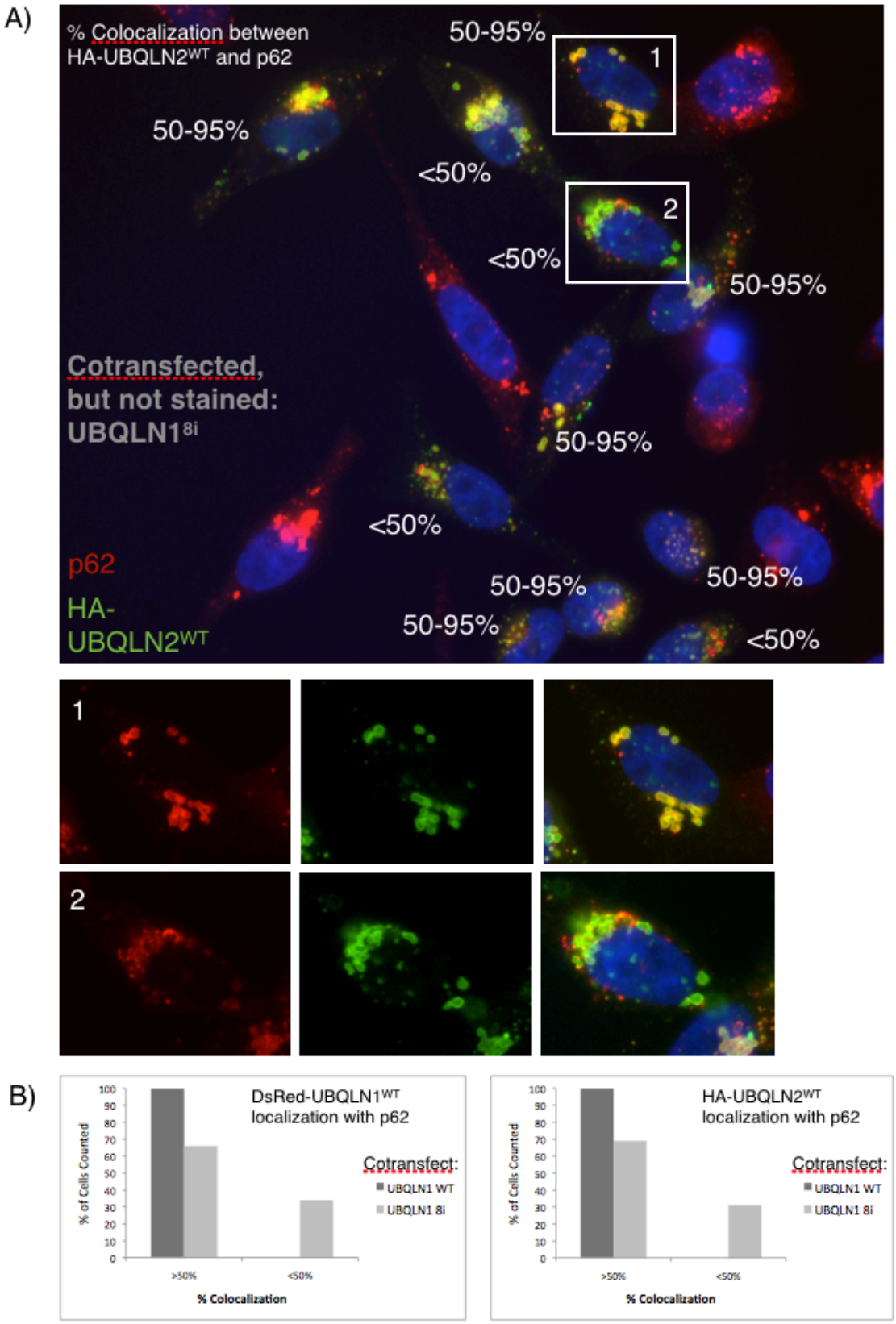
A)
% Colocalization between HA-UBQLN2WT and p62
50-95%
1
50-95%
<50%
2
<50%
50-95%
Cotransfected, but not stained: UBQLN18i
50-95%
<50%
p62
HA-UBQLN2WT
50-95%
50-95%
50-95%
<50%
1
2
B)
DsRed-UBQLN1WT localization with p62
Cotransfect:
UBQLN1 WT
UBQLN1 8i
% of Cells Counted
100
90
80
70
60
50
40
30
20
10
0
>50%
<50%
% Colocalization
HA-UBQLN2WT localization with p62
Cotransfect:
UBQLN1 WT
UBQLN1 8i
% of Cells Counted
100
90
80
70
60
50
40
30
20
10
0
>50%
<50%
% Colocalization

Quantification of $UQ1^{8i}$ disruption. **A)** Representative image of HA-$UQ2^{WT}$ and endogenous p62 in the presence of $UQ1^{8i}$ (but not stained). Cells were classified according to how much $UQ2^{WT}$ localized with p62, marked as either greater than 50%, or less than 50%. Select cells shown in the inserts are magnified for closer inspection. **B)** Quantification of localization. Expression of $UQ1^{8i}$ disrupts localization of $UQ1^{WT}$ or $UQ2^{WT}$ in roughly 40% of cells.

Figure 2.7

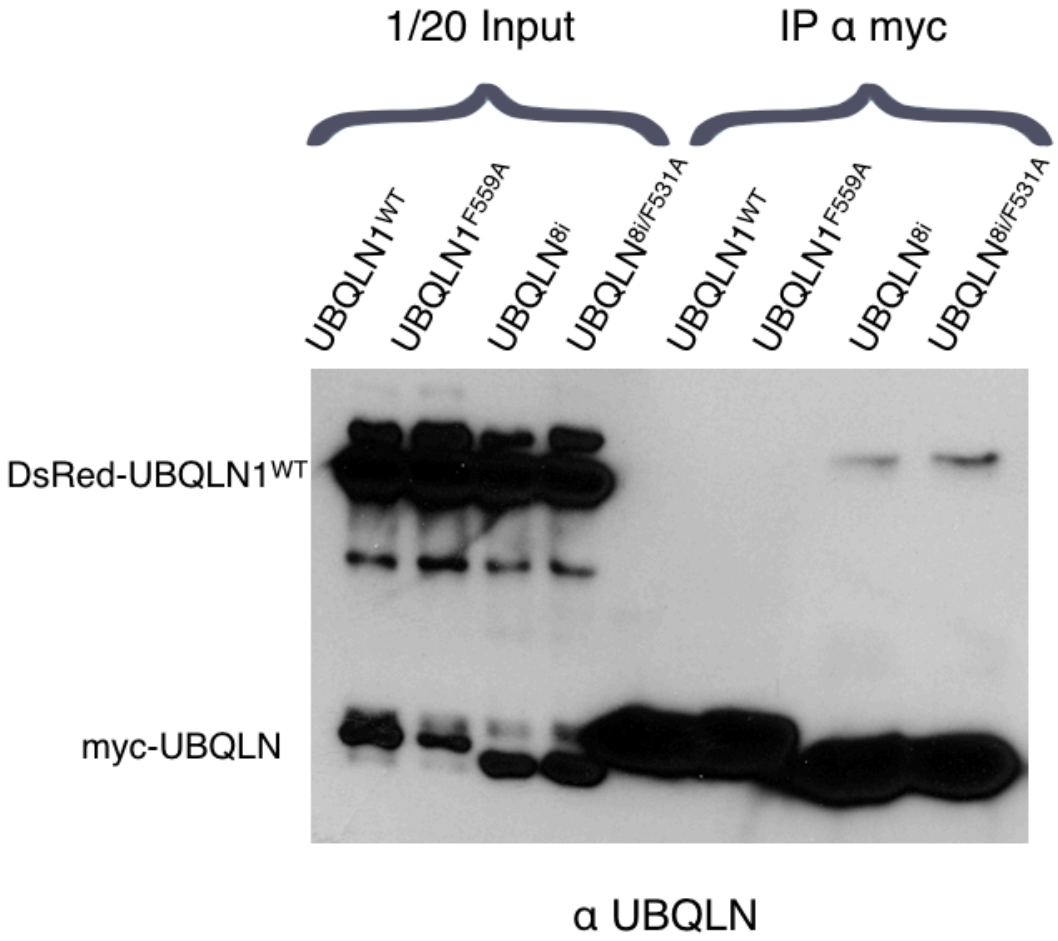

Enhanced dimerization of $UQ1^{8i}$ does not depend on UBA domain. HEK 293T cells were transfected with DsRed-$UBQLN1^{WT}$ in combination with myc-$UBQLN1^{WT}$, Myc-$UQ1^{F559A}$, Myc-$UBQLN1^{8i}$, or the compound mutant Myc-$UQ1^{8i/F531A}$, 24 h later, cell extracts were IP with α-myc. Bound proteins were analyzed by SDS-PAGE and immunoblotting with α-UBQLN antibody, which reacts with both myc- and DsRed-tagged UBQLN proteins.

Figure 2.8

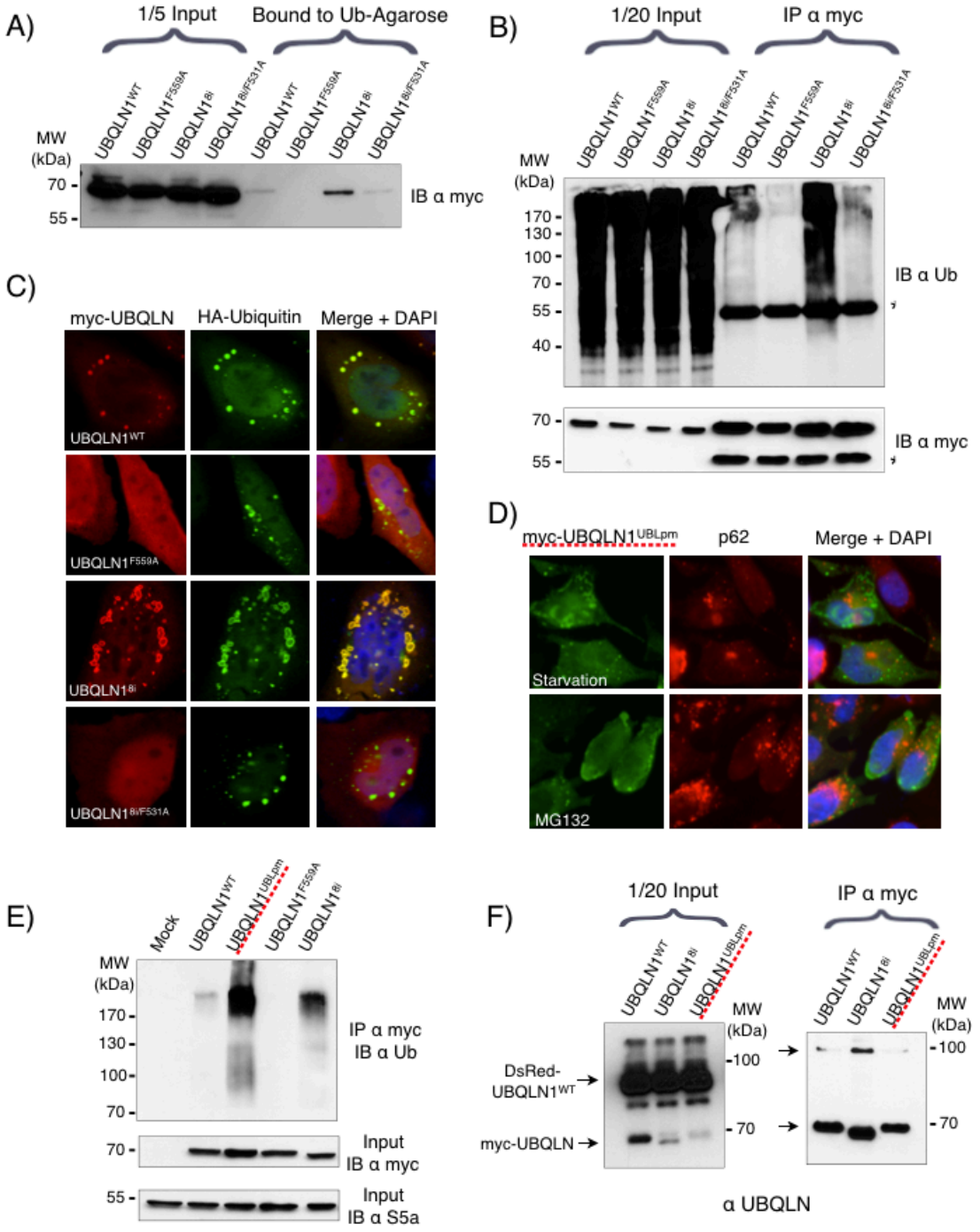

Enhanced Ub-binding of UBQLN1^{8i} **A)** HEK 293T cells were transfected with myc-UBQLN1^{WT}, myc-UBQLN1^{8i}, or their respective UBA point mutants (F559A and F531A), and lysed 24 h later. Lysate was incubated with monoUb-conjugated agarose beads and bound proteins analyzed by SDS-PAGE and immunoblotting with α-myc. **B)** HEK 293T cells were transfected as in (A) and incubated with 4 μM MG132 for 4 h. Immunoprecipitated myc-tagged proteins were analyzed by SDS-PAGE and

immunoblotting with α-Ub and α-myc. Asterisks indicate reactivity against Ig heavy chain. **C)** HeLa cells were transfected with HA-Ub and myc-UBQLN constructs, 24 h later cells were fixed and stained using α-myc (red) and α-HA (green) antibodies. Arrow designates unique UBQLN1^{8i} fused vesicle structure. **D)** HeLa cells were transfected with myc-UBQLN1^{UBLpm} and starved for 30 minutes (top) or treated with 4 μM MG132 for two h (bottom) immediately preceding fixation and staining with α-myc (red) and α-p62 (green) antibodies. **E)** HEK 293T cells were transfected with myc-UBQLN1^{WT}, myc-UBQLN1^{8i}, or myc-UBQLN1^{UBLpm}. Myc-tagged proteins were immunoprecipitated and analyzed by immunoblotting with antibodies as indicated. **F)** HEK 293T cells were transfected with DsRed-UBQLN1^{WT} alone or in combination with myc-UBQLN1^{WT}, myc-UBQLN1^{8i}, or myc-UBQLN1^{UBLpm} as described in (Fig. 3F). Twenty-four h later, IP was performed with the α-myc and analyzed by immunoblotting with α-UBQLN antibody, which reacts with both myc- and DsRed-tagged ubiquilin proteins, as indicated by arrows.

Figure 2.9

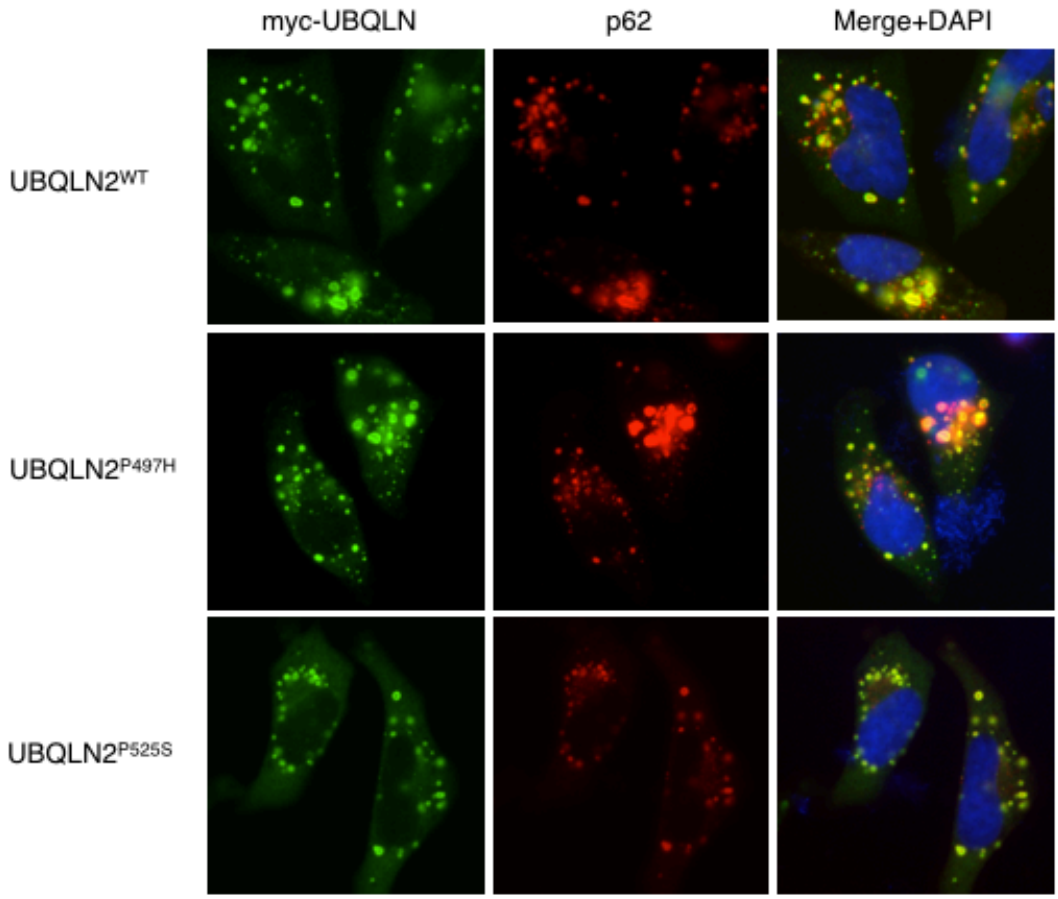

ALS mutations do not grossly disrupt UQ2 localization. HeLa cells were transfected with the indicated constructs and stained with Myc and p62 antibodies. UQ2 ALS mutants shown are representative and did not disrupt interaction with p62.

Figure 2.10

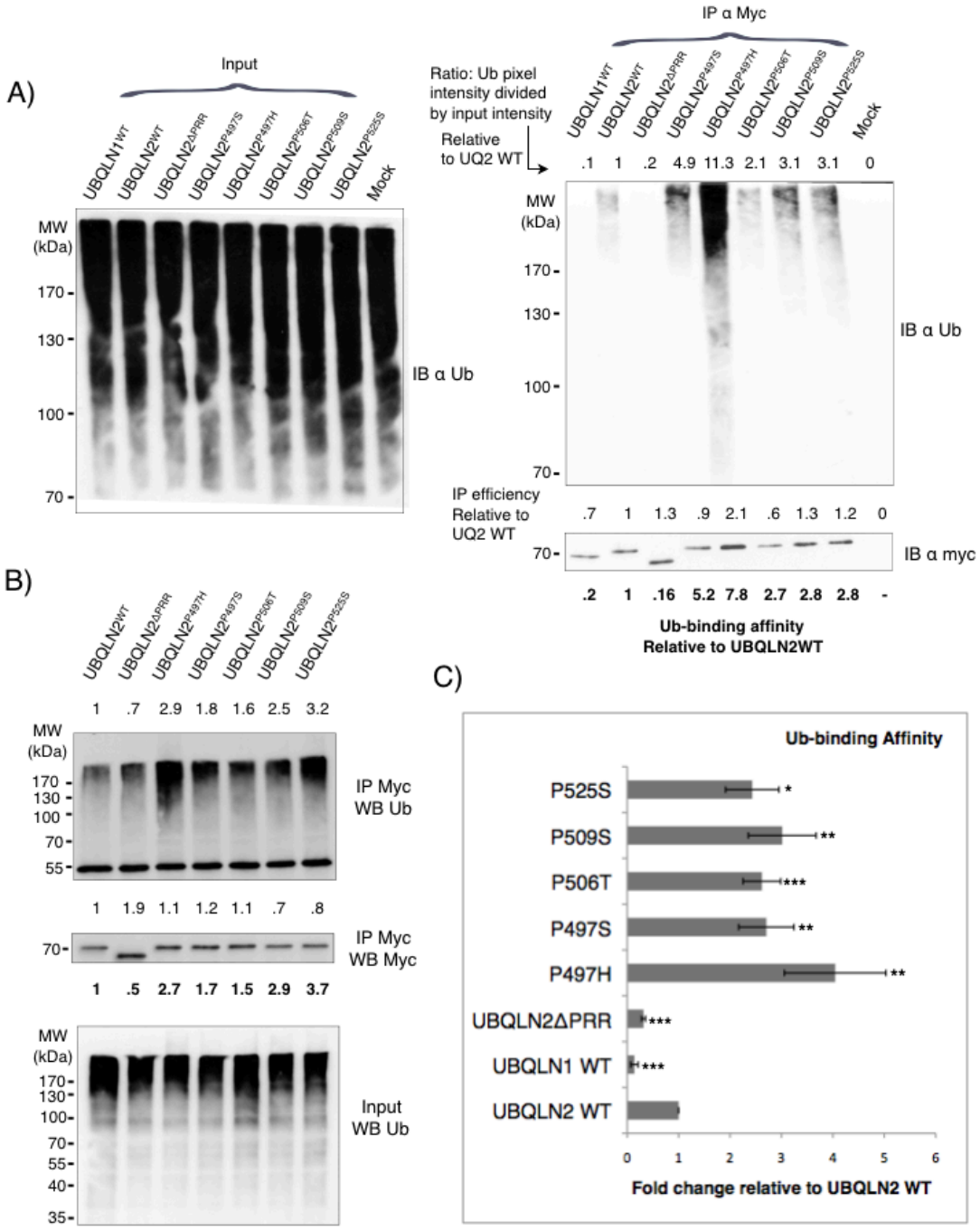

Enhanced Ub-binding of UBQLN2 ALS mutants **A)** HEK 293T cells were transfected with indicated constructs, and incubated with MG132 for 4 h preceding lysis. The a-myc immunoprecipitates were analyzed by immonoblotting with α-Ub and α-myc. The input levels confirm equal amounts of Ub in extract. The signal intensity of the Myc band in the IP was set as a ratio relative to the intensity of the $UQ2^{WT}$ band, and this was then used to gauge the amount of polyUb in the IP, or the relative pulldown capacity. All UQ2

ALS mutants are elevated relative to $UQ2^{WT}$, whereas $UQ1^{WT}$ and the PRR deletion construct are lower. **B)** As in (A). **C)** Quantification of Ub IP intensity.

Figure 2.11

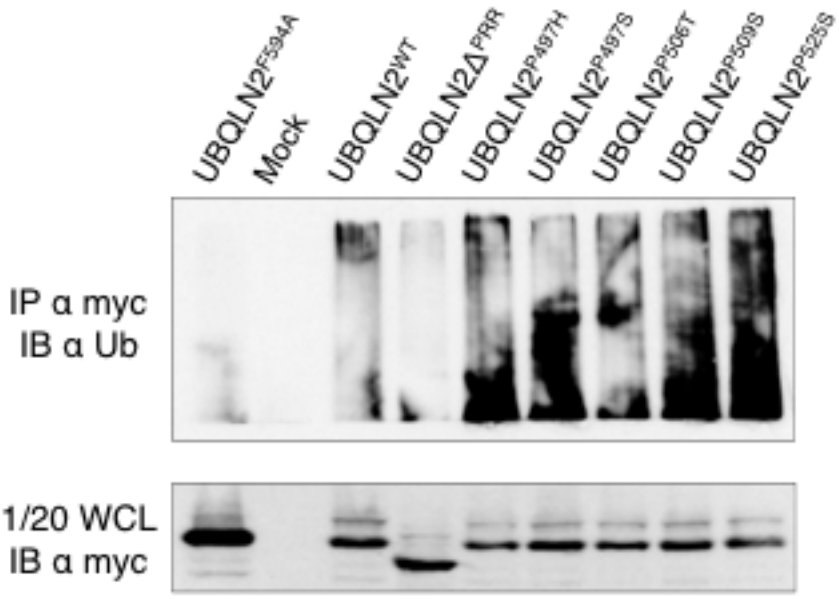

$UQ2^{F594A}$ mutant does not bind Ub. Indicated constructs transfected and Myc IP analyzed by SDS-PAGE and immunoblotting with Ub antibody. Far left lane, $UQ2^{F594A}$, is abundantly expressed but does not bind Ub.

Figure 2.12

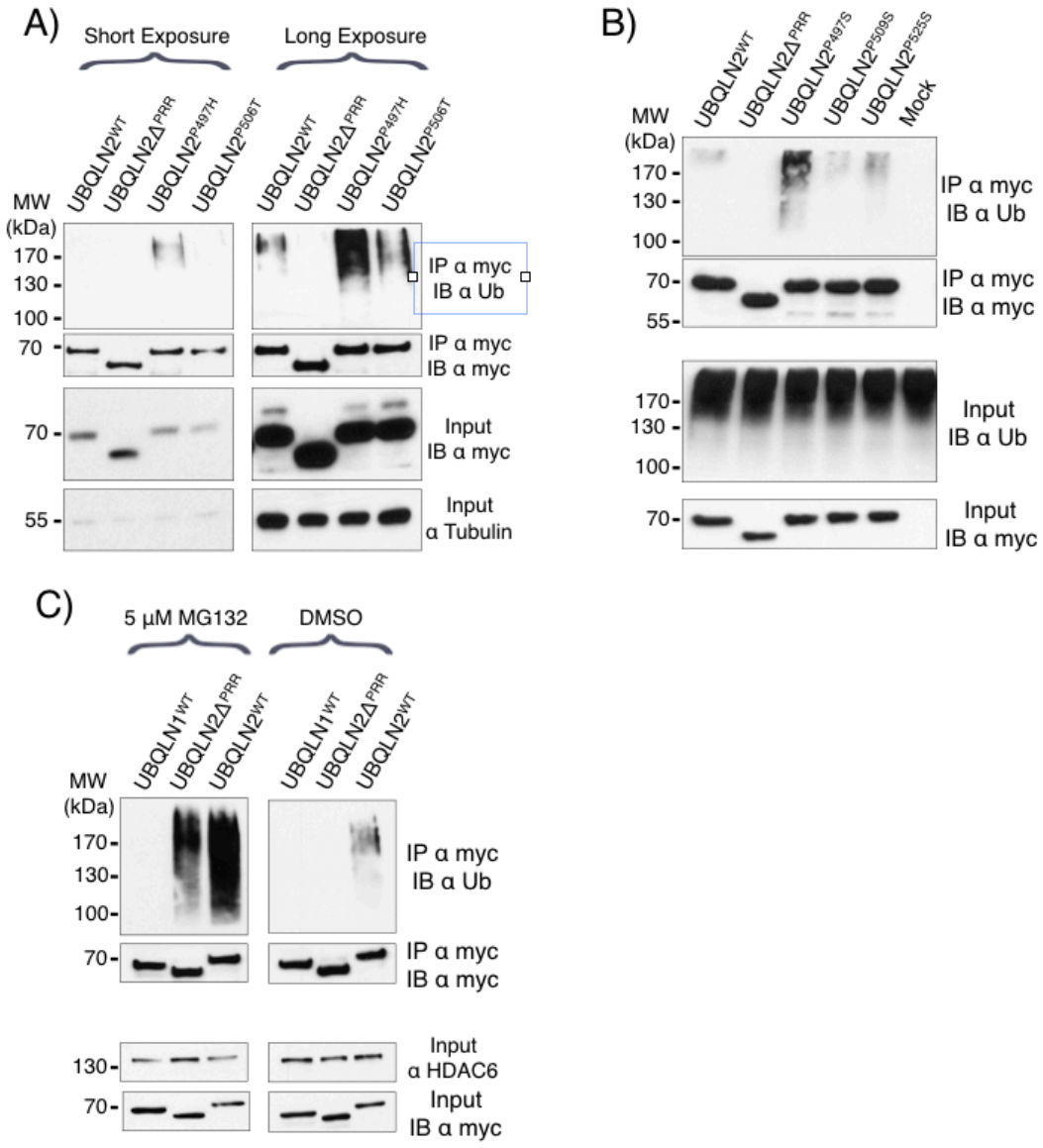

Enhanced Ub-binding by UQ2 ALS mutants relative to UQ2, and enhanced Ub-binding of UQ2 relative to UQ1. **A)** Indicated constructs transfected in 293T and IP with Myc antibody analyzed by SDS-PAGE and immunoblotting. UQ2 ALS mutants bind more Ub than UQ2, which binds more than UQ2$^{\Delta PRR}$. **B)** As in (A), independent experiment. **C)** Independent sets of HEK 293T cells were transfected with myc-UBQLN1^{WT}, myc-UBQLN2Δ^{PRR}, or myc-UBQLN2^{WT} and either treated or not with MG132 as indicated. Myc IP analyzed using the indicated antibodies. HDAC6 serves as loading control.

Figure 2.13

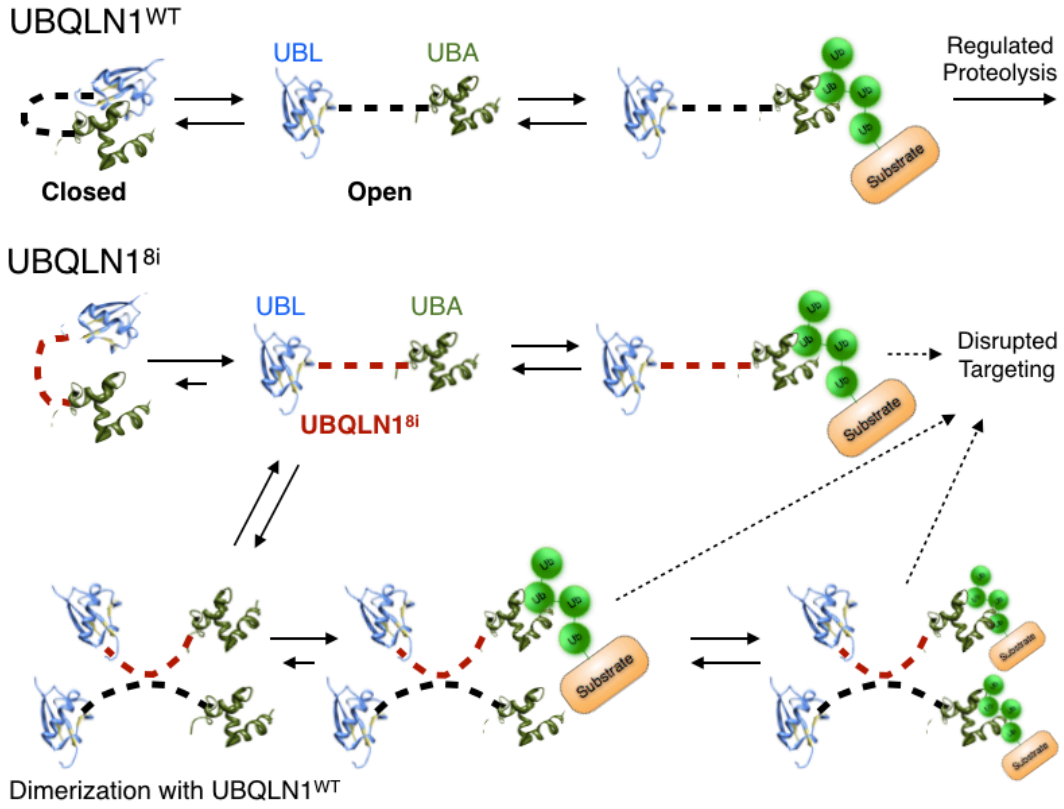

Model of Ubiquilin intramolecular regulation. In this model, Ubiquilins are in a conformational equilibrium between closed and open states. The UBL and UBA domains interact in the closed state, preventing association with Ub-modified substrates. Disruptions in UBQLN1^{8i} that perturb this equilibrium will increase occupancy of the open state, resulting in enhanced Ub-binding. We propose that dimerization of UBQLN1^{8i} is enhanced relative to UBQLN1^{WT} independent of its Ub-binding activity, and that this property disturbs the normal targeting of UBQLN1^{8i} to degradative vesicles.

Figure 2.14

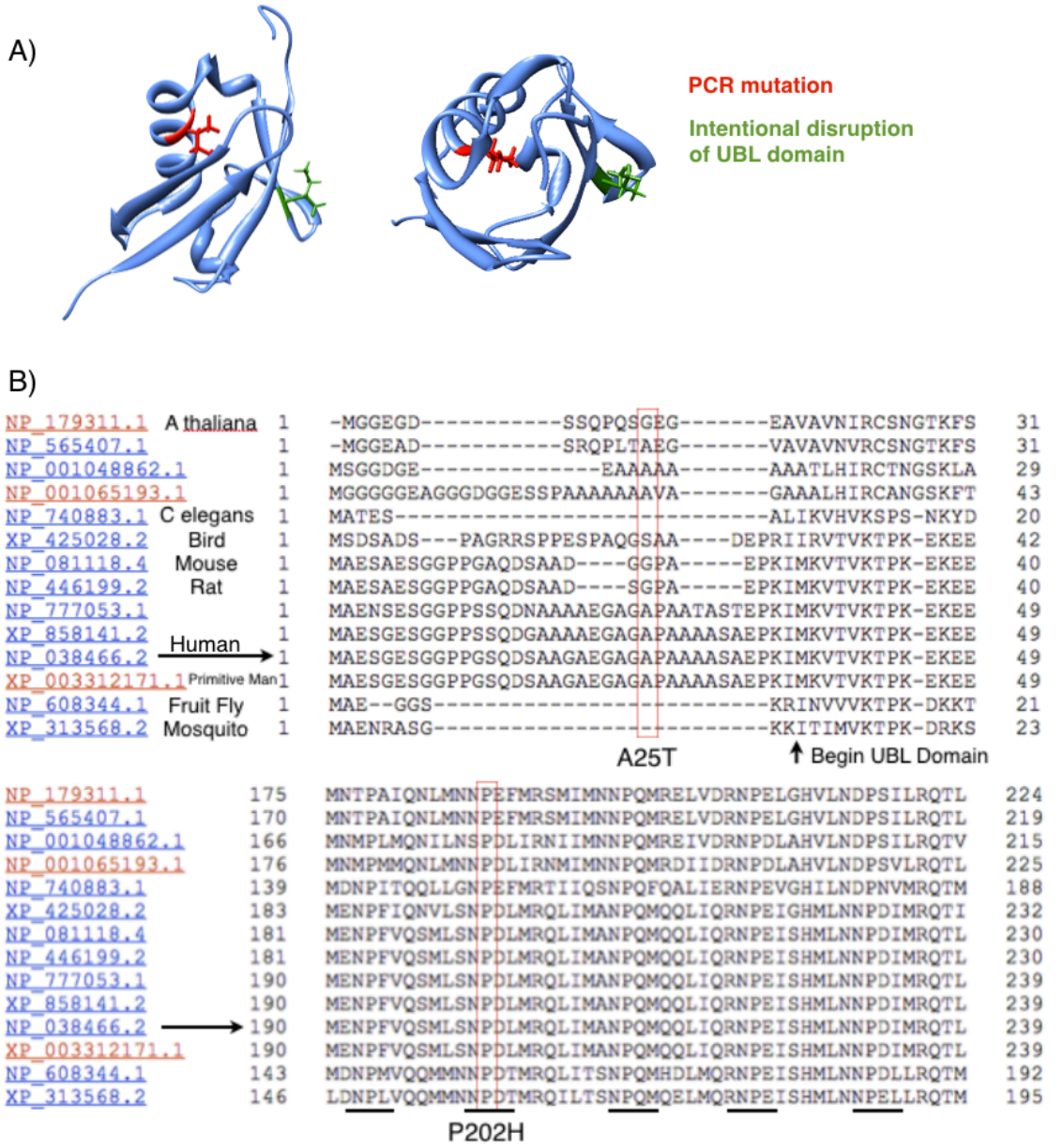

Discovery of mutations in UQ1^{8i} and UQ1^{WT}. **A)** NMR structure of UQ1 UBL domain with intentional I79T mutation used to generate UQ1^{UBLpm} highlighted in green. The PCR error, I65T, is highlighted in red. Ile65 is highly conserved. **B)** Depiction of two SNPs in UQ1, A25T and P202H. The former is predicted to be neutral, the latter is disruptive and sits in a conserved N-P-(E/D)-Ψ motif, in which Ψ is an aliphatic amino acid.

Figure 2.15

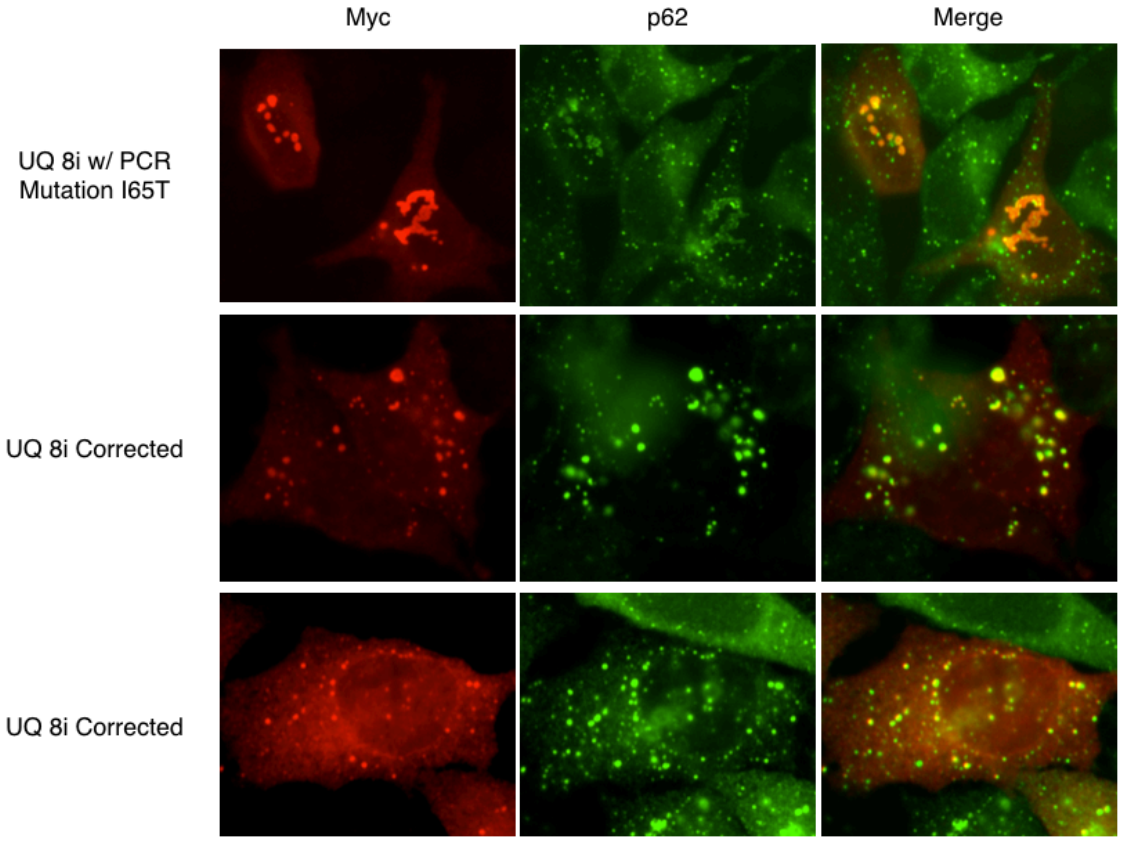

Correction of the UQ1^{8i} I65T mutation reverts localization phenotype. The corrected version now localizes with p62, invalidating several figures in this manuscript.

2.9 References

1. Bertram, L. *et al.* Family-based association between Alzheimer's disease and variants in UBQLN1. *N Engl J Med* **352,** 884–894 (2005).
2. Smemo, S. *et al.* Ubiquilin 1 polymorphisms are not associated with late-onset Alzheimer's disease. *Ann Neurol* **59,** 21–26 (2006).
3. Arias-Vásquez, A. *et al.* Relationship of the Ubiquilin 1 gene with Alzheimer‘s and Parkinson’s disease and cognitive function. *Neurosci Lett* **424,** 1–5 (2007).
4. Brouwers, N. *et al.* The UBQLN1 polymorphism, UBQ-8i, at 9q22 is not associated with Alzheimer's disease with onset before 70 years. *Neurosci Lett* **392,** 72–74 (2006).
5. Winklhofer, K. F., Tatzelt, J. & Haass, C. The two faces of protein misfolding: gain- and loss-of-function in neurodegenerative diseases. *EMBO J* **27,** 336–349 (2008).
6. Bird, T. D. Genetic aspects of Alzheimer disease. *Genet. Med.* **10,** 231–239 (2008).
7. Ross, C. A. & Poirier, M. A. Protein aggregation and neurodegenerative disease. *Nat Med* **10 Suppl,** S10–7 (2004).
8. Andersen, P. M. & Al-Chalabi, A. Clinical genetics of amyotrophic lateral sclerosis: what do we really know? *Nat Rev Neurol* **7,** 603–615 (2011).
9. Gitcho, M. A. *et al.* TDP-43 A315T mutation in familial motor neuron disease. *Ann Neurol* **63,** 535–538 (2008).
10. Kabashi, E. *et al.* TARDBP mutations in individuals with sporadic and familial amyotrophic lateral sclerosis. *Nat Genet* **40,** 572–574 (2008).
11. Rutherford, N. J. *et al.* Novel mutations in TARDBP (TDP-43) in patients with familial amyotrophic lateral sclerosis. *PLoS Genet* **4,** e1000193 (2008).
12. Sreedharan, J. *et al.* TDP-43 mutations in familial and sporadic amyotrophic lateral sclerosis. *Science* **319,** 1668–1672 (2008).
13. Van Deerlin, V. M. *et al.* TARDBP mutations in amyotrophic lateral sclerosis with TDP-43 neuropathology: a genetic and histopathological analysis. *Lancet Neurol* **7,** 409–416 (2008).
14. Yokoseki, A. *et al.* TDP-43 mutation in familial amyotrophic lateral sclerosis. *Ann Neurol* **63,** 538–542 (2008).
15. Neumann, M., Kwong, L. K., Sampathu, D. M., Trojanowski, J. Q. & Lee, V. M.-Y. TDP-43 proteinopathy in frontotemporal lobar degeneration and amyotrophic lateral sclerosis: protein misfolding diseases without amyloidosis. *Arch Neurol* **64,** 1388–1394 (2007).
16. Gidalevitz, T., Kikis, E. A. & Morimoto, R. I. A cellular perspective on conformational disease: the role of genetic background and proteostasis networks. *Curr Opin Struct Biol* **20,** 23–32 (2010).
17. Morimoto, R. I. Proteotoxic stress and inducible chaperone networks in neurodegenerative disease and aging. *Genes Dev* **22,** 1427–1438 (2008).
18. Watts, G. D. J. *et al.* Inclusion body myopathy associated with Paget disease of bone and frontotemporal dementia is caused by mutant valosin-containing protein. *Nat Genet* **36,** 377–381 (2004).
19. Johnson, J. O. *et al.* Exome sequencing reveals VCP mutations as a cause of

familial ALS. *Neuron* **68,** 857–864 (2010).
20. Fecto, F. *et al.* SQSTM1 Mutations in Familial and Sporadic Amyotrophic Lateral Sclerosis. *Arch Neurol* **68,** 1440–1446 (2011).
21. King, A., Maekawa, S., Bodi, I., Troakes, C. & Al-Sarraj, S. Ubiquitinated, p62 immunopositive cerebellar cortical neuronal inclusions are evident across the spectrum of TDP-43 proteinopathies but are only rarely additionally immunopositive for phosphorylation-dependent TDP-43. *Neuropathology* **31,** 239–249 (2011).
22. Kuusisto, E., Kauppinen, T. & Alafuzoff, I. Use of p62/SQSTM1 antibodies for neuropathological diagnosis. *Neuropathol Appl Neurobiol* **34,** 169–180 (2008).
23. Deng, H.-X. *et al.* Mutations in UBQLN2 cause dominant X-linked juvenile and adult-onset ALS and ALS/dementia. *Nature* 1–7 (2011). doi:10.1038/nature10353
24. Kim, S. H. *et al.* Potentiation of amyotrophic lateral sclerosis (ALS)-associated TDP-43 aggregation by the proteasome-targeting factor, ubiquilin 1. *J Biol Chem* **284,** 8083–8092 (2009).
25. Hanson, K. A., Kim, S. H., Wassarman, D. A. & Tibbetts, R. S. Ubiquilin modifies TDP-43 toxicity in a Drosophila model of amyotrophic lateral sclerosis (ALS). *J Biol Chem* **285,** 11068–11072 (2010).
26. Ko, H. S., Uehara, T., Tsuruma, K. & Nomura, Y. Ubiquilin interacts with ubiquitylated proteins and proteasome through its ubiquitin-associated and ubiquitin-like domains. *FEBS Lett* **566,** 110–114 (2004).
27. Kleijnen, M. F. *et al.* The hPLIC proteins may provide a link between the ubiquitination machinery and the proteasome. *Molecular cell* **6,** 409–419 (2000).
28. Ford, D. L. & Monteiro, M. J. Dimerization of ubiquilin is dependent upon the central region of the protein: evidence that the monomer, but not the dimer, is involved in binding presenilins. *Biochem J* **399,** 397–404 (2006).
29. Ko, H. S., Uehara, T. & Nomura, Y. Role of ubiquilin associated with protein-disulfide isomerase in the endoplasmic reticulum in stress-induced apoptotic cell death. *J Biol Chem* **277,** 35386–35392 (2002).
30. Kaye, F. J. *et al.* A family of ubiquitin-like proteins binds the ATPase domain of Hsp70-like Stch. *FEBS Lett* **467,** 348–355 (2000).
31. N'Diaye, E.-N. *et al.* PLIC proteins or ubiquilins regulate autophagy-dependent cell survival during nutrient starvation. *EMBO Rep* **10,** 173–179 (2009).
32. Bensemain, F. *et al.* Association study of the Ubiquilin gene with Alzheimer's disease. *Neurobiol Dis* **22,** 691–693 (2006).
33. Kamboh, M. I., Minster, R. L., Feingold, E. & DeKosky, S. T. Genetic association of ubiquilin with Alzheimer's disease and related quantitative measures. *Mol. Psychiatry* **11,** 273–279 (2006).
34. Ganguly, A., Feldman, R. M. R. & Guo, M. ubiquilin antagonizes presenilin and promotes neurodegeneration in Drosophila. *Hum Mol Genet* **17,** 293–302 (2008).
35. Li, A. *et al.* Isolation and characterization of the Drosophila ubiquilin ortholog dUbqln: in vivo interaction with early-onset Alzheimer disease genes. *Hum Mol Genet* **16,** 2626–2639 (2007).
36. Wang, H. *et al.* Suppression of polyglutamine-induced toxicity in cell and animal models of Huntington's disease by ubiquilin. *Hum Mol Genet* **15,** 1025–1041 (2006).

37. Williams, K. L. *et al.* UBQLN2/ubiquilin 2 mutation and pathology in familial amyotrophic lateral sclerosis. *Neurobiol Aging* (2012). doi:10.1016/j.neurobiolaging.2012.05.008
38. Pankiv, S. *et al.* p62/SQSTM1 binds directly to Atg8/LC3 to facilitate degradation of ubiquitinated protein aggregates by autophagy. *J Biol Chem* **282,** 24131–24145 (2007).
39. Komatsu, M. *et al.* Homeostatic Levels of p62 Control Cytoplasmic Inclusion Body Formation in Autophagy-Deficient Mice. *Cell* **131,** 1149–1163 (2007).
40. Seibenhener, M. L. *et al.* Sequestosome 1/p62 is a polyubiquitin chain binding protein involved in ubiquitin proteasome degradation. *Mol Cell Biol* **24,** 8055–8068 (2004).
41. Bjørkøy, G. *et al.* p62/SQSTM1 forms protein aggregates degraded by autophagy and has a protective effect on huntingtin-induced cell death. *J Cell Biol* **171,** 603–614 (2005).
42. Henne, W. M., Buchkovich, N. J. & Emr, S. D. The ESCRT pathway. *Dev Cell* **21,** 77–91 (2011).
43. Regan-Klapisz, E. *et al.* Ubiquilin recruits Eps15 into ubiquitin-rich cytoplasmic aggregates via a UIM-UBL interaction. *J Cell Sci* **118,** 4437–4450 (2005).
44. Polo, S. *et al.* A single motif responsible for ubiquitin recognition and monoubiquitination in endocytic proteins. *Nature* **416,** 451–455 (2002).
45. Ohno, A. *et al.* Structure of the UBA domain of Dsk2p in complex with ubiquitin molecular determinants for ubiquitin recognition. *Structure* **13,** 521–532 (2005).
46. Raasi, S., Ranjani Varadan, Fushman, D. & Pickart, C. M. Diverse polyubiquitin interaction properties of ubiquitin-associated domains. *Nat Struct Mol Biol* **12,** 708–714 (2005).
47. Walters, K. J., Lech, P. J., Goh, A. M., Wang, Q. & Howley, P. M. DNA-repair protein hHR23a alters its protein structure upon binding proteasomal subunit S5a. *Proc Natl Acad Sci USA* **100,** 12694–12699 (2003).
48. Lowe, E. D. *et al.* Structures of the Dsk2 UBL and UBA domains and their complex. *Acta Cryst (2006). D62, 177-188 [doi:10.1107/S0907444905037777]* 1–12 (2006). doi:10.1107/S0907444905037777
49. Heir, R. *et al.* The UBL domain of PLIC-1 regulates aggresome formation. *EMBO Rep* **7,** 1252–1258 (2006).
50. Ichimura, Y. *et al.* Structural basis for sorting mechanism of p62 in selective autophagy. *J Biol Chem* **283,** 22847–22857 (2008).
51. Rothenberg, C. & Monteiro, M. J. Ubiquilin at a crossroads in protein degradation pathways. *Autophagy* **6,** 979–980 (2010).
52. Biggins, S., Ivanovska, I. & Rose, M. D. Yeast ubiquitin-like genes are involved in duplication of the microtubule organizing center. *J Cell Biol* **133,** 1331–1346 (1996).
53. Hoeller, D. *et al.* Regulation of ubiquitin-binding proteins by monoubiquitination. *Nat Cell Biol* **8,** 163–169 (2006).
54. Bedford, F. K. *et al.* GABA(A) receptor cell surface number and subunit stability are regulated by the ubiquitin-like protein Plic-1. *Nature neuroscience* **4,** 908–916 (2001).
55. Lim, P. J. *et al.* Ubiquilin and p97/VCP bind erasin, forming a complex involved

in ERAD. *J Cell Biol* **187,** 201–217 (2009).
56. Massey, L. K. *et al.* Overexpression of ubiquilin decreases ubiquitination and degradation of presenilin proteins. *J. Alzheimers Dis.* **6,** 79–92 (2004).
57. Kay, B. K., Williamson, M. P. & Sudol, M. The importance of being proline: the interaction of proline-rich motifs in signaling proteins with their cognate domains. *FASEB J* **14,** 231–241 (2000).
58. Ren, X. & Hurley, J. H. Proline-rich regions and motifs in trafficking: from ESCRT interaction to viral exploitation. *Traffic* **12,** 1282–1290 (2011).
59. Suzuki, R. & Kawahara, H. UBQLN4 recognizes mislocalized transmembrane domain proteins and targets these to proteasomal degradation. *EMBO Rep* (2016). doi:10.15252/embr.201541402
60. Hjerpe, R. *et al.* UBQLN2 Mediates Autophagy-Independent Protein Aggregate Clearance by the Proteasome. *Cell* 1–16 (2016). doi:10.1016/j.cell.2016.07.001

Chapter 3) Exploring the UBQLN Interactome

Overview

I initiated this collaboration through a friend of mine, Dr. Julia Kennedy-Darling, who was a graduate student with Professor Lloyd Smith. She set me up with a scientist in her lab, Dr. Mark Scalf, and we set up the collaboration. I also collaborated extensively on this project with Dr. Sang Hwa Kim, a scientist in my lab. Sang Hwa performed the transfections, harvested the material, and performed the IP; I then performed all of the MS workup and cleanup before handing the sample off to Mark. Mark would send the data back to me, and I performed all of the analysis and validation presented herein. Overall, while informative, the runs were highly variable. In general, these qualitative experiments helped to identify several ubiquilin-interacting proteins and post-translational modifications of ubiquilins, including ubiquitylation and proline-hydroxylation. In this chapter, I will present data from the co-IP-LC-MS/MS and validation by co-IP and WB. The post-translational ubiquitylation of ubiquilins will be presented, but is fully developed in chapter 4.

3.1 Introduction

Our original hypothesis for this project was that the PRR of UQ2 might serve as a unique protein-protein interaction domain. The PRR contains several overlapping PXXP tetrapeptides, which support interaction with a variety of binding domains, including SH3, GYF, and WW domains[1]. We therefore performed co-IP-LC-MS/MS experiments to identify proteins that co-precipitated with ubiquilins. The majority of our experiments were conducted in buffer containing TX-100 or NP-40 (hydrophobic detergents), and we performed one run in buffer containing the zwitterionic detergent, CHAPS. The majority

of the interacting proteins returned were common between UQ1, UQ2, UQ2$^{\Delta PRR}$, and UQ2 ALS mutants. In retrospect, this result is not surprising, considering the conserved UBL and UBA domains that likely share the same interacting partners. Additionally, the proteins isolated by co-IPs are typically either high affinity interacting partners or sticky – interactions mediated by the PRR may be lower affinity, detergent-sensitive, or non-existent.

We carried out proteomic analyses of HA-UQ IPs in HEK 293T cells with the goal of identifying factors that interact with UQ2 in a PRR- or ALS mutation-dependent manner. We performed multiple iterations of this experiment, ultimately settling on in-solution digests, although in the first run, we performed separation by SDS-PAGE, dehydrated the gel slices, and performed in-gel digests. Overall, we had five separate runs with highly variable results – unfortunately there are no records of input/expression levels for the HA-tagged constructs, leading me to hypothesize that the data sets are variable due to variable expression level (transfection efficiency). Our single set of data collected in CHAPS buffer was far and away the most robust in terms of identifying interacting proteins, especially those proteins localized to the ER and mitochondria.

Overall, this was a qualitative analysis, but it revealed several proteasomal subunits, ERAD proteins, and components of the BAG6 complex recently linked to ubiquilins[2,3]. We did not identify any PRR-dependent interactions, but we decided to pursue specific hits in our screen in order to investigate other published interactions and to place ubiquilins in different cellular degradation pathways.

3.2 Results

3.2.1 Ubiquilins interact with the proteasome

Co-precipitation of proteasome subunits was robust, especially in CHAPS buffer. We anticipated strong interaction with the proteasome, as this is a well-characterized interaction. Nonetheless, I performed co-IP and western blotting for endogenous proteasome subunits to validate these hits. Early in my graduate career, I detected robust interaction with the proteasome, in this case examining the UBA*, UBL* and K*R mutants, which are a Ub-binding null mutant (F594A)[4], a corrupted UBL domain variant (T39A, I75T)[5], and a UQ2 with all lysine amino acids in the UBL mutated to arginine, respectively. I tested three subunits to assess if ubiquilins were pulling out full proteasomes. I examined 20Sα1, a small subunit in the 20S core, PSMD2 (also known as S2, RPN1), a subunit in the 19S that binds the UBL domain of a related UBL-UBA shuttling protein[6], and S5a (RPN10), a non-stoichiometric component of the 19S with Ub-binding domains and a characterized interaction with ubiquilins[7]. Although I was able to successfully co-IP all of these proteins (Fig. 3.1A), the situation changed with time and now it's quite challenging for reasons I don't fully understand. It was recently published that UQ2 ALS mutants have a diminished interaction with the proteasome, but I never explicitly tested this by co-IP[8]. I did examine cells by immunofluorescence and found that proteasome components are contained within vesicles formed by ubiquilin proteins, both wild type and ALS mutants (Fig. 3.1B).

3.2.2 Ubiquilins interact with UBXD8

Among the identified UQ2 interactions in our screen was Fas-associated factor 2 (FAF2)/UBXD8, an ER-anchored protein with cytosolic Ub-like and Ub-binding domains that is implicated in lipid droplet regulation and ERAD[9]. In light of a report that ALS mutations disrupted interaction between UQ2 and UBXD8 and cause ERAD defects

and ER stress[10], we investigated the UQ2-UBXD8 interaction in further detail. We found that $UQ2^{WT}$ and $UQ2^{ALS}$ mutants interacted with endogenous UBXD8 to a similar extent and that the interaction of UBXD8 with $UQ2^{WT}$ and $UQ2^{P497H}$ was abolished by the F594A UBA domain mutation (Fig. 3.2A). Overall, we found that the ubiquilin-UBXD8 interaction correlated with the amount of precipitated polyUb in the IP, and thus UQ2 had a more robust interaction with UBXD8 than UQ1 in buffer containing TX, suggesting that UBXD8 interacts with ubiquitylated UQ2, associated polyUb, or Ub-binding factors (Fig. 3.2B). Finally we investigated the localization patterns of Myc-UQ1, Myc-UQ2 and S-tagged UBXD8 in HeLa cells and found that UBXD8-S containing vesicles were distinct from, but in close proximity to ubiquilin-containing vesicles (Fig. 3.2C) [9].

3.2.3 Interaction with ERAD E3 Ligases, GP78 and HRD1

We identified the E3 Ub ligase, GP78 (also known as AMFR), in our MS experiments. GP78 has seven transmembrane domains that pass through the smooth ER – the cytosolic C-terminus of GP78 contains a RING motif bestowing E3 activity, an Ub-binding CUE domain, a dedicated E2 binding surface, and a VCP-interacting domain at its extreme C-terminus[11]. The RING, CUE, and E2 binding domains are all required for Ub ligase activity. GP78 is one of the most well characterized E3 Ub ligases in endoplasmic reticulum-associated degradation (ERAD), a process by which misfolded ER proteins are degraded by the proteasome[12]. We selected GP78 to validate by co-IP experiments, but found the antibody (Santa Cruz) showed no immunoreactivity. We therefore acquired a vector encoding S-tagged GP78/pcDNA3.1 (a kind gift from the lab of Ron Kopito) and performed co-transfection experiments to validate the interaction[13]. As a specificity control, I decided to investigate an additional E3 Ub ligase that is very

well characterized in ERAD, known as HRD1 (also known as SYVN1)[14]. HRD1 is similar to GP78 in that it is a multi-pass transmembrane E3 embedded in the ER with well characterized associations with the retrotranslocon complex, proteasome subunits, and VCP[15,16]. The S-tagged Hrd1/pcDNA3.1 vector was also from the Kopito lab.

I investigated binding in TX buffer initially, but expanded my analysis such that binding was measured in both TX and CHAPS buffers in order to determine if the interactions were detergent-sensitive. In TX, GP78-S was detected as a discrete band at its expected MW, as well as a high molecular weight smear, described by several labs as a Ub-modified form of the protein resulting from auto-ubiquitylation (Fig. 3.3A)[17]. In CHAPS, only the high MW smear was visible in the soluble fraction, but was highly abundant in the insoluble (pellet) fraction. In TX, UQ2 precipitated GP78-S to a greater extent than UQ1; UQ2 also precipitated more endogenous UBXD8 than UQ1 in these experiments, consistent with previous findings in TX (Fig. 3.3A). In CHAPS, however, both UQ1 and UQ2 precipitated similar amounts of polyUb, UBXD8, and GP78-S, although the amount of GP78-S was markedly reduced, perhaps owing to its relative insolubility in this detergent (Fig. 3.3A).

The interactions of UQ1 and UQ2 with Hrd1-S were very similar to those observed with GP78-S – indicating that the interaction likely isn't very specific in this experimental system (Fig. 3.3B). In brief, Hrd1-S expression results in a band at the predicted MW, as well as high MW smears likely corresponding to the ubiquitylated form of the protein, and it resistant to extraction in CHAPS, although not as insoluble as GP78-S. In TX, binding to Hrd1 again seems to correlate with the amount of precipitated Ub, whereas in CHAPS, UQ1 co-IPs similar amounts of Hrd1 (Fig. 3.3B).

$UQ2^{WT}$ and UQ2 ALS mutants interacted with GP78-S and Hrd1-S to a similar extent, suggesting that ALS mutations do not disrupt this interaction (Fig. 3.4A). Additionally, $UQ2^{\Delta PRR}$ precipitated more GP78-S and Hrd1-S than $UQ1^{+PRR}$, indicating that this interaction does not require the PRR and is likely an indirect interaction mediated through polyUb or associated Ub-binding factors (Fig. 3.4B). As with UBXD8-S, I also performed IF analysis of Myc-ubiquilins co-transfected with Hrd1-S and performed two different fixation methods. When fixed in 4%PFA and permeabilized with .2% TX, Hrd1-S was distributed in cytosolic foci that were connected to a reticular network and excluded from the nucleus (Fig. 3.5A). Myc-UQ1 and Myc-UQ2 both formed small punctate structures that were partially overlapping with Hrd1-S (Fig. 3.5A). When fixed in 4%PFA followed by methanol, Hrd1-S formed a very similar staining pattern, indicating that these structures are not lipid droplets[9]. A similar localization pattern was also observed for ubiquilins, with some overlapping structures (Fig. 3.5B).

3.2.4 Ubiquilins interact with BAG6 complex

We identified BAG6 and an additional protein from the BAG6 complex, UBL4A, in our MS analysis of the ubiquilin interactome. BAG6 was also identified in a screen for UQ1-interacting proteins by an independent lab[3], and was recently linked to UQ4 in the degradation of cytosolic model substrates bearing transmembrane (hydrophobic) domains, known as mislocalized proteins (MLPs)[2]. BAG6 functions as a chaperone for tail-anchored (TA) membrane proteins and is required for proper targeting of TA proteins as well as for efficient degradation of those TA proteins that fail to localize – the BAG6 complex is at once required for proper insertion and timely degradation of TA proteins,

functioning as a cytosolic triage complex with physical connections to both E3 Ub ligases and the post-translational membrane insertion machinery[18,19].

BAG6 contains a UBL domain at its N-terminus that allows it to engage E3 Ub ligases, and several proline-rich hydrophobic domains that are required for its interaction with client proteins containing exposed hydrophobic motifs[20,21]. In this way, BAG6 supports the ubiquitylation of client proteins that do not become anchored in the membrane. Knockdown of BAG6 results in hypo-ubiquitylation of clients, whereas overexpression of BAG6 stabilizes clients bearing Ub chains, thus it is thought that BAG6 regulates the stability of proteins that fail to localize within an adequate timeframe[22]. BAG6 is also known for its roles in promoting the degradation of newly synthesized proteins, known as defective ribosomal products (DRiPs), and for its function in apoptotic signaling from DNA damage or ribosomal stress[23,24].

Originally, I was able to detect interaction with endogenous BAG6 in certain detergents, but not in TX. However, after getting a new lot of the same antibody, I could hardly detect any protein, even when running massive amounts of whole cell lysate (data not shown). I therefore switched over to a plasmid expressing BAG6-V5[25]. When co-expressed with Myc-ubiquilins, interaction with BAG6-V5 was pretty weak and once again trended with the amount of co-precipitated Ub (Fig 3.6A). The extraction of BAG6-V5 was affected by ubiquilin co-expression, with $UQ2^{P497H}$ driving BAG6 to the pellet fraction (Fig. 3.6A). I also attempted to repeat a very recent paper suggesting the specific interaction of BAG6 with UQ4 (but not UQ1)[2]. In my hands, I found that BAG6 interacted most strongly with UQ2 following MG132 treatment, and that this interaction was visible but not robust for UQ4. Interestingly, co-expression with UQ4 led to the most

dramatic reduction in BAG6 solubility, despite the observation that UQ4 is primarily soluble (Fig. 3.6B).

3.2.5 Post-translational modifications of ubiquilins

Throughout the series of MS experiments, we detected abundant peptides corresponding to Ub and Ub-modified ubiquilins. When a protein is Ub-modified, the modified lysine is protected from trypsin cleavage and the C-term of Ub (^{69}LVLRLRGG^{76}) is cleaved after R^{74}, leaving a characteristic di-glycine appendage. There were several runs that contained di-glycine Ub remnants indicating precipitated polyUb chains. The sum of five separate experiments yielded 12 K11-linked peptides, 13 K48-linked peptides, and 4 K63-linked peptides. The relative abundance of the different polyUb chains in basal cells is estimated to be ~30% K11, ~30% K48, and ~15% K63[26,27]. Interestingly, in *S. cerevisiae*, knockout of the ubiquilin homolog, Dsk2, causes increases in the steady state levels of K11- and K48- linked chains, but no change to K63-linked polyUb[26]. This might be reflected in our data set – although there are several variables, including the qualitative nature of our experiments that prevent a proper quantitative analysis. We also identified di-glycine remnants on eight lysine amino acids of UQ2 in one run (0303_2012), corresponding to K31, 2 x K41, 2 x K43, K58, and K82. In an additional run, we identified five lysine amino acids bearing a Ub modification (0628_2012): K31, K41, K43, K58, K79 (Fig. 3.7). However, in three other runs, no Ub-modified lysine amino acids were detected in UQ2. Notably, we did not detect Ub modifications on UQ2^{P497H}, although we only performed one MS run on this protein.

We also detected abundant proline hydroxylation on ubiquilins, occurring most frequently at P219 (4), P262 (9), and P278 (3). This was very exciting and we attempted

to find proline hydroxylation within the PRR domain but did not succeed, perhaps owing to the primary sequence of the domain, which lacks basic amino acids. I spent a bit of time playing with sealed plastic bags as mock hypoxic chambers and also with dimethyloxaloylglycine, which is a generic prolyl hydroxylase inhibitor (data not shown)[28]. Ultimately, I considered that proline hydroxylation could be an oxidation artifact during MS preparation because of how often we saw the modification, so I did not pursue it further, but will revisit this idea in the following discussion.

3.3 Discussion

Seeing that several labs previously published data about ubiquilins with the proteasome, I pursued less well-characterized interactions in order to contribute novel findings. This does not mean that the proteasome is not an interesting interacting partner, but it did not pique our interest in light of some of the other data coming in. In retrospect, it might have been useful to characterize this interaction more carefully, as proteasome dysfunction is likely therapeutically relevant in ALS and related neurodegenerative diseases[8,29].

The ERAD pathway and several mitochondrial proteins were most abundant in CHAPS, perhaps because indirect interactions are more likely to persist in CHAPS due to its incomplete penetration of the lipid membrane[30]. Proteins associated with membranes will be more likely to maintain association in complexes and this is a possible explanation for the robust co-IP of several factors that were not present in TX. We approached these experiments loosely and received qualitative results – meaning we would see proteins or we wouldn't. It was impossible to gauge relative amounts in the IPs for two reasons: i) the experiments were not quantitative (no SILAC, no iTRAQ, etc.)

and ii) the variability of samples between runs made it very difficult to construct an interaction hierarchy.

One set of interactions that I did not mention in the results, nor did I pursue experimentally, was the robust precipitation of HSP70 family members, including HSC70, HSP70, GRP75, and GRP78. We considered the precipitation of these peptides to be largely artifact, as they were present in the control IPs, although to a lesser extent. Very recently, one week before my oral defense, a lab published a large study on the stress-induced activation of UQ2 in cooperation with the HSP70 pathway[31]. Hjerpe et al. generated a knock-in mouse model of $UQ2^{P506T}$ and characterized its interactome through quantitative mass spectrometry, making the general conclusions that $UQ2^{P506T}$ interacted to a lesser degree with HSP70 and to a greater degree with endogenous Ub[31]. Their overall model was that UQ2 is a stress-activated chaperone that cooperates with HSP70, and in the event of the P506T mutation, the protein does not cooperate as efficiently with HSP70, rendering cells sensitive to different stressors (heat and puromycin), and resulting in the inefficient clearance of proteins destined for proteasome degradation. I will explore their results and possible follow-up experiments in greater detail in Chapter 6.

The post-translational ubiquitylation of ubiquilins is explored in depth in Chapter 4, but the proline hydroxylation of ubiquilins is ripe for exploration. Although my initial impression of this data was that it might be an artifact occurring during the MS workflow, I have since learned that proline hydroxylation requires a great deal of energy, and is not likely to oxidize nonspecifically during MS preparation (Professor Laura Kiessling, personal communication). In light of this new information, it is quite interesting that we observed proline hydroxylation at the same positions in several different peptides. There

are reports suggesting that ubiquilins are involved in the cellular response to hypoxia[32] and oxidative stress[33]. Although I did not explore these topics in my dissertation, oxidative stress and neuro-inflammation are currently trending hypotheses regarding the etiology of neurodegenerative disease, including ALS[34,35]. If ubiquilins are prolyl-hydroxylated, it is conceivable that this event could alter the protein structure and/or function, and is a potential avenue for further inquiry.

In sum, I have developed a greater appreciation for the complexity of measuring protein-protein interactions in different detergents; these types of experiments merit careful interpretation. Just because two things interact by co-IP doesn't mean they localize together in the cell (for example, UBXD8, Figure 3.2). On the other hand, just because two things don't IP each other doesn't mean they don't interact, as we're seeing in a newer project in the lab investigating UQ2 in the endocytosis pathway[36] (Dr. Sang Hwa Kim, personal communication). These studies, while qualitative, were nonetheless of great interest to me and to the lab. The indisputable evidence that several lysine amino acids in UQ2 are Ub-modified provided a solid foundation for investigating the role of this post-translational modification, as explored in Chapter 4. Additionally, the interaction of ubiquilins with several different proteins in specific pathways also shaped my choice of model substrates for investigating functional impacts of ubiquilin expression and deficiency, as elaborated in Chapter 5.

3.4 Materials and Methods

DNA Construction

Ubiquilin constructs subcloned into pCMV-Myc or pCMV-HA are as described in Materials and Methods of Chapter 2. The open reading frame of UQ4 was PCR amplified

out of a UQ4/pENTR construct obtained from the non-profit plasmid repository, Addgene (ID 16170) and subcloned into pCMV-Myc using EcoRI and XhoI restriction sites[37]. Point mutations were introduced by site-directed mutagenesis using Phusion DNA polymerase (NEB). $UQ2^{UBL*}$ and $UQ2^{K*R}$ were made by iterative mutagenesis. A former graduate student in the lab, Dr. Lihong Zhan, designed primers for the UQ2 ALS mutations. Constructs expressing UBXD8-S, UBXD8-Myc, GP78-S, and Hrd1-S were cloned into pcDNA3.1 and were a kind gift from Professor Ron Kopito's lab (Stanford University) [9,13]. The construct expressing BAG6-V5 was cloned into pcDNA5/FRT/TO and was a kind gift from Professor Stephen High's lab (University of Manchester) [22,38].

Construct	Mutation	F Primer	R Primer	Location + ID
UQ^{UBA*}	F594A	GCTCAACGCAAT GGGG**GC**C**C**TTAA ACCGTGAAGC	GCTTCACGGTTT AA**GG**CCCCCATT GCGTTGAGC	Primers Box I 12587+12588
$UQ2^{UBL*}$	T39A	CGGTGAAG**GC**T**C** CCAAAGAGAAA GAGGAGTTCG	CGAACTCCTCTT TCTCTTTGGG**AG** **C**CTTCACCG	Primers Box I 12589+12590
$UQ2^{UBL*}$	I75T	GCTAGTGCTG**AC** **T**TTTGCCGGAAA AATCTTAAAAG	CTTTTAAGATTTT TCCGGCAAA**AGT** CAGCACTAGC	Primers Box I 12591+12592
$UQ2^{K*R}$	K31/34R	GGCTGAGCCT**AG** **A**ATCATC**AGA**GT CACGGTGAAGAC TCC	GGAGTCTTCACC GTGAC**TCT**GATG AT**TCT**AGGCTCA GCC	Primers Box II 61056+61057
$UQ2^{K*R}$	K38/41/ 43R	GTCACGGTG**AGG** ACTCCC**AGA**GAG **AGA**GAGGAGTTC GCG	CGCGAACTCCTC **TCT**CTC**TCT**GGG AGT**CCT**CACCGT GAC	Primers Box II 61058+61059
$UQ2^{K*R}$	K58R	GGTTCAGCAGTT T**AGG**GAAGCGA TTTCG	CGAAATCGCTTC **CCT**AAACTGCTG AACC	Primers Box II 61060+61061
$UQ2^{K*R}$	K63/66R	GCGATTTCG**AGA** CGCTTC**AGA**TCC CAAACCG	CGGTTTGGGA**TC** **T**GAAGCG**TCT**CG AAATCGC	Primers Box II 61062+61063
$UQ2^{K*R}$	K79/82R	GCTGATTTTTGC CGGAA**AGA**ATCTT A**AGA**GATCAAG ATACC	GGTATCTTGATC **TCT**TAAGAT**TCT** TCCGGCAAAAAT CAGC	Primers Box II 61064+61065

$UQ2^{K*R}$	K103R	CACCTTGTCATC **AGA**AGCCAGAA CCGACC	GGTCGGTTCTGG CT**TCT**GATGACA AGGTG	Primers Box III 65957+65958

Cell Culture and Transfection

HEK 293T and HeLa cells were maintained in Dulbecco's modified Eagle's medium (DMEM) containing 5% fetal bovine serum and 100u/ml of penicillin and streptomycin in a 5% CO_2 atmosphere in Thermo Forma II water-jacketed incubators (medium and FBS sourced from Cellgro). Dox-inducible Flp-In HeLa cells were a kind gift from Don Cleveland's lab (University of California, San Diego)[39]. The parental Flp-In HeLa cells were simultaneously transfected with ubiquilin constructs in pcDNA5/FRT/TO and the Flp recombinase in vector pOG44 at a plasmid ratio of 9:1, followed by selection in hygromycin, per the manufacturer's instructions (Invitrogen). Cells were maintained in 200ug/ml hygromycin and 5ug/ml blasticidin, resistance to the former conveyed by successful recombination and resistance to the latter conveyed by the previously integrated and constitutively expressed Tet-repressor. HeLa cells were transfected by Lipofectamine 3000 (Invitrogen) according to the manufacturer's instructions. Typically 1-2ug of DNA was transfected in a 60mm plate. HEK 293T cells were transfected by the calcium phosphate method, typically with 1-2ug of DNA per construct per 60mm plate, and 4ug of ubiquilin DNA / 2-3ug of S-tagged ERAD DNA per construct per 10cm plate.

Antibodies

Antibody Target	Species	Supplier/Reference	Application
Myc	Mouse	Santa Cruz Biotechnology SC-40	IF, IP, IB
Myc	Rabbit	Santa Cruz Biotechnology SC-789	IF, IB
HA	Mouse	Santa Cruz Biotechnology SC-7392	IB, IP
HA	Rabbit	Santa Cruz Biotechnology SC-805	IB, IP
S	Rabbit	Cell Signaling	IF, IB
VCP	Rabbit	Santa Cruz Biotechnology SC-20799	IB
UBXD8	Rabbit	Proteintech 16251-1-AP	IF, IB
S5a (PSMD4)	Rabbit	Abcam ab20239	IF
S2 (PSMD2)	Rabbit	Proteintech 14747-1-AP	IB
20Sa1	Rabbit	Santa Cruz Biotechnology SC-67046	IF, IB
Ub P4D1	Mouse	Santa Cruz Biotechnology SC-8017	IB
V5	Rabbit	Bethyl A190-120A	IB
Ub FK2	Mouse	Enzo BML-PW8810-0500	IB, IF
UQ1	Rabbit	Cell Signaling 14526	IB, IF, IP
UQ2	Rabbit	Cell Signaling 85509	IB, IF, IP
HSP70	Rabbit	Cell Signaling 4872	IB, IF
UQ1	Rabbit	Abcam 3341	IB
BAG6	Rabbit	Cell Signaling 8523	
UQ1 / UQ2	Mouse	Invitrogen 37-7700	

Immunoprecipitation

HEK 293T or HeLa cells were transfected with varying amounts of plasmid DNA and incubated for 24-72h, as indicated. Plates of cells were withdrawn from incubator, scraped in ice cold PBS and transferred to micro-eppendorf tubes on ice. Cells were centrifuged at 1,200g, 4C, for 2m. PBS was aspirated, followed by suspension of cells in roughly fifty volume equivalents (V_{EQ}) of lysis buffer, as indicated in each experiment (typically 400uL is used for a ~80-95% confluent 60mm plate). Cells were incubated on ice for 20-30m with gentle, intermittent mixing by shaking on Vortex Genie 2 (Scientific Industries, Inc.) at setting 2, 2x10s stirring, ~once/10m. Alternatively, cells were disrupted by gentle finger flicks (8 flicks in a row, ~once/10m). Cell suspensions were centrifuged at 21,837g, 4C, for 12m, and resulting supernatant transferred to a new tube. 40uL of the supernatant was removed and mixed with an equal volume of 2x Laemmli

loading dye and heated at 95C for 5-8m. To the remaining supernatant, antibody added (1.2ug Myc 9E10 per 60mm plate) and rotated with gentle inversion overnight on a mini-rotator at 20% speed (Glas-Col, LLC) or on a mini-labroller (Labnet International, Inc.), typically 10-18h at 4C.

Day 2: Equilibrate A/G agarose suspension in lysis buffer and chill on ice. The way I like to do this is to have roughly 5uL of bead volume per reaction, then I dilute that to 5uL beads / 100uL buffer. For example, if I'm doing 8 IP reactions, I'll move 45uL bead volume to a new tube, equilibrate it, and after the final wash, suspend the beads in 900uL volume. Using a p200 pipette with the tip cut to allow for a wider diameter, aliquot 100uL A/G agarose suspension to each IP reaction, and tumble for an addition 2-4h at 4C. To wash, chill the appropriate wash buffer (For TX and CHAPS, I use .2%TX/PBS and .1%CHAPS/PBS, respectively). Retrieve samples and allow them to sit on ice for 3-5m. Centrifuge at 100g for 1m, aspirate the sample leaving ~40-50uL volume, then add $20V_{EQ}$ wash buffer, slowly invert twelve times, then allow to sit on ice 3-5m. Repeat three times, then aspirate leaving ~30uL volume, add 12uL 4x Laemmli loading dye, and incubate at 95C for 5-8m.

Immunofluorescence

HeLa cells were grown on glass coverslips and a total of 0.8 μg of plasmid DNA was introduced into each well of a 12-well plate, or 2 μg of plasmid DNA was transfected in 60mm plates that had been fitted with six coverslips, using Lipofectamine 3000 (Invitrogen) according to manufacturer's instructions. Cells were washed with three times with PBS and fixed with 4% paraformaldehyde in PBS for 10m at room temperature. Fixed cells were permeabilized with 0.2% Triton-X 100 (in PBS) for 10m

at room temperature, followed by three washes with PBS. Alternatively, cells were fixed and permeabilized in ice-cold methanol at -20C for 10m. Cells were blocked in sterile-filtered 3% bovine serum albumin (BSA) in PBS (w/v) for 30m at room temperature, followed by overnight incubation at 4C with primary antibody at a final concentration of 0.1-0.5 μg/ml in 3% BSA, depending on the antibody and determined experimentally. Cells were washed five times in ice-cold PBS, then incubated with appropriate Alexa-Fluor secondary antibody, varying between experimental conditions, at a final concentration of 1:1000. Cells were then incubated for 15m at room temperature with DAPI diluted in PBS at a final concentration of 0.15μg/ml, followed by extensive washing in PBS. Coverslips were mounted on glass slides using Vectashield mounting medium (Vector Labs, Inc. H-1000). Once dried, coverslips were sealed using clear nail polish and stored at -20C. Photographs were taken on an inverted Nikon A1R scanning confocal microscope with four laser lines: 408, 488, 561, and 638nm. Image acquisition metadata appended to each image; all acquisition specifications within a given microscope session were uniform.

Sample Preparation for in-solution MS

Precipitated material was washed extensively in lysis buffer, followed by extensive washing in PBS, and samples were eluted with 500μL 100mM glycine. Final volume of collected elution was typically 450μL from 10x10cm dishes of material. Sample volume was reduced to 25μL by speed vacuum, which typically required 10-12h of operation. 125μL 8M urea (in 25mM NH_4HCO_3 pH 8) was added to sample, followed by boiling at 95C for 10m. Sample cooled to room temperature with gentle inversion mixing, then reduced by adding 10μL 200mM DTT (in 50mM NH_4HCO_3 pH 8) and

incubated 45m at room temperature with gentle vortex at 10m intervals. Samples then alkylated by adding 10µL 200mM iodoacetamide (in 50mM NH_4HCO_3 pH 8) and incubated 45m at room temperature with gentle vortex at 10m intervals. Sample then diluted with 50mM NH_4HCO_3 pH 8 to reduce urea concentration below 1M (e.g., add 1.1mL bicarbonate solution to achieve final urea concentration of ~.8M). Trypsin added (Promega V511A) to a final ratio of 1:20 trypsin:substrate per manufacturer's instructions. Samples gently vortexed and centrifuge briefly, followed by overnight incubation at 37C (at least 18H). Digest quenched with 60µL 10% trifluoroacetic acid/water (v/v) and vortexed, then stored at -20C until submitted for MS analysis.

HPLC-ESI- MS/MS analyses

Samples were analyzed by HPLC-ESI- MS/MS using a system consisting of a high performance liquid chromatograph (nanoAcquity, Waters) connected to an electrospray ionization (ESI) Orbitrap mass spectrometer (LTQ Velos, ThermoFisher Scientific). HPLC separation employed a 100 x 365 mm fused silica capillary micro-column packed with 20 cm of 3mm-diameter, 100 Angstrom pore size, C18 beads (Magic C18, Bruker), with an emitter tip pulled to approximately 1 mm using a laser puller (Sutter instruments). Peptides were loaded on-column at a flow-rate of 400nL/minute for 30 minutes and then eluted over 120 min at a flow-rate of 300 nl/minute with a gradient of 2% to 30% acetonitrile, in 0.1% formic acid. Full-mass profile scans were performed in the FT orbitrap between 300-1500 m/z at a resolution of 60,000, followed by ten MS/MS HCD scans of the ten highest intensity parent ions at 42% relative collision energy and 7,500 resolution, with a mass range starting at 100 m/z. Dynamic exclusion

was enabled with a repeat count of two over the duration of 30 seconds and an exclusion window of 120 seconds.

Mass Spectrometry Data Analysis

The acquired precursor MS and MS/MS spectra were searched against a human protein database (Uniprot reviewed canonical database, containing 16,886 sequences) using SEQUEST, within the Proteome Discoverer 1.3.0.339 software package (Thermo Fisher Scientific). Masses for both precursor and fragment ions were treated as mono-isotopic. Oxidized methionine (+15.995 Da) and the gly-gly footprint on lysine (+114.043 Da) were allowed as dynamic modifications and carbamidomethylated cysteine (+57.021 Da) was searched as a static modification. The database search permitted for up to two missed trypsin cleavages and ion masses were matched with a mass tolerance of 10 ppm for precursor masses and 0.1 Da for HCD fragments. The output from the SEQUEST search algorithm was validated using the Percolator algorithm. The data were filtered using a 5% false discovery rate (Rohrbough et al., 2006), based on q-Values, with a minimum of two peptide matches required for confident protein identification.

3.5 Figures

Figure 3.1

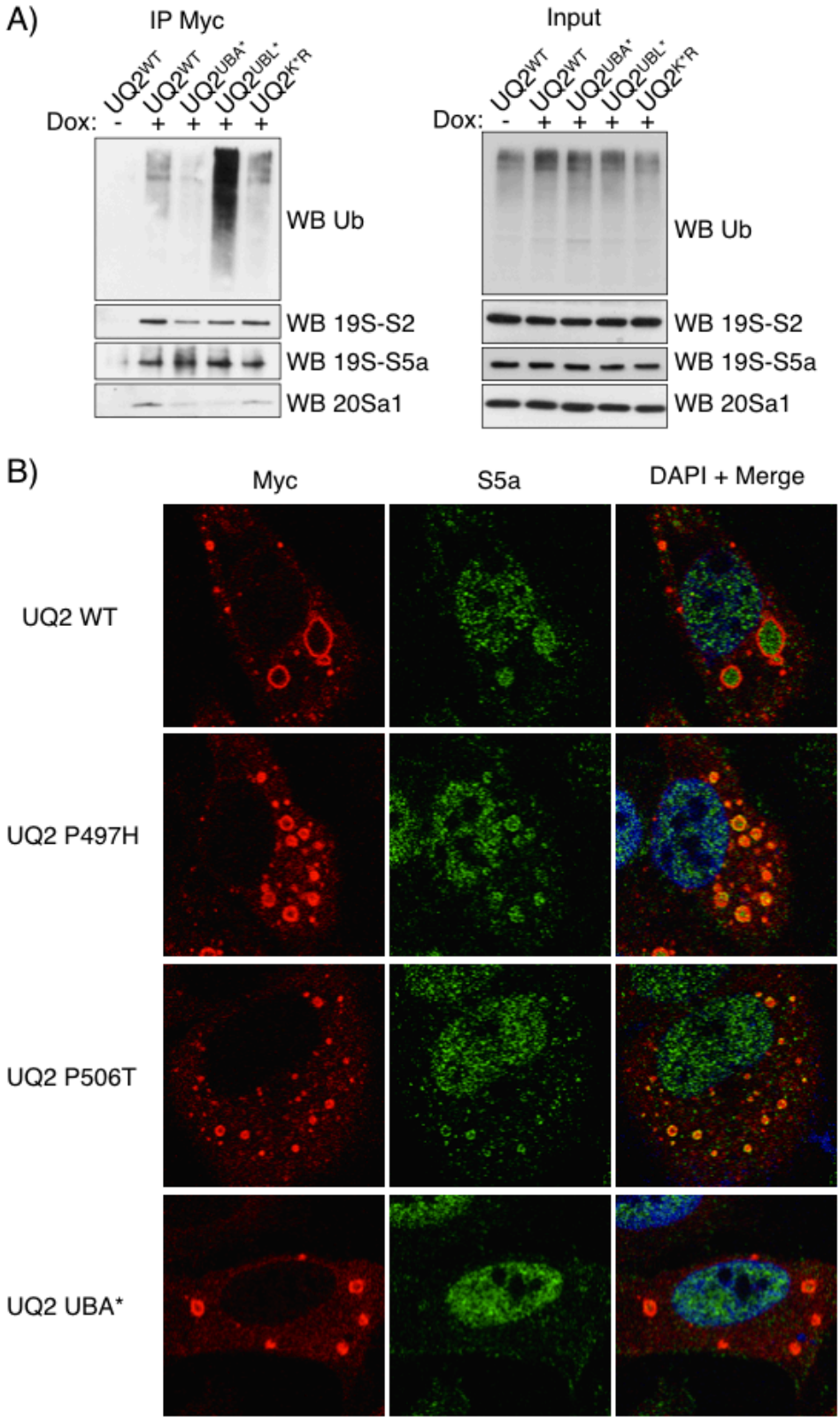
A)
IP Myc
Input
UQ2WT
UQ2WT
UQ2UBA*
UQ2UBL*
UQ2K*R
Dox: - + + + +
WB Ub
WB 19S-S2
WB 19S-S5a
WB 20Sa1
B)
Myc
S5a
DAPI + Merge
UQ2 WT
UQ2 P497H
UQ2 P506T
UQ2 UBA*

Ubiquilins associate with the proteasome. **A)** Dox-inducible HeLa cells expressing the indicated construct were induced with 500ng/ml Dox overnight prior to harvest in PBS and lysis in TX buffer. IP was performed with Myc antibody and bound proteins analyzed by SDS-PAGE and immunoblotting. Robust interaction with proteasome subunits was detected for all ubiquilins, despite differences in IP of Ub. An input blotted for the same factors demonstrates that ubiquilin expression does not affect the abundance of proteasome subunits or Ub in this system. **B)** HeLa cells transfected with lipofectamine 3000 were grown for ~24h, then fixed in 4%PFA and permeabilized in .2% TX. IF performed with Myc antibody and S5a, recognizing endogenous proteasome subunit. $UQ2^{WT}$ and ALS mutants (P497H and P506T shown) exhibit diverse staining patterns following transient transfection. The majority of Myc-ubiquilin vesicles also stain positive for S5a. The $UQ2^{UBA*}$ construct does not stain as strongly for S5a, suggesting that in addition to the UBL domain, polyUb bound by ubiquilins may serve to recruit proteasomes.

Figure 3.2

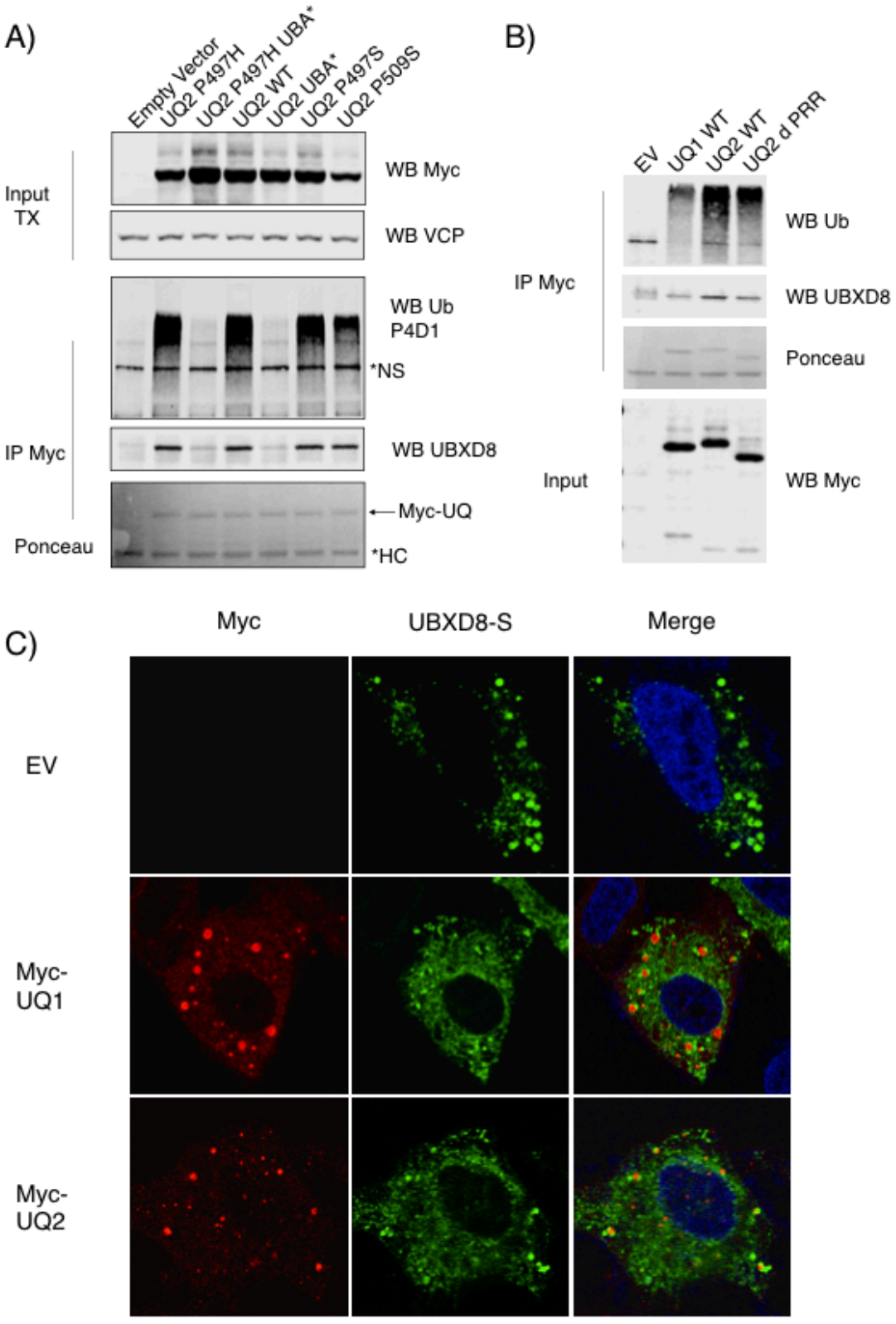
A)
Empty Vector
UQ2 P497H
UQ2 P497H UBA*
UQ2 WT
UQ2 UBA*
UQ2 P497S
UQ2 P509S
Input TX
WB Myc
WB VCP
WB Ub P4D1
*NS
IP Myc
WB UBXD8
←Myc-UQ
Ponceau
*HC
B)
EV
UQ1 WT
UQ2 WT
UQ2 d PRR
IP Myc
WB Ub
WB UBXD8
Ponceau
Input
WB Myc
C)
Myc
UBXD8-S
Merge
EV
Myc-UQ1
Myc-UQ2

IP of UBXD8 correlates with levels of precipitated polyUb. **A)** HeLa cells were transfected by Lipofectamine 3000, grown for ~27h, and lysis and IP with Myc antibody performed in TX buffer. $UQ2^{WT}$ and ALS mutants precipitate roughly equal amounts of Ub and UBXD8 in UBA-dependent manner. * marks nonspecific band in IP. **B)** As in (A), demonstrating correlation between Ub and UBXD8 in IP. **C)** HeLa cells were transfected by Lipofectamine 3000 with plasmids encoding Myc-UQ and UBXD8-S, followed by fixation in 4%PFA, permeabilization in .2%TX, and staining with Myc and S-tag antibodies. UBXD8 localizes to lipid droplets that are proximal to but not co-localized with Myc-ubiquilin vesicles.

Figure 3.3

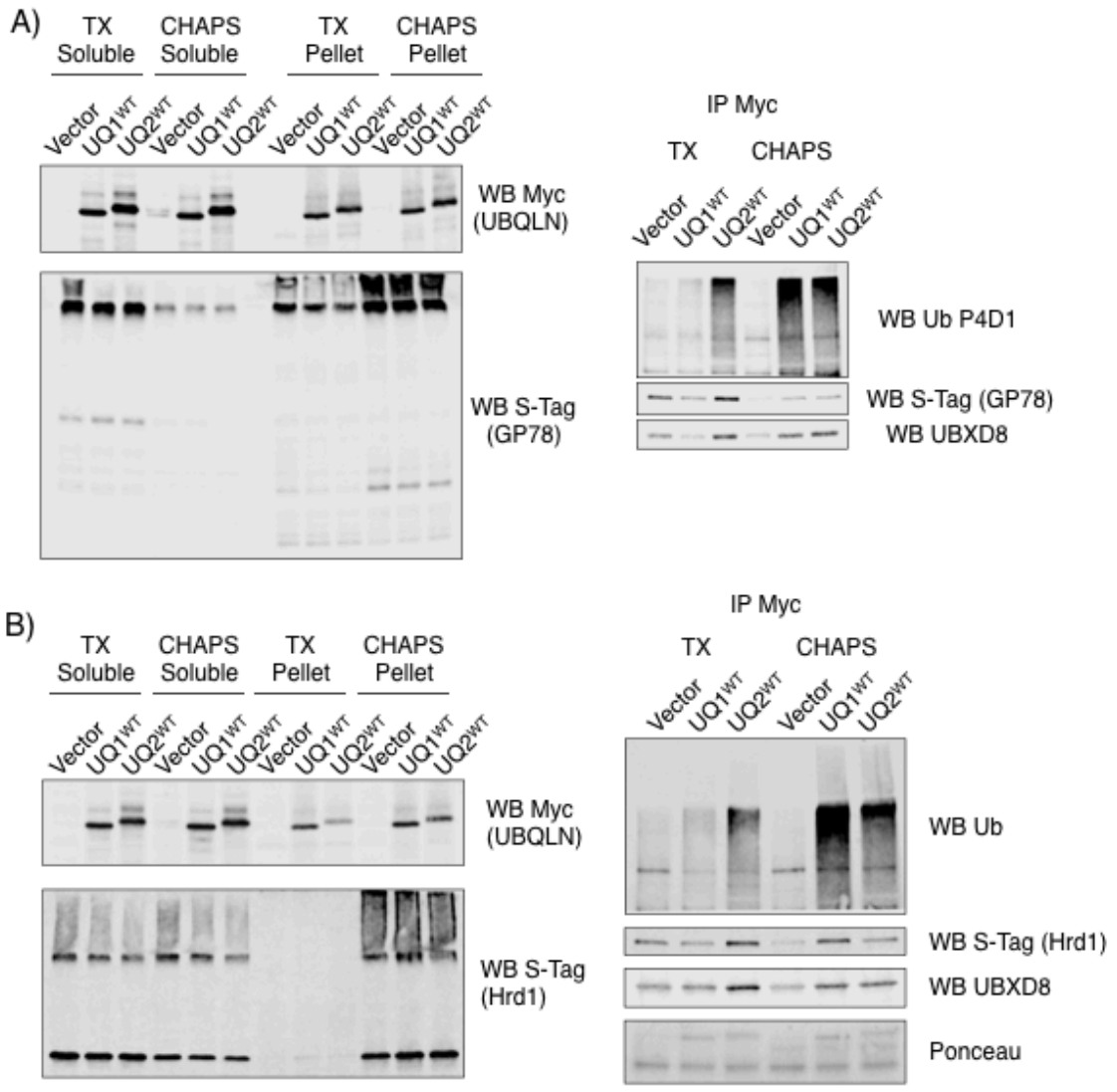

Detergent-sensitive interaction of ubiquilins with Ub and ERAD E3 Ub ligases. **A)** HEK 293T cells were transfected by $CaPO_4$ with the indicated Myc-UQ construct and GP78-S, grown for 30h, harvested in PBS and split to two portions, then lysed in either TX or CHAPS and IP with Myc antibody. Soluble and pellet fractions (top) and IP (bottom) analyzed by SDS-PAGE and immunoblotting. **B)** As in (A), except that cells were transfected with Hrd1-S instead of GP78-S.

Figure 3.4

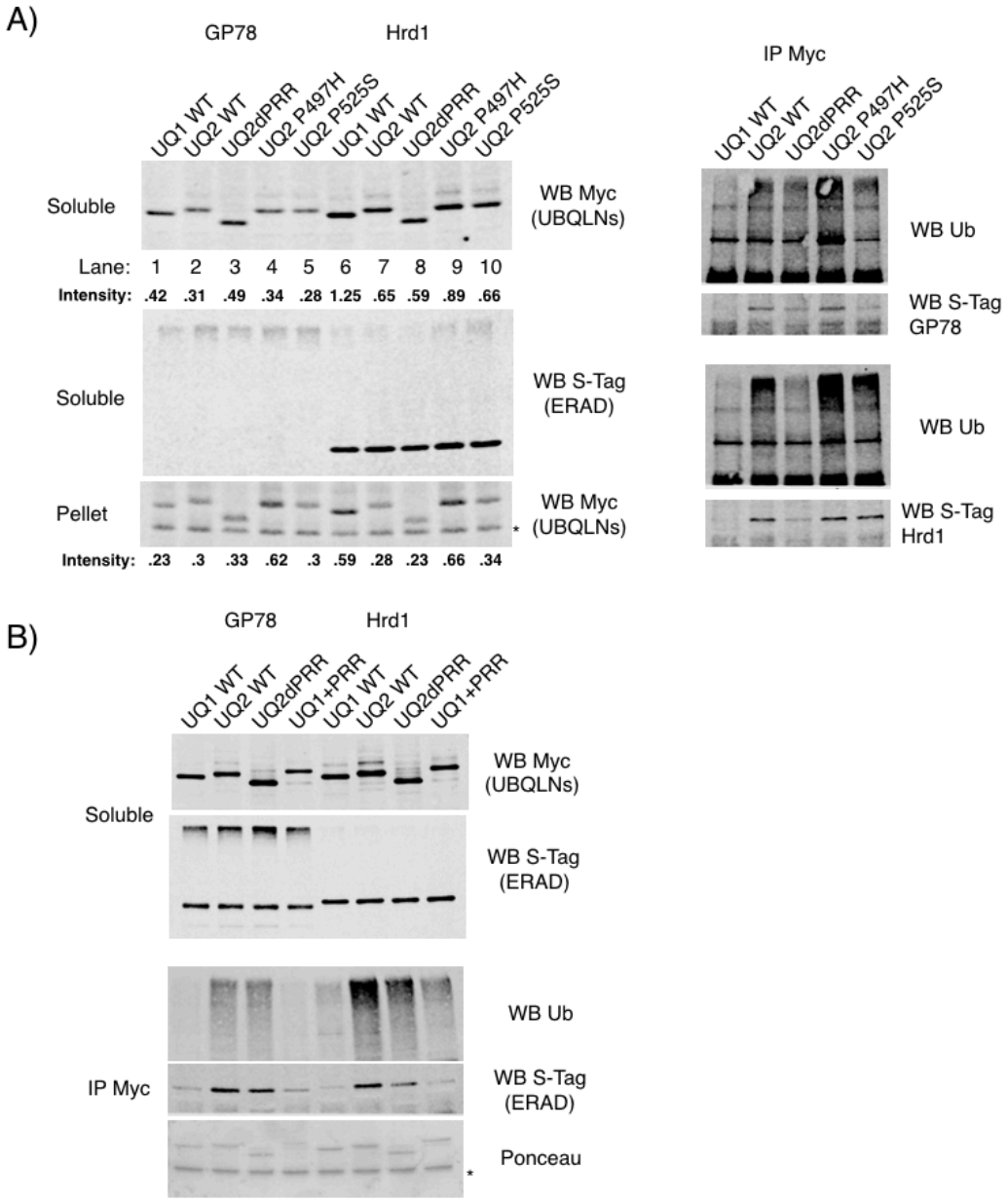

UQ2 ALS mutants do not disrupt interaction with ERAD E3 Ub ligases **A)** HEK 293T cells were transfected by $CaPO_4$ with the indicated Myc-UQ construct and GP78-S or Hrd1-S, as indicated, grown for 26h, harvested in PBS and lysed in TX followed by IP with Myc antibody. In this experiment, the amount of bound S-tagged E3 ligase correlated well with the amount of precipitated Ub. * marks nonspecific band in the pellet that also serves as a loading control. **B)** As in (A), cells were grown for 28h prior to lysis in TX and IP with Myc antibody. Observed correlation between S-tag E3 and Ub in the IP, which is unaffected by the PRR domain. * marks the heavy chain in th ponceau stain of the IP, in which the precipitated Myc-ubiquilin bands are visible at the predicted MW.

Figure 3.5

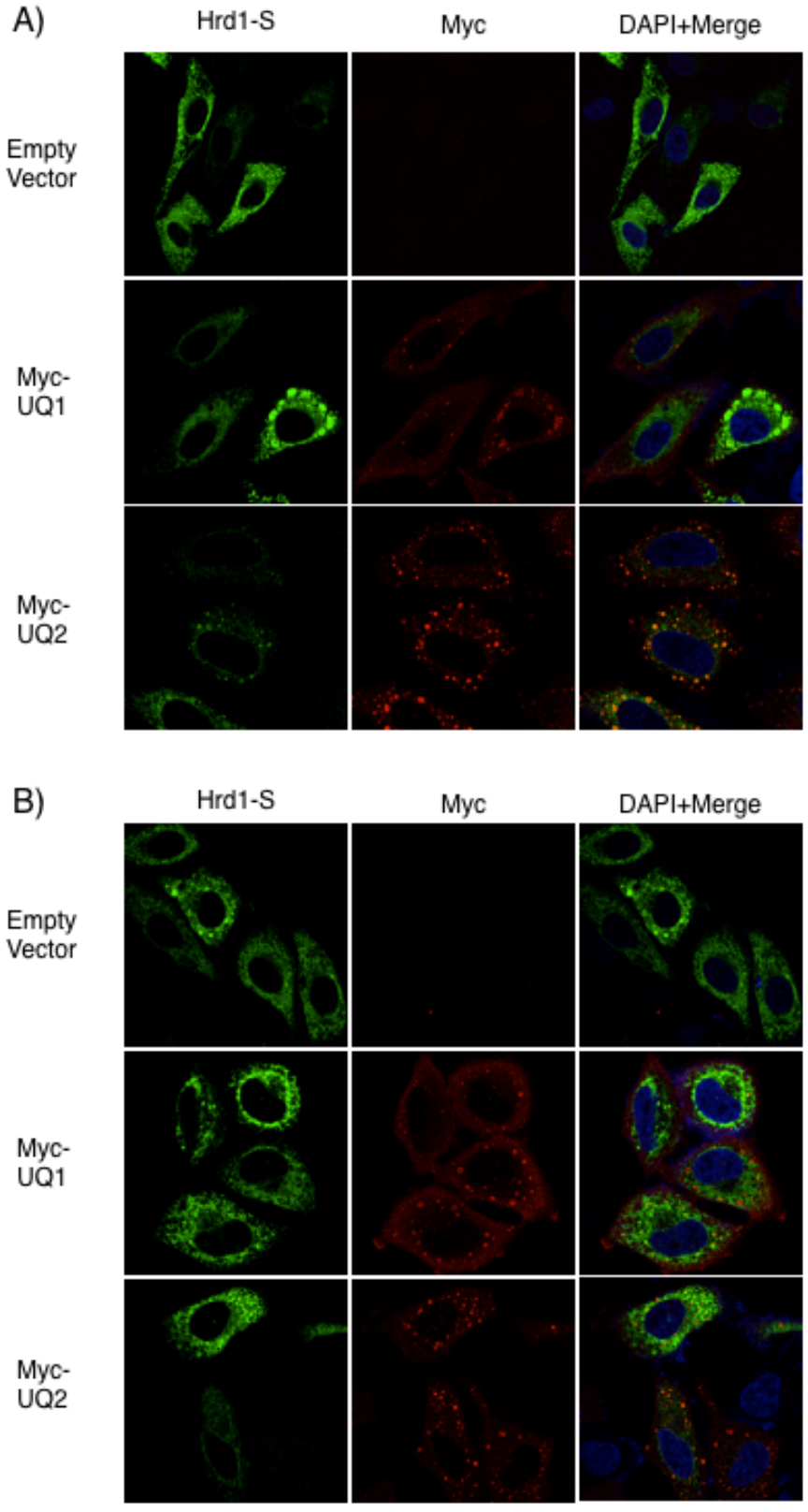
A)
Hrd1-S
Myc
DAPI+Merge
Empty Vector
Myc-UQ1
Myc-UQ2
B)
Hrd1-S
Myc
DAPI+Merge
Empty Vector
Myc-UQ1
Myc-UQ2

Ubiquilins exhibit partial localization with Hrd1-S. **A)** HeLa cells were transfected by lipofectamine 3000 with plasmids expressing Hrd1-S and the indicated Myc-UQ construct. Cells were fixed in 4%PFA, permeabilized in .2%TX, and stained with Myc and S-tag antibodies. Hrd1-S localizes in a reticular mesh pattern and occasionally forms vesicular structures (top). Co-expression with Myc-UQ1 (middle) results in some cells displaying overlapping vesicles, while the proteins clearly occupy non-overlapping compartments in other cells. Co-expression with Myc-UQ2 results in a similar localization pattern. **B)** As in (A), except that cells were fixed in 4%PFA and then permeabilized in methanol at -20C. The reticular pattern of Hrd1-S is still observed, as are Hrd1-S vesicles. Although proximal, the majority of Hrd1-S and Myc-ubiquilin vesicles are non-overlapping in methanol-fixed cells.

Figure 3.6

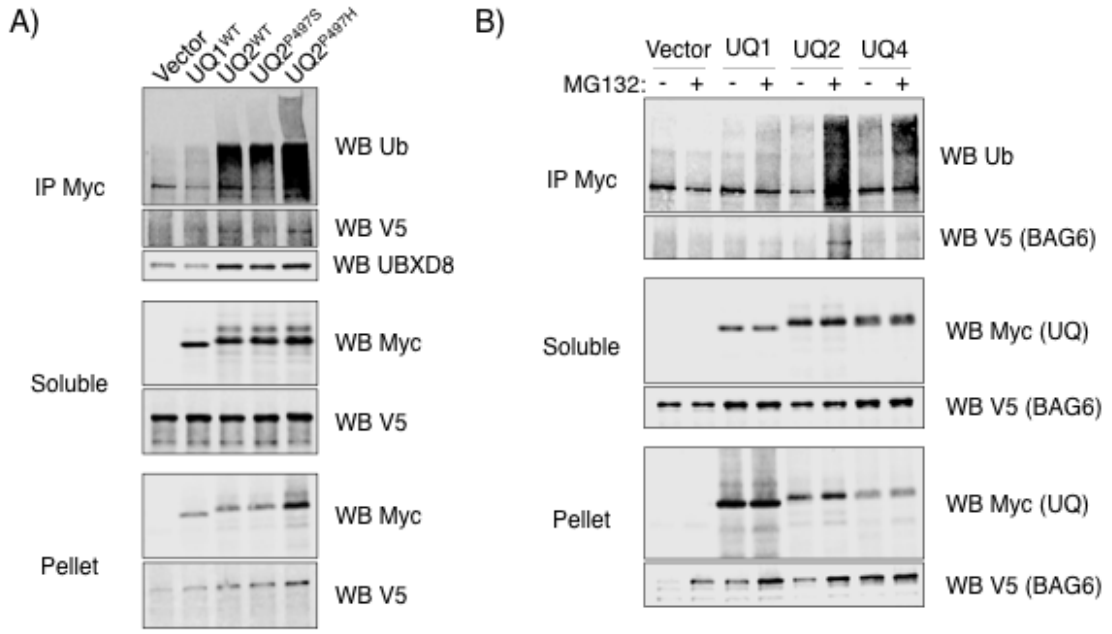

Ubiquilins interact with BAG6. **A)** HEK 293T cells were transfected by $CaPO_4$ with plasmids encoding Myc-UQ and BAG6-V5, grown for 27h, and lysed in TX followed by IP with Myc antibody. Precipitation of BAG6 correlated with the amount of precipitated Ub, as did UBXD8. BAG6 solubility was also reduced in the presence of ubiquilins, with $UQ2^{P497H}$ driving BAG6 to the pellet more than the other ubiquilins. **B)** HEK 293T cells were transfected by $CaPO_4$ with plasmids encoding Myc-UQ and BAG6-V5, grown 24h, then split to 4 plates and grown for an additional ~48h. Cells were treated with MG132 (5μM 5h) prior to lysis in TX, followed by IP with Myc antibody. In this case, Myc-UQ2 interacted most strongly with BAG6 following proteasome inhibition, whereas Myc-UQ4 interacted with BAG6 to the same extent in mock or MG132-treated cells. BAG6 shifted to the insoluble phase following proteasome inhibition, except in cells expressing Myc-UQ4, in which BAG6 was markedly insoluble under basal conditions (n=2).

Figure 3.7

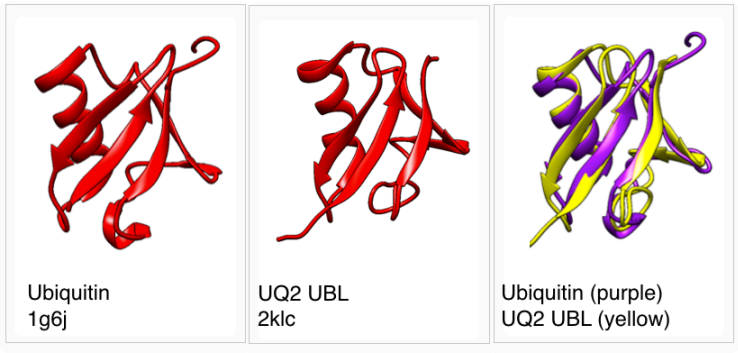


```
                 *         *  *           *                   *  *
UQ1 31-112 SAEPKIMKVTVKTPK-EKEEFAVPENSSVQQFKEEISKRFKSHTDQLVLIFAGKILKDQDGIHDGLTVHLVIKTQNRP
UQ2 27-108 PAEPKIIKVTVKTPK-EKEEFAVPENSSVQQFKEAISKRFKSQTDQLVLIFAGKILKDQDGIHDGLTVHLVIKSQNRP
Ubiquitin  ------MQIFVKTLTGKTITLEVEPSDTIENVKAKIQDKEGIPPDQQRLIFAGKQLEDGRNIQKESTLHLVLRLRGG-
                  ::: *** . :.  : *  ..:::::.*  *..:    .**  ****** *:*  .*:.  *:***:: :.
```

UQ2 is Ub-modified. Crystal structure of Ub (1g6j) and NMR structure of the UBL domain of UQ2 (2klc) superimposed to show structural similarity. Below is a sequence alignment of the UBL domains of UQ1, UQ2, and Ub, in which a red * marks a lysine amino acid that we identified as Ub-modified in the mass spectrometry data sets.

3.6 References

1. Kay, B. K., Williamson, M. P. & Sudol, M. The importance of being proline: the interaction of proline-rich motifs in signaling proteins with their cognate domains. *FASEB J* **14,** 231–241 (2000).
2. Suzuki, R. & Kawahara, H. UBQLN4 recognizes mislocalized transmembrane domain proteins and targets these to proteasomal degradation. *EMBO Rep* (2016). doi:10.15252/embr.201541402
3. Yun Lee, D., Arnott, D. & Brown, E. J. Ubiquilin4 is an adaptor protein that recruits Ubiquilin1 to the autophagy machinery. *EMBO Rep* **14,** 373–381 (2013).
4. Ohno, A. *et al.* Structure of the UBA domain of Dsk2p in complex with ubiquitin molecular determinants for ubiquitin recognition. *Structure* **13,** 521–532 (2005).
5. Walters, K. J., Kleijnen, M. F., Goh, A. M., Wagner, G. & Howley, P. M. Structural studies of the interaction between ubiquitin family proteins and proteasome subunit S5a. *Biochemistry* **41,** 1767–1777 (2002).
6. Chen, X. *et al.* Structures of Rpn1 T1:Rad23 and hRpn13:hPLIC2 Reveal Distinct Binding Mechanisms between Substrate Receptors and Shuttle Factors of the Proteasome. *Structure* 1–15 (2016). doi:10.1016/j.str.2016.05.018
7. Ryu, K.-S. *et al.* Binding surface mapping of intra- and interdomain interactions among hHR23B, ubiquitin, and polyubiquitin binding site 2 of S5a. *J Biol Chem* **278,** 36621–36627 (2003).
8. Chang, L. & Monteiro, M. J. Defective Proteasome Delivery of Polyubiquitinated Proteins by Ubiquilin-2 Proteins Containing ALS Mutations. *PLoS ONE* **10,** e0130162 (2015).
9. Olzmann, J. A., Richter, C. M. & Kopito, R. R. Spatial regulation of UBXD8 and p97/VCP controls ATGL-mediated lipid droplet turnover. *Proceedings of the National Academy of Sciences* **110,** 1345–1350 (2013).
10. Xia, Y. *et al.* Pathogenic mutation of UBQLN2 impairs its interaction with UBXD8 and disrupts endoplasmic reticulum-associated protein degradation. *J Neurochem* n/a–n/a (2013). doi:10.1111/jnc.12606
11. Fang, S. *et al.* The tumor autocrine motility factor receptor, gp78, is a ubiquitin protein ligase implicated in degradation from the endoplasmic reticulum. *Proc Natl Acad Sci USA* **98,** 14422–14427 (2001).
12. Zhang, T., Xu, Y., Liu, Y. & Ye, Y. gp78 functions downstream of Hrd1 to promote degradation of misfolded proteins of the endoplasmic reticulum. *Mol Biol Cell* **26,** 4438–4450 (2015).
13. Christianson, J. C. *et al.* Defining human ERAD networks through an integrative mapping strategy. *Nat Cell Biol* **14,** 93–105 (2012).
14. Carvalho, P., Goder, V. & Rapoport, T. A. Distinct ubiquitin-ligase complexes define convergent pathways for the degradation of ER proteins. *Cell* **126,** 361–373 (2006).
15. Kikkert, M. *et al.* Human HRD1 is an E3 ubiquitin ligase involved in degradation of proteins from the endoplasmic reticulum. *J Biol Chem* **279,** 3525–3534 (2004).
16. Bernasconi, R., Galli, C., Calanca, V., Nakajima, T. & Molinari, M. Stringent requirement for HRD1, SEL1L, and OS-9/XTP3-B for disposal of ERAD-LS substrates. *J Cell Biol* **188,** 223–235 (2010).
17. de Bie, P. & Ciechanover, A. Ubiquitination of E3 ligases: self-regulation of the

ubiquitin system via proteolytic and non-proteolytic mechanisms. *Cell Death Differ* **18,** 1393–1402 (2011).
18. Hessa, T. *et al.* Protein targeting and degradation are coupled for elimination of mislocalized proteins. *Nature* **475,** 394–397 (2011).
19. Kawahara, H., Minami, R. & Yokota, N. BAG6/BAT3: emerging roles in quality control for nascent polypeptides. *J Biochem* **153,** 147–160 (2013).
20. Rodrigo-Brenni, M. C., Gutierrez, E. & Hegde, R. S. Cytosolic quality control of mislocalized proteins requires RNF126 recruitment to Bag6. *Molecular cell* **55,** 227–237 (2014).
21. Leznicki, P. *et al.* The Association of BAG6 with SGTA and Tail-Anchored Proteins. *PLoS ONE* **8,** e59590 (2013).
22. Payapilly, A. & High, S. BAG6 regulates the quality control of a polytopic ERAD substrate. *J Cell Sci* **127,** 2898–2909 (2014).
23. Minami, R. *et al.* BAG-6 is essential for selective elimination of defective proteasomal substrates. *J Cell Biol* **190,** 637–650 (2010).
24. Krenciute, G. *et al.* Nuclear BAG6-UBL4A-GET4 complex mediates DNA damage signaling and cell death. *J Biol Chem* **288,** 20547–20557 (2013).
25. Wunderley, L., Leznicki, P., Payapilly, A. & High, S. SGTA regulates the cytosolic quality control of hydrophobic substrates. *J Cell Sci* **127,** 4728–4739 (2014).
26. Xu, P. *et al.* Quantitative proteomics reveals the function of unconventional ubiquitin chains in proteasomal degradation. *Cell* **137,** 133–145 (2009).
27. Newton, K. *et al.* Ubiquitin chain editing revealed by polyubiquitin linkage-specific antibodies. *Cell* **134,** 668–678 (2008).
28. Semenza, G. L. Hypoxia-Inducible Factors in Physiology and Medicine. *Cell* **148,** 399–408 (2012).
29. Rubinsztein, D. C. The roles of intracellular protein-degradation pathways in neurodegeneration. *Nature* **443,** 780–786 (2006).
30. Rodi, P. M., Gianello, M. D. B., Corregido, M. C. & Gennaro, A. M. Biochimica et Biophysica Acta. *BBA - Biomembranes* **1838,** 859–866 (2014).
31. Hjerpe, R. *et al.* UBQLN2 Mediates Autophagy-Independent Protein Aggregate Clearance by the Proteasome. *Cell* 1–16 (2016). doi:10.1016/j.cell.2016.07.001
32. Ko, H. S., Uehara, T. & Nomura, Y. Role of ubiquilin associated with protein-disulfide isomerase in the endoplasmic reticulum in stress-induced apoptotic cell death. *J Biol Chem* **277,** 35386–35392 (2002).
33. Liu, Y. *et al.* Ubiquilin-1 Protects Cells from Oxidative Stress and Ischemic Stroke Caused Tissue Injury in Mice. *J Neurosci* **34,** 2813–2821 (2014).
34. Philips, T. & Robberecht, W. Neuroinflammation in amyotrophic lateral sclerosis: role of glial activation in motor neuron disease. *Lancet Neurol* **10,** 253–263 (2011).
35. McGoldrick, P., Joyce, P. I., Fisher, E. M. C. & Greensmith, L. Biochimica et Biophysica Acta. *BBA - Molecular Basis of Disease* **1832,** 1421–1436 (2013).
36. Farg, M. A. *et al.* C9ORF72, implicated in amytrophic lateral sclerosis and frontotemporal dementia, regulates endosomal trafficking. *Hum Mol Genet* **23,** 3579–3595 (2014).
37. Lim, J. *et al.* A Protein–Protein Interaction Network for Human Inherited Ataxias

and Disorders of Purkinje Cell Degeneration. *Cell* **125,** 801–814 (2006).
38. Leznicki, P. & High, S. SGTA antagonizes BAG6-mediated protein triage. *Proceedings of the National Academy of Sciences* **109,** 19214–19219 (2012).
39. Ling, S.-C. *et al.* ALS-associated mutations in TDP-43 increase its stability and promote TDP-43 complexes with FUS/TLS. *Proc Natl Acad Sci USA* **107,** 13318–13323 (2010).

Chapter 4) Differential ubiquitylation and solubility of UQ2 ALS mutants

Overview

This chapter comprises the most complete work I've done in the Tibbetts lab, in collaboration with Dr. Mark Scalf from the Smith Lab, (soon to be Dr.) Chris Hooper from the Miyamoto Lab, and a very talented undergraduate student in my lab, Chi Chi Xie. Much of this work is being packaged together with a Drosophila model of UQ2 toxicity for publication. Although I helped to design and interpret some of the fly data, Chi Chi has performed the characterization of transgenic Drosophila lines expressing UQ2 and UQ2 ALS mutants, with material contributions from a former graduate student in the lab, Dr. Lihong Zhan. I am excluding the Drosophila data from this chapter in order to focus on my contributions. Drawing on MS data from chapter 3, the major findings in this chapter are that UQ2 is more ubiquitylated than UQ1, and there exists a single hypermorphic ALS mutant, $UQ2^{P497H}$, with unique biochemical properties. Other significant findings include insolubility of $UQ2^{P497H}$ through both Ub-dependent and –independent mechanisms and that there is an ubiquitylation-directing N-terminal sequence in UQ2 that is not conserved in UQ1.

4.1 Abstract

Members of the ubiquilin (UBQLN) family of ubiquitin (Ub)-binding chaperones participate in proteasome- and autophagosome-mediated protein degradation and are broadly implicated in neurodegenerative disease. Notably, mutations in a proline-rich-repeat (PRR) domain of UBQLN2 (UQ2) cause X-linked amyotrophic lateral sclerosis (ALS)/frontotemporal lobar degeneration (FTD); however, neither the normal functions of the PRR nor impacts of ALS-associated mutations in UQ2 are well understood. We

performed a comparative analysis of UQ2 and its closely related paralog, UQ1, and found that the PRR domain contributes to increased ubiquitylation of UQ2. Ub modification of UQ2 is diminished by disruption of the UBA domain, as well as by removal or replacement of the first 30aa of UQ2, which contains unique proline motifs. A comparison of $UQ2^{ALS}$ mutants revealed increased ubiquitylation and reduced solubility of a single mutant, $UQ2^{P497H}$, whereas other ALS mutants were similar to wild-type UQ2.

4.2 Introduction

The proteotoxicity hypothesis for neurodegeneration emerged from the histologic characterization of several diseases, including Alzheimer's Disease, Parkinson's Disease, Huntington's Disease, and ALS[1]. These heterogeneous conditions are collectively referred to as proteinopathies, in which pathology is characterized by aggregates of disease-specific proteins in affected tissues of the central nervous system. The discovery that dominant mutations in superoxide dismutase 1 (SOD1) cause ~20% of familial ALS (fALS) cases first established the proteotoxic etiology of ALS[2]. Mutant SOD1 proteins assume toxic folds, disrupt intracellular regulation, and kill motor neurons through autonomous and non-autonomous mechanisms[3]. More recently, mutations in the nuclear RNA-binding proteins, TDP-43 and FUS/TLS, were identified in fALS, with most disease mutations occurring in low-complexity regions of the proteins, resulting in a proclivity for aggregation[4-7]. Furthermore, cytosolic aggregation of wild-type TDP-43 is observed in affected brain and spinal cord of >90% of sporadic ALS cases, establishing TDP-43 inclusion pathology among the most reliable histopathologic markers of non-SOD1 ALS[8]. The most recent discovery of G4C2 hexanucleotide repeat expansions (HREs) in the *C9ORF72* gene[9,10]—which are far-and-away the most common genetic

cause of ALS—may also instigate toxicity, at least in part, through proteotoxic mechanisms involving dipeptide repeat proteins that are produced from the G4C2 repeat via repeat associated non-ATG (RAN) translation[11,12].

The toxicity of ALS disease proteins may result from burdened cellular pathways related to protein trafficking and degradation, altering the localization and abundance of proteins that contribute to degeneration in vulnerable populations of neurons[13]. Mutations in several genes that regulate protein homeostasis are implicated in ALS and other neurodegenerative diseases. These genes include optineurin (OPTN) and Tank-binding kinase 1 (TBK1), which participate in a common pathway to regulate autophagy[14-16]; valosin-containing protein (VCP, p97 in mouse) and p62/SQSTM1, which are dual mediators of proteasomal and autophagosomal protein degradation[17-19]; and additional genes involved in endosome traffic and membrane remodeling, including CHMP2B, Alsin, and VAPB[20](reviewed here[21]). In 2011, Deng and colleagues reported that mutations in *UBQLN2* cause rare, X-linked forms of ALS/FTD. The *UBQLN2* gene product, UQ2, belongs to a family of eukaryotic ubiquilin proteins that are thought to participate in both proteasomal and autophagosomal protein degradation. Development and application of UQ2-specific antibodies in post-mortem immunohistochemistry have revealed that UQ2 is abundant in Ub-positive protein aggregates, both in cases of *UBQLN2* mutation and in sALS [22,23]. UQ2 is strikingly abundant in pathological inclusions related to the *c9ORF72* expansion, as well as in additional, genetically distinct neurodegenerative diseases, implying that UQ2 might function more generally in Ub-mediated aggregation[24 25,26].

Ubiquilins harbor a similar domain architecture comprised of an N-terminal Ub-like (UBL) domain and C-terminal Ub-associated (UBA) domain. The UBL domain mediates interactions with the proteasome[27-29], Ub-binding endosome proteins, such as EPS15 and Hrs[30], and likely with several additional Ub-binding domains. The UBA binds with roughly equal affinity to all homotypic tetraUb chains, including M1-, K48-, and K63-linked polyUb, and shows modest binding to monoUb[31,32]. The central region of ubiquilins is comprised of a series of STI1 repeats and is thought to mediate protein-protein interactions and self-association[33,34]. Through their dual UBL-UBA configuration, ubiquilins are thought to mediate delivery of Ub-modified substrates to the proteasome [28,35]. Importantly, ubiquilins physically and genetically interact with proteins implicated in several neurodegenerative diseases, including TDP-43[36,37], presinilin[38,39], amyloid precursor protein[40], and polyQ expansions[41,42], indicating that ubiquilins function in relevant proteotoxic stress response pathways.

Among the seven mammalian ubiquilin family members, UQ1 and UQ2 are more similar to each other than any other pairwise combination[43], exhibiting 95% amino acid similarity. The most obvious difference between UQ1 and UQ2 is the presence of a proline-rich-repeat (PRR) segment in UQ2 that contains iterations of the tripeptide sequence P-[I/X]-[G/X] (Fig.). Interestingly, several clinically validated UQ2 ALS mutations occur in the PRR, suggesting that this domain is connected to UQ2-associated neurodegeneration[22]. Neither the normal cellular functions of UQ2 nor the biochemical functions of the PRR have been elucidated. In this study, we found that UQ1 and UQ2 are biochemically distinct entities that are differentially ubiquitylated; the PRR contributes to, but is not wholly responsible for these biochemical differences. Through a

series of chimeric constructs, we identified an additional amino-terminal sequence in UQ2 that modifies ubiquitylation status. Heightened ubiquitylation correlates with heightened detergent solubility, which is uncoupled by the P497H substitution, resulting in both hyper-ubiquitylation and detergent resistance of this particular mutant. We report that both wild type and UQ2 ALS mutants disrupt proteasome-dependent degradation of a model substrate in an Ub-binding dependent manner. Collectively, this work demonstrates divergent properties of UQ2 ALS mutants in cell culture models that do not translate to differential disruption of the Ub-proteasome system.

4.3 Results

4.3.1 UQ2 is more Ub-modified than UQ1

UQ1 and UQ2 are highly similar with the notable exception of the UQ2-specific PRR (Fig. 4.1A). To investigate possible functional differences between UQ1 and UQ2, we first assessed association with endogenous Ub in co-immunoprecipitation (co-IP) experiments[44]. As seen in Fig. 4.1B, we found that transiently transfected Myc-UQ1 or Myc-UQ2 in HEK 293T cells co-precipitated comparable levels of polyUb in the presence of the zwitterionic detergent CHAPS; however, Myc-UQ2 precipitated considerably more polyUb than Myc-UQ1 in the presence of the non-ionic detergent, Triton X-100 (TX) (Fig. 4.1B). In both conditions, we observed that a band likely corresponding to mono-ubiquitylated (monoUb) UQ2 was relatively more abundant than the equivalent band for UQ1 (Fig. 1B, arrow). We analyzed the ubiquilin immunoprecipitates by LC-MS/MS to verify Ub modification of UQ2. DiGly-signatures in our MS dataset confirmed Ub-modified residues within UQ2 to several Lys (K31, K41, K43, K58, K79), all of which reside in the UBL domain. Additionally, K11-, K48-,

and K63-polyUb chains were identified by LC-MS/MS, although it is not known if these Ub chains were covalently attached to UQ2 or co-precipitated via binding to the UBA domain.

We hypothesized that the presence of the PRR might alter the Ub-binding affinity of UQ2. To test this, we performed pull-down experiments using monoUb-conjugated agarose beads incubated with lysates from cells expressing Myc-UQ1 or Myc-UQ2, and observed similar affinity of ubiquilins for monoUb (Fig. 4.7A). Additionally, we performed several *in vitro* GST-fusion pull-down experiments conducted with a variety of purified and heterogeneous Ub substrates and conclude that the PRR does not directly enhance Ub-binding by UQ2 (Fig 4.2). We formulated that the polyUb signal in non-denaturing IPs likely represents both Ub-modified ubiquilin and polyUb substrates bound non-covalently through the UBA domain. We therefore carried out IP experiments under more stringent conditions (RIPA buffer) to selectively visualize covalent Ub modification of UQ2. As expected, we observed increased IP of polyUb by Myc-UQ2 relative to Myc-UQ1 in TX buffer, and MG132 treatment increased polyUb IP by both ubiquilins (Fig 4.1C). In RIPA, the signal for UQ1 IPs was near baseline, whereas UQ2 IPs retained Ub-positive signal in both mock- and MG132-treated cells (Fig 4.1C), indicating that Myc-UQ2 is likely ubiquitylated to a greater extent than Myc-UQ1.

We also analyzed endogenous ubiquilin proteins to confirm differential Ub-modification of UQ2. We performed IPs with UQ1- and UQ2-specific antibodies and observed polyUb enrichment in the UQ2 IP following MG132, but not in the UQ1 IP (data not shown). We employed a third antibody that recognizes both proteins to perform IP experiments in HeLa cells stably expressing shRNA targeting either *UBQLN1* or

UBQLN2. This approach allows selective enrichment of endogenous UQ1 following *UBQLN2* knockdown and vice-versa, while maintaining the same antibody for enrichment. We found that knockdown of *UBQLN2* resulted in reduction of polyUb IP, whereas depletion of *UBQLN1* resulted in a slight increase of polyUb IP under normal conditions (Fig 4.1D). Analysis of mRNA levels corresponding to *UBQLN1* and *UBQLN2* revealed a compensatory increase in message of the remaining paralog, i.e., *UBQLN2* is transcriptionally upregulated in *UBQLN1* knockdown, although the converse induction is not as strong (Fig. 4.3). Collectively, these findings indicate regulatory ubiquitylation of UQ2 not shared with UQ1, which we investigated further.

4.3.2 Ubiquilins undergo coupled mono-ubiquitylation

We wanted to identify the minimal sequence elements required for ubiquitylation of UQ2, beginning with the PRR. We measured the ubiquitylation of a deletion mutant of UQ2 lacking the PRR ($UQ2^{\Delta PRR}$) and an insertion mutant of UQ1 containing the PRR ($UQ1^{+PRR}$) (Fig. 4.4). Deletion of the PRR only slightly diminished the ubiquitylation of $UQ2^{\Delta PRR}$, whereas insertion of the PRR into $UQ1^{+PRR}$ failed to increase its ubiquitylation (Fig. 4.5A). In CHAPS, all of the proteins bound equally well to polyUb, indicating that regions outside of the PRR must dictate modification of UQ2 (data not shown). We disrupted the UBA domain by installing a single point mutation, F559A in UQ1, F594A in UQ2 (denoted ^{UBA*})[45], and found that UBA* mutants neither bind Ub nor are they efficiently ubiquitylated, suggesting that Ub-binding is required for ubiquitylation (Fig. 4.5B). This is reminiscent of endocytic proteins that are ubiquitylated in a Ub-binding dependent manner, a process termed coupled mono-ubiquitylation[46,47]. We also find that the PRR does not alter the solubility of ubiquilins: UQ1 is relatively more insoluble than

UQ2, most clearly observed when cells are harvested 72H after transfection, and the solubility of both proteins is increased by the UBA* mutation (Fig. 4.5B, 4.5C).

Transfected ubiquilins form punctate cytosolic structures that localize with endocytic proteins, as well as with endogenous Ub, p62, and subunits of the proteasome (see chapters 2 and 3 for IF images of transfected ubiquilins) [30,36,48]. The localization pattern is punctate and typically concentrated around the periphery of the vesicles, which stain strongly for Ub. The UBA* mutants exhibit an unexpected localization pattern in more than 80% of cells: large, malformed vesicles that strongly localize with the endosome marker, EEA1, and rarely localize with Ub (Fig. 4.6A, 4.6B). To more accurately assess the localization of UQ1 and UQ2, we generated doxycycline-inducible U-2 OS cells in which expression of the transgenes could be titrated (Fig. 4.5D). Although both proteins formed small cytoplasmic vesicles, they were much more abundant for UQ2 than UQ1 (Fig. 4.5E). We found that removal of the PRR resulted in diminished punctate localization of $UQ2^{\Delta PRR}$, but not to the level observed for UQ1, while $UQ1^{+PRR}$ localization was similar to $UQ1^{WT}$ (Fig. 4.5E, 4.5F). Expression of the $UQ2^{UBA*}$ in this system yielded a diffuse signal in the cytosol, in agreement with previously published data on $UQ2^{\Delta UBA}$ and indicating a possible lipofection artifact (Fig 4.6C)[36]. ALS mutations did not have an obvious impact on UQ2 localization by either method (Fig 3.1B, 4.6C), prompting us to examine the biochemistry of UQ2 ALS mutants.

4.3.3 Specific impact of P497H mutation on UQ2 ubiquitylation and solubility

We hypothesized that ALS mutations in the PRR might disrupt the Ub-binding / Ub-modification cycle of UQ2 because of the proximity between the two domains. To

test this, we first measured the interaction of Myc-UQ2^{WT} and a panel of Myc-UQ2^{ALS} mutants with monoUb beads and found that all proteins bound to monoUb comparably (Fig 4.7A). We then performed co-IP experiments following fractionation in a variety of detergents to investigate alterations in ubiquitylation and/or Ub-binding. IPs were performed on cells treated with the broad-spectrum deubiquitylase (DUB) inhibitor, PR-619, to assess changes in ubiquitylation and possible regulation by DUBS. In TX buffer, Myc-UQ2^{WT} and UQ2^{P525S} precipitated similar amounts of polyUb, as assessed by K48-Ub and pan-Ub antibodies, while the levels of polyUb in the Myc-UQ2^{P497H} IP were roughly twofold above UQ2^{WT}. In RIPA, UQ2^{P497H} is highly enriched for endogenous polyUb, including K48-linked polyUb species (Fig. 4.7B). We performed UbiCRest analysis of UQ2^{P497H} IP and found that the polyUb signal is complex, as only treatment with a nonspecific DUB efficiently cleaved the precipitated polyUb (Fig. 4.8A)[49]. We further measured the ubiquitylation of additional clinical mutations in the PRR and found that all mutants, except UQ2^{P497H}, behaved similarly to UQ2^{WT} in this assay, including the P497S ALS mutation at the same position (Fig. 4.7C).

We analyzed the insoluble fractions from these experiments and found abundant K48-linked Ub species in the pellet from all cells treated with PR-619, but only UQ2^{P497H} was highly enriched in the pellet fraction (Fig. 4.7B, Fig. 4.8B). We considered that the P497H substitution is unique in that it is the only basic amino acid substitution within the PRR domain, which is otherwise devoid of basic amino acids. We therefore generated two additional Pro to His substitutions at disease relevant codons 506 and 509, but found that these proteins are ubiquitylated and extracted comparably to UQ2^{WT} (Fig 4.7C). To assess the broader impact of mutant ubiquilins on protein solubility, we examined an

endogenous Ub-binding autophagy adaptor implicated in ALS, p62/SQSTM1, which colocalizes with transfected ubiquilins and functions in the regulated formation of inclusion bodies (see chapter 2 for IF localization) [19,50,51]. However, p62 solubility was unaffected by $UQ2^{P497H}$ expression (Fig. 4.7C), indicating that insoluble $UQ2^{P497H}$ aggregates do not sequester p62 under the conditions tested.

We further characterized $UQ2^{P497H}$ insolubility by performing a two-step TX-based fractionation with minor procedural modifications adapted from[52 53]. Cells expressing Myc-$UQ2^{WT}$, -$UQ2^{P497H}$, or $UQ2^{P525S}$ were extracted in TX and subject to sequential centrifugations. The pellet of the first spin (P1) primarily contains nuclei and insoluble material. An aliquot of the supernatant (S1) is removed before high-speed centrifugation to sediment protein aggregates, generating additional pellet (P20) and supernatant fractions (S20). $UQ2^{P497H}$, but not $UQ2^{WT}$ or $UQ2^{P525S}$, was enriched in the P20 fraction, while UBXD8 distribution was uniform across the samples (Fig 4.7D). We also performed this experiment with Myc-$UQ1^{WT}$, which we found to be more detergent resistant than $UQ2^{WT}$. As can be seen, $UQ1^{WT}$ is enriched in the P1 fraction relative to $UQ2^{WT}$, but this partitioning does not correlate with enrichment in the P20 fraction, suggesting that $UQ2^{P497H}$ is forming unique aggregates that sediment at high speeds (Fig. 4.7E). Given its heightened Ub modification, we assessed the stability of $UQ2^{P497H}$ by CHX chase experiments, but we did not observe differences in turnover rate, indicating that the Ub-modified protein is not subject to rapid degradation (Fig. 4.8C). From the combined findings we conclude that the Ub-binding affinity of UQ2 ALS mutants is not altered, and that $UQ2^{P497H}$ is unique among ALS mutations in its pronounced effects on UQ2 solubility and ubiquitylation.

4.3.4 PRR and N-terminus are required for maximal UQ2 Ub modification

We were interested to determine whether the PRR domain harboring a P497H mutation could dominantly confer hyper-ubiquitylation to UQ1. We mutated the PRR of the $UQ1^{+PRR}$ construct to generate $UQ1^{+P497H}$, but found that this protein behaved comparably to $UQ1^{WT}$ when transfected in 293T cells (Fig. 4.9A). It should be noted that $UQ1^{+PRR}$ and $UQ1^{+P497H}$ precipitate polyUb in CHAPS buffer, so the UBA domain is still functional in this regard (Fig. 4.9B). We rebuilt these chimeras and constructed seamless fusions of the first 482aa of UQ1 with the remaining C-term of UQ2 ($UQ1^{N}$-2^{C} and $UQ1^{N}$-P497H) to retest this hypothesis (Fig 4.10A). In this case, the chimera containing the P497H mutation was substantially more Ub-modified than the wild type construct as assessed by IP in RIPA. IPs in TX corroborated earlier data that the PRR supports robust Ub enrichment in this particular detergent (Fig. 4.10B). We noted that the monoUb band above the chimeric species in the input was reduced (Fig. 4.10B, arrow), despite enrichment of Ub by IP. We also found that $UQ1^{N}$-P497H was more readily extracted than $UQ2^{P497H}$ (Fig. 4.10B).

A second region of sequence divergence between UQ1 and UQ2 exists at the amino-termini of the proteins, which is the basis for commercially available antibodies that can distinguish between UQ1 and UQ2 (Fig. 4.11A). Notably, UQ2 harbors two conserved PXXP motifs absent from UQ1 (Fig. 4.11B). Of interest, the N-terminus is predicted to be unstructured and is adjacent to the UBL domain, which contains all of the lysine amino acids in the protein (Fig. 4.11C). To test the role of these amino-terminal sequence differences, we measured the ubiquitylation of UQ1-UQ2 chimeras containing either the amino terminus of UQ1 through the UBL domain ($UQ1^{UBL}$-$UQ2^{C}$), or just the

first 31aa of UQ1 ($UQ1^{31}$-$UQ2^{C}$), either with or without the P497H mutation (denoted $UQ1^{UBL}$-P497H and $UQ1^{31}$-P497H) (Fig 4.10A). As shown in Fig. 4.10C, the P497H mutation stimulated hyperubiquitylation of both $UQ1^{UBL}$-$UQ2^{C}$ and $UQ1^{31}$-$UQ2^{C}$ chimeras. Once again, we observed that the monoUb band in the input was reduced for the N-terminal chimeras (Fig 4.10C, arrow), and the P497H-harboring chimeras were more efficiently extracted than the parental $UQ2^{P497H}$.

4.3.5 P497H mutation uncouples UQ2 ubiquitylation from solubility

We hypothesized that truncation of the N-terminal 30aa from UQ2 should hamper its ubiquitylation. We generated $UQ2^{\Delta N30}$ and $P497H^{\Delta N30}$ constructs and repeated IP experiments (Fig 4.10A). The ΔN30 constructs exhibited similar Ub IP in TX, likely a reflection of non-covalent UBA-dependent interactions with polyUb (Fig. 4.12A). In RIPA, $P497H^{\Delta N30}$ precipitated less Ub relative to the parental $UQ2^{P497H}$, although $P497H^{\Delta N30}$ was still increased relative to $UQ2^{\Delta N30}$ (Fig. 4.12A). Strikingly, the monoUb band was dramatically reduced for the ΔN30 proteins and both proteins were highly detergent resistant, suggesting that ubiquitylation might promote solubility (Fig. 4.12B). We generated constructs with all lysine amino acids in the UBL mutated to arginine (denoted ^{K*R}) in order to formally test this idea. It can be plainly observed that the monoUb band is reduced (although not ablated, possibly due to a lysine in the Myc epitope and a free N-terminal amine) and these proteins are highly detergent resistant (Fig. 4.12C). As expected, the amount of precipitated Ub is highly reduced for $P497H^{K*R}$ (Fig. 4.9C). The $UQ2^{K*R}$ constructs also exhibit a unique localization pattern defined by abundant, very small vesicles, confirming that Ub-binding and Ub-modification regulate ubiquilin trafficking (Fig. 4.12D).

Although several independent lines of data seem to indicate that Ub-modification promotes solubility of various ubiquilin proteins, $UQ2^{P497H}$ is both hyper-ubiquitylated and insoluble. We generated a compound mutant of $UQ2^{P497H}$ harboring the F594A mutation in its UBA domain to assess the contributions of Ub binding to the aberrant properties of $UQ2^{P497H}$. As expected, the ubiquitylation and Ub-binding of $P497H^{UBA*}$ resembled $UQ2^{UBA*}$, indicating that the UBA domain is required for these properties (Fig 4.12E). To our surprise, we found that $UQ2^{P497H/UBA*}$ was highly resistant to detergent as a function of time. At 24H after transfection, the UBA* mutants exhibit greater solubility than their Ub-binding counterparts. At 72H after transfection, the $P497H^{UBA*}$ double mutant is markedly insoluble, while $UQ2^{UBA*}$ is highly soluble (Fig. 4.12F). Other ALS mutants analyzed in this method were similar to $UQ2^{WT}$ (Fig. 4.13A), and the relative insolubility of $UQ1^{WT}$ was greater at 72H than at 24H (Fig. 4.13B). It seems that $UQ2^{P497H}$ can aggregate in both Ub-dependent and –independent mechanisms (Fig. 4.13C), and that hyper-ubiquitylation of $UQ2^{P497H}$ may be occurring due to an uncoupling mechanism, explored further in the discussion.

4.3.6 Wild-type and ALS mutant UQ2 proteins inhibit protein degradation

We characterized the functional impact of mutant ubiquilin expression on the ubiquitin-proteasome system. A previous study reported that $UQ2^{ALS}$ mutants retard the degradation of an unstable proteasome substrate in mammalian cells, known as Ub^{G76V}-GFP [22]. The stabilizing effects of the mutants in this assay were greater than those observed for $UQ2^{WT}$, which was surprising given several other studies showing that $UQ2^{WT}$ expression stabilizes proteasome substrates (see discussion). To address this issue further, we transfected HeLa cells stably expressing an integrated Ub^{G76V}-GFP reporter

with wild-type and ALS mutant UQ2 plasmids, and analyzed Ub^{G76V}-GFP stabilization by Western blotting and fluorescence microscopy[54]. Expression of $UQ2^{WT}$ stabilized Ub^{G76V}-GFP in a dose-dependent manner, whereas the Ub-binding null $UQ2^{UBA*}$ mutant had no activity (Fig 4.14A). ALS mutants also stabilized Ub^{G76V}-GFP and, in the case of $UQ1^{WT}$ and $UQ2^{P497H}$, stabilization required a functional UBA domain (Fig. 4.14B).

By live cell imaging, Ub^{G76V}-GFP was not visible in cells under basal conditions. After a short treatment with MG132, we observed uniformly increased fluorescence across all cells[55]. Cells transfected with $UQ2^{WT}$ harbored fluorescence in vesicular structures that varied in size and were qualitatively similar in cells transfected with UQ2 ALS mutants, but were absent from cells transfected with $UQ2^{UBA*}$ (Fig. 4.14C). Using immunofluorescence microscopy, we found that Ub^{G76V}-GFP was strongly localized with both wild type and ALS mutant UQ2 proteins, suggesting that UQ2 overexpression may inhibit Ub^{G76V}-GFP degradation directly through sequestration of exposed polyUb chains (Fig. 4.14D). Notably, these vesicles were consistently smaller in cells expressing K*R variants, which also stabilized Ub^{G76V}-GFP. We observed the characteristic, malformed vesicles in cells expressing $UQ2^{UBA*}$, but many structures did not contain GFP signal or were weakly positive for Ub^{G76V}-GFP (Fig. 4.14D).

4.4 Discussion

This study lends to a growing body of evidence that ubiquilin proteins fulfill distinct roles in proteostasis and are differentially regulated[56-58]. We report that the PRR domain functions together with the N-terminus of UQ2 to promote its ubiquitylation, and our data provide new insights into the divergent biochemical impacts of ALS mutations in UQ2.

Despite greater than 70% amino acid identity, UQ1 and UQ2 exhibited differential ubiquitylation and detergent solubility in cell culture experiments. Although the PRR is the most conspicuous difference between UQ1 and UQ2, it is only partially responsible for the distinct biochemical behaviors of UQ2. Deletion of the PRR caused a small reduction in UQ2 ubiquitylation, but had little impact on UQ2 solubility. Truncation of the N-terminal 30aa, on the other hand, reduced UQ2 ubiquitylation and profoundly reduced solubility in common detergents. The UBA-dependent ubiquitylation of UQ2 indicates that the first 30aa is not sufficient to direct Ub-modification, despite its proximity to the UBL. We hypothesize that the UBA may engage nascent or elongating polyUb chains proximal or directly attached to E3 Ub ligases, fulfilling an essential targeting role required for ubiquitylation. Of the five ALS mutants tested, only P497H caused overt changes in UQ2 solubility and ubiquitylation in transient transfection experiments. Remarkably, neither the P497S mutation nor alternative Pro to His substitutions recapitulated the P497H insolubility or hyperubiquitylation phenotype, indicating that both the nature of the substitution (i.e., Pro to His) and its position within the PRR are critically important.

A caveat to these experiments is overexpression of ubiquilin proteins, which are estimated to be at fairly low concentration in commonly used cell lines[59]. However, this approach allowed for the study of UQ2 ALS mutants and chimeric constructs that have provided valuable insight into ubiquilin regulation by ubiquitin. Although expression of $UQ2^{P497H}$ resulted in a striking biochemical phenotype, it does not elicit a cellular stress response in mammalian cell culture (data not shown), nor does it inhibit the UPS to a greater extent than $UQ2^{WT}$ as assessed by degradation of Ub^{G76V}-GFP, a rapidly degraded

model that accumulates during stress-related alterations to proteostasis [54,60,61]. Our results are in contrast to a previously published study[22], but are consistent with a non-specific inhibitory impact of ubiquilin expression on Ub-mediated protein degradation. As such, overexpressed ubiquilins retard the degradation of a variety of proteins, including endogenous signaling molecules such as presenilin[26,62], IκBα[63], and p53[64], as well as model hydrophobic substrates from the cytosol[58] and the ER[44]. Nonetheless, such findings do not rule out proteasome disruption as a pathologic mechanism in cases of UQ2 ALS[65]; however, such effects may not be discernible in transfected cell lines.

We have constructed a model for UQ2 ubiquitylation in the context of substrate capture and release (Fig. 4.15). We posit that ubiquilins can exist in a "closed," auto-inhibited state, in which the UBL and UBA are docked in an intramolecular manner, and an "open" state, in which the UBA is free to interact with Ub, similar to a recently proposed model[66]. Important parameters in this model include the affinity of the UBA domain for Ub, polyUb, and the UBL. It is estimated that the binding affinity of the Dsk2 UBA domain (and by analogy, ubiquilin) for its own UBL domain is roughly five- to ten-fold lower than the affinity of the Dsk2 UBA domain for Ub[31,67]. However, the dissociation constant for the UBA-UBL interaction was measured using purified, isolated UBA and UBL domains, not the full-length Dsk2/ubiquilin protein. Because the UBL and UBA are connected in the same molecule, the estimated k_d is likely an underestimate of the affinity, as intramolecular events are typically more favorable than intermolecular events due to high local concentration and low entropy cost.

In the context of overexpression, we envision non-specific stabilization of many substrates bearing polyUb modifications. One possible outcome of ubiquilin binding to

the polyUb chain on a substrate would be to block chain elongation and prevent further modification[38]. If this occurs in the proximity of charged E2-Ub / E3 complex, then the UBL domain, harboring 11 lysine amino acids, may serve as the Ub acceptor, resulting in Ub modification of UQ2. At this point, the Ub-modified UBL domain resembles di-Ub and may allow for an inter- to intramolecular UBA switch, releasing the Ub-modified substrate (Fig. 4.15). It is also possible that substrate release won't occur after a single modification, due to multivalent interactions between ubiquilin and its client[66]. In the presence of a kinetically competent E3 enzyme, it is conceivable that multiple ubiquitylation events could occur on the UBL domain, forming polyUb chains anchored to a single lysine or resulting in multiple monoUb attachments[68]. We propose that the covalent attachment of many Ub moieties to the UBL domain elicits stronger intramolecular UBA binding, prompting substrate release. Of interest, the ubiquilin UBA is remarkably nonspecific and recognizes the spectrum of polyUb chains[32,69], allowing flexibility in which lysine on UQ2 is modified to induce self binding.

It is also possible this modification will recruit other Ub-binding proteins, such as p62 or OPTN, shunting the pathway towards autophagy through a nucleation event[70]. In the case of transfection, given the abnormally high concentration, it seems likely that Ub-modification may recruit more ubiquilins, leading to oligomerization through UBA/UBL dependent and independent mechanisms[34]. Although the exact role of ubiquitylation in the relationship between microscopic inclusions bodies and solubility is not known, our data suggests that Ub modification promotes the solubility of ubiquilin proteins. Thus, the affinity of UQ1 for Ub is similar to that of UQ2, but the protein is not efficiently ubiquitylated and is therefore less soluble. This hypothesis is supported by data with

$UQ2^{K*R}$ mutants, which are markedly insoluble. How the N-terminal 30aa of UQ2 supports ubiquitylation will be an important question to address in future studies.

Returning to $UQ2^{P497H}$, one interpretation of the heightened Ub-modification and insolubility of $UQ2^{P497H}$ is an uncoupling mechanism. We hypothesize that hyper-ubiquitylation of $UQ2^{P497H}$ is an attempt to solubilize the protein, which is insoluble independently of its Ub-binding activity. It's also possible that $UQ2^{P497H}$ is being ubiquitylated during the course of IP experiments, as the monoUb band above various chimeras and truncations is reduced without significant reduction of precipitated Ub. Of note, the contrasting data sets for $UQ1^{+P497H}$ vs. $UQ1^{N}$-P497H indicate that the mutated PRR is not simply a misfolded domain – insertion of the PRR is not sufficient to induce ubiquitylation of $UQ1^{+P497H}$ unless it is inserted with some modicum of care. The biophysical aspects of this particular mutant and other ALS mutants should be addressed in future studies. Although non-P497H mutations did not lead to overt changes in UQ2 solubility or ubiquitylation under the conditions tested, it is possible that alternative mutations manifest in an age- or stress-dependent manner *in vivo* to instigate neurodegeneration.

It is possible that inclusion formation is a protective adaptation to adverse conditions. In the case of certain long-lived *C. elegans* mutants, the ability to sequester proteins in insoluble aggregates serves to maintain a balanced proteome[71]. Additional studies describing the selective aggregation of specific proteins in response to stress support a model in which protein aggregation can be protective[72,73]. We speculate that UPS deficiencies related to normal aging or acute stress cause reversible, Ub-regulated protein aggregation – the aggregates can be disassembled by the action of specialized

ATPases, e.g., HSP110 in yeast, VCP in mammals, and subject to proteasomal degradation

[74,75]. There's also evidence to suggest that large protein aggregates can be directly degraded by the autophagy/lysosomal pathway[76]. Observations of UQ2-positive aggregates across a wide spectrum of disease, independent of *UBQLN2* mutations, supports the notion that UQ2 is a specialized mediator of Ub-regulated inclusion formation.

If UQ2 plays a pivotal role in inclusion formation, then perhaps a single point mutation in the PRR domain is sufficient to alter the equilibrium of aggregate formation and dissolution, resulting in the pathologic structures described in post-mortem analysis. A recent mouse model of UQ2 toxicity demonstrated that transgenic expression of $UQ2^{P497H}$ in mouse brain elicited inclusion pathology, dendritic spine abnormalities, and mild behavior defects but not overt degeneration, although this study did not employ a wild type UQ2-expressing mouse as a control[77]. An additional study in mice used viral vectors and demonstrated heightened inclusion pathology for all $UQ2^{ALS}$ mutants relative to $UQ2^{WT}$, although inclusion formation correlated with expression level[78]. Notably, in a neuronal culture model, Ceballos-Diaz et al. also found $UQ2^{P497H}$ to be much more insoluble than other ALS mutants, in agreement with our observations of this particular mutant as a biochemical outlier[78]. Further work is required to probe the consequences of PRR mutations, how they affect the reaction cycle of UQ2, and if they instigate UQ2 aggregation and ultimately neurodegeneration.

4.5 Materials and Methods

DNA Construction

pGEX6p-1 (GE Healthcare) was used for GST-fusion expression and production of recombinant proteins. UQ1 UBA (aa 523-589), UQ2 UBA (aa 557-624), and UQ2 PRR-UBA (aa 474-624) were cloned 3' of the GST-fusion and inserted into pGEX6p-1 with BamHI and EcoRI (NEB) restriction enzymes.

Several ubiquilin constructs have been previously described in Chapters 2 and 3. All point mutations were generated by site-directed mutagenesis using Phusion DNA polymerase (NEB). All targets, primers, and primer locations are listed in the master Excel spreadsheet titled, "Primers_BWF," which is available on the lab server.

$UQ1^{+PRR}$ was inserted into pCMV-Myc by inverse PCR using custom-made "ultramers" (Integrated DNA Technologies):

1) Part 1: 5' PRR reverse complement

CCCAATGGGGCCTATGGGGGTAAAAGGGACTATAGGGCCTATGGGGCCTATG

GGGGTGACTGGGCCTACAGGTCCAGTGCTTCCTAATGCC

2) Part 2: 3' PRR

CCCATAGGACCCACTGGCCCTGCAGCCCCCCCTGGCTCCACCGGCTCTGGTG

GCCCCACGGGGCCTACTGTGTCTAACGCCACACCTAGTG

The primers were designed such that amplification proceeded outward from the insertion site (NEB Phusion DNA polymerase), leaving long, non-homologous overhangs containing the PRR. The overhangs were then *in vitro* phosphorylated using T4 polynucleotide kinase (NEB) and then ligated with T4 DNA ligase (NEB) in the presence of PEG6000. Following heat inactivation according to manufacturer's instructions, the amplifications were subject to DpnI digest (Promega) to remove template, then transformed into DH5a. Colonies were selected and DNA was prepared according to

standard practices, followed by analytical restriction digests and Sanger sequencing to verify insertion. This construct was further mutagenized to generate $UQ1^{+P497H}$.

The $UQ1^{N}$-2^{C} construct was generated by Dr. Sang Hwa Kim with assistance from the boss man, himself, Randy. In this construct, an internal SmaI in UQ1 was employed with gene blocks (IDT) containing the desired C-terminal sequence – either $UQ2^{WT}$ or bearing the P497H mutation. $UQ2^{UBL}$-$UQ1^{C}$ was made by amplifying UQ2 with EcoRI and BamHI restriction overhangs (aa 1-103) and UQ1 with BamHI and KpnI restriction overhangs (aa 109-589), then digesting the amplicons and performing a three-part ligation. $UQ1^{UBL}$-2^{C} and $UQ1^{31}$-2^{C} were made by custom gene blocks (IDT) with the desired sequence, flanked by EcoRI and SalI restriction sites, there is a naturally occurring SalI site in UQ1, rendering this set of chimeras scar-free. The EcoRI sites in the N-terminus of UQ1 were altered with silent mutations to allow for the same vector appendage at the 5' site in these constructs. gBlocks are located in Primers Box VII (ID 1237 and 1238). These same conditions were used with $UQ2^{P497H}$ to make the corresponding mutant chimeric constructs.

Detailed Calcium Phophate protocol

Reagents Required:

2.5M $CaCl_2$, 2x HEPES-Buffered Saline (HBS), .1x TE Buffer, clean plasmid DNA

General Considerations:

- Use 100uL Ca^{2+}/PO_4^{2-}/DNA solution per 2ml culture medium
    - 200uL per 60mm plate (containing 3.5ml medium)
    - 400ul per 10cm dish (containing 8-10ml medium)

- Cells should be ~40% confluent at time of transfection, best expression levels are ~48H post treatment

Step-by-step:

1) Change medium on plates 2-3H before transfection (important for pH of the medium)
2) For 60mm plate, dilute DNA in .1x TE, add 10uL $CaCl_2$, solution should be 100uL total
3) Mix one volume of the Ca/DNA solution with an equivalent volume of 2x HBS by slowly dropping the 2x HBS over the Ca/DNA solution while gently finger flicking to mix. It's really important to add the Ca/DNA drop wise while flicking so that it mixes properly.
4) Pipet up and down evenly 4 times.
5) Add solution drop wise to plate with minimal rocking of the plate. Try to drop evenly over the plate from a height of about 1 inch.
6) Expose cells to precipitate for 6h - overnight, and then change medium (no PBS wash).
7) Incubate cells for desired amount of time; see references for selecting stable transfections or other downstream applications.

Notes:

- For a 10cm dish, mix 20uL $CaCl_2$ with desired amount of DNA in .1x TE, 200uL final volume. Final concentration of $CaCl_2$ in the precipitate should be 125mM, and therefore ~12.5mM in the culture medium.

- pH your 2x HBS! pH is an important parameter (see CSH protocols for recipe)

pLKO Packaging

Transfect HEK293T at ~70% confluence in DMEM containing 2% FBS, no Pen/Strep

Transfection: Lipofectamine 2K

For each shRNA:4 ug pLKO, 3 ug psPAX2, 1ug pMD2.G

Transfect evening Day 1

Change medium Day 2, switch to 2% FBS + Pen/Strep (6ml)

Harvest medium Day 3, replenish with new medium 2% FBS + P/S (6ml)

Harvest medium Day 4 or 5, depending on cells (Harvest on Day 5 has slightly higher titer, as assessed empirically)

Spin harvested medium to pellet cell debris (slow spin) and collect supernatant

Aliquot to 1ml, labeled ep tubes and snap freeze in LN2

Note: Can also be done by calcium phosphate transfection

4.6 Figures

Figure 4.1

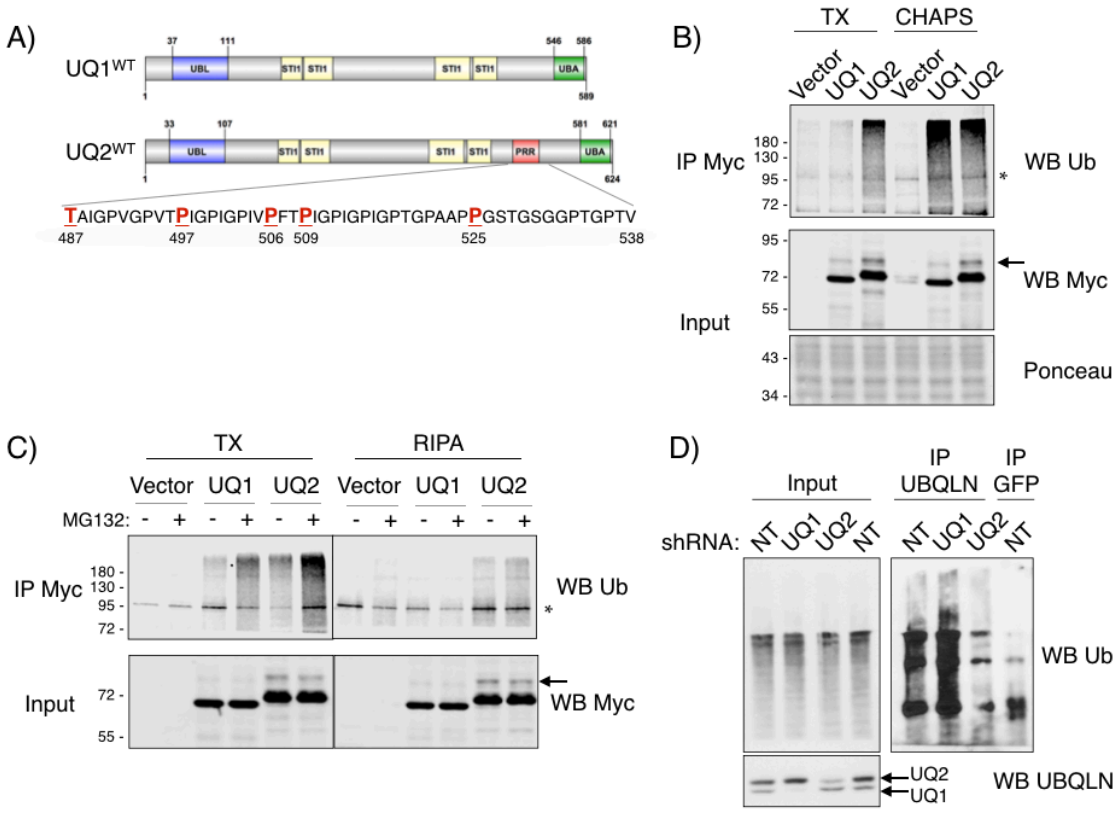

UQ2 is more Ub-modified than UQ1. **A)** Schematic diagram of UQ1^{WT} and UQ2^{WT}, which share 74% amino acid identity and 95% similarity. Proline-rich-repeat (PRR) in UQ2 is highlighted in red and primary sequence is shown; ALS-causing missense substitutions are highlighted at amino acids within the PRR. **B)** HEK 293T cells were transfected by $CaPO_4$ and grown for ~24h. Cells were harvested in PBS, split to two equal portions, and lysed in either TX or CHAPS buffer. IPs were performed with Myc antibody, separated by SDS-PAGE, and immunoblotted for endogenous Ub. Arrow indicates upper band of UQ2 that corresponds to monoUb modification. * indicates non-specific band. Ponceau stain for loading. **C)** HEK 293T were transfected by $CaPO_4$ and after 24h, plates were split to 4 plates each and grown for an addition ~48h. Where indicated, cells were treated with MG132 (10μM 4h) prior to lysis in either TX or RIPA buffer. IPs and immunoblotting performed as in (A). Arrow indicates monoUb modification and * indicates nonspecific band. **D)** HeLa cells expressing non-targeting (NT), *UBQLN1* (UQ1), or *UBQLN2* (UQ2) shRNA were subject to IP using UBQLN antibody that reacts with both UQ1 and UQ2, or using GFP antibody. IP was analyzed as in (A). In UBQLN blot, upper band corresponds to UQ2 and lower band to UQ1.

Figure 4.2

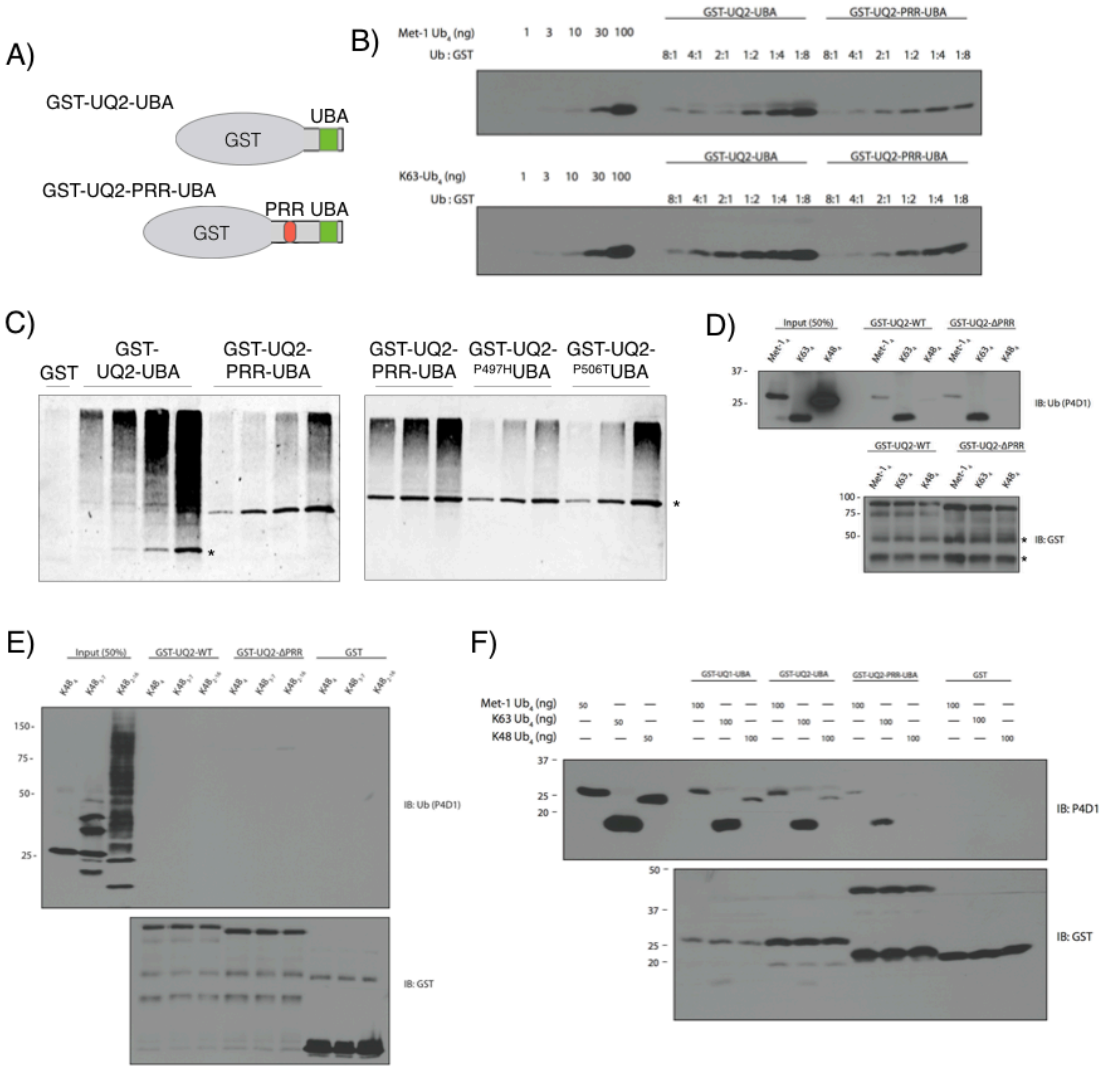

PRR does not alter Ub-binding affinity *in vitro*. **A)** Schematic of recombinant GST-fusion constructs. **B)** Hooper **C)** Increasing amounts of the indicated GST-fusions were incubated with clarified cellular extract, bound to GSH agarose and washed. The beads were boiled and analyzed by SDS-PAGE and immunoblotting against Ub. * Indicates fusion protein cross-reactivity with Ub antibody. **D) E) F)**

Figure 4.3

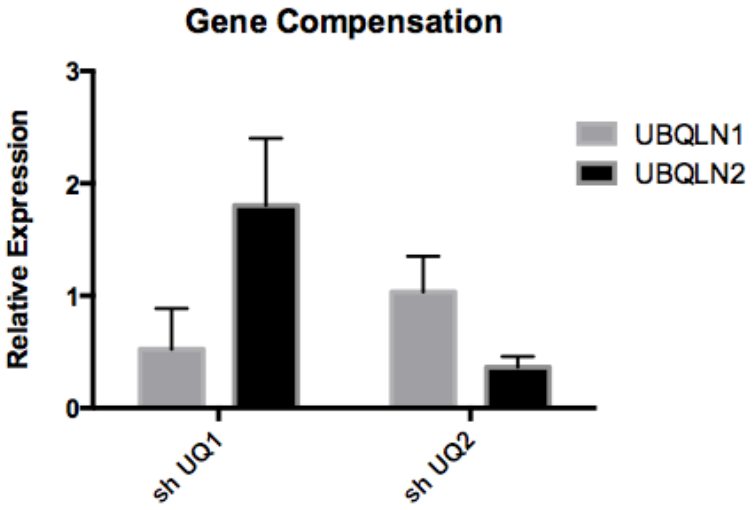

Ubiquilin compensation during stable knockdown. mRNA was prepared from HeLa cells stably expressing non-targeting, *UBQLN1*, or *UBQLN2* shRNA and analyzed by RT-PCR with primers to UQ1 and UQ2. N=4 total, n=2 in cell lines with coding sequence-directed shRNA and n=2 in cell lines with 3'UTR-directed shRNA. Expressed relative to NT shRNA.

Figure 4.4

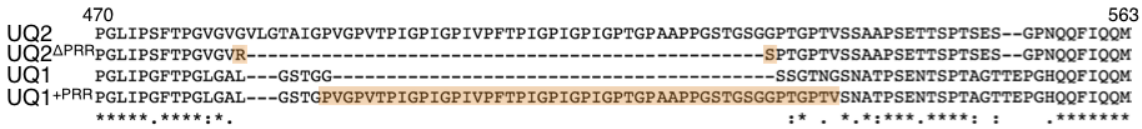

Sequence alignment of ubiquilin deletion and insertion mutants. Dr. Sang Hwa Kim constructed UQ2$^{\Delta PRR}$ by outward PCR and the introduction of a restriction site to ligate the two pieces. The scar is highlighted in orange. UQ1^{+PRR} was generated by inverse PCR with primers carrying the insertion. Following amplification, DNA was *in vitro* phosphorylated and annealed, yielding the insertion highlighted in orange.

Figure 4.5

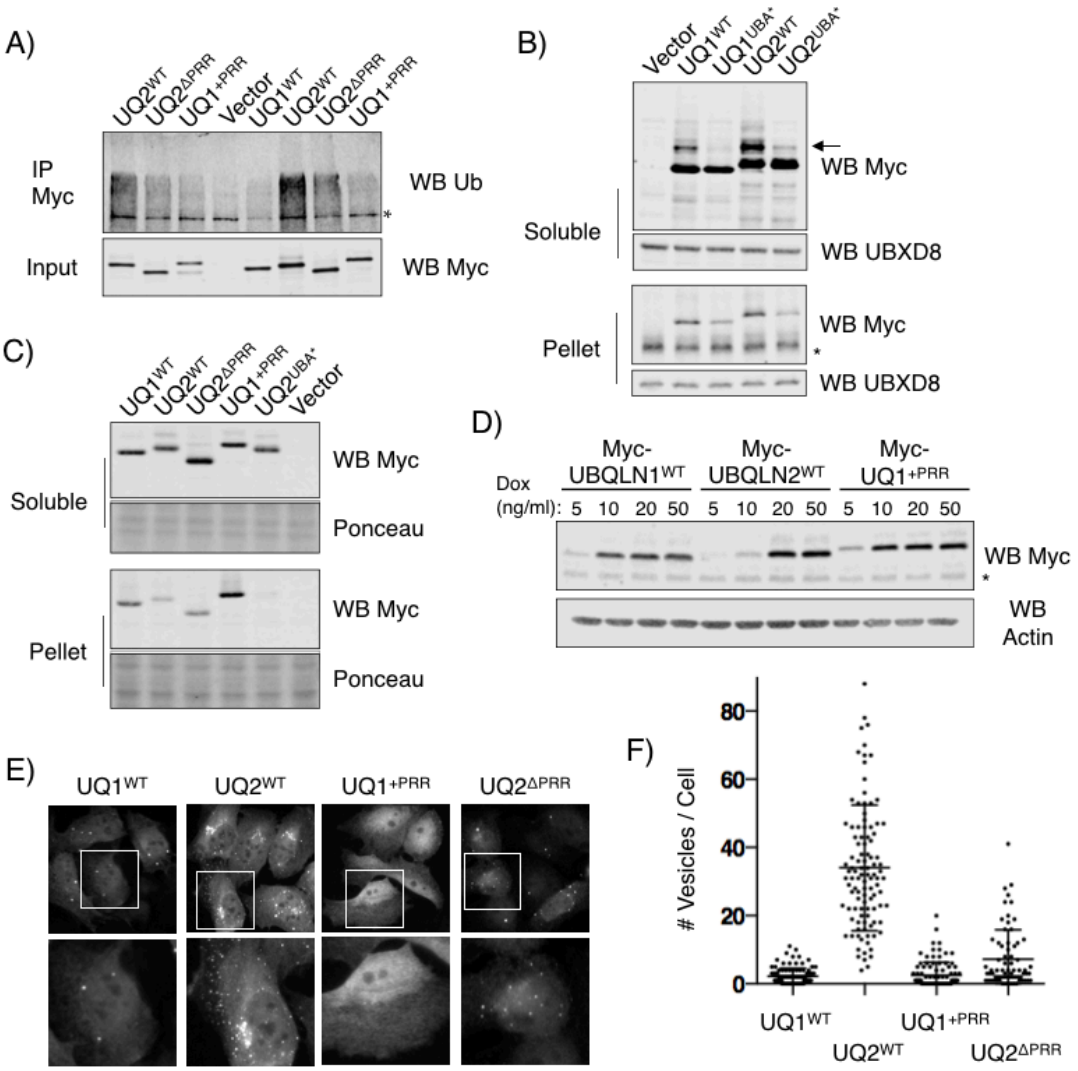

Ubiquitylation of ubiquilins does not require PRR domain, but requires the UBA domain. **A)** HEK 293T cells transfected by $CaPO_4$ were harvested after ~27h and subject to lysis in RIPA buffer. Myc IP analyzed by immunoblotting for endogenous Ub. **B)** HEK 293T cells transfected by $CaPO_4$ were harvested after ~24h and lysed in TX buffer. UBA* mutants of UQ1 and UQ2 exhibit reduced intensity of band with retarded mobility, corresponding to monoUb-modified form of protein (arrow). The UBA* mutants are also more readily extracted in detergent. * Marks immunoreactive band of protein that is not readily extracted in TX. **C)** HEK 293T cells transfected by $CaPO_4$ and analyzed as in (B). The PRR domain does not appreciably alter solubility. **D)** Dox-inducible U-2 OS cells were treated with the indicated concentration of Dox for 16h prior to harvest in TX buffer. * marks immunoreactive band not related to ubiquilins. **E)** Localization of dox-inducible ubiquilins in U-2 OS. Cells were induced with 50ng/ml Dox overnight, prior to fixation in 4% PFA, permeabilization in .2% TX, and staining with Myc antibody. Representative images are shown. **F)** Quantification of number of vesicles per cell in the

dox-inducible system. Roughly 100 cells were quantified from two separate staining experiments, and vesicles were counted manually.

Figure 4.6

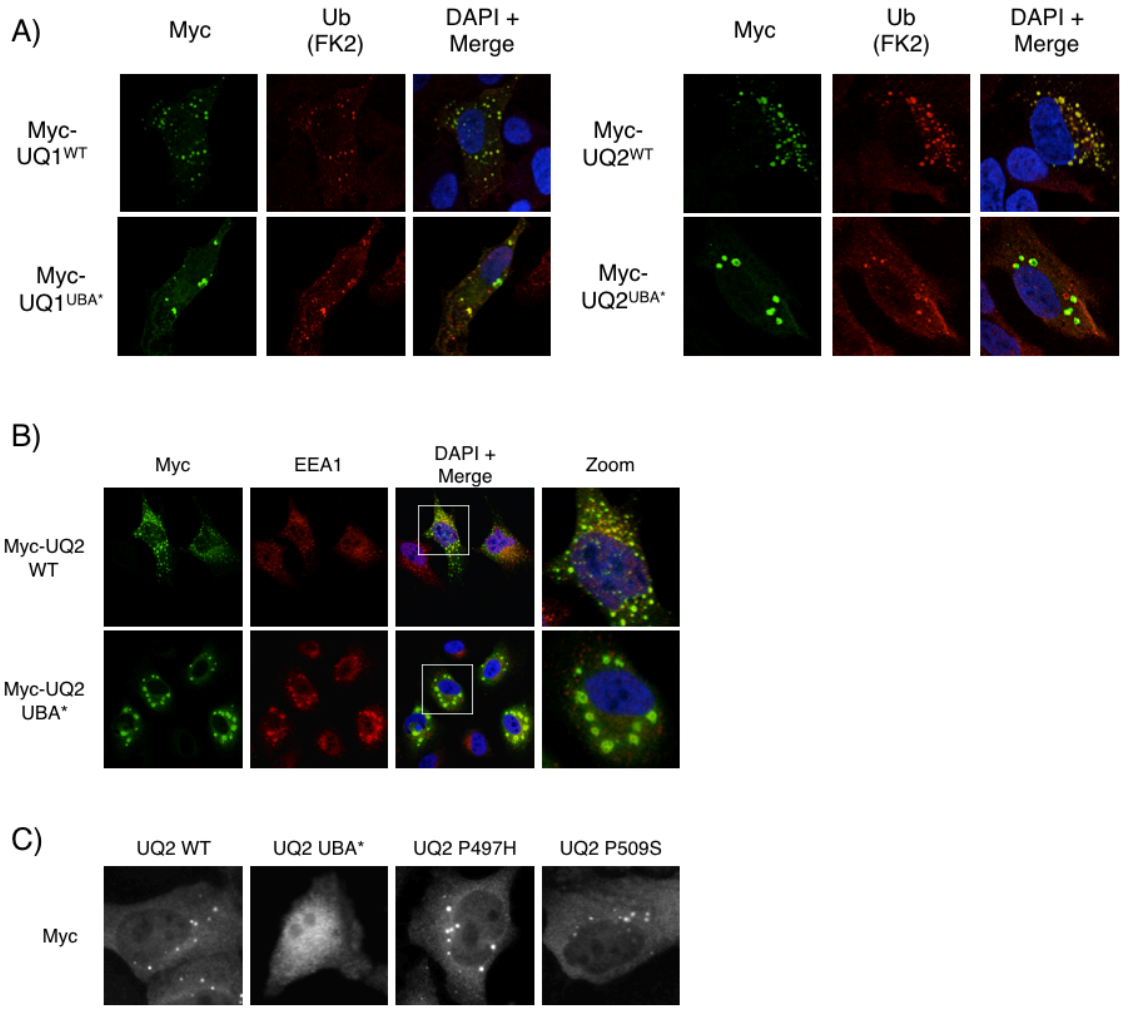

Ubiquilin localization following transfection differs from stable expression. **A)** HeLa cells were transfected by Lipofectamine 3000, grown for ~24h, then fixed in 4% PFA, permeabilized in .2% TX, and stained for Myc and endogenous Ub (FK2). Both UQ1 and UQ2 form punctate, cytosolic structures that are positive for Ub, whereas the UBA* mutants form fewer, large vesicles with irregular patterns that are only partially localized with Ub. **B)** As in (A), but stained with the endosome marker, EEA1. The UBA* mutant vesicles are strongly enriched for EEA1. **C)** Dox-inducible U-2 OS cells reveal a diffuse pattern for the UBA* mutant, whereas $UQ2^{WT}$ and the UQ2 ALS mutants (representative images) look similar.

Figure 4.7

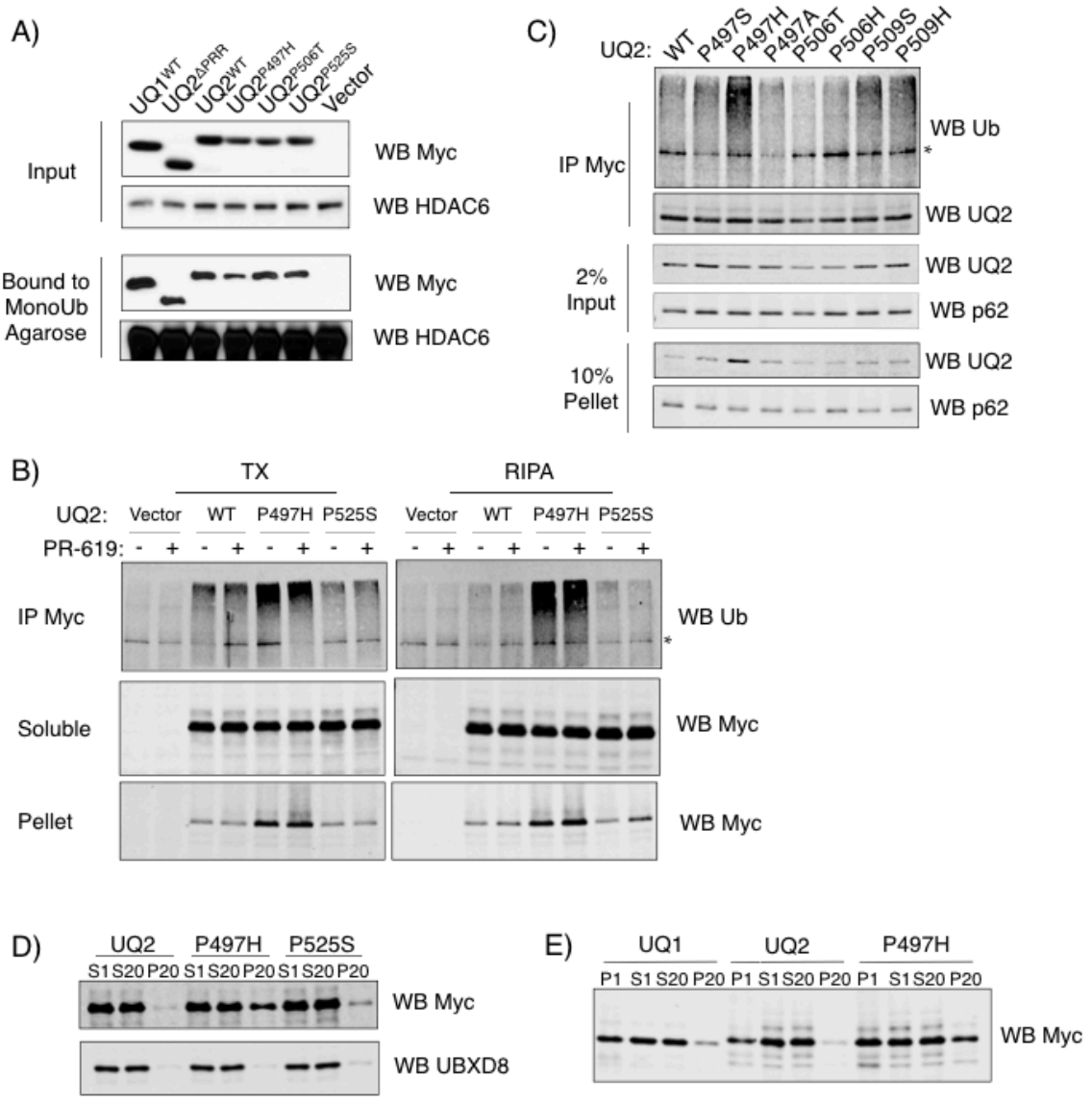

Unique ubiquitylation and insolubility of $UQ2^{P497H}$. **A)** HEK 293T cells transfected by $CaPO_4$ were harvested ~24h later and lysed in TX buffer. Clarified extract was applied to monoUb-conjugated agarose beads, which were washed and then boiled. Proteins bound to beads analyzed by SDS-PAGE and immunoblotting. HDAC6 was used as a positive control due to its high affinity for monoUb. **B)** HEK 293T were transfected by $CaPO_4$ and after 24h, plates were split to 4 plates each and grown for an addition ~48h. Where indicated, cells were treated with PR-619 (2.5μM 5h) prior to lysis in either TX or RIPA buffer. IPs performed with Myc antibody; soluble, pellet, and IP analyzed by immunoblotting with indicated antibodies. **C)** HEK 293T cells transfected by $CaPO_4$, harvested ~27h later, and IP performed in RIPA, analyzed as in (B). **D)** HEK 293T cells transfected by $CaPO_4$ and subject to 2-Step spin TX fractionation. Following 1,000g spin, the supernatant (S1) is spun at 20,000g, resulting in an additional supernatant (S20) and a

high speed pellet (P20). Fractions analyzed by immunoblotting as indicated. **E)** As in (D), in this case the P1 fraction was also analyzed.

Figure 4.8

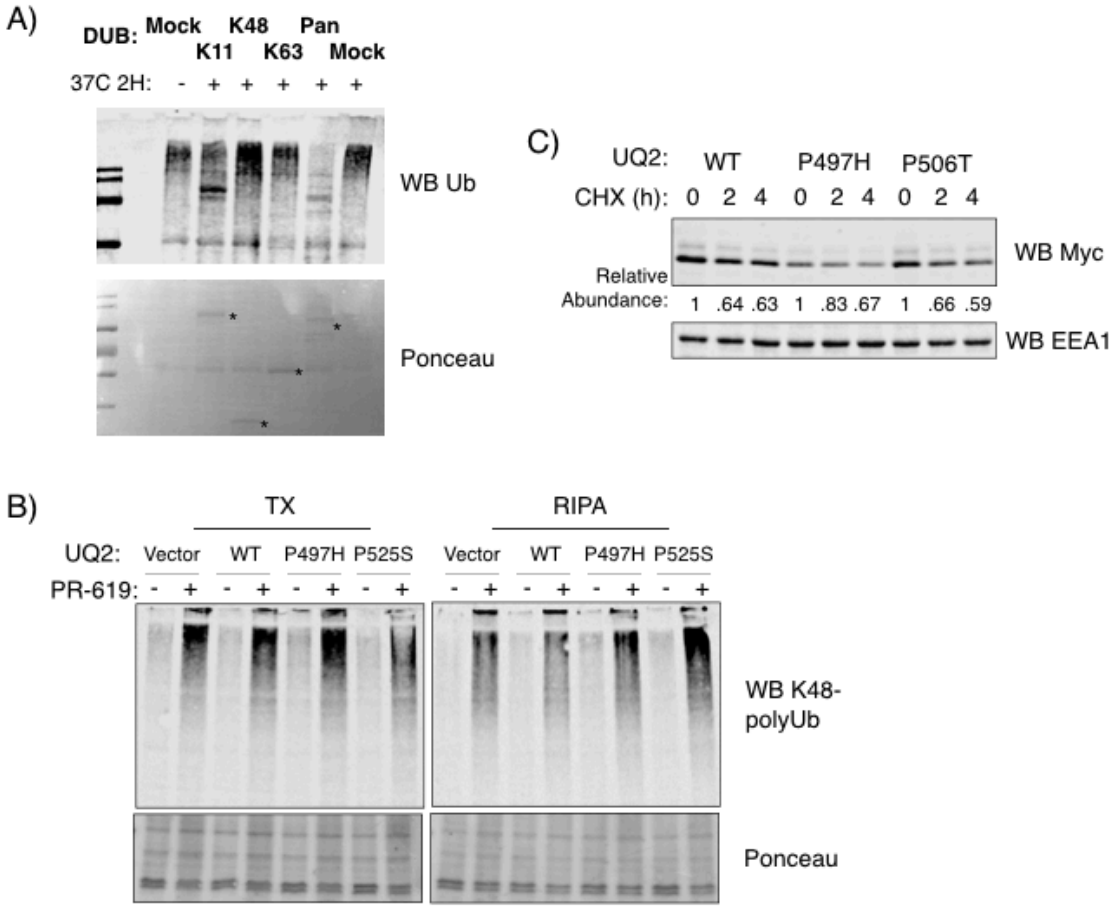

UQ2^{P497H} ubiquitylation is not homotypic and does not impact stability. **A)** UQ2^{P497H} was transfected by $CaPO_4$ in HEK 293T cells, harvested after ~27h, and IP performed in TX. Following washing, bead-bound complexes were aliquoted to 6 tubes and treated with polyUb chain specific DUBs as indicated. Only treatment with a nonspecific DUB caused loss of signal. **B)** Pellet analysis from Fig. 4.7B. Insolubility of K48-linked polyUb resulting from PR-619 treatment does not cause ubiquilins to shift into the insoluble phase. **C)** HEK 293T cells transfected by $CaPO_4$ grown for 24h, then split to multiple dishes and treated for the indicated amount of time (h) with 50µg/ml CHX to inhibit protein synthesis. Similar degradation rates were observed for UQ2 and UQ2 ALS mutants (representative experiment).

Figure 4.9

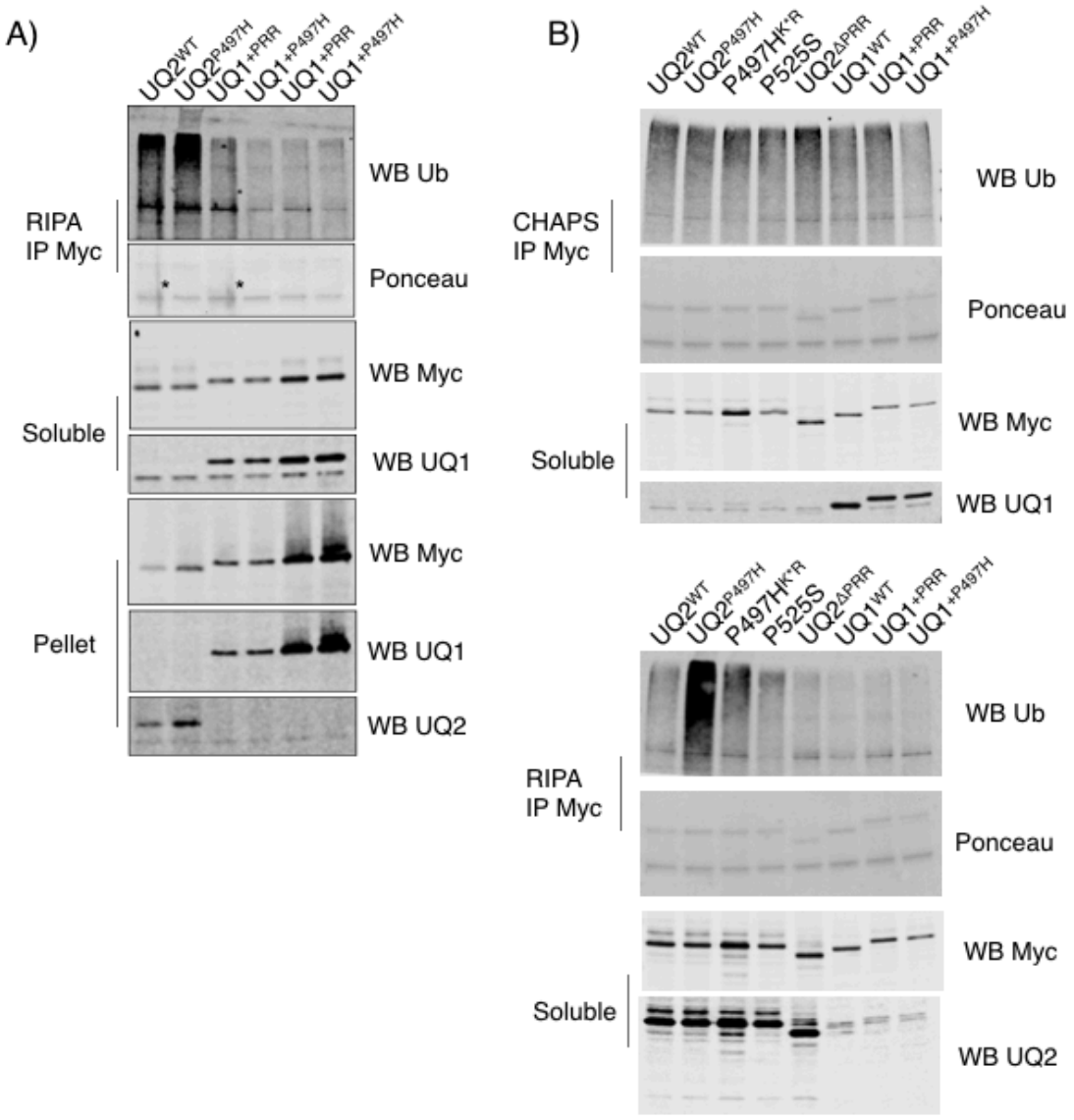

$UQ1^{+P497H}$ does not undergo hyperubiquitylation. **A)** HEK 293T cells transfected by $CaPO_4$ harvested after ~27h and IP with Myc antibody in RIPA. * in ponceau stain indicate contaminating streaks that caused increased intensity in lanes 1 and 3. $UQ1^{+PRR}$ and $UQ1^{+P497H}$ were each transfected at 2 doses to clearly demonstrate lack of Ub reactivity in IP. **B)** HEK 293T cells transfected by $CaPO_4$ harvested after ~27h in PBS, then split to 2 portions and IP with Myc antibody in either CHAPS (top) or RIPA (bottom). In CHAPS, all ubiquilins exhibit roughly equal precipitation of Ub, whereas in RIPA, $UQ2^{P497H}$ is elevated above $UQ2^{WT}$ and all other constructs tested. $P497H^{K*R}$ lacks lysine amino acids in the UBL domain, but contains a lysine in the Myc epitope and a free amine at its N-terminus. This construct is less ubiquitylated than $UQ2^{P497H}$, but still more than any other construct examined in this experiment.

Figure 4.10

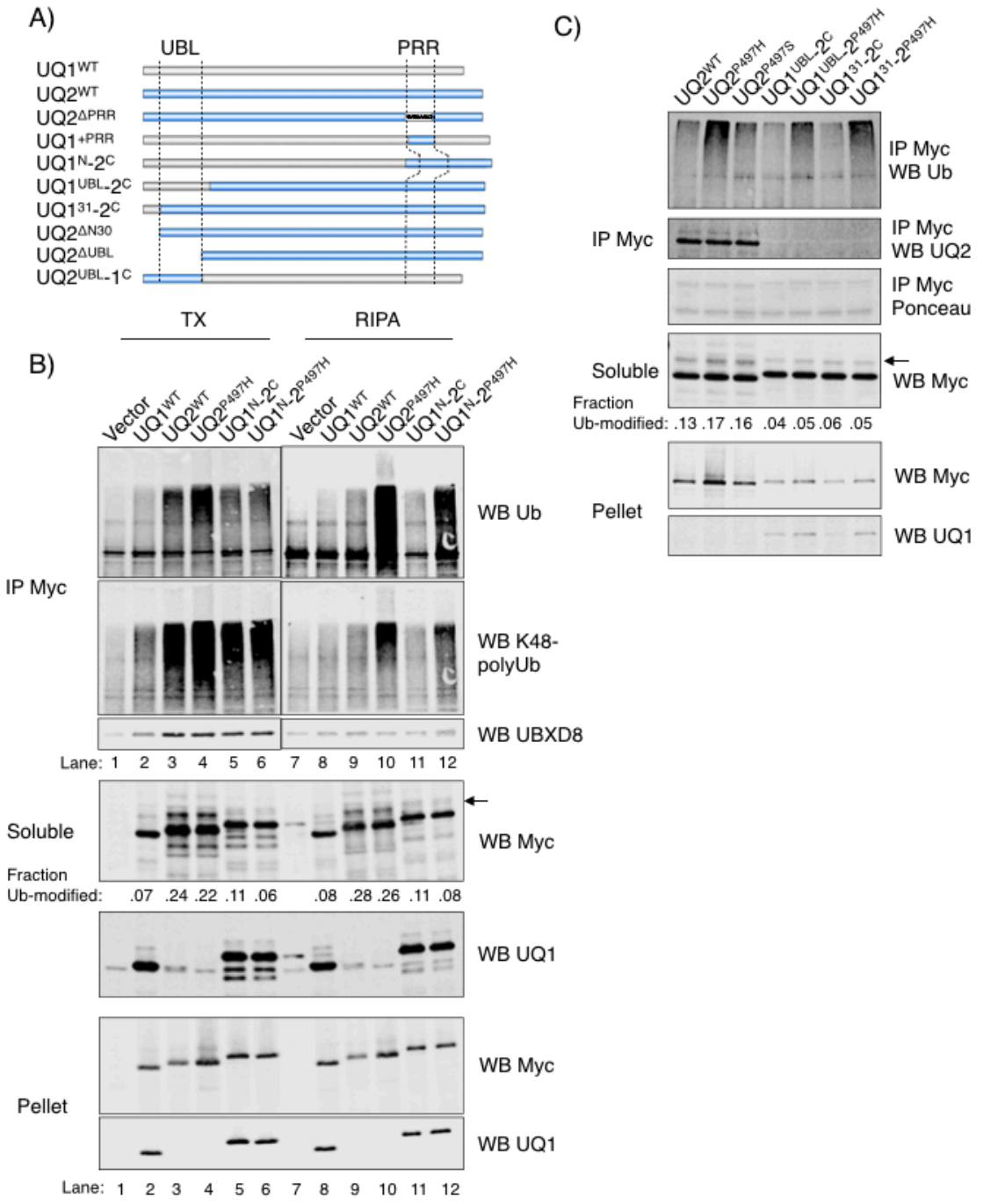

P497H mutation can confer dominant hyperubiquitylation. **A)** Schematics of chimeric constructs analyzed in this work. UQ1 sequence is gray and UQ2 sequence is blue. Dashed lines mark regions of interest: in this case, the influence of the PRR (marked) on UQ2 ubiquitylation in the UBL domain (marked), which contains all of the lysine amino acids. **B)** HEK 293T cells transfected by $CaPO_4$, grown for ~27h, harvested in PBS and split to two portions for IP in TX (left) or RIPA (right). IP of Ub, as assessed by pan-Ub antibody and K48-specific antibody, is clearly increased in TX for all constructs bearing

the PRR. In RIPA, constructs bearing the P497H mutation precipitate more Ub. Quantification of monoUb fraction suggests that although polyUb IP is elevated, chimeric constructs are not as efficiently monoUb modified. **C)** HEK 293T cells transfected by $CaPO_4$, grown for ~27h, and IP performed with Myc antibody in RIPA buffer as in (B). P497H-bearing constructs IP more polyUb, but again the monoUb mark is reduced. In both (B) and (C), the P497H-bearing chimeras are more readily extracted than the $UQ2^{P497H}$ construct.

Figure 4.11

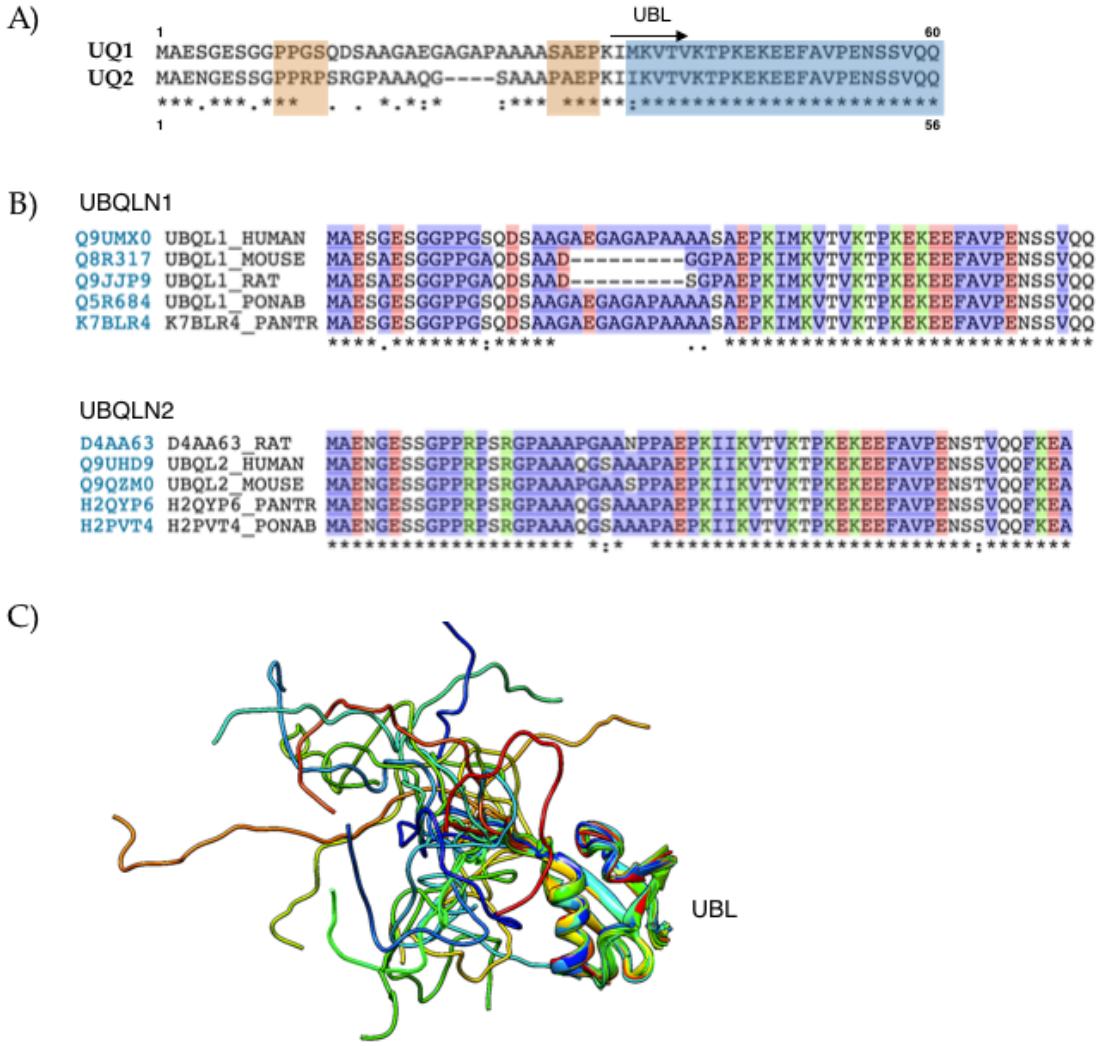

Unique N-terminal PXXP motifs in UQ2. **A)** Alignment of UQ1 and UQ2 N-termini. PXXP motifs in UQ2 highlighted in orange, UBL domain highlighted in blue. **B)** Sequence alignment of N-termini show that UQ1 has a unique polyA tract not present in rodents, whereas the PXXP motifs of UQ2 are conserved. **C)** Superposition of the 20 lowest energy NMR structures of the UQ2 UBL domain corresponding to PDB accession: 1j8c. The UBL domain helix and sheets are clearly observed, while it appears that the N-terminal section containing the PXXP motifs is disorganized and likely available for binding.

Figure 4.12

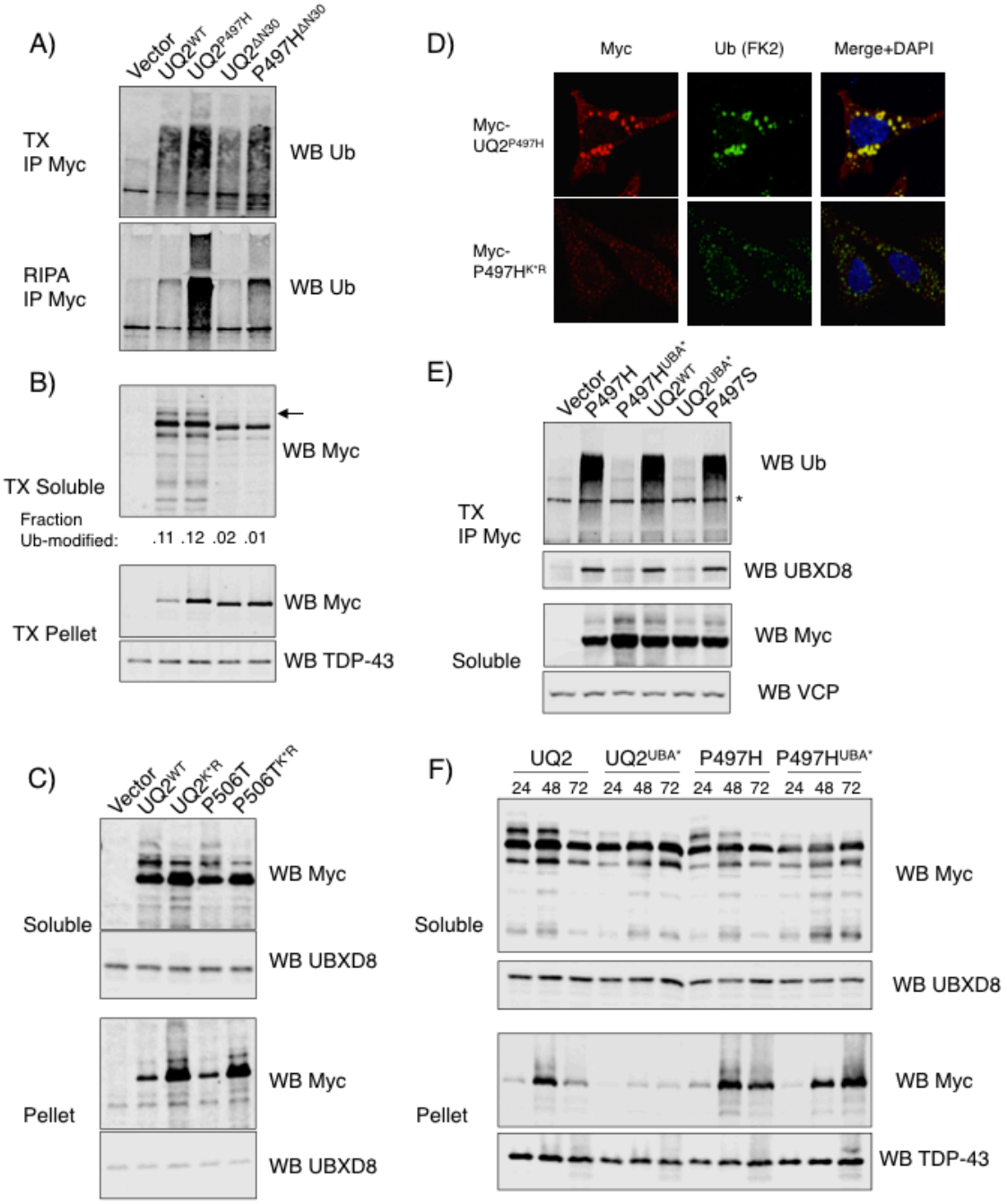

UQ2 N-terminus enhances ubiquitylation; P497H mutation uncouples ubiquitylation from increased solubility. **A)** HEK 293T cells transfected by $CaPO_4$, grown for ~27h, harvested in PBS and split to two portions for IP in TX (top) or RIPA (bottom). Ub precipitation is similar in TX, whereas Δ30 constructs IP less Ub in RIPA. **B)** Soluble and pellet analysis from IPs in (A). Δ30 constructs show strong reduction in the monoUb band (arrow) and are also apparently highly insoluble. **C)** HEK 293T cells transfected by $CaPO_4$, grown for ~27h, and lysed in TX. Soluble and pellet fractions analyzed by SDS-PAGE and immunoblotting, $UQ2^{K*R}$ mutants are highly insoluble. **D)** HeLa cells were

transfected by Lipofectamine 3000, grown for ~24h, then fixed in 4% PFA, permeabilized in .2% TX, and stained for Myc and endogenous Ub (FK2). K*R variants localize to small, numerous vesicles that are positive for Ub. Representative image shown. **E)** HeLa cells were transfected by Lipofectamine 3000, grown for ~27h, and lysis and IP with Myc antibody performed in TX buffer. $UQ2^{WT}$ and ALS mutants precipitate roughly equal amounts of Ub and UBXD8 in a UBA-dependent manner. * marks nonspecific band in IP. **F)** HEK 293T cells transfected by $CaPO_4$, grown for 24h, then trypsinized. A portion of the cells was extracted in TX, and remaining material was plated and grown for an additional 24h or 48h, as indicated. $UQ2^{UBA*}$ is soluble at all times tested, whereas $P497H^{UBA*}$ is TX-resistant at later time points.

Figure 4.13

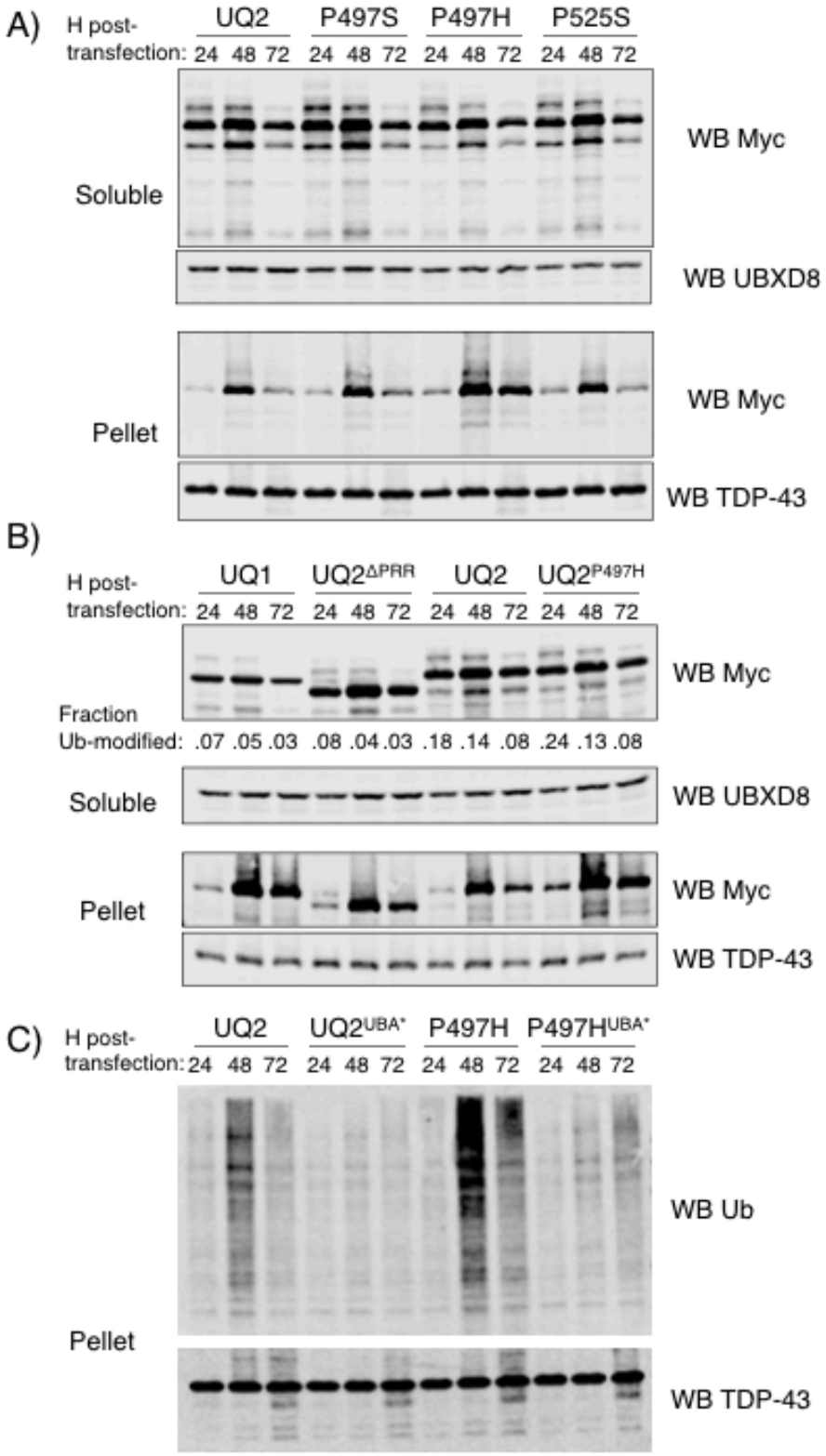
A)
H post-transfection:
UQ2
P497S
P497H
P525S
24 48 72 24 48 72 24 48 72 24 48 72
Soluble
WB Myc
WB UBXD8
Pellet
WB Myc
WB TDP-43
B)
H post-transfection:
UQ1
UQ2ΔPRR
UQ2
UQ2P497H
24 48 72 24 48 72 24 48 72 24 48 72
WB Myc
Fraction Ub-modified:
.07 .05 .03 .08 .04 .03 .18 .14 .08 .24 .13 .08
Soluble
WB UBXD8
Pellet
WB Myc
WB TDP-43
C)
H post-transfection:
UQ2
UQ2UBA*
P497H
P497HUBA*
24 48 72 24 48 72 24 48 72 24 48 72
WB Ub
Pellet
WB TDP-43

Ub-dependent and –independent insolubility of $UQ2^{P497H}$. **A)** HEK 293T cells transfected by $CaPO_4$, grown for 24h, then trypsinized. A portion of the cells was extracted in TX, and remaining material was plated and grown for an additional 24h or 48h, as indicated. $UQ2^{WT}$ and non-P497H mutants display similar extraction profiles. **B)** As in (A). UQ1 is more insoluble than UQ2, most clearly observed at later time points. **C)** Pellet extracts from Fig. 4.12F were blotted for Ub, revealing accumulation of Ub in insoluble fraction that tracks with ubiquilin proteins. However, the $P497H^{UBA*}$ compound mutant becomes insoluble without recruiting Ub into this fraction.

Figure 4.14

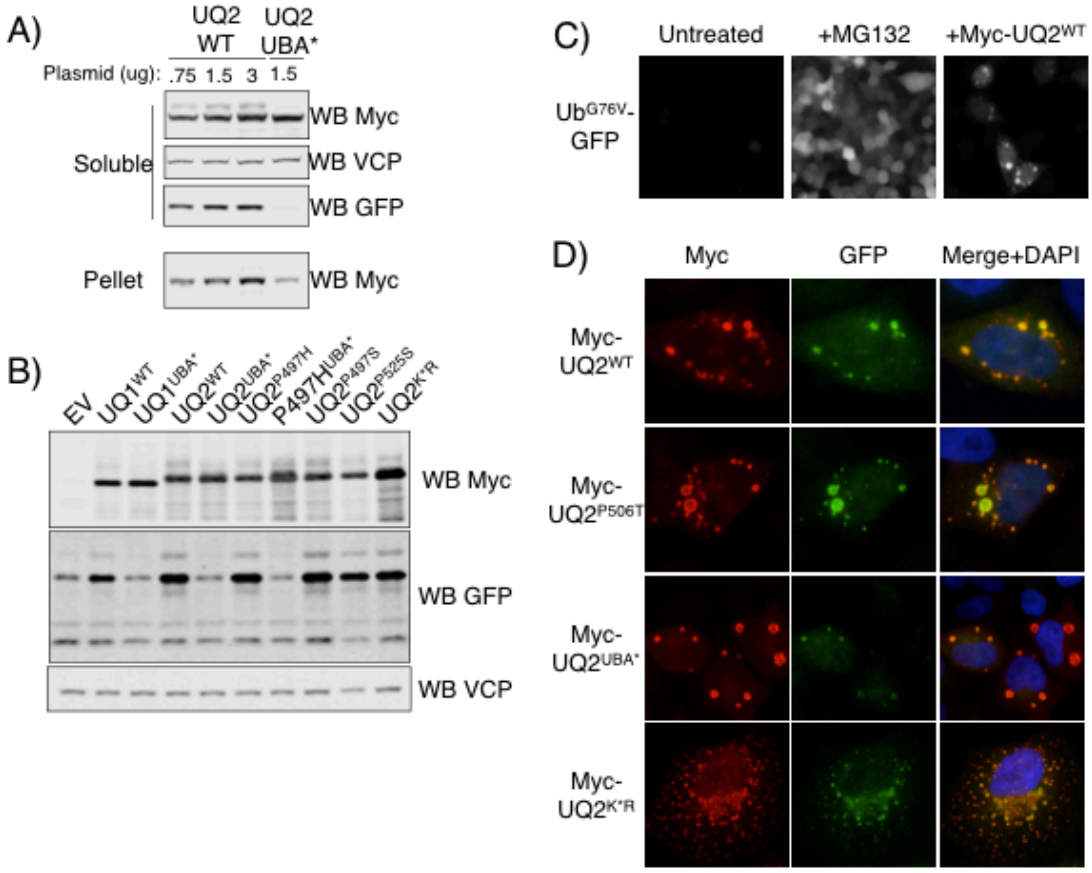

UBA domain is required for stabilization of Ub^{G76V}-GFP. **A)** HeLa cells stably expressing Ub^{G76V}-GFP were transfected with lipofectamine 3000 with the indicated amount of plasmid expressing either Myc-$UQ2^{WT}$ or Myc-$UQ2^{UBA*}$. Cells were lysed in TX and fractions analyzed by SDS-PAGE and immunoblotting with indicated antibodies. **B)** As in (A). $UQ2^{WT}$ and UQ2 ALS mutants stabilize Ub^{G76V}-GFP to a similar extent by UBA-dependent mechanism. **C)** HeLa stably expressing Ub^{G76V}-GFP HeLa examined by live cell microscopy under basal conditions, following proteasome inhibition (10μM 2h), or expressing Myc-$UQ2^{WT}$. Uniform fluorescence is observed with MG132 treatment; $UQ2^{WT}$ transfection results in punctate fluorescence. **D)** Ub^{G76V}-GFP HeLa cells were transfected by lipofectamine 3000, fixed in 4%PFA, permeabilized in .2% TX, and analyzed by IF. $UQ2^{WT}$ and ALS mutants ($UQ2^{P506T}$ shown) exhibited similar punctate patterns that were positive for GFP. $UQ2^{UBA*}$ localized in large inclusion bodies that were partially positive for GFP, whereas $UQ2^{K*R}$ mutants localized in characteristically small vesicles that were positive for GFP signal.

Figure 4.15

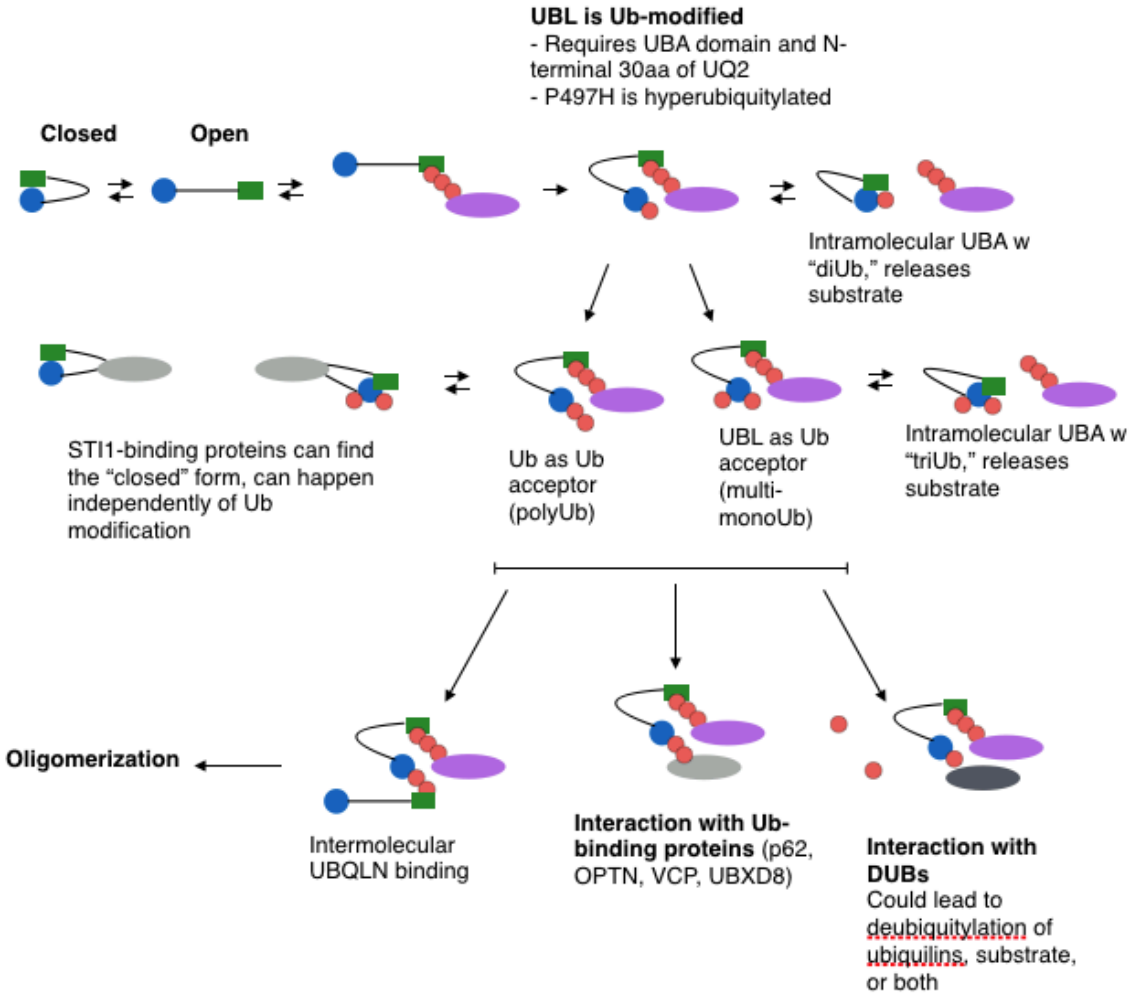

Model for ubiquitylation of ubiquilins might regulate intramolecular dynamics or recruit additional Ub-binding proteins.

4.7 References

1. Douglas, P. M. & Dillin, A. Protein homeostasis and aging in neurodegeneration. *J Cell Biol* **190,** 719–729 (2010).
2. Rosen, D. R. *et al.* Mutations in Cu/Zn superoxide dismutase gene are associated with familial amyotrophic lateral sclerosis. *Nature* **362,** 59–62 (1993).
3. Boillee, S. *et al.* Onset and Progression in Inherited ALS Determined by Motor Neurons and Microglia. *Science* **312,** 1389–1392 (2006).
4. Neumann, M. *et al.* Ubiquitinated TDP-43 in frontotemporal lobar degeneration and amyotrophic lateral sclerosis. *Science* **314,** 130–133 (2006).
5. Johnson, B. S. *et al.* TDP-43 is intrinsically aggregation-prone, and amyotrophic lateral sclerosis-linked mutations accelerate aggregation and increase toxicity. *J Biol Chem* **284,** 20329–20339 (2009).
6. Kwiatkowski, T. J. *et al.* Mutations in the FUS/TLS gene on chromosome 16 cause familial amyotrophic lateral sclerosis. *Science* **323,** 1205–1208 (2009).
7. Vance, C. *et al.* Mutations in FUS, an RNA processing protein, cause familial amyotrophic lateral sclerosis type 6. *Science* **323,** 1208–1211 (2009).
8. Mackenzie, I. R. A. *et al.* Pathological TDP-43 distinguishes sporadic amyotrophic lateral sclerosis from amyotrophic lateral sclerosis with SOD1 mutations. *Ann Neurol* **61,** 427–434 (2007).
9. DeJesus-Hernandez, M. *et al.* Expanded GGGGCC Hexanucleotide Repeat in Noncoding Region of C9ORF72 Causes Chromosome 9p-Linked FTD and ALS. *Neuron* 1–12 (2011). doi:10.1016/j.neuron.2011.09.011
10. Renton, A. E. *et al.* A Hexanucleotide Repeat Expansion in C9ORF72 Is the Cause of Chromosome 9p21-Linked ALS-FTD. *Neuron* 1–12 (2011). doi:10.1016/j.neuron.2011.09.010
11. Zu, T. *et al.* RAN proteins and RNA foci from antisense transcripts in C9ORF72 ALS and frontotemporal dementia. *Proceedings of the National Academy of Sciences* (2013). doi:10.1073/pnas.1315438110
12. Gitler, A. D. & Tsuiji, H. Brain Research. *Brain Res* 1–11 (2016). doi:10.1016/j.brainres.2016.04.004
13. Morimoto, R. I. Proteotoxic stress and inducible chaperone networks in neurodegenerative disease and aging. *Genes Dev* **22,** 1427–1438 (2008).
14. Maruyama, H. *et al.* Mutations of optineurin in amyotrophic lateral sclerosis. *Nature* **465,** 223–226 (2010).
15. Wild, P. *et al.* Phosphorylation of the autophagy receptor optineurin restricts Salmonella growth. *Science* **333,** 228–233 (2011).
16. Freischmidt, A. *et al.* Haploinsufficiency of TBK1 causes familial ALS and fronto-temporal dementia. *Nature neuroscience* (2015). doi:10.1038/nn.4000
17. Johnson, J. O. *et al.* Exome sequencing reveals VCP mutations as a cause of familial ALS. *Neuron* **68,** 857–864 (2010).
18. Tresse, E. *et al.* VCP/p97 is essential for maturation of ubiquitin-containing autophagosomes and this function is impaired by mutations that cause IBMPFD. *Autophagy* **6,** 217–227 (2010).
19. Fecto, F. *et al.* SQSTM1 Mutations in Familial and Sporadic Amyotrophic Lateral Sclerosis. *Arch Neurol* **68,** 1440–1446 (2011).

20. Cirulli, E. T. *et al.* Exome sequencing in amyotrophic lateral sclerosis identifies risk genes and pathways. *Science* **347,** 1436–1441 (2015).
21. Renton, A. E., Chiò, A. & Traynor, B. J. State of play in amyotrophic lateral sclerosis genetics. *Nature neuroscience* **17,** 17–23 (2013).
22. Deng, H.-X. *et al.* Mutations in UBQLN2 cause dominant X-linked juvenile and adult-onset ALS and ALS/dementia. *Nature* 1–7 (2011). doi:10.1038/nature10353
23. Williams, K. L. *et al.* UBQLN2/ubiquilin 2 mutation and pathology in familial amyotrophic lateral sclerosis. *Neurobiol Aging* (2012). doi:10.1016/j.neurobiolaging.2012.05.008
24. Brettschneider, J. *et al.* Pattern of ubiquilin pathology in ALS and FTLD indicates presence of C9ORF72 hexanucleotide expansion. *Acta Neuropathol* (2012). doi:10.1007/s00401-012-0970-z
25. Rothenberg, C. *et al.* Ubiquilin functions in autophagy and is degraded by chaperone-mediated autophagy. *Hum Mol Genet* **19,** 3219–3232 (2010).
26. Mah, A. L., Perry, G., Smith, M. A. & Monteiro, M. J. Identification of ubiquilin, a novel presenilin interactor that increases presenilin protein accumulation. *J Cell Biol* **151,** 847–862 (2000).
27. Walters, K. J., Kleijnen, M. F., Goh, A. M., Wagner, G. & Howley, P. M. Structural studies of the interaction between ubiquitin family proteins and proteasome subunit S5a. *Biochemistry* **41,** 1767–1777 (2002).
28. Ko, H. S., Uehara, T., Tsuruma, K. & Nomura, Y. Ubiquilin interacts with ubiquitylated proteins and proteasome through its ubiquitin-associated and ubiquitin-like domains. *FEBS Lett* **566,** 110–114 (2004).
29. Chen, X. *et al.* Structures of Rpn1 T1:Rad23 and hRpn13:hPLIC2 Reveal Distinct Binding Mechanisms between Substrate Receptors and Shuttle Factors of the Proteasome. *Structure* 1–15 (2016). doi:10.1016/j.str.2016.05.018
30. Regan-Klapisz, E. *et al.* Ubiquilin recruits Eps15 into ubiquitin-rich cytoplasmic aggregates via a UIM-UBL interaction. *J Cell Sci* **118,** 4437–4450 (2005).
31. Raasi, S., Ranjani Varadan, Fushman, D. & Pickart, C. M. Diverse polyubiquitin interaction properties of ubiquitin-associated domains. *Nat Struct Mol Biol* **12,** 708–714 (2005).
32. Kristariyanto, Y. A. *et al.* K29-Selective Ubiquitin Binding Domain Reveals Structural Basis of Specificity and Heterotypic Nature of K29 Polyubiquitin. *Molecular cell* **58,** 83–94 (2015).
33. Kaye, F. J. *et al.* A family of ubiquitin-like proteins binds the ATPase domain of Hsp70-like Stch. *FEBS Lett* **467,** 348–355 (2000).
34. Ford, D. L. & Monteiro, M. J. Dimerization of ubiquilin is dependent upon the central region of the protein: evidence that the monomer, but not the dimer, is involved in binding presenilins. *Biochem J* **399,** 397–404 (2006).
35. Kleijnen, M. F. *et al.* The hPLIC proteins may provide a link between the ubiquitination machinery and the proteasome. *Molecular cell* **6,** 409–419 (2000).
36. Kim, S. H. *et al.* Potentiation of amyotrophic lateral sclerosis (ALS)-associated TDP-43 aggregation by the proteasome-targeting factor, ubiquilin 1. *J Biol Chem* **284,** 8083–8092 (2009).
37. Hanson, K. A., Kim, S. H., Wassarman, D. A. & Tibbetts, R. S. Ubiquilin modifies TDP-43 toxicity in a Drosophila model of amyotrophic lateral sclerosis (ALS). *J*

Biol Chem **285,** 11068–11072 (2010).
38. Massey, L. K. *et al.* Overexpression of ubiquilin decreases ubiquitination and degradation of presenilin proteins. *J. Alzheimers Dis.* **6,** 79–92 (2004).
39. Ganguly, A., Feldman, R. M. R. & Guo, M. ubiquilin antagonizes presenilin and promotes neurodegeneration in Drosophila. *Hum Mol Genet* **17,** 293–302 (2008).
40. Ayadi, El, A., Stieren, E. S., Barral, J. M. & Boehning, D. Ubiquilin-1 regulates amyloid precursor protein maturation and degradation by stimulating K63-linked polyubiquitination of lysine 688. *Proceedings of the National Academy of Sciences* **109,** 13416–13421 (2012).
41. Wang, H. *et al.* Suppression of polyglutamine-induced toxicity in cell and animal models of Huntington's disease by ubiquilin. *Hum Mol Genet* **15,** 1025–1041 (2006).
42. Rutherford, N. J. *et al.* Unbiased screen reveals ubiquilin-1 and -2 highly associated with huntingtin inclusions. *Brain Res* 1–12 (2013). doi:10.1016/j.brainres.2013.06.006
43. Marin, I. The ubiquilin gene family: evolutionary patterns and functional insights. *BMC Evol. Biol.* **14,** 1–22 (2014).
44. Lim, P. J. *et al.* Ubiquilin and p97/VCP bind erasin, forming a complex involved in ERAD. *J Cell Biol* **187,** 201–217 (2009).
45. Ohno, A. *et al.* Structure of the UBA domain of Dsk2p in complex with ubiquitin molecular determinants for ubiquitin recognition. *Structure* **13,** 521–532 (2005).
46. Polo, S. *et al.* A single motif responsible for ubiquitin recognition and monoubiquitination in endocytic proteins. *Nature* **416,** 451–455 (2002).
47. Hoeller, D. *et al.* Regulation of ubiquitin-binding proteins by monoubiquitination. *Nat Cell Biol* **8,** 163–169 (2006).
48. Osaka, M., Ito, D., Yagi, T., Nihei, Y. & Suzuki, N. Evidence of a link between ubiquilin 2 and optineurin in amyotrophic lateral sclerosis. *Hum Mol Genet* (2014). doi:10.1093/hmg/ddu575
49. Hospenthal, M. K., Mevissen, T. E. T. & Komander, D. Deubiquitinase-based analysis of ubiquitin chain architecture using Ubiquitin Chain Restriction (UbiCRest). *Nat Protoc* **10,** 349–361 (2015).
50. Pankiv, S. *et al.* p62/SQSTM1 binds directly to Atg8/LC3 to facilitate degradation of ubiquitinated protein aggregates by autophagy. *J Biol Chem* **282,** 24131–24145 (2007).
51. King, A., Maekawa, S., Bodi, I., Troakes, C. & Al-Sarraj, S. Ubiquitinated, p62 immunopositive cerebellar cortical neuronal inclusions are evident across the spectrum of TDP-43 proteinopathies but are only rarely additionally immunopositive for phosphorylation-dependent TDP-43. *Neuropathology* **31,** 239–249 (2011).
52. Yonashiro, R. *et al.* The Rqc2/Tae2 subunit of the ribosome-associated quality control (RQC) complex marks ribosome-stalled nascent polypeptide chains for aggregation. *Elife* **5,** (2016).
53. Fang, N. N., Ng, A. H. M., Measday, V. & Mayor, T. Hul5 HECT ubiquitin ligase plays a major role in the ubiquitylation and turnover of cytosolic misfolded proteins. *Nat Cell Biol* **13,** 1344–1352 (2011).
54. Chou, T.-F. & Deshaies, R. J. Quantitative cell-based protein degradation assays to

identify and classify drugs that target the ubiquitin-proteasome system. *J Biol Chem* **286,** 16546–16554 (2011).
55. Alvarez-Castelao, B., Martín-Guerrero, I., García-Orad, A. & Castaño, J. G. Cytomegalovirus promoter up-regulation is the major cause of increased protein levels of unstable reporter proteins after treatment of living cells with proteasome inhibitors. *J Biol Chem* **284,** 28253–28262 (2009).
56. N'Diaye, E.-N. *et al.* The ubiquitin-like protein PLIC-2 is a negative regulator of G protein-coupled receptor endocytosis. *Mol Biol Cell* **19,** 1252–1260 (2008).
57. Yun Lee, D., Arnott, D. & Brown, E. J. Ubiquilin4 is an adaptor protein that recruits Ubiquilin1 to the autophagy machinery. *EMBO Rep* **14,** 373–381 (2013).
58. Suzuki, R. & Kawahara, H. UBQLN4 recognizes mislocalized transmembrane domain proteins and targets these to proteasomal degradation. *EMBO Rep* (2016). doi:10.15252/embr.201541402
59. Geiger, T., Wehner, A., Schaab, C., Cox, J. & Mann, M. Comparative Proteomic Analysis of Eleven Common Cell Lines Reveals Ubiquitous but Varying Expression of Most Proteins. *Mol Cell Proteomics* **11,** M111.014050–M111.014050 (2012).
60. Dantuma, N. P., Lindsten, K., Glas, R., Jellne, M. & Masucci, M. G. Short-lived green fluorescent proteins for quantifying ubiquitin/proteasome-dependent proteolysis in living cells. *Nat Biotechnol* **18,** 538–543 (2000).
61. Salomons, F. A. *et al.* Selective Accumulation of Aggregation-Prone Proteasome Substrates in Response to Proteotoxic Stress. *Mol Cell Biol* **29,** 1774–1785 (2009).
62. Li, A. *et al.* Isolation and characterization of the Drosophila ubiquilin ortholog dUbqln: in vivo interaction with early-onset Alzheimer disease genes. *Hum Mol Genet* **16,** 2626–2639 (2007).
63. Feng, P. *et al.* Kaposi's sarcoma-associated herpesvirus K7 protein targets a ubiquitin-like/ubiquitin-associated domain-containing protein to promote protein degradation. *Mol Cell Biol* **24,** 3938–3948 (2004).
64. Kleijnen, M. F., Alarcon, R. M. & Howley, P. M. The ubiquitin-associated domain of hPLIC-2 interacts with the proteasome. *Mol Biol Cell* **14,** 3868–3875 (2003).
65. Chang, L. & Monteiro, M. J. Defective Proteasome Delivery of Polyubiquitinated Proteins by Ubiquilin-2 Proteins Containing ALS Mutations. *PLoS ONE* **10,** e0130162 (2015).
66. Itakura, E. *et al.* Ubiquilins Chaperone and Triage Mitochondrial Membrane Proteins for Degradation. *Molecular cell* **63,** 21–33 (2016).
67. Lowe, E. D. *et al.* Structures of the Dsk2 UBL and UBA domains and their complex. *Acta Cryst (2006). D62, 177-188 [doi:10.1107/S0907444905037777]* 1–12 (2006). doi:10.1107/S0907444905037777
68. Pierce, N., Kleiger, G., Shan, S. & Deshaies, R. Detection of sequential polyubiquitylation on a millisecond timescale. *Nature* (2009).
69. Zhang, D., Raasi, S. & Fushman, D. Affinity makes the difference: nonselective interaction of the UBA domain of Ubiquilin-1 with monomeric ubiquitin and polyubiquitin chains. *J Mol Biol* **377,** 162–180 (2008).
70. Itakura, E. & Mizushima, N. p62 Targeting to the autophagosome formation site requires self-oligomerization but not LC3 binding. *J Cell Biol* **192,** 17–27 (2011).
71. Walther, D. M. *et al.* Widespread Proteome Remodeling and Aggregation in Aging

C. elegans. *Cell* **161,** 919–932 (2015).
72. Miller, S. B. M., Mogk, A. & Bukau, B. Spatially Organized Aggregation of Misfolded Proteins as Cellular Stress Defense Strategy. *J Mol Biol* **427,** 1564–1574 (2015).
73. Wallace, E. W. J. *et al.* Reversible, Specific, Active Aggregates of Endogenous Proteins Assemble upon Heat Stress. *Cell* **162,** 1286–1298 (2015).
74. Rampelt, H. *et al.* Metazoan Hsp70 machines use Hsp110 to power protein disaggregation. *EMBO J* 1–15 (2012). doi:10.1038/emboj.2012.264
75. Verma, R., Oania, R. S., Kolawa, N. J. & Deshaies, R. J. Cdc48/p97 promotes degradation of aberrant nascent polypeptides bound to the ribosome. *Elife* **2,** e00308 (2013).
76. Johansen, T. & Lamark, T. Selective autophagy mediated by autophagic adapter proteins. *Autophagy* **7,** 279–296 (2011).
77. Gorrie, G. H. *et al.* Dendritic spinopathy in transgenic mice expressing ALS/dementia-linked mutant UBQLN2. *Proceedings of the National Academy of Sciences* (2014). doi:10.1073/pnas.1405741111
78. Ceballos-Diaz, C. *et al.* Viral expression of ALS-linked ubiquilin-2 mutants causes inclusion pathology and behavioral deficits in mice. *Mol Neurodegener* 1–13 (2015). doi:10.1186/s13024-015-0026-7

Chapter 5) Ubiquilins perturb the degradation of cytosolic proteins

Overview

This section comprises a series of experiments studying the effect of ubiquilins on a variety of model substrates. The choice of substrates was partially informed by our co-IP-LC-MS/MS experiments (chapter 3), in which identification of different proteins implicated ubiquilins in specific pathways. Previously published work from other labs also informed substrate scope and selection. The substrates include a cytosolic Ub fusion substrate, Ub^{G76V}-GFP, which was touched on in the last chapter, although in this chapter I explore both stable cells expressing the Ub-fusion substrate and co-transfection experiments, which yielded some interesting data about alterations in solubility. I also explored an endoplasmic reticulum-associated degradation (ERAD) substrate, which I found was not strongly affected by ubiquilins. I examined another cytosolic substrate, a model that harbors a transmembrane domain but lacks a targeting sequence, resulting in a mislocalized protein (MLP)[1]. Finally, I attempted to investigate the consequences of puromycin, which generates many truncated proteins that are misfolded and mislocalized, and how ubiquilins affect puromycin metabolism.

5.1 Abstract

The majority of cellular proteins in eukaryotes are degraded by the ubiquitin-proteasome system. Disposal of proteins derived from the nucleus, cytosol, or a membrane-bound organelle will require different cellular machinery for efficient degradation. However, the majority of proteasomes are found in the cytosol – and thus cytosolic targeting factors that deliver clients to the proteasome can regulate a wide variety of UPS substrates from many different cellular compartments. Ubiquilin proteins harbor a nonspecific Ub-binding domain that permits interaction with a variety of polyUb

chains, although the true substrate scope of ubiquilins remains poorly defined. In this work, I assessed the effect of ubiquilin knockdown and overexpression on a variety of model substrates. Novel findings in this section include alterations in MLP substrate abundance and solubility, and that UQ2 stabilizes defective ribosomal products (DRiPs), which are produced during autofragmentation of GFP and in high abundance during puromycin treatment.

5.2 Introduction

The Ub-fusion model is a rapidly degraded fusion of Ub and GFP, in which the C-terminal glycine of Ub is mutated to valine such that it is no longer efficiently recognized and cleaved by DUBs[2]. The Ub^{G76V}-GFP fusion protein is interpreted by cellular Ub-binding proteins as an intermediate en route to degradation and directed to specialized Ub chain extension enzymes, also known as "E4" ligases[3]. Most E3 Ub ligase enzymes are capable of directly modifying substrate proteins with Ub, but some enzymes are dedicated to extending chains on substrates bearing Ub modifications too short to efficiently engage the degradation machinery, and are called E4 Ub ligases[4]. The pathway for Ub^{G76V}-GFP degradation relies on VCP, an AAA^+ ATPase implicated in many facets of Ub-dependent protein remodeling and also implicated in rare instances of familial ALS[5,6].

CD3-δ is another model substrate that is widely employed to gauge the efficiency of a specialized pathway for degradation of ER-resident proteins, in this case denoted ERAD-L_M (luminal, type-I membrane) [7]. CD3-δ is typically part of the T-cell receptor-CD3 complex involved in activation of T-cells. When expressed without the other CD3 subunits, CD3-δ cannot be assembled into a functional receptor and does not fold

properly, leading to its degradation. Degradation of CD3-δ relies on specific ERAD complexes based around different E3 Ub ligases, in this case depending on GP78, but not on HRD1[8,9]. Although it was originally reported that GP78 overexpression enhanced the rate of degradation of CD3-δ[8] (now 15 years old), this result was challenged recently by the finding that GP78 overexpression stabilizes CD3-δ, and that perturbation of the balance between E3 Ub ligases, DUBs, and Ub-binding chaperones will reduce the efficiency of degradation[10].

With respect to the ubiquilin project, the first paper to suggest an impact on ERAD found that *UBQLN1/UBQLN2* double knockdown by siRNA stabilized CD3-δ, but accelerated degradation of the Ub-fusion substrate, although these conclusions were based on results that left some room for interpretation[11]. The other major paper on this topic suggested that *UBQLN1*/*UBQLN2* double knockdown reduced the degradation rate of CD3-δ, whereas overexpression of UQ1 accelerated its degradation[12]. This same paper found that *UBQLN1/UBQLN2* double knockdown stabilized a different ERAD substrate, α1-anti-trypsin null Hong Kong mutant (NHK), which represents a different class of ERAD substrate, ERAD-L_S (luminal, soluble). The paper concluded with analysis of the UBQLN homolog in *C. elegans*, describing ER stress-induced *UBQLN* expression, dependent on the IRE-1 branch of the UPR[13], and *UBQLN* knockdown causing ER stress in the whole organism. Although some of the western blotting data in this paper was interpreted favorably for its publication (e.g., Figure 4A is the basis for suggesting that UBQLN knockdown stabilizes the model, even though the quantification is based on film and the error bars are overlapping), this paper was nonetheless pretty convincing and pretty interesting. My interest in this pathway was rekindled by a publication suggesting

that UQ2 ALS mutants stabilized NHK to a greater extent than $UQ2^{WT}$[14]. This is the same paper claiming that UQ2 ALS mutations disrupt the interaction of UQ2 with UBXD8, which I carefully and rigorously tested, but ultimately my conclusion was that UQ2 ALS mutations do not disrupt interaction with UBXD8 (see chapter 3). Based on my general interest in reproducing published work as a good starting point, I investigated the impact of ubiquilins on the type I luminal membrane ERAD substrate, CD3-δ.

I became interested in puromycin because of a publication that came out in 2010 suggesting that ubiquilins are degraded by puromycin-induced autophagy[15]. The more time I spent studying this paper, the more inconsistencies I found with the interpretation of western blotting data, e.g., cf. LC3 levels in figure 4, panels B and D[15]. Most importantly, the basis for the paper – that puromycin induces autophagy – seemed to be an unjustified assumption. In fact, alternative research suggests that the majority of puromycin-adducts are degraded by the proteasome[16]. I became very intrigued by puromycin, which is a really cool drug with a unique mechanism of action.

Puromycin is a member of the aminonucleoside family of antibiotics and is a structural mimetic of the 3' end of an aminoacyl-tRNA molecule. Puromycin interferes with translation by intercepting nascent polypeptides as they are being translated by ribosomes, resulting in a covalent puromycin-peptide bond[17], blocking peptide elongation, and thus producing truncated polypeptides with a propensity to misfold due to missing domains and lack of targeting signals. Puromycin-adducts are degraded rapidly and grouped into the category of defective ribosomal products (DRiPs). DRiPs are produced in surprising abundance in cells under normal conditions; it is thought that roughly 30% of peptides are rapidly targeted for degradation, representing a pool of

proteins that presents a continuous challenge to protein surveillance and degradation pathways, and also serves as the primary source of peptides for antigen presentation[18].

An additional paper played a guiding role in my research on puromycin, concluding that the ubiquilin-interacting protein, BAG6, is required for the efficient degradation of DRiPs [19]. Minami et al. demonstrated that BAG6 is precipitated with an anti-puromycin antibody following puromycin treatment of cells. BAG6 forms punctate, cytosolic inclusions that localize with puromycin positive structures and also strain strongly for endogenous Ub[20,21]. The work also suggested that RNAi against *BAG6* caused sensitivity to puromycin stress, indicating that the clearance of puromycylated peptides was an essential element of the stress response. The concluding data focused on the role of BAG6 in MHC-class I presentation, bringing the connection between DRiP degradation and antigen presentation full circle[22]. Looking back on this now, it seems clear that those proteins involved in the degradation of the DRiP pool might also have an impact on antigen presentation, at least in simple cell culture models. This paper was among the first in a larger literature describing the function of BAG6 in targeting hydrophobic domains and functioning as a triage unit for membrane proteins loitering in the cytosol[23], referred to as mislocalized proteins (MLPs)[24], which very much spurred my interest in the additional model substrate, TASK85[1].

Finally, the connection between ubiquilins, DRiPs, and Ub^{G76V}-GFP can be summarized by the observation that ubiquilin expression with transfected Ub^{G76V}-GFP results in the stabilization of a GFP-reactive band of roughly 20kDa that is detergent resistant. This led me to the work of Jon Yewdell, whose lab focuses on immune surveillance and the efficiency of antigen presentation. His work characterized a faster

migrating band of GFP that is produced in cells (not lysate), accumulates during proteasome inhibition, and is highly resistant to biological detergents[25]. His lab described this fragment as GFP(f1), and characterized it as a C-terminal peptide resulting from chromophore-induced autofragmentation of the GFP protein, which occurs in all fluorescent proteins they tested[26]. His work on this topic led me to re-evaluate much of my work on Ub^{G76V}-GFP, because I observed faster migrating GFP-reactive bands by western blotting that were highly enriched in the insoluble fraction. I found that UQ2 causes an accumulation of GFP(f1) to a greater extent than UQ1 when co-transfected with Ub^{G76V}-GFP in HEK 293T cells, and UQ2 exerts this effect on EGFP independently of the Ub fusion, suggesting that UQ2 is a bona fide regulator of DRiPs independently of Ub modification. In sum, my investigations into model substrates suggest that ubiquilin deficiency did not have a major impact on degradation of a variety of substrates, and that in general, ubiquilins are more potent regulators of cytosolic proteins than ERAD substrates.

5.3 Results

5.3.1 Ub-fusion model substrate, Ub^{G76V}-GFP

I began by asking if ubiquilin proteins are required for the degradation of Ub^{G76V}-GFP by performing co-transfection of siRNA targeting *UBQLN1, UBQLN2,* or both genes simultaneously, along with plasmid expressing Ub^{G76V}-GFP. I found that individual or combined knockdown of UQ1 and UQ2 does not stabilize Ub^{G76V}-GFP to an appreciable extent (Fig. 5.1A). I also tried siRNA transfections in HeLa cells stably expressing Ub^{G76V}-GFP, but found again that knockdown of ubiquilins, alone or in combination, does not inhibit the degradation of Ub^{G76V}-GFP as assessed by western

blotting following CHX chase (Fig. 5.1B). In this experiment, cells were pre-treated with MG132 to accumulate Ub^{G76V}-GFP, followed by a short CHX time course. It can be clearly observed that the GFP-reactive band is rapidly degraded and its disappearance is unaffected by ubiquilin knockdown (Fig. 5.1B).

In the next set of experiments, I assessed if ubiquilin overexpression would stabilize Ub^{G76V}-GFP. Of special interest, the Nature paper describing the *UBQLN2* mutations also concluded their paper with experiments suggesting that ALS mutants stabilize Ub^{G76V}-GFP to a greater extent than $UQ2^{WT27}$. Because of my additional interests in divergent functions of the ubiquilin proteins, I performed assays comparing UQ1, UQ2, ALS mutants, and several other mutants to address the requirement for different domains of ubiquilin and to get at the most important question: do ALS mutants disrupt the UPS? In the HeLa cells stably expressing Ub^{G76V}-GFP, I found that $UQ2^{WT}$ and ALS mutants stabilize Ub^{G76V}-GFP to a similar extent in a manner that is clearly dose and UBA-dependent (See Fig. 4.14A, 4.14B). I also performed CHX chase experiments in the stable HeLa cells: plates were transfected with Myc-UQ proteins, then split to 12 w dishes, treated with CHX and harvested in 1x laemmli buffer do in the plate, which is a pretty efficient way to do these types of experiments. Once again, I observed clear stabilization of Ub^{G76V}-GFP in a UBA-dependent manner that did not appear different between wild type and ALS mutant UQ2 proteins (Fig. 5.2A).

As described in chapter 4, I performed live cell imaging and fixed cell immunofluorescence on these cells. Ub^{G76V}-GFP accumulates in large punctate structures that are positive for Myc-ubiquilins. ALS mutations do not perturb localization patterns, which are unique to ubiquilin expression, as MG132 results in diffuse fluorescence (Fig.

5.2B). The UBA* mutants did not exhibit fluorescence in live cells, but did show some GFP signal in their characteristic odd structures by immunofluorescence (Fig. 4.14D). It is possible that non-fluorescent proteins were captured in those structures, such as GFP fragments, although I did not look into it too much further besides the conclusion that the large, irregular vesicles formed by UBA* mutants were infrequently and weakly positive for GFP signal. As a general conclusion, UQ2 and the ALS mutants tested exerted a similar stabilizing impact on Ub^{G76V}-GFP in an UBA-dependent manner.

I also performed co-transfection experiments with Myc-UQ and Ub^{G76V}-GFP plasmids in HEK 293T cells in an attempt to more faithfully reproduce work reported in the original Nature paper, in which they performed co-transfection in both neuronal-like SHSY cells and 293T cells[27]. A brief summary of findings would be that ubiquilins stabilize Ub^{G76V}-GFP to a similar extent when co-transfected. The variable expression level of Ub^{G76V}-GFP, despite my best efforts, makes it difficult to compare results from experiment to experiment – one of the many challenges of transfection-based experiments. However, I generated crude fractions in TX buffer and found that ubiquilins have a profound and reproducible effect on the stabilization of Ub^{G76V}-GFP in the TX-resistant (pellet) fraction, even more interesting, there's a clear distinction between the effects of UQ1 and UQ2, but this difference is not PRR-dependent, nor is it disrupted by ALS mutations (Fig. 5.3). This observation boggled me until I came across a very interesting paper on autofragmentation of GFP[26]. This will be elaborated in detail in section 5.3.4.

5.3.2 Endoplasmic reticulum-associated degradation (ERAD) substrate, CD3-δ

I explored this model substrate by co-transfection of Myc-UQ constructs with CD3-δ-YFP. I compared the stabilizing effects of ubiquilins against known ERAD disruptors, such as GP78 overexpression[10]. I found that ubiquilin expression stabilizes CD3-δ-YFP, and the effect of UQ1 is similar to that of UQ2 (Fig. 5.4A). However, compared to transfection with GP78, I found that ubiquilins stabilized CD3-δ-YFP only modestly (Fig. 5.4). Because the most striking feature of this this data is the amount of CD3-δ-YFP in the pellet, I also examined the impact of $UQ2^{P497H}$, which is markedly insoluble. Co-expression of CD3-δ-YFP with $UQ2^{P497H}$ did not cause stabilization of the reporter relative to $UQ2^{WT}$ in either the soluble or insoluble fractions, despite the increased amount of $UQ2^{P497H}$ in the pellet fraction (Fig 5.5A). Once again, co-expression with GP78-S caused a massive accumulation of the reporter in the TX-insoluble fraction (Fig. 5.5A).

I was really fascinated by the detergent resistance of this model, so I assessed cells expressing CD3-δ-YFP by live cell fluorescence microscopy, and observed striking localization patterns in the presence of GP78 or Hrd1, which resulted in punctate foci, typically two per cell, occurring on either side of the nucleus (Fig. 5.5B). Localization patterns in the presence of ubiquilins varied from small vesicles to not very changed at all relative to the vector (Fig. 5.5B). I did not dig in to this as aggressively as the others, in part because it seemed that ubiquilins did not strongly stabilize this model.

5.3.3 Mislocalized protein (MLP) substrate, TASK85

I obtained the TASK85 plasmid and an antibody directed against it from the lab of Stephen High[1]. This model is an N-terminal fragment of a transmembrane protein known as TASK1, containing a hydrophobic transmembrane domain (TMD) and an opsin

glycosylation signal, but the fragment is too short to be efficiently profiled by SRP and inserted into the membrane. As such, TASK85 contains a TMD but does not target to the membrane, and ends up mislocalized in the cytosol, hence the mislocalized protein (MLP) designation. Upon co-transfection and CHX chase with Myc-UQ1 or Myc-UQ2, the 8kDa band at the predicted MW corresponding to TASK85 is clearly visible in whole cell lysate, but in the lanes with Myc-UQ2, there is strong signal at higher MW as well, similar to a polyUb smear (Fig. 5.6A). As a control, I also co-transfected SGTA-V5, which has been shown to stabilize TASK85 through two possible non-exclusive mechanisms: prevention of substrate binding to BAG6, and / or recruitment of DUBs[28,29]. When expressed with UQ1, the signal for TASK85 is steadily decreasing as a function of CHX incubation. However, when expressed with UQ2 or SGTA, the band at the predicted MW is more stable, although the high MW smear is depleted with time (Fig. 5.6A).

In follow-up experiments, I sought to investigate if stabilization of TASK85 was occurring in a PRR- or UBA-dependent manner. What I found was really baffling at the time, but in light of a recently published paper, I think I have an idea of what might be happening[30]. In multiple experiments, I found that the UQ2^{UBA*} mutant strongly stabilized TASK85 in both TX-soluble and –insoluble fractions (Fig. 5.6B), in contrast to my previous results with the Ub-fusion substrate. I also attempted CHX chase experiments with the UBA* mutant and made the same observation (Fig. 5.7). I abandoned this line of investigation because I didn't understand what was happening, but will provide my working hypothesis in the discussion.

5.3.4 GFP(F1), Puromycin, and the degradation of DRiPs

As I alluded to in the Ub^{G76V}-GFP section, I noted the stabilization of a faster migrating, GFP-reactive band that was primarily TX-insoluble when the Ub-fusion reporter was co-transfected with ubiquilins. I stumbled on a paper from Jon Yewdell's lab that all fluorescent proteins undergo autofragmentation as a result of chromophore maturation, resulting in a C-terminal peptide that is rapidly degraded[26]. In this section, I will begin with some findings that were the result of a cloning artifact, and I think speak to the sensitivity of crude fractionation of cells. My line of thinking was as follows: if the Ub^{G76V}-GFP fusion has the Ub at the N-terminus of GFP, and the fragment I'm observing is in the C-terminus of GFP, then will ubiquilins stabilize this fragment independently of Ub?

In the first experiment to address if UQ2 selectively stabilizes GFP(f1) in the insoluble fraction, I performed co-transfections of UQ proteins with EGFP and Ub^{G76V}-GFP at the same time and ran on the same gel. I also used GFP-fusions of UQ1 and UQ2, with the hypothesis that UQ2 should have this stabilizing effect in *cis*, meaning that its own fusion should be subject to cleavage and partition to the insoluble phase. For both EGFP and the UFD substrate, I included vector controls, one of which was left untreated and the other treated with MG132. I was surprised to find that the EGFP by itself was very insoluble – it accumulated massively in the pellet fraction. This shift to the insoluble phase was enhanced by co-expression of UQ2, and the same shift to the insoluble phase was observed when UQ2 was expressed with Ub^{G76V}-GFP (Fig. 5.8). Additional data supporting the idea that UQ2 selectively stabilizes this C-term fragment of GFP in the pellet was the GFP-UQ fusions, where a clear GFP-reactive band is observed at ~60kDa, which I interpreted as a C-terminal GFP fused to the N-term of UQ2, which is also

subject to cleavage (Fig 5.8, arrow and label). All of this data fit my hypothesis, namely that UQ2 was stabilizing the GFP C-term fragment more strongly than UQ1.

What was surprising about this data was the insolubility of EGFP – normally EGFP is a pretty soluble protein. In the event that it is misfolded, it is rapidly degraded – so what gives? I repeated the experiment with the same EGFP construct and once again observed that even in the vector control, there was a lot of insoluble protein – in fact, in this experiment, the majority of EGFP signal was in the TX-insoluble fraction (Fig. 5.9A). I knew something was wrong, and at this point I more carefully examined the vector. The EGFP I was using had come from Addgene in the pcDNA5 backbone and was meant to be an N-terminal fusion. As I looked more carefully at the sequence, I realized that there was no stop codon for EGFP and it was reading through the multiple cloning site and appending a C-terminal tail to EGFP with the following amino acid sequence:

GSTSPVWWNSADIQHSGGRSSLEGPFKPADQPRLCLLVASHLLFAPPPCLP

Yikes! This is a terrible looking sequence – it's an ugly, hydrophobic garbage sequence. Unfortunately, in several experiments throughout 2015, I had used this plasmid as a transfection efficiency marker. I would take a peek at cells on the microscope to gauge transfection efficiency by adding in a small amount of this GFP plasmid. It was confusing to me how ubiquilins were much more insoluble in its presence, but then I had my Eureka moment, so to speak, after which I threw out a lot of samples. I named this construct $EGFP^{Tail}$, and the next experiment I performed was with EGFP from the Clontech vector, pEGFP-C1.

Expression of EGFP in the Clontech vector results in primarily soluble protein, with protein turning up in the insoluble fraction in an MG132-dependent fashion. In the first experiment I performed with the corrected EGFP, I found that expression of any UQ protein was sufficient to drive some portion of EGFP to the insoluble fraction (Fig. 5.9B). However, UQ1 did not stabilize the faster migrating GFP(f1) peptide, whereas UQ2, UQ2dPRR, UQ1^{+PRR}, UQ2^{P497H} all stabilized GFP(f1) to a similar extent. I interpreted the data cautiously and attributed the difference in stabilization of GFP(f1) to differences in expression level of the different ubiquilin constructs. One other noteworthy aspect of EGFP^{Tail} is that it forms inclusions in cells, as assessed by live cell imaging. Treatment with MG132 results in a single focus, whereas co-expression with ubiquilins redistributes EGFP^{Tail} to small cytosolic vesicles – indicating that the C-terminal hydrophobic extension is sufficient to garner capture by ubiquilins, either directly or perhaps via Ub-mediated recognition (Fig. 5.9C).

I focused on UQ1 and UQ2, and performed a two-step titration of each Myc-UQ construct against a fixed amount of EGFP. This time I was convinced that there were clear differences between UQ1 and UQ2 in their ability to cause the accumulation of EGFP and GFP(f1) in the TX-resistant fraction (Fig. 5.10). The data is pretty striking, and suggests that UQ2 has some novel role in stabilizing DRiPs, which will be discussed further at the end of this chapter. The final experiment I did was a two-way titration, first of Myc-UQ2 against EGFP and then EGFP against Myc-UQ2. I included a couple of additional reference controls in this experiment to see if other proteins known to affect the stability of DRiPs would have an impact on GFP(f1). Increasing the amount of EGFP expression with fixed UQ2 expression resulted in the accumulation of EGFP in the pellet,

as well as reduction of UQ2 from the soluble fraction (with a roughly constant amount in the pellet) (Fig. 5.11). I wasn't sure how to interpret this experiment, thinking that it could be promoter competition. Neither BAG6 nor SGTA had an impact on GFP(f1), which was surprising(Fig 5.11). I was satisfied by the extractions, however, which showed the accumulation of the Myc-reactive non-UQ band in the pellet with MG132 (unaffected by UQ expression), and a significant amount of BAG6 in the pellet as a result of MG132 treatment (Fig. 5.11).

Long before I did experiments on GFP(F1), I attempted to co-IP puromycin-peptide adducts by performing an IP on cells expressing either UQ1 or UQ2 and exposing them to puromycin (data not shown). I was really surprised to find that UQ2 turned over very rapidly in response to puromycin treatment, while UQ1 was pretty much unaffected. I didn't really follow up these observations for several months… not sure why! When I returned to this idea, I performed a puromycin treatment in HeLa cells at 500ng/ml over a 24H time course. This was an exciting experiment, because I observed the degradation of endogenous UQ2, but not UQ1 (Fig. 5.12A). I did many iterations of this experiment, only to later discover a crossreactive band with the UBQLN1/2 antibody that is coincidentally at the same size as UQ1. The crossreactive band has a much thicker shape, consistent with an abundant protein and not a relatively rare protein like UQ1. Eventually, I figured this out with shRNA-expressing cells and starvation / add-back experiments (Fig. 5.12B). I hypothesize that the crossreactive band corresponds to an abundant serum protein, one that is not affected by puromycin treatment. As I discovered much later using Myc-tagged UQ constructs, all ubiquilins are diminished by puromycin

treatment, partially due to degradation and partially due to reduced translation (data not shown).

I do have some beautiful IF data that is worth sharing, as endogenous ubiquilins don't form punctate structures very often – in fact, they seem to form them exclusively following insult with puromycin. I performed IF with the UQ1/UQ2 antibody following puromycin insult and heat shock (Fig. 5.13A). I observed punctate ubiquilin staining in roughly half of the cells following puromycin insult, but no foci following heat shock. This stands in contrast to the RNA-binding protein, G3BP1, which is a well-known component of stress granules. Following heat shock, G3BP1 formed cytoplasmic foci in roughly 99% of cells, but its localization was unchanged after insult with puromycin. I found similar results with arsenite (data not shown), suggesting that ubiquilins are not part of stress granules[31], but do aggregate in puromycin-induced bodies, termed ALIS[20]. I also examined endogenous UQ1 and UQ2 with specific antibodies following puromycin treatment, this time comparing my normal method of fixation with a pre-extraction technique. I found that both UQ1 and UQ2 form cytosolic punctae in response to puromycin, but the structures formed by UQ1 were sensitive to pre-extraction in .2% TX, whereas UQ2 structures persisted (Fig. 5.13B). The final piece of this dataset is the shift of UQ2 away from EEA1-containing vesicles during puromycin insult. When U-2 OS cells stably expressing Myc-UQ2^{WT} are processed for IF, there is frequent overlap between UQ2 and EEA1, and infrequent overlap between UQ2 and the inclusion body marker, p62[16]. Following insult with puromycin, there is a shift of UQ2 out of EEA1-containing structures and into p62-positive inclusion bodies (Fig. 5.14).

5.4 Discussion

The UFD pathway is thought to synthesize predominantly K48- and K29-linked chains on its substrates. RAD23, another UBL-UBA containing shuttling factor, is much more abundant than UQ1 or UQ2[32]. In fact, according to a recent study of the HeLa proteome by label-free quantitative MS, RAD23 is more than an order of magnitude more abundant than UQ2, which is itself five times more abundant than UQ1[33,34]. Additionally, the UBA domain of RAD23 is specific for K48-linked polyUb chains, while the UBA of UQ proteins exhibits roughly equal affinity for all known polyUb regioisomers[35,36]. Given these important differences in copy number, it seems unlikely that UQ proteins would be limiting for the degradation of a molecule that is thought to carry K48-linked polyUb. This theory is in agreement with our experimental findings that UQ knockdown does not inhibit degradation of Ub^{G76V}-GFP. Although I make the same conclusion from co-transfected cells, the substrate accumulates in cells with high plasmid dose due to its strong pCMV promoter and is much more variable from cell to cell. The stable cells exhibit significantly lower and more uniform substrate expression, which is a better system for the application of high-efficiency siRNA transfections.

I envision a simple model in which the UFD substrate is bound and protected by the UBA domain of ubiquilin. When overexpressed, ubiquilin is in extremely high abundance, far exceeding normal concentration and resulting in stabilization of Ub-modified proteins by direct interaction. This concept can be generalized such that ubiquilin overexpression should result in the stabilization of any Ub-proteasome substrates, and it does. As described in the discussion of chapter 4, ubiquilin overexpression purportedly stabilizes p53, IkBa, presenilin, APP, TDP-43, and probably many more. Ubiquilin overexpression likely stabilizes Ub-modified substrates directly,

and there are not enough ubiquilin-binding proteins in the cells to efficiently transduce the signal to the proteasome. An alternative model is that ubiquilin overexpression disrupts the stoichiometry of the proteasome, resulting in less efficient proteasomal degradation of many different proteins. As for the Nature paper – my data do not support their claim that the UQ2 ALS mutants stabilize the reporter more strongly than the wild type protein. It's difficult to imagine an indirect mechanism by which the mutants would be more detrimental, with the exception of cell death from UQ2 ALS mutant expression, which has not been reported.

CD3 discussion: This model substrate doesn't seem to be regulated by ubiquilins in a special way. I'm not sure that ubiquilins are involved in ERAD in these cells, but it's possible that ubiquilins do fulfill these types of roles in more complex cells with greater cell volume. That said, earlier work describing the role of ubiquilins in ERAD was conducted in run-of-the-mill Hela and 293T.

I contacted Jon Yewdell about the GFP(F1) data, sharing first the Ub^{G76V}-GFP data and then the Ub-independent stabilization of GFP(f1). I presented it to him in a straightforward way – here's what I did, here's what I saw, and here's how the experiments were informed by your work[25,26]. He was really interesting – very cool and he's genuinely curious about some of the fundamental facets of antigen presentation, cell division, and protein concentration. As I understand his work, and I am a novice, he's interested in understanding how infected cells are detected by the immune system. The formation of "viral factories" occurs rapidly after infection, within 4h of exposure to virus[37]. How does the immune system know that a cell has been infected early, before the cell becomes lytic? If, as Jon's earlier work suggests, up to 30% of newly synthesized

proteins are rapidly degraded[18], then viral replication factories should be generating a massive load of viral peptides that can be presented as antigens on the cell surface. This is a cool idea.

I spoke with Jon on the phone and he shared with me the results of an unpublished screen that was performed in his lab by a post-doc. They used a variant of L929 cells stably expressing the mouse class I molecule H-2K^b, called L-K^b cells, and transduced GFP fused to the SIINFEKL peptide. The efficiency of display was measured by flow cytometry using a monoclonal antibody, 25-D1.16, which is specific for the class I K^b molecule bound to the SIINFEKL peptide. This system was then probed by a genome wide siRNA screen to look for modifiers of antigen display, classified as either inhibitors or enhancers. He pulled up this data while we talked on the phone, and informed me that *UBQLN1* knockdown is in the top 20% of hits for inhibitors of MHC-class I display. On the other side of the spectrum sits *UBQLN2* knockdown, which results in a roughly two-fold increase in antigen display (3 different siRNAs, showing 2.6, 1.8, and 1.8-fold enhanced display). These results also fit with my overexpression data – the accumulation of GFP(f1) means the peptide is no longer being efficiency degraded, and therefore not processed for antigen display. This is a really incredible confluence of findings. A very good experiment would be to test the effect of UBQLN knockdown, alone and in combination, on this system. This data suggests that UQ1 and UQ2 may very well have antagonistic roles – a double knockdown could be very informative. So that's the GFP(f1) data… it's pretty cool, and it sort of ties in to the puromycin data that I've generated. It also strongly implies differential functions for UQ1 and UQ2, which is one of my long-standing interests in grad school.

As for the TASK85 and puromycin data, in light of a really excellent paper from a pretty well-known lab[30], I have some new ideas about this. In their paper, they describe the central region of UQ1 as being able to capture hydrophobic substrates, independently of the UBA domain, which Itakura et al. posit is tied up in a UBA-UBL auto-inhibited state, much like the model I propose at the end of the last chapter (Fig. 4.15). When the substrate becomes Ub-modified, the UBA engages the Ub moiety, freeing the UBL to allow for targeting to the proteasome. It's a very clean model and it places ubiquilins in the cytosolic triage pathway[38]. If ubiquilins can bind to hydrophobic motifs, such as TMDs or truncated puromycyl-peptides, prior to Ub modification, then this might explain why the UQ2^{UBA*} mutant stabilized TASK85 to such a large extent. The other interesting experiment in that paper (there were several) was their characterization of proteasome interaction of UQ1^{WT} and two truncation mutants, UQ1$^{\Delta UBL}$ and UQ1 $^{\Delta UBA}$. They found that the UQ1$^{\Delta UBA}$ construct interacts to a much greater extent with the proteasome, due to free UBL targeting (not tied up with its own UBA). I interpreted this to also mean that UQ1^{UBA*} overexpression could disrupt proteasome stoichiometry.

An additional idea based on a couple of observations in other people's work[19,39,40]. When BAG6 is depleted, substrates accumulate, but are not ubiquitylated. When UQ4 is depleted, substrates accumulate in the polyUb-modified form. This suggests that BAG6 is required for directing substrates to E3s, and UQ4 is required for chaperoning those substrates to the proteasome once they are modified. Working out the order of this pathway, whether BAG6 and ubiquilins are antagonistic or cooperative, seems like a viable next step in understanding the role of ubiquilins in cytosolic triage[41].

5.5 Materials and Methods

See previous chapters.

5.6 Figures

Figure 5.1

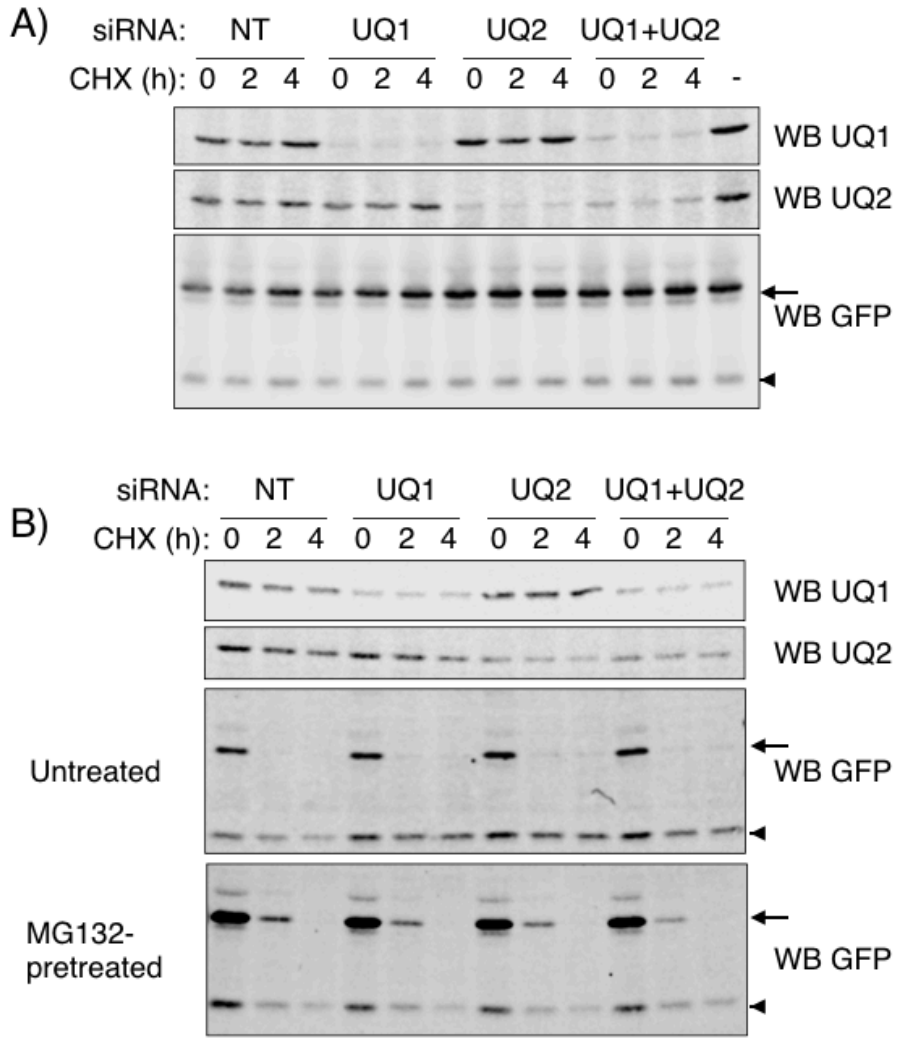

Knockdown of ubiquilins does not stabilize Ub^{G76V}-GFP. **A)** HEK 293T cells were co-transfected by $CaPO_4$ with plasmid encoding Ub^{G76V}-GFP and siRNA targeting a scrambled non-targeting control (NT), UQ1, UQ2, or both ubiquilins at a final concentration of 20nM each. Cells were grown 24H and then split to multiple dishes. 48h later, cells were treated with 50μg/ml CHX for the indicated time (h) and whole cell lysate (WCL) was harvested by suspending cells in PBS and adding equal volume 2x laemmli buffer. WCL was analyzed by SDS-PAGE and immunoblotting. Arrow indicates expected MW of Ub-GFP fusion, arrowhead indicates free GFP. **B)** HeLa cells stably expressing Ub^{G76V}-GFP were transfected with siRNA targeting NT, UQ1, UQ2, or both using Dharmafect I reagent at a final concentration of 30nM each. Cells were split 28h later to multiple dishes and allowed to grow ~48h before treatment with CHX and analysis as in (A). In the bottom panel, cells were pretreated with MG132 (5μM 2h) prior to CHX chase. Arrow indicates expected MW of Ub-GFP fusion, arrowhead indicates free GFP.

Figure 5.2

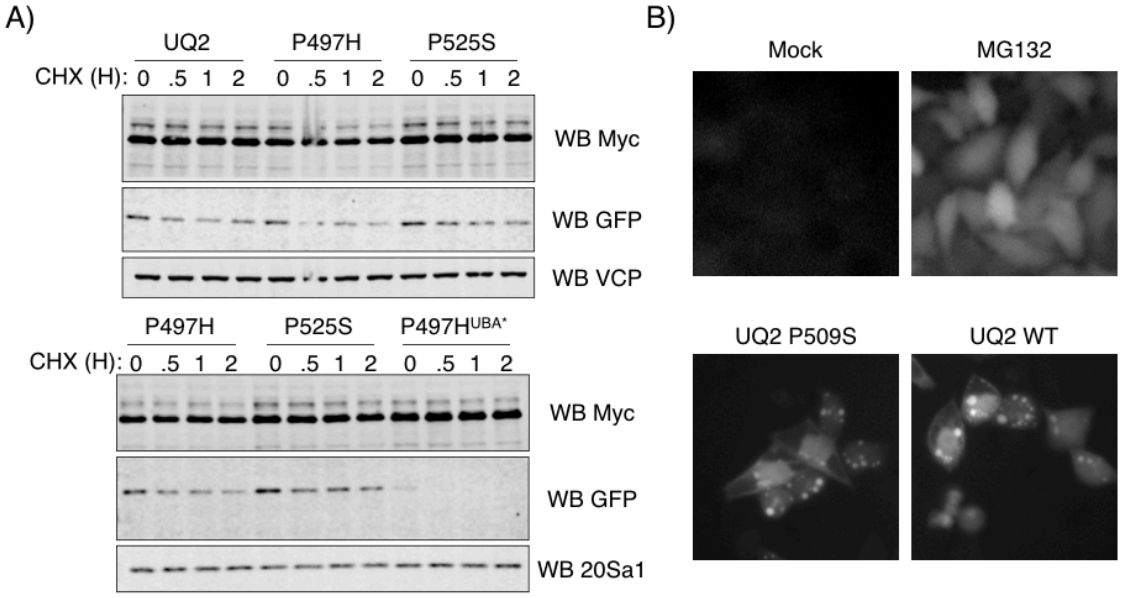

Ubiquilin overexpression stabilizes Ub^{G76V}-GFP in UBA-dependent manner. **A)** HeLa cells stably expressing Ub^{G76V}-GFP were transfected with the indicated constructs by lipofectamine 3000. After 24h, the cells were split and seeded in a 12w dish. 24h later, cells were treated with 50µg/ml CHX for the indicated time (h) and whole cell lysate (WCL) was harvested by adding 1x laemmli buffer directly to plate. Analysis by SDS-PAGE and immunoblotting reveal stabilization of Ub^{G76V}-GFP depends on UBA domain. **B)** Live cell imaging of HeLa cells stably expressing Ub^{G76V}-GFP transfected with the indicated construct or treated with MG132 (5µM 2h).

Figure 5.3

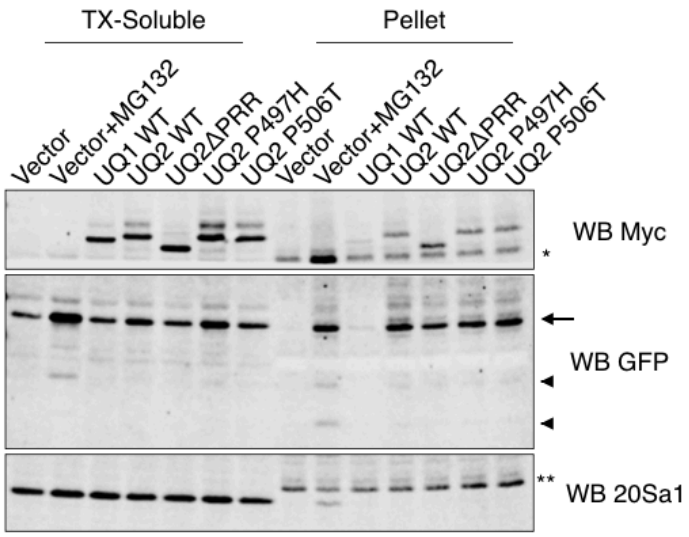

Ubiquilins stabilize Ub^{G76V}-GFP in the TX-resistant fraction. **A)** HEK 293T cells were transfected by $CaPO_4$ with 1.2µg of Myc-UQ and 300ng Ub^{G76V}-GFP, grown for 26h, then lysed and fractioned in TX buffer. Where indicated, cells were treated with MG132 (10µM 8h). Accumulation of Ub^{G76V}-GFP in the pellet is observed with MG132 treatment and with ubiquilin expression, but not with UQ1. * marks insoluble, proteasome-sensitive band. ** marks insoluble NS band. Note the shift of 20Sa1 proteasome subunit to the pellet following MG132. Arrow indicates expected MW of Ub-GFP, arrowheads indicate free GFP and GFP(F1).

Figure 5.4

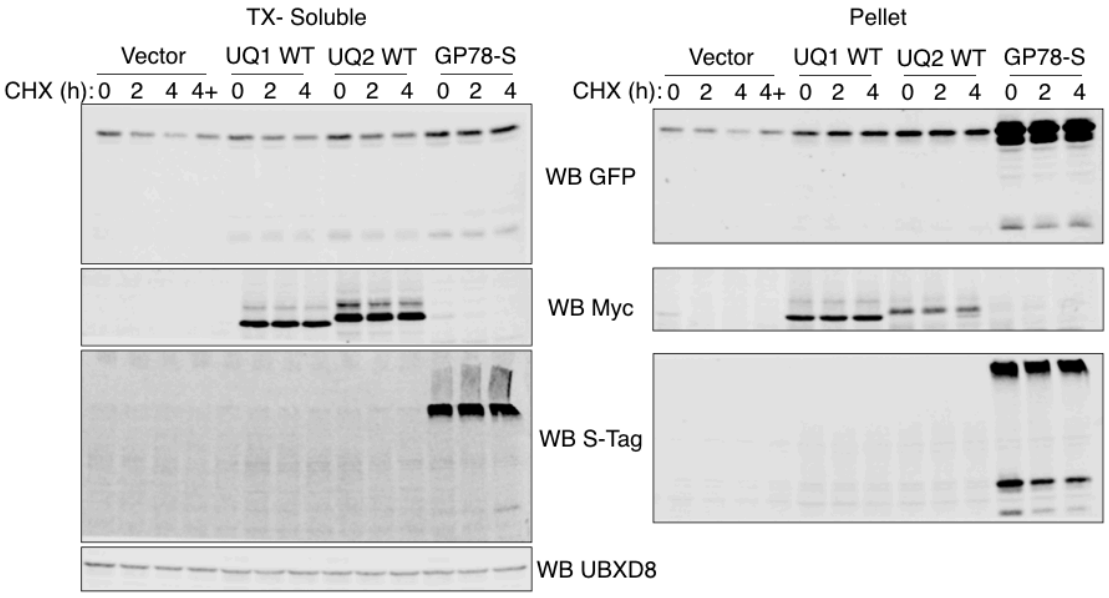

Ubiquilins exert modest stabilizing effect on CD3-δ. **A)** HEK 293T cells were transfected by $CaPO_4$ with 1.5µg of Myc-UQ or GP78-S and 500ng CD3-δ-YFP, grown for 24h, then split to multiple plates. After an additional 24h growth, cells were treated with 50µg/ml CHX for the indicated time (h), harvested and fractioned in TX. Analysis of soluble and pellet fractions reveal mild stabilization of CD3-δ-YFP in the soluble phase, but strong accumulation in the pellet. GP78-S has a much stronger effect than ubiquilins in this assay.

Figure 5.5

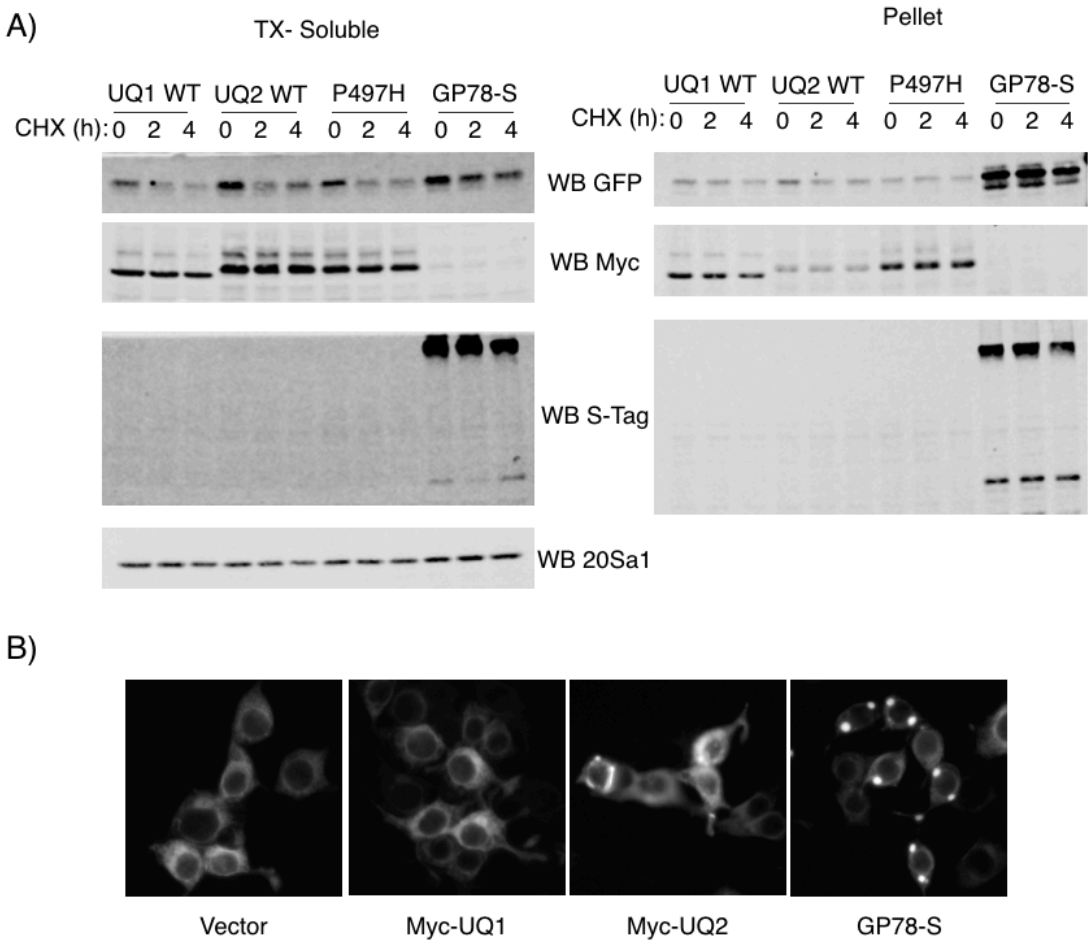

Unique stabilizing effect of GP78-S is not due to detergent resistance. **A)** HEK 293T cells were transfected by $CaPO_4$ with 1.5µg of Myc-UQ or GP78-S and 500ng CD3-δ-YFP, grown for 24h, then split to multiple plates. After an additional 24h growth, cells were treated with 50µg/ml CHX for the indicated time (h), harvested and fractioned in TX. Analysis of soluble and pellet fractions reveal that ubiquilins did not exert strong stabilization in the soluble phase, as evidenced by the rapid turnover of CD3-δ-YFP when compared to its degradation in the presence of GP78-S. The stabilization of CD3-δ-YFP by GP78-S is more dramatic in the insoluble fraction, despite the insolubility of $UQ2^{P497H}$. **B)** Live cell imaging of HEK 293T cells transfected as in (A) reveal unique localization of CD3-δ-YFP to perinuclear inclusions in the presence of GP78-S.

Figure 5.6

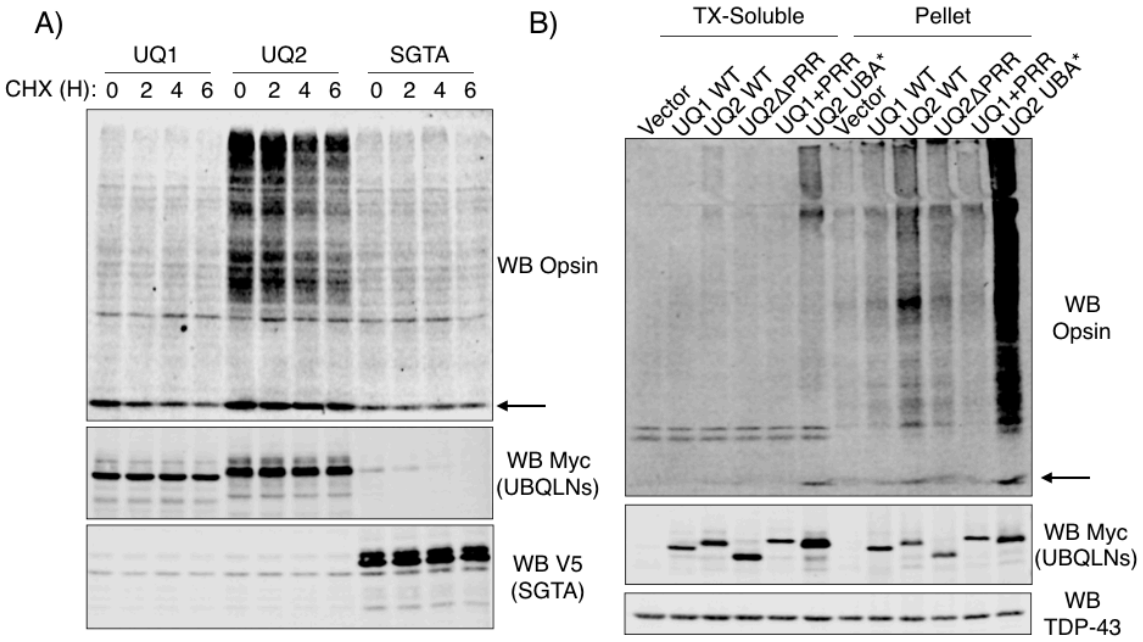

Differential stabilization of MLP substrate, TASK85. **A)** HEK 293T cells were transfected by $CaPO_4$ with 2µg of Myc-UQ or SGTA-V5 and 1µg TASK85, grown for 24h, then split to multiple plates. Roughly 48h later, cells were treated with 50µg/ml CHX for the indicated time (h) and whole cell lysate (WCL) was harvested by suspending cells in PBS and adding equal volume 2x laemmli buffer. SDS-PAGE and immunoblotting with indicated antibodies reveal that UQ2 stabilizes high MW forms of TASK85, in addition to the band at the expected MW (arrow). **B)** HEK 293T cells were transfected by $CaPO_4$ with 1µg of Myc-UQ and 1µg TASK85, grown for 24h, then split to multiple plates. Roughly 48h later, cells were fractioned in TX. $UQ2^{UBA*}$ exhibits the most clear stabilizing effect in both fractions. Notably, $UQ2^{UBA*}$, which is normally very soluble, was enriched in the pellet in this experiment. The greater stabilizing effect of UQ2 over UQ1 was once again observed.

Figure 5.7

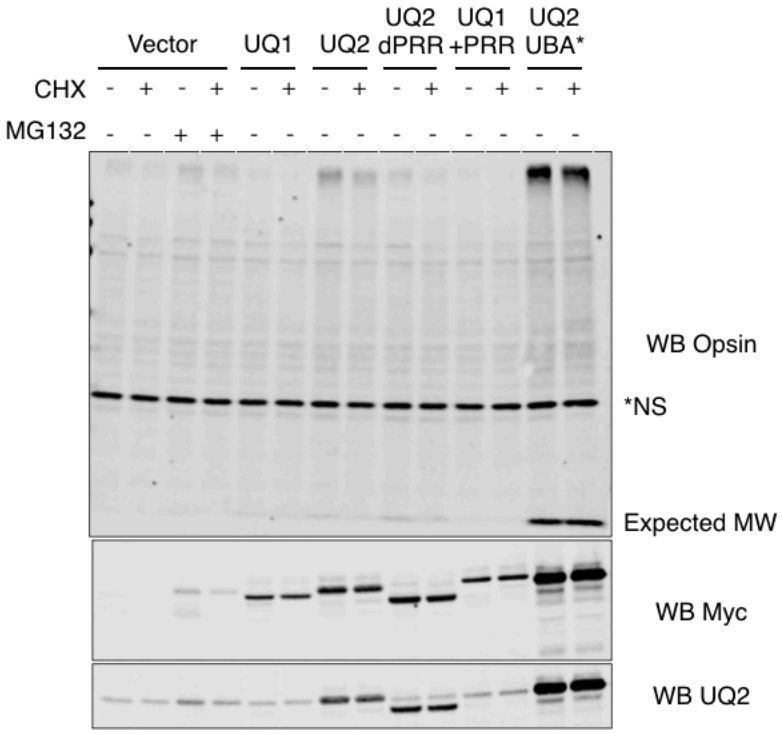

$UQ2^{UBA*}$ exerts greatest stabilizing effect on TASK85. HEK 293T cells were transfected by $CaPO_4$ with 1µg of Myc-UQ and 1µg TASK85, grown for 24h, then split to multiple plates. Roughly 48h later, cells were treated with 50µg/ml CHX for 4h, then fractioned in TX. Soluble fraction analyzed by SDS-PAGE and immunoblotting clearly show TASK85 accumulation in cells expressing $UQ2^{UBA*}$.

Figure 5.8

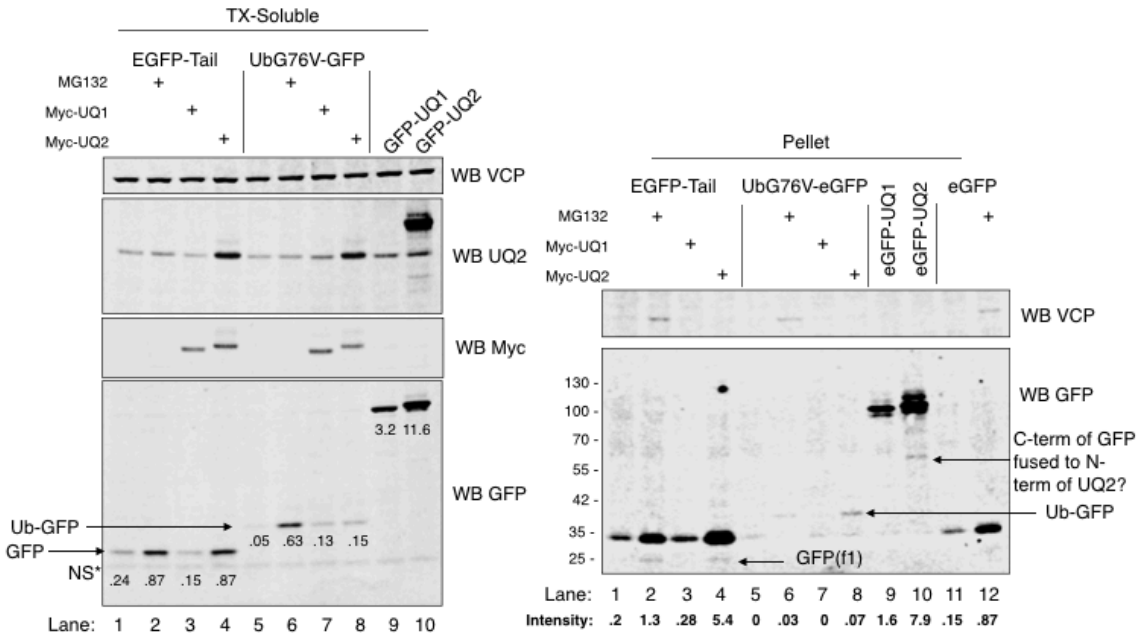

UQ2 promotes TX-resistance of model substrates. HEK 293T cells were transfected with Myc-UQ1 or Myc-UQ2 in combination with $EGFP^{Tail}$ or Ub^{G76V}-GFP, or cells were transfected with EGFP-UQ1 or EGFP-UQ2. Cells were harvested 27h after transfection, and where indicated cells were treated with MG132 (10μM 8h) prior to fractionation in TX. UQ2 promotes the accumulation of detergent-resistant species.

Figure 5.9

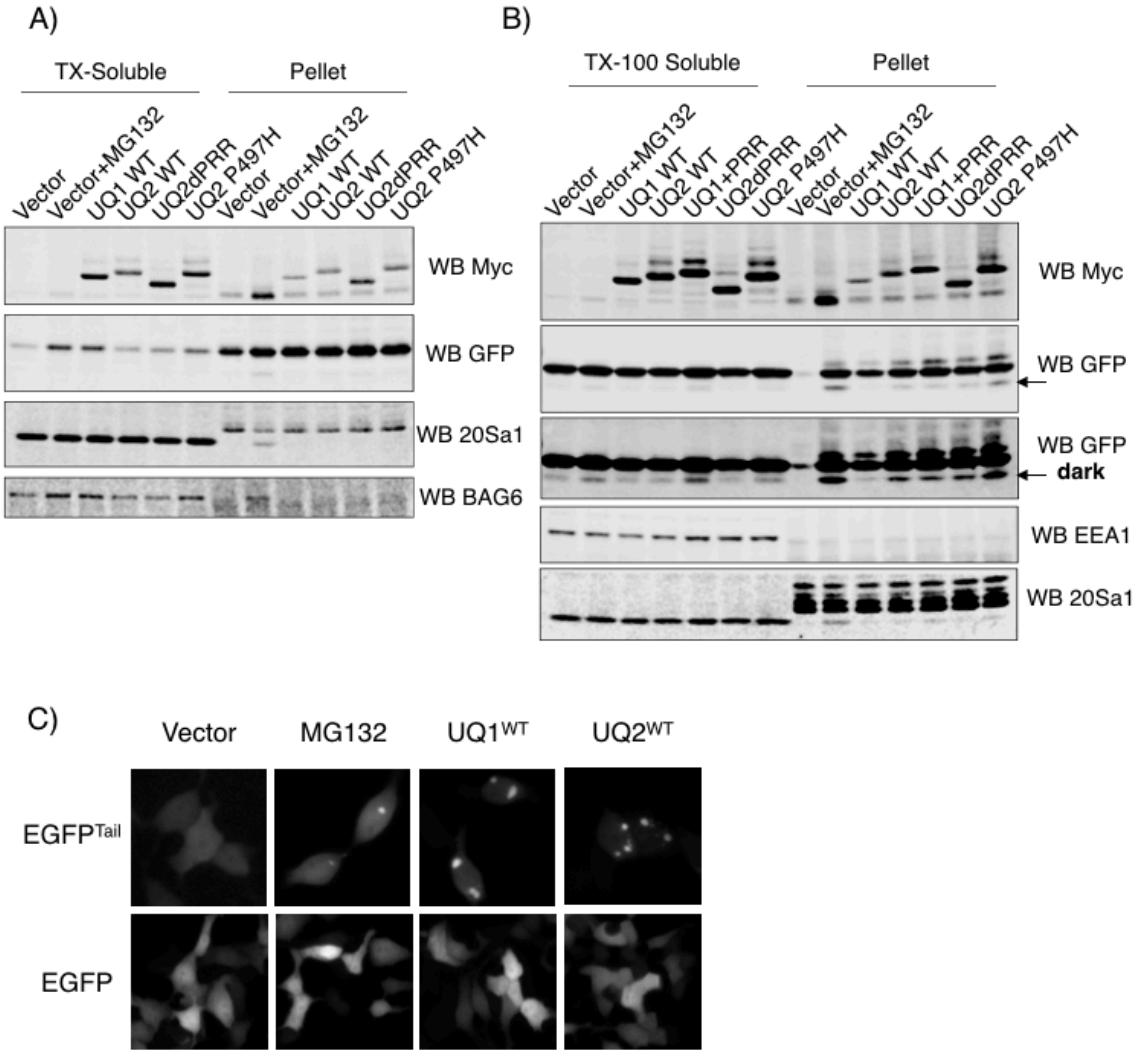

$EGFP^{Tail}$ is detergent resistant. **A)** HEK 293T cells were transfected with the indicated Myc-UQ construct and $EGFP^{Tail}$, grown for 27h, and where indicated treated with MG132 (10μM 8h) before fractionation in TX. Fractions were analyzed by SDS-PAGE and immunoblotting as indicated. $EGFP^{Tail}$ is abundant in the TX-resistant fraction, even in the context of vector expression. **B)** As in (A), except that EGFP was used in place of the $EGFP^{Tail}$ construct. In this case, EGFP is predominantly soluble in the vector only, and is shifted to the pellet by MG132 treatment or expression of ubiquilins. Only UQ1 doesn't stabilize the GFP(F1) fragment (arrow). **C)** Live cell imaging of HEK 293T cells transfected with either Myc-UQ1 or Myc-UQ2 and either $EGFP^{Tail}$ or EGFP, as indicated. Focus formation and vesicle incorporation of $EGFP^{Tail}$ due to hydrophobic tail.

Figure 5.10

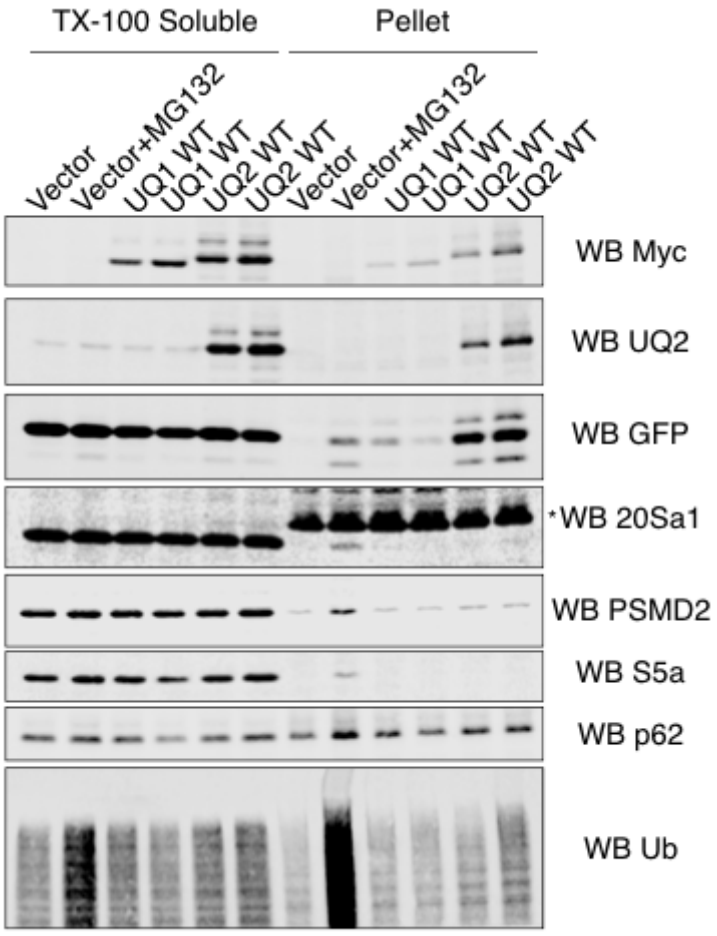

UQ2 stabilizes EGFP in the TX-resistant fraction to a greater extent than UQ1. HEK 293T were transfected by $CaPO_4$ with EGFP alone or in 1:1 or 1:2 ratio with Myc-UQ1 or Myc-UQ2, grown for 30h, and fractioned in TX. Where indicated, cells were treated with MG132 (10μM 6h) prior to lysis. Co-expression with UQ2 results in accumulation of EGFP and GFP(f1) in the TX-resistant fraction. Solubility shift of several proteasome proteins and Ub during MG132 indicate that the effect of UQ2 on GFP(f1) is specific.

Figure 5.11

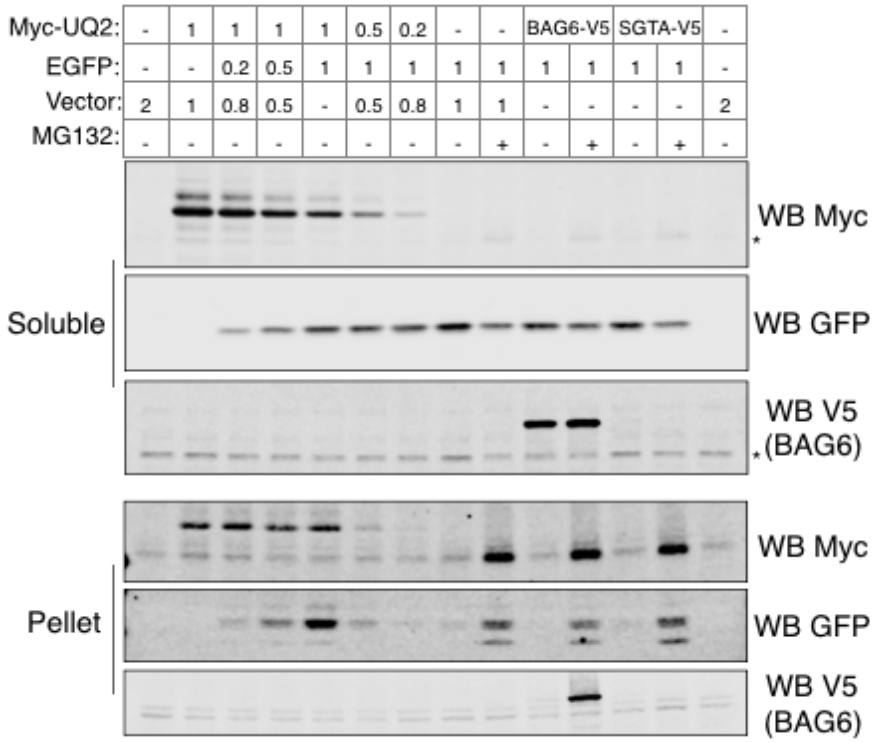

Unique impact of UQ2 on EGFP solubility. HEK 293T cells were transfected by $CaPO_4$ with a total of 2µg per plate as indicated. Titration of UQ2 against EGFP and of EGFP against UQ2 reveal dose-dependent effect of UQ2 on EGFP solubility. Fractionation of EGFP is not altered by BAG6 or SGTA.

Figure 5.12

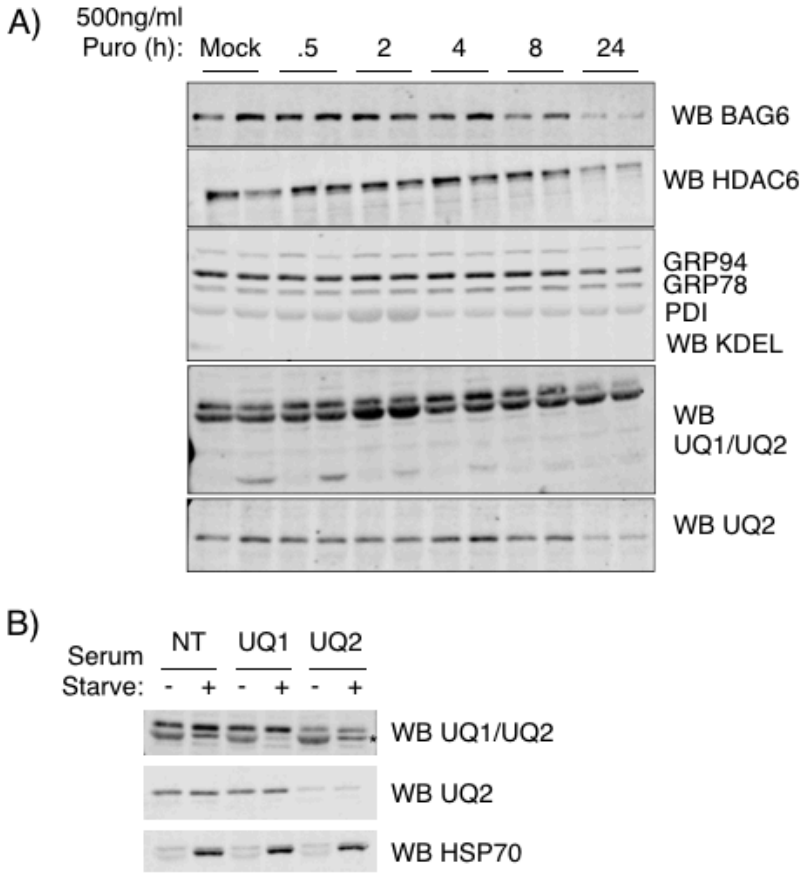

Puromycin induces degradation of DRiP regulators. **A)** HeLa cells were treated with 500ng/ml puromycin for the indicated amounts of time prior to lysis. Analysis by SDS-PAGE and immunoblotting reveal the depletion of BAG6, UQ2, and HDAC6. In this data, the UQ1/UQ2 antibody seems to indicate that UQ1 is stable during the course of treatment. **B)** HeLa cells stably expressing shRNA against a non-targeting control (NT), UQ1, or UQ2, were serum starved for 7h prior to lysis and analysis by SDS-PAGE and immunoblotting. Induction of a band during serum starvation (marked by *) corresponding to UQ1 is blocked by UQ1 shRNA (cf. lanes 2, 4, and 6). The large cross-reactive band at the same MW is not reduced by UQ1 shRNA and is likely a serum protein.

Figure 5.13

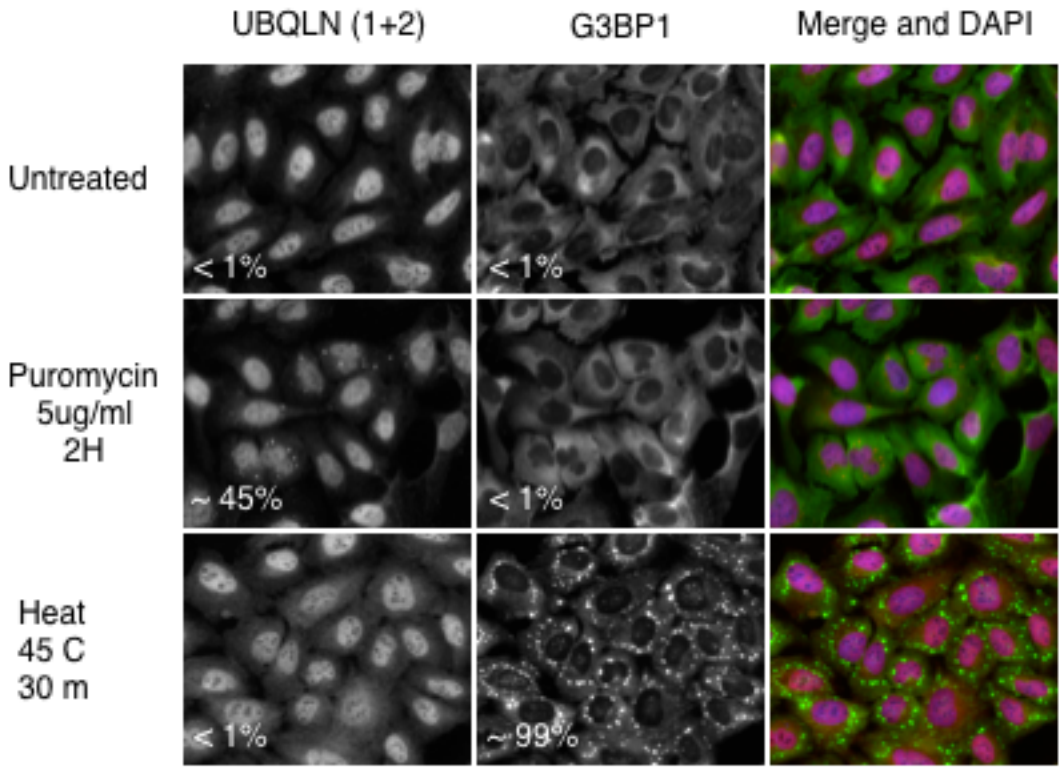

Ubiquilins form cytosolic punctae following puromycin insult. **A)** HeLa cells were either left untreated, treated with puromycin (5µg/ml 2h), heat shocked at 45C for 30m prior to fixation in 4%PFA, permeabilization in .2%TX, and IF with antibodies against UQ1/UQ2 and G3BP1. Ubiquilins form punctate structures in ~45% of cells in response to puromycin, but are unchanged by heat stress. G3BP1 forms stress granules in >99% of cells following heat stress, but does not redistribute in response to puromycin.

Figure 5.13 continued

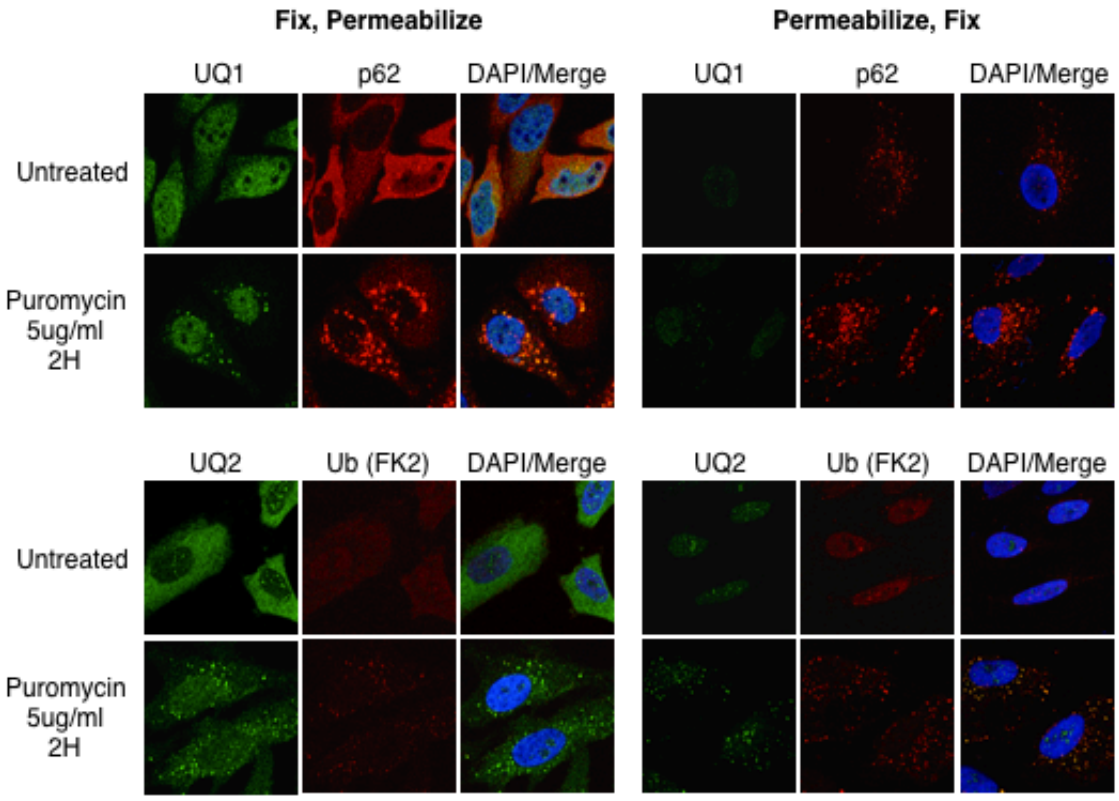

B) HeLa cells were left untreated or insulted with puromycin as in (A). In the left panels, cells were fixed, then permeabilized as in (A); in the right panels, cells were pre-extracted in .2%TX prior to fixation to remove soluble protein. Both UQ1 and UQ2 form punctate inclusions in response to puromycin that localize with p62 and Ub. Only UQ2 inclusions persist through pre-extraction. It also appears that UQ2 exhibits nuclear speckles that are resistant to extraction under basal conditions.

Figure 5.14

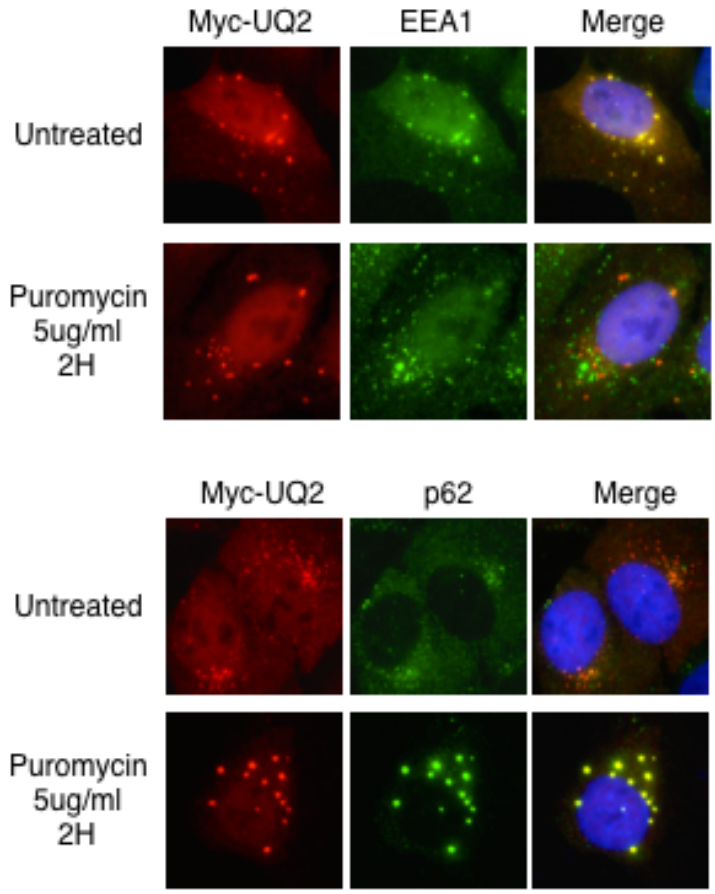

UQ2 exits endosomes and enters inclusion bodies following puromycin. Dox-inducible U-2 OS cells were treated with Dox (50ng/ml) overnight before treatment with puromycin (5µg/ml 2h) where indicated. Cells were fixed in 4%PFA, permeabilized in .2%TX, and stained with the indicated antibodies. Under basal conditions, Myc-UQ2 forms cytosolic vesicles that are frequently positive for EEA1, and only infrequently localizing with p62. Upon treatment with puromycin, Myc-UQ2 rarely localizes with EEA1 and enters large inclusions positive for p62.

5.7 References

1. Wunderley, L., Leznicki, P., Payapilly, A. & High, S. SGTA regulates the cytosolic quality control of hydrophobic substrates. *J Cell Sci* **127,** 4728–4739 (2014).
2. Dantuma, N. P., Lindsten, K., Glas, R., Jellne, M. & Masucci, M. G. Short-lived green fluorescent proteins for quantifying ubiquitin/proteasome-dependent proteolysis in living cells. *Nat Biotechnol* **18,** 538–543 (2000).
3. Hänzelmann, P., Stingele, J., Hofmann, K., Schindelin, H. & Raasi, S. The yeast E4 ubiquitin ligase Ufd2 interacts with the ubiquitin-like domains of Rad23 and Dsk2 via a novel and distinct ubiquitin-like binding domain. *J Biol Chem* **285,** 20390–20398 (2010).
4. Thrower, J. S., Hoffman, L., Rechsteiner, M. & Pickart, C. M. Recognition of the polyubiquitin proteolytic signal. *EMBO J* **19,** 94–102 (2000).
5. Johnson, J. O. *et al.* Exome sequencing reveals VCP mutations as a cause of familial ALS. *Neuron* **68,** 857–864 (2010).
6. Chou, T.-F. & Deshaies, R. J. Quantitative cell-based protein degradation assays to identify and classify drugs that target the ubiquitin-proteasome system. *J Biol Chem* **286,** 16546–16554 (2011).
7. Bernasconi, R., Galli, C., Calanca, V., Nakajima, T. & Molinari, M. Stringent requirement for HRD1, SEL1L, and OS-9/XTP3-B for disposal of ERAD-LS substrates. *J Cell Biol* **188,** 223–235 (2010).
8. Fang, S. *et al.* The tumor autocrine motility factor receptor, gp78, is a ubiquitin protein ligase implicated in degradation from the endoplasmic reticulum. *Proc Natl Acad Sci USA* **98,** 14422–14427 (2001).
9. Yang, H. *et al.* Ubiquitin ligase Hrd1 enhances the degradation and suppresses the toxicity of polyglutamine-expanded huntingtin. *Exp Cell Res* **313,** 538–550 (2007).
10. Liu, Y. *et al.* USP13 antagonizes gp78 to maintain functionality of a chaperone in ER-associated degradation. *Elife* **3,** e01369 (2014).
11. Kim, T.-Y., Kim, E., Yoon, S. K. & Yoon, J.-B. Herp enhances ER-associated protein degradation by recruiting ubiquilins. *Biochem Biophys Res Commun* **369,** 741–746 (2008).
12. Lim, P. J. *et al.* Ubiquilin and p97/VCP bind erasin, forming a complex involved in ERAD. *J Cell Biol* **187,** 201–217 (2009).
13. Yoshida, H., Matsui, T., Yamamoto, A., Okada, T. & Mori, K. XBP1 mRNA is induced by ATF6 and spliced by IRE1 in response to ER stress to produce a highly active transcription factor. *Cell* **107,** 881–891 (2001).
14. Xia, Y. *et al.* Pathogenic mutation of UBQLN2 impairs its interaction with UBXD8 and disrupts endoplasmic reticulum-associated protein degradation. *J Neurochem* n/a–n/a (2013). doi:10.1111/jnc.12606
15. Rothenberg, C. *et al.* Ubiquilin functions in autophagy and is degraded by chaperone-mediated autophagy. *Hum Mol Genet* **19,** 3219–3232 (2010).
16. Wenger, T. *et al.* Autophagy inhibition promotes defective neosynthesized proteins storage in ALIS, and induces redirection toward proteasome processing and MHCI-restricted presentation. *Autophagy* **8,** 350–363 (2012).
17. NATHANS, D. PUROMYCIN INHIBITION OF PROTEIN SYNTHESIS:

INCORPORATION OF PUROMYCIN INTO PEPTIDE CHAINS. *Proc Natl Acad Sci USA* **51,** 585–592 (1964).
18. Schubert, U. *et al.* Rapid degradation of a large fraction of newly synthesized proteins by proteasomes. *Nature* **404,** 770–774 (2000).
19. Minami, R. *et al.* BAG-6 is essential for selective elimination of defective proteasomal substrates. *J Cell Biol* **190,** 637–650 (2010).
20. Szeto, J. *et al.* ALIS are stress-induced protein storage compartments for substrates of the proteasome and autophagy. *Autophagy* **2,** 189–199 (2006).
21. Liu, X.-D. *et al.* Transient aggregation of ubiquitinated proteins is a cytosolic unfolded protein response to inflammation and endoplasmic reticulum stress. *J Biol Chem* **287,** 19687–19698 (2012).
22. Lacsina, J. R. *et al.* Premature Translational Termination Products Are Rapidly Degraded Substrates for MHC Class I Presentation. *PLoS ONE* **7,** e51968 (2012).
23. Hessa, T. *et al.* Protein targeting and degradation are coupled for elimination of mislocalized proteins. *Nature* **475,** 394–397 (2011).
24. Rodrigo-Brenni, M. C., Gutierrez, E. & Hegde, R. S. Cytosolic quality control of mislocalized proteins requires RNF126 recruitment to Bag6. *Molecular cell* **55,** 227–237 (2014).
25. Qian, S.-B., Princiotta, M. F., Bennink, J. R. & Yewdell, J. W. Characterization of rapidly degraded polypeptides in mammalian cells reveals a novel layer of nascent protein quality control. *J Biol Chem* **281,** 392–400 (2006).
26. Wei, J. *et al.* Ubiquitous Autofragmentation of Fluorescent Proteins Creates Abundant Defective Ribosomal Products (DRiPs) for Immunosurveillance. *J Biol Chem* **290,** 16431–16439 (2015).
27. Deng, H.-X. *et al.* Mutations in UBQLN2 cause dominant X-linked juvenile and adult-onset ALS and ALS/dementia. *Nature* 1–7 (2011). doi:10.1038/nature10353
28. Leznicki, P. & High, S. SGTA antagonizes BAG6-mediated protein triage. *Proceedings of the National Academy of Sciences* **109,** 19214–19219 (2012).
29. Leznicki, P. *et al.* Binding of SGTA to Rpn13 selectively modulates protein quality control. *J Cell Sci* **128,** 3187–3196 (2015).
30. Itakura, E. *et al.* Ubiquilins Chaperone and Triage Mitochondrial Membrane Proteins for Degradation. *Molecular cell* **63,** 21–33 (2016).
31. Buchan, J. R., Kolaitis, R.-M., Taylor, J. P. & Parker, R. Eukaryotic stress granules are cleared by autophagy and Cdc48/VCP function. *Cell* **153,** 1461–1474 (2013).
32. Qian, S.-B., Ott, D. E., Schubert, U., Bennink, J. R. & Yewdell, J. W. Fusion proteins with COOH-terminal ubiquitin are stable and maintain dual functionality in vivo. *J Biol Chem* **277,** 38818–38826 (2002).
33. Geiger, T., Wehner, A., Schaab, C., Cox, J. & Mann, M. Comparative Proteomic Analysis of Eleven Common Cell Lines Reveals Ubiquitous but Varying Expression of Most Proteins. *Mol Cell Proteomics* **11,** M111.014050–M111.014050 (2012).
34. Schaab, C., Geiger, T., Stoehr, G., Cox, J. & Mann, M. Analysis of High Accuracy, Quantitative Proteomics Data in the MaxQB Database. *Mol Cell Proteomics* **11,** M111.014068–M111.014068 (2012).
35. Rao, H. & Sastry, A. Recognition of specific ubiquitin conjugates is important for the proteolytic functions of the ubiquitin-associated domain proteins Dsk2 and

Rad23. *J Biol Chem* **277,** 11691–11695 (2002).
36. Zhang, D., Raasi, S. & Fushman, D. Affinity makes the difference: nonselective interaction of the UBA domain of Ubiquilin-1 with monomeric ubiquitin and polyubiquitin chains. *J Mol Biol* **377,** 162–180 (2008).
37. David, A. *et al.* Nuclear translation visualized by ribosome-bound nascent chain puromycylation. *J Cell Biol* **197,** 45–57 (2012).
38. Ast, T. & Schuldiner, M. Protein degradation: BAGging up the trash. *Curr Biol* **21,** R692–R695 (2011).
39. Suzuki, R. & Kawahara, H. UBQLN4 recognizes mislocalized transmembrane domain proteins and targets these to proteasomal degradation. *EMBO Rep* (2016). doi:10.15252/embr.201541402
40. Shao, S., Malsburg, von der, K. & Hegde, R. S. Listerin-dependent nascent protein ubiquitination relies on ribosome subunit dissociation. *Molecular cell* **50,** 637–648 (2013).
41. Guo, L. *et al.* A Cellular System that Degrades Misfolded Proteins and Protects against Neurodegeneration. *Molecular cell* **55,** 15–30 (2014).

Chapter 6: Discussion and future directions

Overview

In the month leading up to my oral defense, two high impact papers on ubiquilins were published in Molecular Cell and Cell, from the labs of Professor Ramanujan Hegde and Professor Thimo Kurz, respectively[1,2]. Seeing as I am one of the world's foremost experts on ubiquilins (pretty cool), I thought I would take a moment to comment on these publications, including a brief description of the approach, major findings, and how this work informs my understanding of ubiquilins. The Mol Cell paper from Manu Hegde's lab is excellent, and I don't think it overlaps significantly with the work presented in this thesis. The Cell paper from the Kurz lab hits closer to home, there are some common experimental threads that I will cover in detail, and I will also share some preliminary data, collected after my oral defense, that I consider due diligence in reproducing their work as a jumping off point for future investigations. Both of these papers focus on detergent-specific and stress-inducible partitioning of ubiquilins, and I would like to expand on a framework for thinking about protein solubility. Finally, I will present a series of gedankenexperiments to explore a few of the experimental avenues that could be pursued with the genetic and biochemical models being developed in our lab.

6.1 Literature Update

Itakura et al. initiated their study by identifying both UQ1 and UQ4 in an unbiased proteomics approach to identify proteins that interacted with an *in vitro* translated substrate bearing an exposed transmembrane domain (TMD). Through a series of *in vitro* binding assays, they concluded that UQ1 preferentially binds mitochondrial TMDs in a manner that is independent of the UBL and UBA domains – drawing attention

to the less well-characterized central region of the protein, which the group deemed the "M domain" because of its high methionine content. The group went on to generate triple deficient UQ1/UQ2/UQ4 CRISPR knockout cells to perform complement experiments to assess the function of UQ1, which they performed with a series of truncations and point mutants. They found that UQ1 is required for the efficient degradation of mitochondrial proteins that fail to insert into the membrane, and were further able to demonstrate a direct and detergent-sensitive interaction between UQ1 and a number of model TMD substrates in multiple experimental models. Another significant finding from the work of Itakura et al. is that pathologic polyglutamine proteins, which are found in neurodegenerative diseases such as Huntington's disease and spinocerebellar ataxias, sequester ubiquilins in an insoluble (and nonfunctional) state.

Ultimately, Itakura et al. propose a model in which ubiquilins exist in an auto-inhibited state, in which the UBL and UBA domains are engaged with each other, preventing the association of ubiquilins with polyUb. Upon binding to a hydrophobic motif with the M domain, ubiquilins recruit E3 Ub ligases through a UBA-dependent mechanism, promoting the ubiquitylation of the substrate. The Ub modification is thought to act as a commitment step to degradation, as it prevents the membrane targeting of the substrate (well demonstrated in supplemental figure 7). The association of UQ1 with the Ub-modified substrate is now bolstered by an avidity mechanism, freeing the UBL domain to target the complex to the proteasome for degradation. I very much like this model, and there are some additional fine points of this model which I developed in the discussion of Chapter 4, considering how Ub modification of the UBL domain might factor into this auto-inhibition mechanism. One noteworthy detail in this paper is the

group's direct comparison of a UBA truncation mutant ($UQ1\Delta^{UBA}$) with a UBA point mutant ($UQ1^{F559A}$), which they found to function identically in a membrane insertion assay – lending support to my data, because I used the same F559A mutation as my $UQ1^{UBA*}$ construct. Another series of noteworthy observations from this work is the UQ1-induced stabilization of TMD reporters in the heavy fractions of cells following centrifugation and in insoluble fractions following differential detergent extraction.

Hjerpe et al. posit that stress stimulates the interaction of UQ2 with HSP70, thereby facilitating the proteasome-dependent degradation of HSP70 clients. Under basal conditions, UQ2 forms homo- and hetero-dimers with UQ1, itself, and UQ4, but does not interact to an appreciable extent with polyUb, HSP70, or the proteasome. Following stress, in this case heat shock, UQ2 can robustly co-IP polyUb, HSP70, and proteasome subunits, but does not efficiently interact with other ubiquilins. The authors claim that UQ2 functions in both the cytosol and the nucleus to degrade polyUb-containing protein aggregates following heat shock, critical to cell survival. Most importantly, the group generated a knock-in mouse model of $UQ2^{P506T}$ ($mUQ2^{P520T}$) and concluded that this particular mutation is a loss-of-function. In their assays, largely conduced in murine embryonic fibroblasts (MEFs) and with brain extract from animals, they found that $mUQ2^{P520T}$ bound with lower affinity to HSP70, but with higher affinity to polyUb under resting conditions. Following heat shock, there was no inducible interaction $mUQ2^{P520T}$ with either HSP70 or polyUb, suggesting that the mutation is a loss-of-function with respect to stress-inducible protein-protein interactions.

In a variety of biophysical assays, the group concluded that UQ2 itself is not aggregation-prone, and mutations that cause ALS do not cause the protein to misfold, nor

do they alter its oligomerization status, localization, or cytosolic-nuclear shuttling. The knock-in mouse did not have a motor phenotype, but did have a subtle object recognition phenotype – I don't have much experience with these types of behavioral assays, but it seems a mild phenotype. Importantly, the knock-in mUQ2^{P520T} mouse develops Ub- and p62-positive protein aggregates throughout the brain as a function of age, recapitulating hallmark pathology of UQ2-associated ALS. Hjerpe et al. also characterized the sequestration of wild type UQ2 with polyglutamine proteins, suggesting that depletion of UQ2 in polyglutamine diseases and related proteinopathies could diminish the aggregated protein response, which is conceivably a new pathway independent of the well-characterized unfolded protein response pathway.

There are some interesting data contained in the supplemental file that I would like to highlight here. First, the Kurz lab also generated a UQ2$^{\Delta PRR}$ construct and found that this protein can bind to HSP70 under basal conditions and following heat stress to a similar extent as that seen for UQ2^{WT}. If mutations in the PRR are loss-of-function with respect to HSP70 binding, then how could UQ2$^{\Delta PRR}$ interact? The authors address this briefly: "We also tested if the PXXP motif is required for interaction; however, deletion of the PXXP motif had no effect on HSP70 binding, demonstrating that this region is not the direct binding site (Figure S5G). Instead, it is likely that the PXXP mutations interfere indirectly with HSP70 binding." Because the lab has expertise in the approach, I would suggest *in vitro* pull down experiments with truncation mutants to address central questions in the loss-of-function model: 1) if the PRR is not the direct binding site, what is? Can UQ1 bind as well? 2) How are mutations disrupting HSP70 interaction?

6.2 What does protein solubility reflect?

An additional piece of data that struck me from this recent paper was the selective accumulation of mUQ2^{P520T} in the insoluble fraction of hippocampus, but not in the cortex or cerebellum (Fig. S7). I am not sure the significance of this observation, but it is striking and potentially an important piece in the puzzle of ALS[2]. Both of these papers and my personal work addressed alterations to protein solubility in the event of ubiquilin deficiency or mutation. Traditionally, extraction resistance of proteins to biological detergents implies membrane localization or membrane association in the cellular context. Given the wide variety of detergents, the solubility of a given protein in a particular detergent may reflect the type of lipid membrane or domain with which it is associated[3]. In neurodegeneration, detergent resistance is a common property of protein aggregates, which are resistant even to strong anionic detergents such as sarkosyl[4]. The meaning of detergent resistance in this context is slightly more nebulous, as protein aggregates and inclusion bodies are typically not membrane-bound. Observation of hippocampus-specific accumulation of insoluble mUQ2^{P520T} complicates this picture further, giving us a peek of the complex biology governing protein solubility.

In a different example of protein solubility in biology, detergent resistance of prions represents a fibrillar, oligomeric form of a protein[5]. In yeast, prionogenic transcription factors can toggle between a soluble, functional state and an insoluble, oligomeric state, resulting in altered transcriptional programs and variable phenotypes that can be passed from mother to daughter cells[6]. Yeast prions have been documented to toggle randomly between soluble and aggregated states at low frequency, allowing for population "bet hedging," in which the few organisms that harbor the prion state of a

transcription factor can sample a new transcriptional program. If the program is beneficial, the prion-carrying yeast will multiple faster and populate the colony – if not, they will be outgrown by the masses. On the other hand, there are prions that respond to cellular and environmental cues, providing phenotypic diversity in response to adverse conditions[7].

However, outside of pathologic proteins, there are no known beneficial prions in humans (to my knowledge)[8]. Nonetheless, one of the most interesting features of protein solubility is that it declines with age in model organisms independently of disease[9,10]. Specific complexes, such as ribosome-associated chaperones, also lose solubility as a function of age, which I interpret to mean that these complexes are no longer functional[11]. How this phenomenon contributes to neurodegeneration is not presently known, but it is conceivable that post-mitotic cells, such as neurons, experience a gradual decline in protein solubility as a function of age, resulting in gradual degeneration and loss of function as a molecular reflection of the aging process[12].

6.3 Stress-induced alterations to protein solubility

Protein solubility fluctuates on a much shorter time scale during acute stress, and these fluctuations are required for adaptation to adverse conditions[13,14]. One of the most fascinating tangential projects I enjoyed was observation of oscillation in Ub solubility following heat shock. I was inspired to try this experiment after seeing a talk by Professor Thibault Mayor at the Cold Spring Harbor Ubiquitin Family meeting[15,16]. I performed heat shock at 45C for 30m, returned cells to the incubator for varying amounts of time to recover, and then lysed the cells and separated into soluble and pellet fractions. In U-2 OS and HEK 293T cells, ubiquilin solubility was not altered under the conditions tested.

However, I observed a pretty unexpected oscillatory pattern of Ub solubility, in which insoluble Ub accumulated dramatically during heat shock, was then absent from the insoluble phase at certain time points, and then the signal was very high in the insoluble phase again (Figure 6.1). At first I thought it was a weird artifact, but I repeated it because it's straightforward to just add one more plate of cells to an experiment, so why not. This was highly reproducible, but the main issue with this experiment in its first iteration was that I was using a non-CO_2 incubator, and I was simply sealing cells in plastic bags for the 30m, shifting them to an incubator at 45C (which, full disclosure, is not a very well-behaved incubator), and then returning them to a CO_2 incubator at 37C. When I performed multiple experiments close together – within a couple weeks – it was reproducible, but when I revisited this experiment months later, the oscillation period changed (perhaps due to a slightly different temperature) and was observed in HEK 293T, but not in HeLa cells (Figure 6.2).

As it turns out, UQ2 in the heat shock response is the main focus of the Cell paper discussed in section 6.1[2]. Hjerpe et al. performed a more mild heat shock (42C) for 2h, and they found that UQ2 shifted to the insoluble phase, and that UQ2 deficiency impeded the clearance of insoluble Ub as assessed by a recovery assay, much like my work. I think it's important to point out how different 42C and 45C is to cells – 2h at 42C is stressful, no doubt, but cells can recover; 2h at 45C is lethal. It seems that heat shock is not trivial, and minor changes in temperature or time can have enormous experimental ramifications. I think it's also important to point out that heat shock is not cell autonomous and heat is not simply a means of inducing protein misfolding. While cells in culture do respond to heat shock, there is significant blunting of the heat shock response at the organismal level

in *C. elegans* when the thermosensory neurons are ablated[17]. Additional work from the Morimoto lab suggests that cellular signaling plays an equally, if not more, important role in protein folding stress as the stressor itself [18].

So – under different conditions, it appears that UQ2 does move to the pellet fraction following heat stress, and Hjerpe et al. found that UQ1 did not. I therefore am in the process of repeating the work from Hjerpe et al., and it is quite clear that UQ2 moves to the insoluble phase following heat shock at 42C for 2h (this time using a well calibrated incubator) (Figure 6.3). However, in my hands, UQ2 deficiency does not impact clearance of Ub from the insoluble phase. It is possible that different experimental conditions account for this discrepancy, and I think it is worth noting that I am employing different lysis conditions. Nonetheless, I do see UQ2 shift to the pellet after heat shock at 42C for 2h. How this heat shock differs from 45C for 30m is not clear to me, but what is clear is that heat shock is an unexpectedly nuanced experimental technique.

6.4 Summary of primary findings

My work suggests that UQ1 and UQ2 are differentially ubiquitylated, resulting in distinct cytological and biochemical properties of these highly similar proteins. Surprisingly, I found that the PRR domain of UQ2 is not solely responsible for these differences, as ubiquitylation is strongly reduced by mutation or truncation of the first 30aa from the UQ2 N-terminus. The N-terminus of UQ2 is not sufficient to cause ubiquitylation, however, as it requires a functional UBA domain and is modulated by the presence of the PRR. ALS mutations concentrated in and around the PRR do not have uniform effects – in my hands, only UQ2^{P497H} had a discernible alteration in transient transfection experiments, resulting in heightened ubiquitylation and reduced solubility.

Even UQ2^{P497S}, bearing a disease-relevant missense mutation at the same position, behaved similarly to UQ2^{WT} in this analysis, which was surprising. Although I can confidently make the conclusion that UQ2^{P497H} is hyper-ubiquitylated and relatively insoluble, this work generates more questions than it answers.

Additionally, my studies indicate that both UQ1 and UQ2 share several common interacting partners, likely mediated by the conserved UBL and UBA domains. As such, I did not discover any alterations to the protein-protein interaction profiles of UQ2 ALS mutants, although absence of evidence is not sufficient to eliminate this working hypothesis. It's not terribly surprising that ubiquilins perturb protein degradation when expressed at high levels, but additional UBA* controls allow me to make the strong conclusion that UQ2^{WT} and ALS mutants retard protein degradation to a similar extent when transfected in the presence of the unstable reporter substrate, Ub^{G76V}-GFP. Although this is negative data, it contrasts with a previously published finding in a high impact journal[19], and I have done my best to include additional controls, both positive and negative, in order to assert this conclusion. I would further posit that the substrate scope of UQ1 and UQ2 may in fact be distinct, given my findings with TASK85 and GFP(f1) – although this work is still preliminary.

6.5 Future directions

There's a lot of interesting leads to pursue with the ubiquilin crew, and I'll organize these final thoughts by priority – what I think is most important for pursuing this project. I've been lucky to collaborate with Chi Chi Xie during my final years as a graduate student, and she developed a series of transgenic Drosophila with tissue-specific, inducible ubiquilin transgenes. The characterization of flies expressing UQ2^{WT},

$UQ2^{P497H}$, and $UQ2^{P525S}$ is underway. One striking observation is a bristle phenotype exhibited by UQ2 ALS mutant flies, but not by wild type or driver only (control) flies, which is a mild degenerative phenotype that occurs when ubiquilins are expressed in the eye. An enhancer screen to look for gene expression combinations that exacerbate this phenotype will be the most logical route for follow-up, as the phenotype is mild and therefore looking for genes that ameliorate the phenotype will be harder to screen. Additional Drosophila experiments directed at behavioral and motor phenotypes, such as climbing assays, will provide a functional readout for neuron-specific ubiquilin expression. The most important upcoming experiment in this case is a climbing comparison of flies expressing $UQ2^{WT}$ and ALS mutants with matched UBA* mutations, i.e., $UQ2^{UBA*}$ and $P497H^{UBA*}$. The prediction is that Ub-binding is required for toxicity, and would be the first example of such a mechanism in ALS.

An alternative genetic model of ubiquilin deficiency is being constructed in the lab by crossing *UBQLN1* knockout mice with *UBQLN2* knockout mice to obtain the double knockout (UQ DKO). The *UBQLN2* knockout rat has no phenotype[20], and the triple UQ1/UQ2/UQ4 knockout HEK cells have only a mild stress compensation phenotype[1], so it will be important to characterize both the cells and whole animals resulting from UQ DKO. Although biochemistry can be performed in many different cell types, I think it would be wise to characterize stress response and recovery in cultured neurons from these animals, rather than working with MEFs.

I also think that the assays described in the discussion of Chapter 5, namely the role of ubiquilins in DRiP metabolism and antigen presentation is a fascinating follow-up project. Considering the work from the Hegde lab, it seems that ubiquilins are bona fide

chaperones for mislocalized proteins containing transmembrane domains, and likely for DRiPs as well. Finally it would be excellent to reproduce some of the biophysical characterization explored by Hjerpe et al. An *in vitro* translation system, like rabbit reticulocyte lysate or the Promega TNT kit, would help to yield functional, folded ubiquilins for biochemical assays and structure elucidation. The work of Itakura et al. specifically touches on lysate-based membrane insertion assays, which I think would be complemented by additional assays, such as luciferase refolding or thermal denaturation assays[21,22]. These experiments could be structured like work from Harm Kampinga by using different concentrations and combinations of ubiquilins and HSP70s to refold model substrates *in vitro* or mitigate toxicity of polyQ proteins in cell culture (as an example) [23,24].

Finally, I would love to follow up on my observations of insoluble Ub oscillation following heat stress. This is mostly just for fun, because it's not necessarily related to ubiquilins. At first pass, I envisioned an siRNA screen to find factors that alter the response to heat stress, which could be measured through immunoblotting of soluble and insoluble ubiquitin. The problem with the approach is that it's incredibly time-consuming to heat shock cells, precisely and reproducibly return them to the incubator for set times, and then fraction them. It's not only time-consuming, it's difficult to stay faithful to the time points, and potentially the most interesting dynamics are being lost in the 15-20m intervals that are necessary for reproducibility. These shortcomings could be addressed by the use of fluorescent protein reporters that aggregate during folding stress[25]. I acquired these reporters from the lab of Ulrich Hartl and I think this would be an excellent live-cell imaging project.

6.6 Figures

Figure 6.1

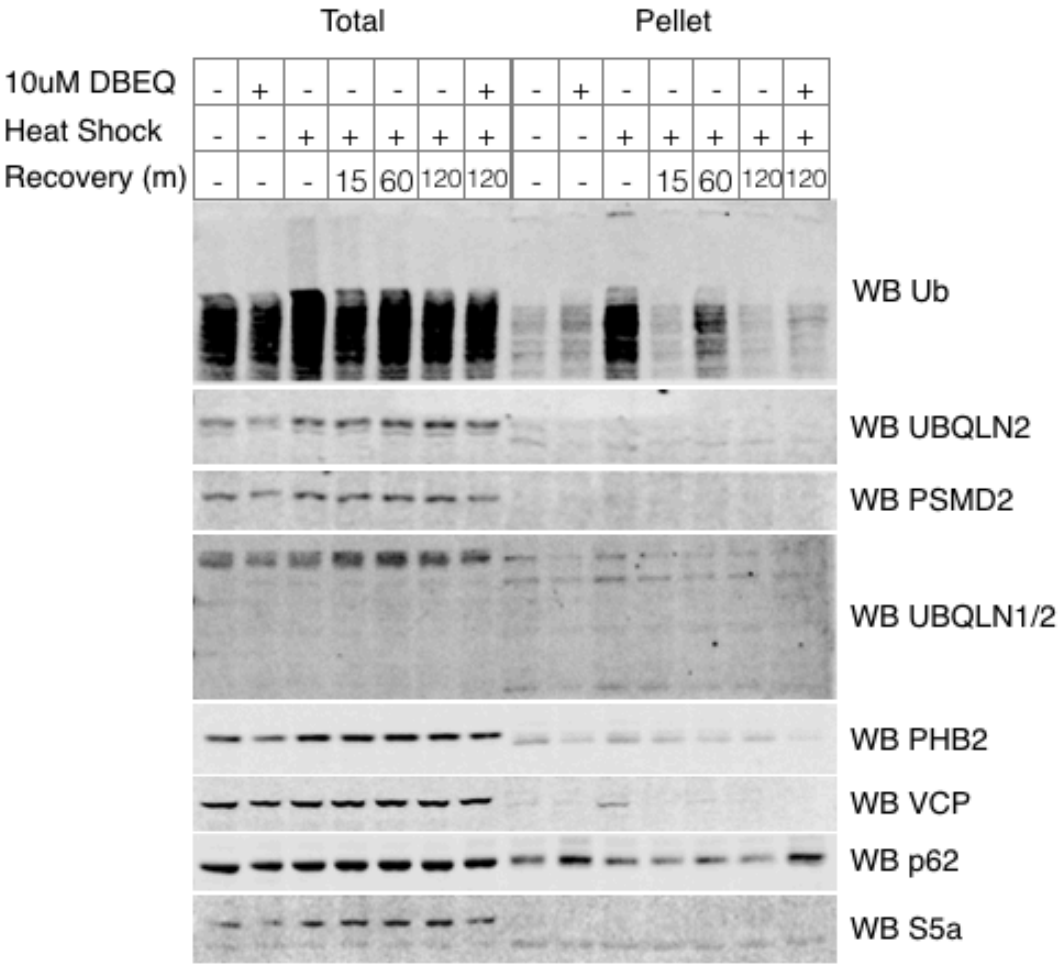

U-2 OS cells were heat shocked at 45C for 30m, and then returned to 37C for the indicated amount of time. Where indicated, cells were pre-treated for 3h with the VCP inhibitor, DBeQ. Cells were harvested, an aliquot of the total lysate taken, and then separated into TX-soluble and –insoluble phases, followed by SDS-PAGE and immunoblotting with indicated antibodies. Heat shock causes a massive accumulation of polyUb in the insoluble phase, which is strongly reduced following 15m recovery. At 1h recovery, polyUb is again strongly enriched in the insoluble phase. VCP inhibition (DBeQ +) does not inhibit the clearance of polyUb from the pellet, but does alter p62 solubility.

Figure 6.2

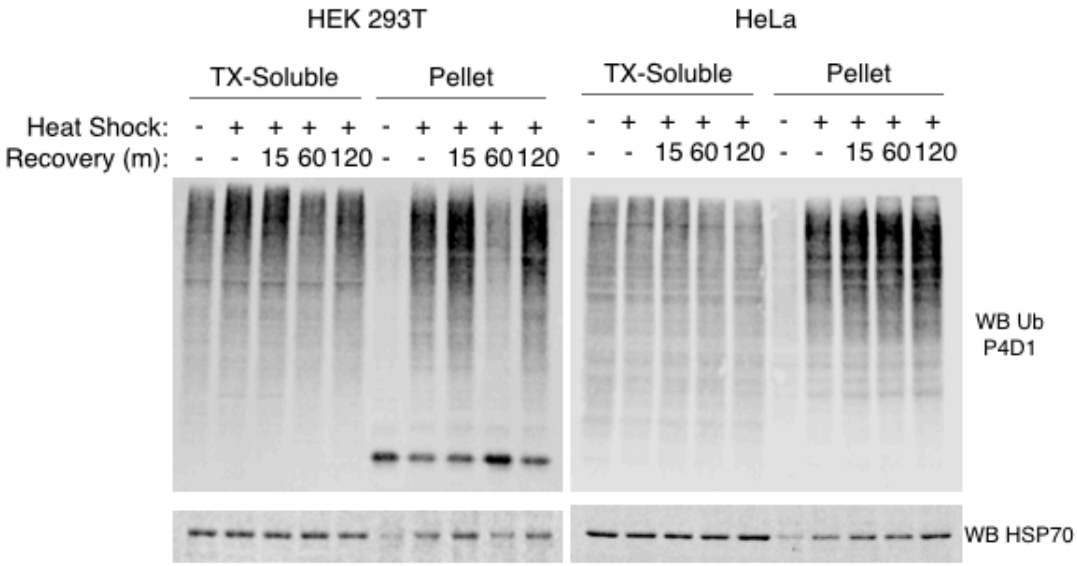

HEK 293T or HeLa cells were heat shocked at 45C for 30m, then returned to 37C for the indicated amount of time. Cells were harvested and separated into TX-soluble and – insoluble phases, followed by SDS-PAGE and immunoblotting with indicated antibodies. Heat shock causes a massive accumulation of polyUb in the insoluble phase for both HEK 293T and HeLa cells. HEK 293T cells exhibit an oscillation of solubility, down at 1h, up at 2h, whereas HeLa cells maintain persistent insoluble polyUb. HSP70 is strongly enriched in the insoluble phase following heat shock.

Figure 6.3

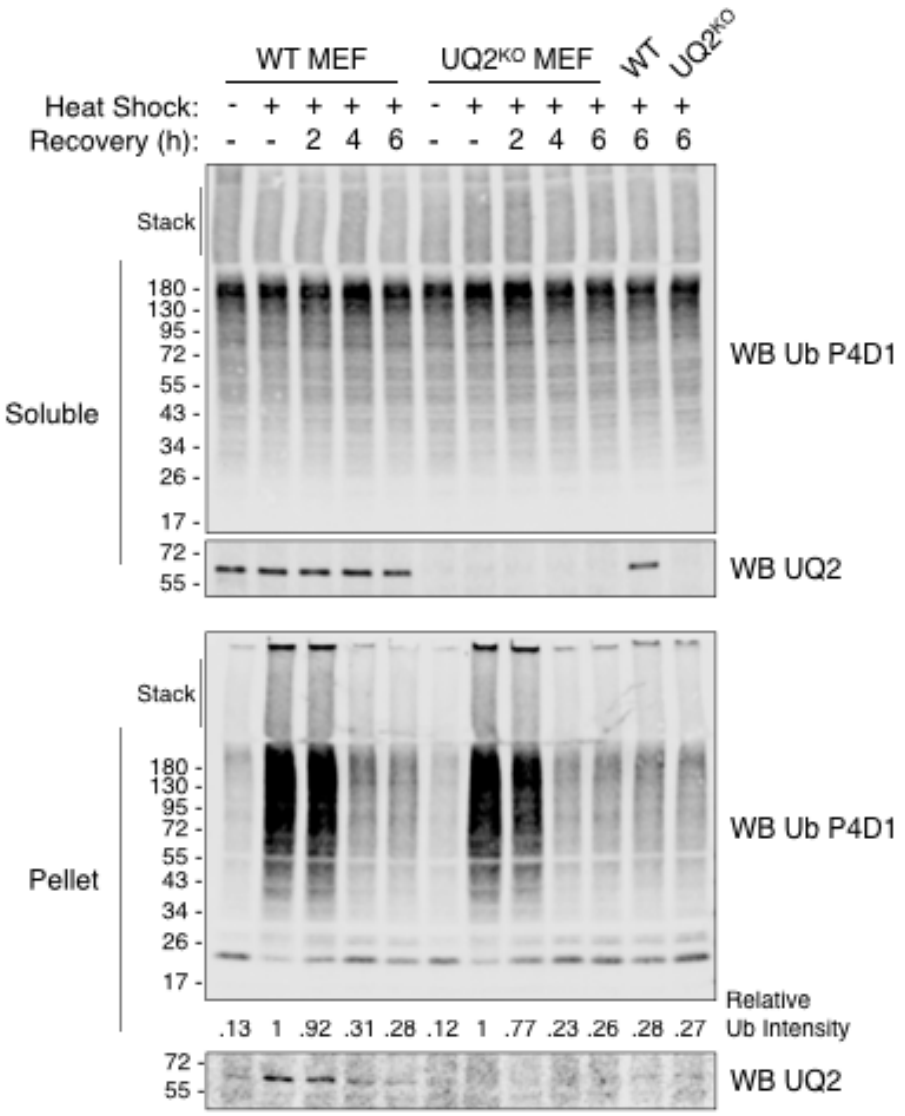

Murine embryonic fibroblasts (MEFs) immortalized with large T antigen were rendered null for UQ2 by CRISPR/Cas9, WT or UQ2^{KO} MEFs were heat shocked at 42C for 2h, then returned to 37C for the indicated amount of time. Cells were harvested and separated into TX-soluble and –insoluble phases, followed by SDS-PAGE and immunoblotting with indicated antibodies. Heat shock causes massive accumulation of polyUb in insoluble phase, but no change in soluble phase. UQ2 can be clearly observed in the insoluble phase following heat shock. UQ2 deficiency does not alter the kinetics of polyUb clearance from the soluble phase. Relative intensities for insoluble Ub set equal to heat shock lane.

6.7 References

1. Itakura, E. *et al.* Ubiquilins Chaperone and Triage Mitochondrial Membrane Proteins for Degradation. *Molecular cell* **63,** 21–33 (2016).
2. Hjerpe, R. *et al.* UBQLN2 Mediates Autophagy-Independent Protein Aggregate Clearance by the Proteasome. *Cell* 1–16 (2016). doi:10.1016/j.cell.2016.07.001
3. Schuck, S., Honsho, M., Ekroos, K., Shevchenko, A. & Simons, K. Resistance of cell membranes to different detergents. *Proc Natl Acad Sci USA* **100,** 5795–5800 (2003).
4. Neumann, M. *et al.* Ubiquitinated TDP-43 in frontotemporal lobar degeneration and amyotrophic lateral sclerosis. *Science* **314,** 130–133 (2006).
5. Alberti, S., Halfmann, R., King, O., Kapila, A. & Lindquist, S. A Systematic Survey Identifies Prions and Illuminates Sequence Features of Prionogenic Proteins. *Cell* **137,** 146–158 (2009).
6. Halfmann, R. *et al.* Prions are a common mechanism for phenotypic inheritance in wild yeasts. *Nature* **482,** 363–368 (2012).
7. Holmes, D. L., Lancaster, A. K., Lindquist, S. & Halfmann, R. Heritable Remodeling of Yeast Multicellularity by an Environmentally Responsive Prion. *Cell* **153,** 153–165 (2013).
8. Polymenidou, M. & Cleveland, D. W. The seeds of neurodegeneration: prion-like spreading in ALS. *Cell* **147,** 498–508 (2011).
9. David, D. C. *et al.* Widespread Protein Aggregation as an Inherent Part of Aging in C. elegans. *PLoS Biol* **8,** e1000450 (2010).
10. Reis-Rodrigues, P. *et al.* Proteomic analysis of age-dependent changes in protein solubility identifies genes that modulate lifespan. *Aging Cell* **11,** 120–127 (2011).
11. Kirstein-Miles, J., Scior, A., Deuerling, E. & Morimoto, R. I. The nascent polypeptide-associated complex is a key regulator of proteostasis. *EMBO J* 1–18 (2013). doi:10.1038/emboj.2013.87
12. Morimoto, R. I. Proteotoxic stress and inducible chaperone networks in neurodegenerative disease and aging. *Genes Dev* **22,** 1427–1438 (2008).
13. Walther, D. M. *et al.* Widespread Proteome Remodeling and Aggregation in Aging C. elegans. *Cell* **161,** 919–932 (2015).
14. Wallace, E. W. J. *et al.* Reversible, Specific, Active Aggregates of Endogenous Proteins Assemble upon Heat Stress. *Cell* **162,** 1286–1298 (2015).
15. Fang, N. N. *et al.* Rsp5/Nedd4 is the main ubiquitin ligase that targets cytosolic misfolded proteins following heat stress. *Nat Cell Biol* **16,** 1227–1237 (2014).
16. Fang, N. N., Ng, A. H. M., Measday, V. & Mayor, T. Hul5 HECT ubiquitin ligase plays a major role in the ubiquitylation and turnover of cytosolic misfolded proteins. *Nat Cell Biol* **13,** 1344–1352 (2011).
17. Prahlad, V., Cornelius, T. & Morimoto, R. I. Regulation of the cellular heat shock response in Caenorhabditis elegans by thermosensory neurons. *Science* **320,** 811–814 (2008).
18. Prahlad, V. & Morimoto, R. I. Neuronal circuitry regulates the response of Caenorhabditis elegans to misfolded proteins. *Proceedings of the National Academy of Sciences* **108,** 14204–14209 (2011).
19. Deng, H.-X. *et al.* Mutations in UBQLN2 cause dominant X-linked juvenile and

adult-onset ALS and ALS/dementia. *Nature* 1–7 (2011). doi:10.1038/nature10353
20. Wu, Q. *et al.* Pathogenic Ubqln2 gains toxic properties to induce neuron death. *Acta Neuropathol* (2014). doi:10.1007/s00401-014-1367-y
21. Glover, J. R. & Lindquist, S. Hsp104, Hsp70, and Hsp40: a novel chaperone system that rescues previously aggregated proteins. *Cell* **94,** 73–82 (1998).
22. Galam, L. *et al.* High-throughput assay for the identification of Hsp90 inhibitors based on Hsp90-dependent refolding of firefly luciferase. *Bioorg Med Chem* **15,** 1939–1946 (2007).
23. Hageman, J. *et al.* A DNAJB chaperone subfamily with HDAC-dependent activities suppresses toxic protein aggregation. *Molecular cell* **37,** 355–369 (2010).
24. Vos, M. J. *et al.* HSPB7 is the most potent polyQ aggregation suppressor within the HSPB family of molecular chaperones. *Hum Mol Genet* **19,** 4677–4693 (2010).
25. Gupta, R. *et al.* Firefly luciferase mutants as sensors of proteome stress. *Nat Methods* **8,** 879–884 (2011).